University of Alberta

Electroweak Phenomenology Beyond the Standard Model

by

David W. Maybury 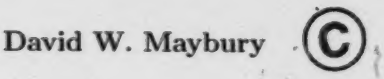

A thesis submitted to the Faculty of Graduate Studies and Research in partial fulfillment of the requirements for the degree of Doctor of Philosophy

Department of Physics

Edmonton, Alberta
Fall 2005

Library and Archives Canada

Published Heritage Branch

395 Wellington Street
Ottawa ON K1A 0N4
Canada

Bibliothèque et Archives Canada

Direction du Patrimoine de l'édition

395, rue Wellington
Ottawa ON K1A 0N4
Canada

0-494-08692-0

Your file *Votre référence*
ISBN:
Our file *Notre reference*
ISBN:

NOTICE:
The author has granted a non-exclusive license allowing Library and Archives Canada to reproduce, publish, archive, preserve, conserve, communicate to the public by telecommunication or on the Internet, loan, distribute and sell theses worldwide, for commercial or non-commercial purposes, in microform, paper, electronic and/or any other formats.

The author retains copyright ownership and moral rights in this thesis. Neither the thesis nor substantial extracts from it may be printed or otherwise reproduced without the author's permission.

AVIS:
L'auteur a accordé une licence non exclusive permettant à la Bibliothèque et Archives Canada de reproduire, publier, archiver, sauvegarder, conserver, transmettre au public par télécommunication ou par l'Internet, prêter, distribuer et vendre des thèses partout dans le monde, à des fins commerciales ou autres, sur support microforme, papier, électronique et/ou autres formats.

L'auteur conserve la propriété du droit d'auteur et des droits moraux qui protège cette thèse. Ni la thèse ni des extraits substantiels de celle-ci ne doivent être imprimés ou autrement reproduits sans son autorisation.

In compliance with the Canadian Privacy Act some supporting forms may have been removed from this thesis.

While these forms may be included in the document page count, their removal does not represent any loss of content from the thesis.

Conformément à la loi canadienne sur la protection de la vie privée, quelques formulaires secondaires ont été enlevés de cette thèse.

Bien que ces formulaires aient inclus dans la pagination, il n'y aura aucun contenu manquant.

Canada

Before I came here, I was confused about this subject. Having listened to your lecture I am still confused - but on a much higher level.

Enrico Fermi

To the women of my life:

my mother, Diane, my sister, Janet,
and of course, my
Laurie

Abstract

This thesis examines low energy consequences of extensions of the Standard Model that call for new particle content and symmetries. In particular, we examine the ramifications of new scalar interactions on pion physics, of induced lepton flavour violation (LFV) in the constrained minimal supersymmetric standard model (CMSSM) with see-saw generated neutrino masses, and of induced LFV in lopsided $SO(10)$ models.

New interactions with Lorentz scalar structure, arising from physics beyond the standard model of electroweak interactions, will induce effective pseudoscalar interactions after renormalization by weak interaction loop corrections. Such induced pseudoscalar interactions are strongly constrained by data on $\pi^{\pm} \to l^{\pm}\nu_l$ decay. These limits on induced pseudoscalar interactions imply limits on the underlying fundamental scalar interactions that in many cases are substantially stronger than limits on scalar interactions from direct β-decay searches.

The see-saw mechanism of neutrino mass generation, when incorporated in supersymmetric theories with supergravity mediated supersymmetry breaking, results in low-energy lepton-flavour violation arising from the soft supersymmetry breaking slepton masses. The parameter space of supergravity theories with conserved R-parity is severely constrained by the requirement that the LSP provide cold dark matter with a relic density in the range indicated by the recent Wilkinson Microwave Anisotropy Probe (WMAP) measurements, as well as by laboratory constraints. We calculate the $\mu \to e\gamma$ branching ratio for the CMSSM, over the range of parameters consistent with WMAP and laboratory constraints, in families of see-saw model parameterizations which fit the low energy neutrino measurements.

A class of predictive $SO(10)$ grand unified theories with highly asymmetric mass matrices, known as lopsided textures, which was developed to accommodate the observed mixing in the neutrino sector, can effectively determine the rate for charged lepton flavour violation, and in particular the branching ratio for $\mu \to e\gamma$. Assuming that

the supersymmetric GUT breaks directly to the CMSSM, we find that in light of the combined constraints on the CMSSM parameters from direct searches and from the WMAP satellite observations, the resulting predicted rate for $\mu \to e\gamma$ in this model class can be within the current experimental bounds for low $\tan\beta$, but that the next generation of $\mu \to e\gamma$ experiments would effectively rule out this model class if LFV is not detected.

Acknowledgements

The last five and a half years have been the most rewarding and the most fulfilling of my life. In this time, I have grown and matured in both my outlook towards physics and as a human being.

First, I would like to thank my mother, Diane. She is truly an inspiration. As a child of eight, I watched my mother, a single parent, bravely go back to school at the age of thirty-five to pursue a better life for our family. I can remember the late and long hours she diligently put in to studying after taking care of the needs of both me and my sister. I also remember, at the age of eleven, attending the award ceremony where she received Lambton College's Presidential Medal of Academic Excellence for graduating top of her class. Simply stated, I would not be the man I am today without her encouragement or example as guidance.

I would also like to thank my sister, Janet. She has been a pillar of support even when separated by great distances. Also, I would like to acknowledge my late father, George, whose love of reading was never tempered by his lack of formal opportunities as a child of the Great Depression. Truly, our discussions have lead me to always appreciate the good fortune that we enjoy today. My parents-in-law have been a source of great support. Both Ernie and Doris are always present with a listening ear.

It has been a privilege to learn from and laugh with excellent colleagues, and friends that I have made during my time at the University of Alberta. In particular, I am a better person for having known Kirk Kaminsky, David Shaw, and Kipp Cannon. In my undergraduate years, I had the wonderful, and life changing opportunity of attending Roger Migneron's Advanced Calculus course. It was during this year that Roger took me under his wing. Besides exposing me to new areas of physics and mathematics, he helped me to develop a confidence in myself for which I will always be grateful. He passed away shortly after I began graduate school; he will be missed. My supervisor, Bruce Campbell, I find nothing short of extraordinary. His constant encouragement and optimism helped me through the most difficult times of my program and his deep understanding of the field has set an example to which I hope one day to aspire.

Finally, I would like to thank my wife, Laurie. The last two years have been the happiest of my life. Her constant, unconditional love has revealed a whole new world to me. I have much to learn from her and I am forever grateful that she has walked into my life.

Preface

This thesis is organized into two parts. Part I, containing chapters 1 - 3, provides the reader the necessary preliminary background detail for exploring the phenomenological implications of the models in Part II. As the underlying framework of the Standard Model, quantum field theory with an emphasis on quantum gauge theories is developed in chapter 1. Since at present supersymmetry provides the best known solution to the gauge hierarchy problem, chapter 2 gives an introduction to supersymmetric field theory and the minimal supersymmetric standard model (MSSM). Finally, chapter 3 is devoted to neutrino mass, neutrino oscillations, and grand unification. As the subject material of the background chapters is vast and has developed greatly over the past 25 years, no attempt has been made at providing an exhaustive (or exhausting) review. Further details may be found in the references cited.

Part II is essentially the heart of this thesis. Each chapter (4-6) contains original contributions to research in the form of three published papers over the course of the author's Ph.D. program at the University of Alberta between September 1999 and April 2005. Part II is based on the following published works:

- Bruce A. Campbell and David Maybury, Constraints on Scalar Couplings from $\pi^{\pm} \to l\nu$, Nucl. Phys. **B709**, 419 (2005), preprint: hep-ph/0303046
- Bruce A. Campbell, David Maybury and Brandon Murakami, See-Saw Induced CMSSM Lepton Flavour Violation Post-WMAP, JHEP **0403**, 052 (2004), preprint: hep-ph/0311244
- Ernest Jankowski and David Maybury, Lepton Flavour Violation in a Class of Lopsided SO(10) Models, Phys. Rev. **D70**, 035004 (2004), pre-print: hep-ph/0401132

Table of Contents

I From Gauge Theories to Grand Unification 1

1 Gauge Field Theory 2
- 1.1 A Geometrical Picture of Fundamental Interactions . . . 2
- 1.2 A Brief Overview of Path Integral Quantization of Gauge Theories . . . 9
- 1.3 A Survey of Renormalization . . . 13
- 1.4 Spontaneous Symmetry Breaking . . . 19

Bibliography 26

2 Supersymmetry for Model Building 29
- 2.1 Naturalness and the Standard Model . . . 29
- 2.2 The Supersymmetry Algebra . . . 31
- 2.3 Superfields . . . 34
- 2.4 A Cursory View of Spontaneous Supersymmetry Breaking . . . 41
- 2.5 The Minimal Supersymmetric Standard Model . . . 45

Bibliography 55

3 Neutrino Mass and a Grand Unification Primer 59
- 3.1 The Lepton Sector of the Standard Model . . . 59
- 3.2 Patterns of Neutrino Mass . . . 62
- 3.3 Neutrino Oscillations: Experimental Evidence for Neutrino Mass . . . 67
- 3.4 The Prototype GUT: $SU(5)$ . . . 72
- 3.5 A Larger Group for Model Building: $SO(10)$ . . . 79

Bibliography 80

II Constraints on Extensions of the Standard Model from Observations 85

4 Constraints on Scalar Couplings from $\pi^{\pm} \to l\nu$ 89
- 4.1 Introduction . . . 89
- 4.2 Pion Physics and New Pseudoscalar Interactions . . . 90
- 4.3 Local Scalar Operator Analysis . . . 92
  - 4.3.1 Type A Operator Analysis: O_A . . . 93

4.3.2 Type B Operator Analysis: O_B 95
4.4 Pseudoscalar Interactions From Threshold Effects 98
4.5 Comparison with β-Decay Constraints 101
4.6 Flavour Dependent Couplings 107
4.7 Discussion 109

Bibliography **110**

5 See-Saw Induced CMSSM LFV Post-WMAP **113**
5.1 Introduction 113
5.2 Supersymmetric See-Saw Parameterization 116
5.3 Supersymmetry Breaking and the CMSSM 118
5.4 $\mu \to e\gamma$ In The CMSSM See-Saw 119
5.4.1 Hierarchical ν_Rs 120
5.4.2 Degenerate ν_Rs 121
5.5 Conclusion 122

Bibliography **123**

6 LFV in a Class of Lopsided SO(10) Models **134**
6.1 Introduction 134
6.2 The AB Model Definition 135
6.3 Numerical Results for $\mu \to e\gamma$ 137
6.4 Conclusions 141

Bibliography **141**

A Spinors **149**

B $l_j \to l_i + \gamma$ **154**

C The One-Loop RGEs for the MSSM-RN **156**

List of Figures

1.1 Parallel transporting a vector on the globe: Starting with vector V at point p, the two distinct paths lead to different vectors at q. 6
1.2 Parallel transporting vector V_0 around an infinitesimal parallelogram on a curved manifold along two distinct paths. 7

2.1 Feynman diagrams that contribute quadratic divergences to the Higgs mass. 30

3.1 Feynman diagrams that contribute to the process $\mu \to e\gamma$. 67

4.1 $\mathcal{O}_1$ and $\mathcal{O}_2$, Type A contact interactions 94
4.2 Example of electroweak corrections to Type A contact interactions. All permutations are required including wavefunction renormalization; the vector bosons are the $W_\mu^{1,2,3}$ and B_μ. 94
4.3 Type A operator RGE analysis. Panel (a) shows how each operator evolves with scale. Panel (b) displays the induced pseudoscalar proportionality factor. 95
4.4 $\mathcal{O}_1$ and $\mathcal{O}_2$, Type B contact interactions 96
4.5 Example of electroweak corrections to Type B contact interactions. All permutations are required including wavefunction renormalization; the vector bosons are the $W_\mu^{1,2,3}$ and B_μ. 96
4.6 Type B operator RGE analysis. Panel (a) shows how each operator evolves with scale. Panel (b) displays the induced pseudoscalar proportionality factor. 97
4.7 Dressed Z^0 exchange diagrams. 99
4.8 Dressed W exchange diagrams. 100
4.9 Radiative corrections to the quark-scalar vertex. 100
4.10 Constraint plots on the real parts of $\tilde{C}_s$ and $\tilde{C}'_s$ at Λ =200 GeV. Panel (a) corresponds to a phase of 0°; panel (b) to ±45°; and panel (c) to 45° and −45° for $\tilde{C}_s$ and $\tilde{C}'_s$ respectively. The diagonal band is the experimental limit set by the b-Fierz interference term from β-decay at the 90% confidence level and the solid annulus is the approximate experimental bound given in [3]. In all cases, the allowed region is the band between the two ellipses. An enlargement of the figures is displayed in figure 4.11. 103

4.11 Constraint plots on the real parts of $\tilde{C}_s$ and $\tilde{C}'_s$ at Λ =200 GeV. Panel (a) corresponds to a phase of 0°; panel (b) to ±45°; and panel (c) to 45° and −45° for $\tilde{C}_s$ and $\tilde{C}'_s$ respectively. The diagonal band is the experimental limit set by the b-Fierz interference term from β-decay at the 90% confidence level. In all cases, the allowed region is the band between the two ellipses. The enlarged area more clearly shows the width of the region. . . 104

4.12 Constraint plots on the imaginary parts of $\tilde{C}_s$ and $\tilde{C}'_s$ at Λ =200 GeV. Panel (a) corresponds to a phase of ±90°; panel (b) to ±45°; and panel (c) to 45° and −45° for $\tilde{C}_s$ and $\tilde{C}'_s$ respectively. The solid ellipse is the approximate experimental bound on the imaginary part of the couplings assuming nothing about the phase [3]. In panel (a), the unshaded interior ellipse is the constraint from pion decay. In the remaining plots, the allowed region is the band between the two ellipses. An enlargement of the figures is displayed in figure 4.13. 105

4.13 Constraint plots on the imaginary parts of $\tilde{C}_s$ and $\tilde{C}'_s$ at Λ =200 GeV. Panel (a) corresponds to a phase of ±90°; panel (b) to ±45°; and panel (c) to 45° and −45° for $\tilde{C}_s$ and $\tilde{C}'_s$ respectively. In panel (a), the interior of the ellipse is the constraint. In the remaining plots, the allowed region is the band between the two ellipses. The enlarged area more clearly shows the width of the region. 106

4.14 Constraint plots on the $|C_e|$ and $|C_\mu|$ couplings at Λ = 200 GeV. Panel (a) corresponds to phases for C_e and C_μ of 0°, 0°; panel (b) to 90°, 90°; panel (c) to 180°, 180°; panel (d) to ±45°, ±45° respectively. The allowed region is the bounded area in the lower left corner. The horizontal line is the muon capture bound [18]. 108

5.1 **Hierarchical ν_Rs**: BR($\mu \to e\gamma$) as a function of the seesaw parameter θ_1; $\mu > 0$ and $a = 0$. The solid curve corresponds to $\tan\beta = 5$, $m_0 = 140$ GeV, $m_{1/2} = 700$ GeV. The dash-dot curve corresponds to $\tan\beta = 10$, $m_0 = 125$ GeV, $m_{1/2} = 560$ GeV. The dashed curve corresponds to $\tan\beta = 20$, $m_0 = 200$ GeV, $m_{1/2} = 760$ GeV. The dotted curve corresponds to $\tan\beta = 40$, $m_0 = 390$ GeV, $m_{1/2} = 900$ GeV. Each parameter set is chosen to lie inside the CMSSM allowed region [12]. The upper horizontal line indicates the present experimental bound and the lower line indicates the expected upcoming experimental sensitivity from MEG. 123

5.2 **Hierarchical ν_Rs**: WMAP and laboratory constraint parameterization of the CMSSM, and LFV compliance, based on the current LFV bound, BR($\mu \to e\gamma$) $< 1.2 \times 10^{-11}$ for $\tan\beta = 5$, 10, 15, 20, 25, 30, 35, 40, 45, 50, 55, $\mu > 0$ and $a = 0$. Grey indicates that less than 25% of the range of θ_1 is allowed. Red indicates that between 25% and 50% of θ_1 is allowed. Green and blue illustrate that 50% to 75%, and 75% to 100%, are allowed respectively. The constraint regions are reproduced from [12]. 124

5.3 **Hierarchical ν_Rs**: WMAP and laboratory constraint parameterization of the CMSSM, and LFV compliance, based on the expected LFV bound from MEG, $\mathrm{BR}(\mu \to e\gamma) \lesssim 5 \times 10^{-14}$ for $\tan\beta = 5$, 10, 15, 20, 25, 30, 35, 40, 45, 50, 55, $\mu > 0$ and $a = 0$. Grey indicates that less than 25% of the range of θ_1 is allowed. Red indicates that between 25% and 50% of θ_1 is allowed. Green and blue illustrate that 50% to 75%, and 75% to 100%, are allowed respectively. The constraint regions are reproduced from [12]. ¶25

5.4 **Hierarchical ν_Rs**: WMAP and laboratory constraint parameterization of the CMSSM, and LFV compliance, based on the current LFV bound, $\mathrm{BR}(\mu \to e\gamma) < 1.2 \times 10^{-11}$ for $\tan\beta = 10, 35$, $\mu < 0$ and $a = 0$. Grey indicates that less than 25% of the range of θ_1 is allowed. Red indicates that between 25% and 50% of θ_1 is allowed. Green and blue illustrate that 50% to 75%, and 75% to 100%, are allowed respectively. The constraint regions are reproduced from [13]. 126

5.5 **Hierarchical ν_Rs**: WMAP and laboratory constraint parameterization of the CMSSM, and LFV compliance, based on the expected LFV bound from MEG, $\mathrm{BR}(\mu \to e\gamma) \lesssim 5 \times 10^{-14}$ for $\tan\beta = 10, 35$, $\mu < 0$ and $a = 0$. Grey indicates that less than 25% of the range of θ_1 is allowed. Red indicates that between 25% and 50% of θ_1 is allowed. Green and blue illustrate that 50% to 75% and 75% to 100% are allowed respectively. The constraint regions are reproduced from [13]. 127

5.6 **Degenerate ν_Rs**: WMAP and laboratory constraint parameterization of the CMSSM, and LFV compliance, based on the current LFV bound, $\mathrm{BR}(\mu \to e\gamma) < 1.2 \times 10^{-11}$ for $\tan\beta = 5, 10, 15, 20, 25, 30, 35, 40, 45, 50, 55$, $\mu > 0$ and $a = 0$. Blue indicates the allowed region. The constraint regions are reproduced from [12]. 128

5.7 **Degenerate ν_Rs**: WMAP and laboratory constraint parameterization of the CMSSM, and LFV compliance, based on the current LFV bound, $\mathrm{BR}(\mu \to e\gamma) < 1.2 \times 10^{-11}$ for $\tan\beta = 10, 35$, $\mu < 0$ and $a = 0$. Blue indicates the allowed region. The constraint regions are reproduced from [13]. 129

6.1 Feynman diagrams contributing to $\mu \to e\gamma$. 140

6.2 Contour Plots of $\mathrm{BR}(\mu \to e\gamma)$ in the $m_0 - m_{1/2}$ plane: Panels (a),(c),(d), and (f) show the contours of the branching ratio for $\tan\beta = 5, 15, 25, 50$ respectively with $\mu > 0$. Panels (b) and (e) show the contours with $\tan\beta = 10, 35$ respectively with $\mu < 0$. In all cases the shaded region corresponds to the approximate combined WMAP and laboratory constraints. 142

Part I

From Gauge Theories to Grand Unification

Chapter 1

Gauge Field Theory

1.1 A Geometrical Picture of Fundamental Interactions

The strong, the weak, and the electromagnetic forces, mediated by spin 1 fields, form the basis of non-gravitational physics. Remarkably, these interactions can be understood in the geometrical language of gauge theories [1, 2, 3, 4, 5, 6], which completely specify how these forces interact. Reformulated as quantum field theories [7, 8, 9], gauge theories and the principle of local gauge invariance form the foundation of the Standard Model - a gauge theory based on $SU(3)_c \times SU(2)_L \times U(1)_Y$ - and moreover, all of elementary particle theory. As gauge theories play a central role in modern theoretical physics, it is worth exploring the structure of gauge theories in some detail.

The earliest and simplest gauge theory is quantum electrodynamics (QED). Starting with the Lagrangian for a free Dirac field,

$$\mathcal{L} = \bar{\psi}(i\gamma^\mu \partial_\mu - m)\psi \tag{1.1}$$

we see that the global phase transformation,

$$\psi(x) \rightarrow e^{-ig\Lambda}\psi(x) \tag{1.2}$$

leaves eq.(1.1) invariant provided that Λ, an arbitrary real parameter, does not depend on spacetime and g is some real constant. Let us examine the consequences of relaxing the spacetime independence requirement of Λ by promoting Λ to a local phase; i.e. $\Lambda \rightarrow \Lambda(x)$. Clearly, the free Dirac Lagrangian will no longer be invariant under this new local transformation,

$$\mathcal{L} \rightarrow \mathcal{L} + g\bar{\psi}\gamma^\mu \psi \partial_\mu \Lambda. \tag{1.3}$$

However, we may construct a Lagrangian that remains invariant under the local trans-

formation by adding new terms that cancel the unwanted contributions. Suppose we replace the derivative ∂_μ with a covariant derivative,

$$\partial_\mu \rightarrow D_\mu = \partial_\mu + igA_\mu \tag{1.4}$$

where the new field in eq.(1.4), called a gauge field, transforms as,

$$A_\mu \rightarrow A_\mu + \partial_\mu \Lambda. \tag{1.5}$$

Using this property, together with the local phase transformation on ψ, we see that the term $D_\mu \psi$ transforms in the same way as ψ (hence the name covariant),

$$D_\mu \psi \rightarrow e^{-ig\Lambda} D_\mu \psi. \tag{1.6}$$

The free Dirac Lagrangian becomes,

$$\mathcal{L} = \bar{\psi}(i\gamma^\mu D_\mu - m)\psi \tag{1.7}$$

$$= \bar{\psi}(i\gamma^\mu \partial_\mu - g\gamma^\mu A_\mu - m)\psi \tag{1.8}$$

which by construction remains invariant under the transformation of eq.(1.2). Having introduced the new field A_μ, there now appears another object that remains invariant under the local phase transformation. Clearly, the term

$$F_{\mu\nu} = \partial_\mu A_\nu - \partial_\nu A_\mu \tag{1.9}$$

is invariant under eq.(1.5) and, as a result, should be included in the theory, namely,

$$\mathcal{L} = \bar{\psi}(i\gamma^\mu D_\mu - m)\psi - \frac{1}{4} F_{\mu\nu} F^{\mu\nu}. \tag{1.10}$$

The object $F_{\mu\nu}$ has been contracted with itself to form a Lorentz invariant and the factor of 1/4 is chosen for future convenience. The Lagrangian of eq.(1.10) is fully invariant under the local transformation.

Systems that remain invariant under local phase rotations, called gauge transformations, possess a gauge symmetry. In the case under discussion, the phase parameterizes the Abelian group $U(1)$. Thus, this Lagrangian describes a massless $U(1)$ vector field interacting with Dirac fermions and therefore serves as the Lagrangian for QED. The electromagnetic field and its interactions with fermions arise simply by insisting on local gauge invariance. This amazing result has far reaching consequences. Gauge theories characterize all the forces of nature, including gravity. Gravity, as described by General Relativity (for review see [10]), is a gauge theory of local spacetime transformations

[11], mediated by a spin 2 field with the dimensionful coupling G_N. (The dimensionful coupling presents subtle problems for quantization and as a result render gravity unrenormalizable. We will discuss aspects of renormalization in following sections.)

Having constructed an Abelian gauge theory, we can generalize to the non-Abelian case. Instead of the Abelian phase in eq.(1.2) we may write,

$$\psi(x) \to e^{-ig\mathbf{T}_a\Lambda_a(x)}\psi(x) \tag{1.11}$$

where $\mathbf{T}_a$ are $p \times p$ matrices forming a Lie Algebra in the representation under which the fermions, $\psi(x)$, transform. (ψ is a p dimensional column vector). Again, we would like to construct a Lagrangian that remains invariant under local gauge transformations. Let us begin by generalizing the covariant derivative from the Abelian case, leading to,

$$D^\mu\psi(x) = (\partial^\mu + ig\mathbf{T}\cdot A^\mu)\psi(x) \tag{1.12}$$

where $\mathbf{T}\cdot A^\mu = \mathbf{T}_a A^\mu_a$. Now, consider an infinitesimal gauge transformation using eq.(1.11),

$$\psi(x) \to (\mathbf{I} - ig\mathbf{T}\cdot\Lambda)\psi(x) \tag{1.13}$$

which implies

$$\partial^\mu\psi(x) \to (\mathbf{I} - ig\mathbf{T}\cdot\Lambda)\partial^\mu\psi(x) - ig(\mathbf{T}\cdot\partial\Lambda)\psi(x). \tag{1.14}$$

As in the Abelian case, we require the covariant derivative, $D^\mu\psi(x)$, to transform in the same way as $\psi(x)$. If the gauge field, A^μ_a, transforms according to

$$A^\mu_a \to A^\mu_a + \partial^\mu\Lambda_\mu + gf_{abc}\Lambda_b A^\mu_c \tag{1.15}$$

where f_{abc} are the structure constants of the Lie Algebra ($[\mathbf{T}_a, \mathbf{T}_b] = if_{abc}\mathbf{T}_c$), the appropriate terms will cancel leaving us with the desired result.

It will be useful to consider finite gauge transformations as well. Defining $\mathbf{U}(x) = e^{-ig\mathbf{T}\cdot\Lambda(x)}$, we can rewrite eq.(1.11) as

$$\psi(x) \to \mathbf{U}(x)\psi(x). \tag{1.16}$$

If we multiply eq.(1.15) by $\mathbf{T}_a$ we find that,

$$\mathbf{A}^\mu \to \mathbf{A}^\mu + \mathbf{T}\cdot\partial^\mu\Lambda - ig[\mathbf{T}\cdot\Lambda, \mathbf{A}^\mu] \tag{1.17}$$

where $\mathbf{A}^\mu$ is a $p \times p$ matrix defined as $\mathbf{A}^\mu = A^\mu_a\mathbf{T}_a$ and it becomes clear that eq.(1.17)

corresponds to the linear (in $\Lambda_a(x)$) expansion of the gauge transformation,

$$\mathbf{A}^\mu(x) \to \mathbf{U}(x)(\mathbf{A}^\mu(x) + ig^{-1}\partial^\mu)\mathbf{U}^{-1}(x). \tag{1.18}$$

Finally, we can construct the gauge invariant field strength - the generalization of the last term in eq.(1.10). We require a two indexed Lorentz tensor that transforms covariantly. Of the objects we have at our disposal, and using the Abelian case as a guide, we can construct,

$$\mathbf{F}^{\mu\nu} = F_a^{\mu\nu}\mathbf{T}_a = -ig^{-1}[D^\mu, D^\nu]. \tag{1.19}$$

Clearly $\mathbf{F}^{\mu\nu}$ transforms covariantly since D^μ does. Expanding out the commutator we find

$$F_a^{\mu\nu} = \partial^\mu A_a^\nu - \partial^\nu A_a^\mu - g f_{abc} A_b^\mu A_c^\nu \tag{1.20}$$

and using eq.(1.18) we learn that $\mathbf{F}$ transforms as,

$$\mathbf{F}^{\mu\nu} \to \mathbf{U}(x)\mathbf{F}^{\mu\nu}(x)\mathbf{U}^{-1}(x). \tag{1.21}$$

We see that the term $F_a^{\mu\nu}F_{\mu\nu}^a$, called the Yang-Mills Lagrangian, also remains gauge invariant under a gauge transformation and allows us to write the full non-Abelian gauge invariant Lagrangian,

$$\mathcal{L} = \bar{\psi}(i\gamma^\mu D_\mu - m)\psi - \frac{1}{4}F_a^{\mu\nu}F_{\mu\nu}^a. \tag{1.22}$$

Notice that the gauge fields belong to the adjoint representation of the gauge group, whereas the fermions transform under some arbitrary representation determined empirically. In fact, the chiral components of the Dirac fields are permitted to fall under different representations of the gauge group - a fact of which nature seems keenly aware with the weak interactions.

In the preceding discussion, we approached the construction of gauge theories intuitively by examining the consequence of local phase transformations. We may also understand gauge theories more directly through modern differential geometry in the language fibre bundles [11]. Although we will not explore these aspects of differential geometry here, it is useful to examine the connection between gauge theories and geometry through the concept of parallel transport [11]. Consider a vector, $V^\mu(x)$, tangent to some curve on a manifold at a point p. The set of all tangent vectors at a point p on the manifold forms a vector space, called the tangent space. A distinct tangent space exists at each point and how a tangent vector changes as we move along some curve reveals intrinsic properties of the manifold. However, we cannot naively compare two different vectors at different points because they belong to separate tangent spaces. We

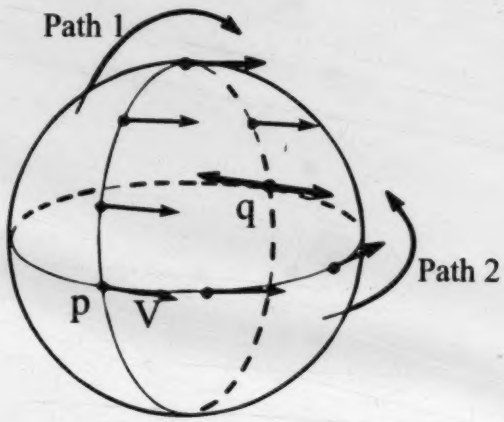

Figure 1.1: Parallel transporting a vector on the globe: Starting with vector V at point p, the two distinct paths lead to different vectors at q.

require a mechanism whereby we can transport a vector in one tangent space into the tangent space of the other without change and then make the comparison; i.e. a parallel transport. Let $V'^{\mu}(x+\Delta x)$ denote the vector $V^{\mu}(x)$ parallel transported to $x+\Delta x$. Let us insist that the vectors satisfy,

$$V'^{\mu}(x+\Delta x) - V^{\mu}(x) \propto \Delta x \tag{1.23}$$

and

$$(V'^{\mu} + W'^{\mu})(x+\Delta x) = V'^{\mu}(x+\Delta x) + W'^{\mu}(x+\Delta x). \tag{1.24}$$

We can satisfy these conditions if we take,

$$V'^{\mu}(x+\Delta x) = V^{\mu}(x) - V^{\lambda}(x)\Gamma^{\mu}_{\nu\lambda}(x)\Delta x^{\nu} \tag{1.25}$$

where the object $\Gamma^{\mu}_{\nu\lambda}$, called the connection coefficients, define the rules of the parallel transport. For our purposes, it can be shown that $\Gamma^{\mu}_{\nu\lambda}$ may be formed from combinations of derivatives of the metric tensor. Now we see how to make the appropriate comparison of two vectors at the same point,

$$\lim_{\Delta x^{\nu}\to 0} \frac{V^{\mu}(x+\Delta x) - V'^{\mu}(x+\Delta x)}{\Delta x^{\nu}} = \frac{\partial V^{\mu}}{\partial x^{\nu}} + V^{\lambda}\Gamma^{\mu}_{\nu\lambda} \tag{1.26}$$

or more succinctly,

$$DV^{\mu} = (\partial_{\nu} + V^{\lambda}\Gamma^{\mu}_{\nu\lambda})dx^{\nu}. \tag{1.27}$$

The part in parenthesis is the covariant derivative of the vector V^μ in curved space. Notice the similarity to the covariant derivative that we constructed using local phase transformations in the preceding discussion. This suggests that somehow the gauge field that we introduced earlier in order to obtain the correct transformation properties for our Lagrangian serves as a connection coefficient.

Using eq.(1.26) it can be shown [12] that if a vector V^μ is parallel transported along a curve, $c(t)$, then it satisfies

$$\frac{dV^\mu}{dt} + \Gamma^\mu_{\nu\lambda}\frac{dx^\nu(c(t))}{dt}V^\lambda = 0. \tag{1.28}$$

If we parallel transport over an infinitesimal distance, ϵ^μ, we see that eq.(1.28) implies,

$$V^\mu(x+\epsilon) = V^\mu(x) - V^\lambda(x)\Gamma^\mu_{\nu\lambda}(x)\epsilon^\nu. \tag{1.29}$$

In order to gain a deeper appreciation of parallel transport, consider figure 1.1. If we

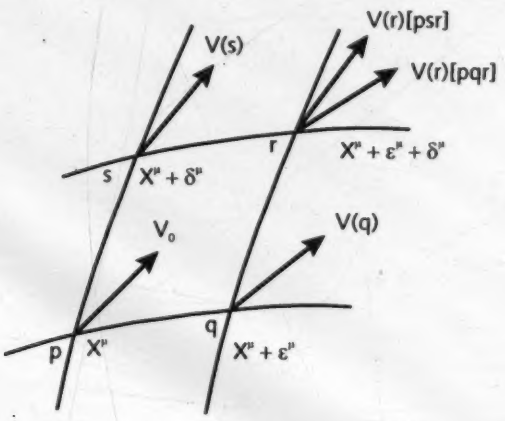

Figure 1.2: Parallel transporting vector V_0 around an infinitesimal parallelogram on a curved manifold along two distinct paths.

start with a vector at the point p and parallel transport to the point q along a longitude line, we see that the resulting vector is different from a transport along the equator to point q. The resulting vector depends on the parallel transport path - a situation unlike usual flat Euclidean space. Let us examine this feature of parallel transport more closely by considering transporting a vector from one corner of a closed, infinitesimal parallelogram to the opposite corner. Figure 1.2 shows a parallelogram $pqrs$ (with coordinates $\{x^\mu\}, \{x^\mu + \epsilon^\mu\}, \{x^\mu + \epsilon^\mu + \delta^\mu\}, \{x^\mu + \delta^\mu\}$) and an initial vector, V_0, parallel transported from p to r by two different paths. Consider the first path, pqr. Transporting from p to

q gives,

$$V^\mu(q) = V_0^\mu - V_0^\lambda \Gamma^\mu_{\nu\lambda}(p)\epsilon^\nu. \tag{1.30}$$

Transporting this new vector to r gives,

$$\begin{aligned} V^\mu(r) &= V^\mu(q) - V^\lambda(q)\Gamma^\mu_{\nu\lambda}(q)\delta^\nu \\ &= V_0^\mu - V^\lambda \Gamma^\mu_{\nu\lambda}(p)\epsilon^\nu - [V_0^\lambda - V_0^\mu \Gamma^\lambda_{\sigma\rho}(p)\epsilon^\sigma][\Gamma^\mu_{\nu\lambda}(p) + \partial_\tau \Gamma^\mu_{\nu\lambda}(p)\epsilon^\tau]\delta^\nu \\ &\approx V_0^\mu - V_0^\lambda \Gamma^\mu_{\nu\lambda}(p)\epsilon^\nu - V_0^\lambda \Gamma^\mu_{\nu\lambda}(p)\delta^\nu \\ &\quad - V_0^\lambda \left[\partial_\tau \Gamma^\mu_{\nu\lambda}(p) - \Gamma^\rho_{\tau\lambda}(p)\Gamma^\mu_{\nu\rho}(p)\right]\epsilon^\tau \delta^\nu \end{aligned} \tag{1.31}$$

where up to order $\epsilon\delta$ terms have been kept. Transporting along the other path, psr, we find,

$$V^\mu(r) \approx V_0^\mu - V_0^\lambda \Gamma^\mu_{\nu\lambda}(p)\delta^\nu - V_0^\lambda \Gamma^\mu_{\nu\lambda}(p)\epsilon^\nu - V_0^\lambda [\partial_\nu \Gamma^\mu_{\tau\lambda}(p) - \Gamma^\rho_{\nu\lambda}(p)\Gamma^\mu_{\tau\rho}(p)]\epsilon^\tau \delta^\nu \tag{1.32}$$

The two vectors of eq.(1.31) and eq.(1.32) differ at the final point r by,

$$\Delta V^\mu = V_0^\lambda [\partial_\tau \Gamma^\mu_{\nu\lambda}(p) - \partial_\nu \Gamma^\mu_{\tau\lambda}(p) - \Gamma^\rho_{\tau\lambda(p)}\Gamma^\mu_{\nu\rho}(p) + \Gamma^\rho_{\nu\lambda}(p)\Gamma^\mu_{\tau\rho}(p)]\epsilon^\tau \delta^\nu \tag{1.33}$$

$$= V_0^\lambda R^\mu_{\lambda\tau\nu}\epsilon^\tau \delta^\nu. \tag{1.34}$$

The Riemann tensor, $R^\mu_{\lambda\tau\nu}$, indicates intrinsic curvature of the manifold. Again, notice the similarity to the earlier discussion of non-Abelian gauge invariance. The Riemann curvature tensor has the same structure as $\mathbf{F}^{\mu\nu}$. The similarities between the gauge field theory discussion and parallel transport point toward a deep connection between geometry and nature. In fact, we can show that $\mathbf{F}^{\mu\nu}$ serves as the "Riemann tensor" for the internal "gauge-charge" space. Recall the covariant derivative of eq.(1.12). The covariant derivative indicates that an infinitesimal coordinate transformation generates the change,

$$\delta\psi(x) = igA_\mu \psi dx^\mu \tag{1.35}$$

since,

$$\psi(x + dx) = (1 + igA_\mu dx^\mu)\psi(x) \tag{1.36}$$

where $A_\mu = \mathbf{T}^a A^a_\mu$. For parallel transport over a finite interval we can write the transformation as an exponential,

$$P(x', x) = \exp\left(ig \int_x^{x'} A_\mu(y)\, dy^\mu\right) \tag{1.37}$$

where x' and x define the endpoints of some path. Transporting ψ around a parallelogram

with sides ϵ and δ with one corner at x^μ, the parallel transportation matrix becomes,

$$\begin{aligned}\mathcal{P} &= P(x, x+dx)P(x+dx, x+dx+\delta x)P(x+dx+\delta x, x+\delta x)P(x+\delta x, x) \\ &= P_1 P_2 P_3 P_4 \end{aligned} \tag{1.38}$$

We see that,

$$\begin{aligned} P_1 P_2 &= \exp[igA_\mu(x)dx^\mu]\exp[igA_\nu(x+dx)\delta x^\nu] \\ &= \exp\left[ig(A_\mu dx^\mu + A_\nu \delta x^\nu + \partial_\mu A_\nu dx^\mu \delta^\nu x) - \frac{g^2}{2}[A_\mu, A_\nu]dx^\mu \delta x^\nu\right] \end{aligned} \tag{1.39}$$

where the Baker-Campbell-Hausdorff theorem,

$$\exp(\lambda A)\exp(\lambda B) = \exp\left(\lambda(A+B) + \frac{\lambda^2}{2}[A,B]\right) + O(\lambda^3) \tag{1.40}$$

has been used. Similarly, applying the Baker-Campbell-Hausdorff theorem on P_3P_4 and then to the final result, we find,

$$\mathcal{P} = \exp[ig(\partial_\mu A_\nu - \partial_\nu A_\mu - ig[A_\mu, A_\nu])dx^\mu \delta x^\nu] \tag{1.41}$$

$$= \exp[igF^{\mu\nu}dx^\mu \delta x^\nu] \tag{1.42}$$

Indeed, $F^{\mu\nu}$ plays the role of the Riemann curvature tensor for the internal gauge-charge space and A_μ behaves as the connection coefficients. This signals that gauge fields have a physical effect and cannot be simply transformed away by some gauge choice.

1.2 A Brief Overview of Path Integral Quantization of Gauge Theories

In the preceding section, we used gauge invariance to understand the interactions of massless spin 1 fields. While gauge theories have given us deep insight into the nature of these interactions, the description thus far has been purely classical. In order to use gauge theories as a candidate for the strong, the weak, and the electromagnetic forces, the uncertainty principle of quantum mechanics must be incorporated - i.e. gauge theories must be quantized. Not all the degrees of freedom in gauge theories are physical. Consider the case of electromagnetism. The photon has two physical degrees of freedom yet the photon appears in the Abelian gauge theory as A_μ which has four degrees of freedom. This does not lead to a contradiction since the gauge field is restricted by some gauge choice, resulting in the physical two degrees of freedom. Thus, gauge theories

are systems of constrained dynamical variables and this makes their quantization a non-trivial matter. To see the problems that arise, consider the generating functional,

$$W[J] = \int \mathcal{D}A_\mu \, \exp\left(i \int d^4x \, [\mathcal{L}_{YM} + J^\mu_a A^a_\mu]\right) \tag{1.43}$$

where $\mathcal{L}_{YM} = -\frac{1}{4} F^{\mu\nu}_a F^a_{\mu\nu}$ and J^a_μ is an external source current. The free field part of the action in eq.(1.43) is,

$$\begin{aligned} \int d^4x \, \mathcal{L}_{\text{free}} &= -\frac{1}{4} \int d^4x \, (\partial_\mu A^a_\nu - \partial_\nu A_{a\mu}) (\partial^\mu A^\nu_a - \partial^\nu A^\mu_a) \\ &= \frac{1}{2} \int d^4x \, A^a_\mu(x) \left(g^{\mu\nu}\partial^2 - \partial^\mu\partial^\nu\right) A_{a\nu} \end{aligned} \tag{1.44}$$

Written in this form, the usual approach of path integral quantization of eq.(1.43) involves evaluating a series of Gaussian intergals using the inverse of the operator $D^{\mu\nu} = \left(g^{\mu\nu}\partial^2 - \partial^\mu\partial^\nu\right)$. However, this approach fails because $D^{\mu\nu}$ has no inverse. To see this, suppose that $D^{\mu\nu}$ had an inverse, such that

$$D_{\mu\nu} G^{\nu\lambda}(x - y) = \delta^\lambda_\mu \delta^4(x - y). \tag{1.45}$$

Fourier transforming this expression we have,

$$(-k^2 g_{\mu\nu} + k_\mu k_\nu) G^{\nu\lambda}(k) = \delta^\lambda_\mu \tag{1.46}$$

with the invariant decomposition of the inverse

$$G^{\nu\lambda} = a(k^2) g^{\nu\lambda} + b(k^2) k^\nu k^\lambda \tag{1.47}$$

for some $a(k^2)$ and $b(k^2)$. Inserting the decomposition into eq(1.46) leads us to a contradiction; i.e. $D^{\mu\nu}$ has no inverse and thus the path integral becomes ill defined. Gauge invariance creates this problem. The path integral sums over all possible field configurations including paths connected by gauge field transformations. Since the gauge connected paths are not distinct, an over counting occurs rendering the path integral singular. In essence, we need to isolate the volume factor in group space that leads to the over counting. Integrating over the gauge group elements while making a particular gauge class choice solves this problem [6, 13, 14, 15]. First, observe that the unitary gauge transformation $U(\Lambda(x)) = \exp(-igT_a\Lambda_a(x))$ implies,

$$U(\Lambda)U(\Lambda') = U(\Lambda\Lambda') \tag{1.48}$$

and restricting to an infinitesimal region in the neighbourhood of the identity we have,

$$U(\Lambda) = 1 + igT_a\Lambda_a + O(g^2). \tag{1.49}$$

We can define an integral of some functional of Λ over the gauge group elements as,

$$\int \mathcal{D}\Lambda\, f[\Lambda] \tag{1.50}$$

where,

$$\mathcal{D}\Lambda = \prod_a \mathcal{D}\Lambda_a. \tag{1.51}$$

Observe that eq.(1.48) implies,

$$\mathcal{D}(\Lambda) = \mathcal{D}(\Lambda\Lambda'). \tag{1.52}$$

As discussed earlier, we must restrict the path integral over the Yang-Mills action by fixing the gauge to eliminate the over counting. A useful gauge choice consists of the generalized Lorentz gauge class,

$$F_a(A^\mu_b) = \partial_\mu A^\mu_a - f_a(x) = 0 \tag{1.53}$$

for some set of functions $f_a(x)$. We can now isolate the gauge group volume factor by writing the gauge invariant functional,

$$\Delta[A_{a\mu}] = \int \mathcal{D}\Lambda\, \delta[F_a(A^\Lambda_{a\mu})]. \tag{1.54}$$

where the delta function fixes the gauge. Inserting the identity, $\Delta^{-1}[A_{a\mu}]\Delta[A_{a\mu}]$, into eq.(1.43), we have,

$$\int \mathcal{D}A^\mu\, e^{iS_{\rm YM}[A_{a\mu}]} = \int \mathcal{D}\, A^\mu \Delta^{-1}[A_{a\mu}] \int \mathcal{D}\Lambda\, \delta[F_a(A^\Lambda_{b\mu})] e^{iS_{\rm YM}[A^\Lambda_{a\mu}]} \tag{1.55}$$

where the gauge invariance of $\Delta^{-1}[A_{a\mu}]$ has been used. Re-writing the gauge group measure as,

$$\int \mathcal{D}\Lambda = \int \prod_a \mathcal{D}\Lambda_a = \int \prod_a \mathcal{D}F_a \det\left(\frac{\delta\Lambda_b(x)}{\delta F_a(x')}\right) \tag{1.56}$$

we find,

$$\Delta^{-1}[A_{a\mu}] = \det\left(\frac{\delta F_a(x')}{\delta\Lambda_b(x)}\right)\Big|_{F_a=0}. \tag{1.57}$$

The generating functional has become

$$W[J_a^\mu] = \int \mathcal{D}A_\mu \det\left(\frac{\delta F_a(x')}{\delta \Lambda_b(x)}\right) \delta[F_a] \exp\left(i \int d^4x \, [\mathcal{L}_{YM} + J_a^\mu A_\mu^a]\right) \tag{1.58}$$

and the over counting has been eliminated. If we multiply the the generating functional of eq.(1.58) by,

$$\int \prod_c \mathcal{D}f_c \, \exp\left(-\frac{i}{2\xi} \int d^4x \, f_c^2(x)\right) \tag{1.59}$$

the delta function will disappear, leaving the expression,

$$W[J_a^\mu] = \int \mathcal{D}A_\mu \det\left(\frac{\delta F_a(x')}{\delta \Lambda_b(x)}\right) \exp\left(i \int d^4x \, \left[\mathcal{L}_{YM} + J_a^\mu A_\mu^a - \frac{1}{2\xi}(\partial_\mu A_a^\mu)^2\right]\right). \tag{1.60}$$

Furthermore, the determinant may be re-expressed as an integral over complex Grassmann variables [4],

$$\begin{aligned} \det\left(\frac{\delta F_a(x')}{\delta \Lambda_b(x)}\right) &\propto \int \mathcal{D}\eta^* \mathcal{D}\eta \, \exp\left(-i \int d^4x \int d^4x' \, \eta_a^*(x') \frac{\delta F_a(x')}{\delta \Lambda_b(x)} \eta_b(x)\right) \\ &= \int \mathcal{D}\eta^* \mathcal{D}\eta \, \exp\left(i \int d^4x \, \partial_\mu \eta_a^* (\partial^\mu \eta_a + g f_{abc} \eta_b A_c^\mu)\right) \end{aligned} \tag{1.61}$$

where eq.(1.15) and eq.(1.53) have been used to carry out the functional differentiation. Finally the generating functional reads,

$$W[J_a^\mu] = \int \mathcal{D}A_\mu \, \mathcal{D}\eta^* \mathcal{D}\eta \exp\left(i \int d^4x \, \left[\mathcal{L}_{YM} + J_a^\mu A_\mu^a - \frac{1}{2\xi}(\partial_\mu A_a^\mu)^2 + \mathcal{L}_{\rm FP}\right]\right) \tag{1.62}$$

where

$$\mathcal{L}_{\rm FP} = \partial_\mu \eta_a^* (\partial^\mu \eta_a + g f_{abc} \eta_b A_c^\mu), \tag{1.63}$$

called the Faddeev-Popov ghost Lagrangian [15], contains ghost fields η and η^* that facilitate a perturbative evaluation of the path integral. Note that the ghost fields are not real particles - they behave as scalar fields with Fermi-Dirac statistics. The ghost fields provide a calculational technique that removes the over counting problem through gauge fixing.

The Faddeev-Popov gauge fixed Lagrangian enables us to write down a sensible path integral that avoids the over counting of the gauge degrees of freedom. The price we pay for handling the gauge group volume factor is the abandonment of a manifestly gauge invariant action. However, the quantum theory is still aware of the underlying gauge invariance and it appears through various relations among Green's functions, called Ward identities [16, 17], or, more generally Slavnov-Taylor identities [18, 19]. These identities

are crucial in proving the renormalizability of the full quantum gauge theory. To sketch the program, consider the full effective quantum Lagrangian,

$$\mathcal{L}_{\text{eff}} = \mathcal{L}_{\text{YM}} - \frac{1}{2\xi}(\partial_\mu A_a^\mu)^2 + \mathcal{L}_{\text{FP}} \tag{1.64}$$

where from eq.(1.63)

$$\mathcal{L}_{\text{FP}} \simeq (\partial_\mu \eta_a^*)(D_{ab}^\mu \eta_b). \tag{1.65}$$

It can be shown that the effective action,

$$S_{\text{eff}} = \int d^4x \, \mathcal{L}_{\text{eff}}, \tag{1.66}$$

remains invariant under a special type of gauge transformation, called BRST transformations [20],

$$\delta A_a^\mu = \theta D_{ab}^\mu \eta_b \tag{1.67}$$

$$\delta \psi = -ig\theta T_a \eta_a \psi \tag{1.68}$$

$$\delta \eta_a^* = -\xi^{-1}\theta(\partial_\mu A_a^\mu) \tag{1.69}$$

$$\delta \eta_a = -\frac{1}{2} g\theta f_{abc}\eta_b \eta_c \tag{1.70}$$

where θ is a spacetime independent real Grassmann parameter. The BRST transformations of eq.(1.67) can be thought of as a usual gauge transformation with gauge parameter $\Lambda_a = \theta\eta_a$. Applying the BRST transformations to the generating functional, $W[\Sigma]$ (where Σ denotes all of the external currents for the fields in $\mathcal{L}_{\text{eff}}$) yields the necessary generalized Ward identities which define relationships amongst Green's functions in accordance with the underlying gauge invariance of the theory.

1.3 A Survey of Renormalization

Using the results of the previous section, we can write the full quantum Lagrangian for a gauge theory with fermions,

$$\mathcal{L} = \bar{\psi}(i\gamma^\mu D_\mu - m)\psi - \frac{1}{4}F_a^{\mu\nu}F_{\mu\nu}^a - \frac{1}{2\xi}(\partial_\mu A_a^\mu)^2 + \partial_\mu \eta^*(\partial^\mu \eta_a + g f_{abc}\eta_b A_c^\mu). \tag{1.71}$$

Calculating with this Lagrangian results in primitively divergent Feynman graphs indicating that the theory must be renormalized. One method of handling the divergences involves dimensional regularization [9] - a method of analytically continuing in dimension in order to isolate pole terms in the Laurent series expansion of one-particle-irreducible

graphs. The initial Lagrangian, eq.(1.71), called the bare Lagrangian, contains unphysical quantities and may be symbolically written as,

$$\mathcal{L}_{\rm B} = \mathcal{L} + \Delta\mathcal{L}. \tag{1.72}$$

The object $\Delta\mathcal{L}$ contains counter terms that cancel against the pole parts of the Laurent series expansion, which amounts to redefinitions of fields and coupling constants, after employing a renormalization prescription that sets boundary conditions on the primitively divergent one-particle-irreducible graphs. The counter terms can be evaluated perturbatively in $(4-\epsilon)$ dimensions through Feynman diagrams. If the field theory is renormalizable, the counter term Lagrangian will have the same structure as the original Lagrangian - new interactions will not be required in order to cancel the pole parts of some divergent graph [21]. Furthermore a renormalizable theory will contain operators of mass dimension four or less as in eq.(1.71). In addition, there exist a number of relationships among the counter terms provided by the generalized Ward identities. These relationships are necessary for consistency. Continuing in dimension introduces a mass scale, M, through the coupling constant, $g \to gM^{\epsilon/2}$, which keeps the action dimensionless and results in a relationship between bare and renormalized Green's functions [4],

$$\tilde{\Gamma}^n(p_1,...,p_n;g(M),\xi,m(M),M) = Z_A^{n_A/2} Z_\psi^{n_\psi/2} \tilde{\Gamma}^n_B(p_1,...,p_n;g_B,\xi_B,m_B). \tag{1.73}$$

The object $\tilde{\Gamma}^n$ denotes a one-particle-irreducible Green's function with n external legs of which n_a are gauge fields and n_ψ are fermions and the subscript B denotes the unphysical bare quantities. The coefficients Z_A and Z_ψ are wavefunction renormalization factors derived perturbatively from the counter term Lagrangian. Since $\tilde{\Gamma}^n_B$ on the right-hand side of eq.(1.73) does not depend on M, we may write,

$$\begin{aligned} &M\frac{\partial\tilde{\Gamma}^n}{\partial M} + M\frac{\partial g(M)}{\partial M}\frac{\partial\tilde{\Gamma}^n}{\partial g(M)} + M\frac{\partial\xi}{\partial M}\frac{\partial\tilde{\Gamma}^n}{\partial\xi} + M\frac{\partial m}{\partial M}\frac{\partial\tilde{\Gamma}^n}{\partial m} \\ &= \frac{n_A}{2} Z_\psi^{n_\psi/2} Z_A^{n_A/2} Z_A^{-1} M\frac{\partial Z_A}{\partial M}\tilde{\Gamma}^n_B + \frac{n_\psi}{2} Z_\psi^{n_\psi/2} Z_A^{n_A/2} Z_\psi^{-1} M\frac{\partial Z_\psi}{\partial M}\tilde{\Gamma}^n_B, \end{aligned} \tag{1.74}$$

leading to the compact renormalization group equation,

$$\begin{aligned} &\left(M\frac{\partial}{\partial M} + \beta_g\frac{\partial}{\partial g} + \beta_\xi\frac{\partial}{\partial\xi} - \gamma_m m\frac{\partial}{\partial m} - n_A\gamma_A - n_\psi\gamma_\psi\right) \\ &\qquad \times\tilde{\Gamma}^n(p_1,...,p_n;g(M),\xi,m(M),M) = 0 \end{aligned} \tag{1.75}$$

where

$$\beta_g = M\frac{\partial g}{\partial M} \tag{1.76}$$

$$\beta_\xi = M\frac{\partial \xi}{\partial m} \tag{1.77}$$

$$\gamma_m = -\frac{M}{m}\frac{\partial m}{\partial M} \tag{1.78}$$

$$\gamma_A = Z_A^{-1/2} M\frac{\partial Z_A^{1/2}}{\partial M} \tag{1.79}$$

$$\gamma_\psi = Z_\psi^{-1/2} M\frac{\partial Z_\psi^{1/2}}{\partial M}. \tag{1.80}$$

Evaluating the coefficients of eq.(1.76) - eq.(1.80) perturbatively through dimensional regularization, we obtain at the one-loop level

$$\beta_g = -bg \tag{1.81}$$

$$\beta_\xi = \left[\left(\frac{13}{6} - \frac{\xi^2}{2}\right) C_1 - \frac{4}{3}\sum_R C_2^R\right]\frac{g^2\xi}{8\pi^2} \tag{1.82}$$

$$\gamma_m = \frac{3C_3^R g^2}{8\pi^2} \tag{1.83}$$

$$\gamma_A = -\left[\left(\frac{13}{6} - \frac{\xi}{2}\right) C_1 - \frac{4}{3}\sum_R C_2^R\right]\frac{g^2}{16\pi^2} \tag{1.84}$$

$$\gamma_\psi = \frac{\xi C_3^R g^2}{16\pi^2} \tag{1.85}$$

where R denote the particular representation of Lie Algebra to which the fermions belong and

$$b = \frac{1}{16\pi^2}\left(\frac{11}{3}C_1 - \frac{4}{3}\sum_R C_2^R\right). \tag{1.86}$$

The group theory factors C_1, C_2, C_3 are defined by,

$$C_1\delta_{ab} = f_{acd}f_{bcd} \tag{1.87}$$

$$C_2\delta_{ab} = \mathrm{Tr}(T_a T_b) \tag{1.88}$$

$$C_3 = \frac{d_G}{d_F}C_2 \tag{1.89}$$

where d_G and d_F are the dimensions of the adjoint representation and the representation of the fermions respectively. The Green's function $\tilde{\Gamma}^n$ is a homogenous function in $p_1, ...p_n; m, M$ of the degree of its mass dimension, $d_{\tilde{\Gamma}} = (4-\epsilon) + (n_A + n_\psi)(\epsilon - 2)/2$. If

we rescale all external leg momentum as, $p_i \to sp_i$, where s is dimensionless we have,

$$\left(s\frac{\partial}{\partial s} + m\frac{\partial}{\partial m} + M\frac{\partial}{\partial M}\right)\tilde{\Gamma}^n(sp_1, ..., sp_n; g(M), \xi, m, M) \tag{1.90}$$

$$= d_{\tilde{\Gamma}}\tilde{\Gamma}^n(sp_1, ..., sp_n; g(M), \xi, m, M). \tag{1.91}$$

The differential operator $M\partial/\partial M$ of eq.(1.75) can be eliminated with the use of eq.(1.90),

$$\left(-s\frac{\partial}{\partial s} + \beta_g\frac{\partial}{\partial g}\beta_\xi\frac{\partial}{\partial \xi} - (1+\gamma_m)m\frac{\partial}{\partial m} - n_A\gamma_A - n_\psi\gamma_\psi + d_{\tilde{\Gamma}}\right) \tag{1.92}$$

$$\times\tilde{\Gamma}^n(sp_1, ..., sp_n; g, \xi, m, M) = 0 \tag{1.93}$$

where the β-functions are now regarded as functions of s,

$$\begin{aligned} s\frac{\partial\bar{g}(s)}{\partial s} &= \beta_g(\bar{g}(s)) \quad ; \quad \bar{g}(1) = g(M) \\ s\frac{\partial\bar{\xi}(s)}{\partial s} &= \beta_\xi(\bar{g}(s)) \quad ; \quad \bar{\xi}(1) = \xi(M) \\ s\frac{\partial\bar{m}(s)}{\partial s} &= \beta_m(\bar{m}(s)) \quad ; \quad \bar{m}(1) = m(M). \end{aligned} \tag{1.94}$$

Solving eq.(1.92) with the relations of eqs.(1.94) using method of characteristic curves leads to,

$$\begin{aligned} \tilde{\Gamma}^n(sp_1, ..., sp_n; g, \xi.m, M) &= s^{d_{\tilde{\Gamma}}}\exp\left(-\int_1^s\frac{ds'}{s}\left[n_A\gamma_A(\bar{g}(s'), \bar{\xi}(s')) + n_A\gamma_\psi(\bar{g}(s'), \bar{\xi}(s'))\right]\right) \\ &\quad \times\tilde{\Gamma}^n(p_1, ..., p_n; \bar{g}(s), \bar{\xi}(s), \bar{m}(s), M) \end{aligned} \tag{1.95}$$

Notice that the system scales unexpectedly. Not only does the coupling constant, g, mass parameter, m, and gauge parameter, ξ, scale with energy but their scaling is relayed to the Green's function itself through the anomalous dimension factors, γ_A and γ_ψ, causing the Green's function to scale non-trivially. The physical effects of renormalization are now apparent. Finite contributions of loop diagrams contribute measurable shifts to tree level quantities and from anomalous scaling of the Green's functions are reflected in the energy dependence of various processes. Furthermore, the preceding analysis extends to composite operators [4, 3] where we may write an inserted Green's function with n_A external gauge field legs, n_ψ external fermion legs and one external leg at zero momentum denoting the composite operator itself, O_i. In general, there may exist many operators of the same type that will mix during the renormalization process and thus O_i becomes one of a set of operators. Analogous to eq.(1.73) we have,

$$\tilde{\Gamma}^n_{O_i}(p_1, ..., p_n; g, \xi, m, M) = Z_{ij}Z_A^{n_A/2}Z_\psi^{n_\psi/2}\tilde{\Gamma}_{O_jB}(p_1, ..., p_n; g_B, \xi_B, m_B) \tag{1.96}$$

where Z_{ij} is the renormalization matrix calculated from Feynman diagrams that mixes the composite operators. Proceeding as before, the renormalization group equation for the inserted Green's function becomes,

$$\left[\delta_{ij}\left(M\frac{\partial}{\partial M}+\beta_g\frac{\partial}{\partial g}+\beta_\xi\frac{\partial}{\partial \xi}-\gamma_m m\frac{\partial}{\partial m}-n_A\gamma_A-n_\psi\gamma_\psi\right)-\gamma_{ij}\right] \times\tilde{\Gamma}^n_{O_j}(p_1,...,p_n;g,\xi,m,M)=0 \tag{1.97}$$

where

$$\gamma_{ij}=M\frac{\partial Z_{ik}}{\partial M}Z^{-1}_{kj}. \tag{1.98}$$

While the techniques of renormalized perturbation theory are successful in dealing mathematically with the divergent behaviour of quantum field theories, the origin of the divergences themselves seems devoid of a physical context. Let us explore these issues more closely. In reality, all field theories must come with an ultra-violet cutoff [22, 3], above which the field theory breaks down as a complete description of nature. In the previous analysis, we assumed that the loop integral momenta in Feynman diagrams could be infinite - the source of the divergences - yet this must be artifical since the theory must break down near the cutoff scale. Let us approach the problem from a more physical perspective, called the Wilsonian approach to renormalization [22], and restrict the generating functional by some hard ultra-violet cutoff, Λ. (This should not be confused with Pauli-Villars regularization where a hard momentum cutoff is introduced to facilitate loop integration only to take the $\Lambda\to\infty$ limit as soon as possible). That is, we will prevent the fields in the path integral from depending on momentum above this scale. Consider a generating functional containing only renormalizable terms and assume that all the couplings are sufficiently weak ,

$$W=\int[\mathcal{D}\phi]_\Lambda\ \exp\left(i\int d^4x\ \mathcal{L}(\phi)\right) \tag{1.99}$$

where ϕ represents all the fields that $\mathcal{L}$ depends on and Λ denotes the ultra-violet momentum cutoff. Instead of immediately writing down a number of Feynman diagrams for one-particle-irreducible graphs, where the divergent behaviour suddenly appears at one loop, suppose we split the path integral into a tower of small momentum slices up to Λ and path integrate out each successive slice in turn. In effect we will remove high momentum fluctuations from the theory systematically. Heuristically, the first iteration, consisting of a momentum slice $b\Lambda<|k|<\Lambda$ where $b\ll 1$, would appear as,

$$W=\int[\mathcal{D}\phi_{|k|<b\Lambda}]\int[\mathcal{D}\phi_{b\Lambda<|k|<\Lambda}]\exp\left(i\int d^4x\ \mathcal{L}(\phi_{|k|<b\Lambda}+\phi_{b\Lambda<|k|<\Lambda})\right) \tag{1.100}$$

which becomes

$$W = \int [\mathcal{D}\phi_{|k|<b\Lambda}] \exp\left(i \int d^4x \, \mathcal{L}(\phi_{|k|<b\Lambda}) + \text{correction terms}\right). \tag{1.101}$$

The correction terms contain shifts to tree level constants in the original theory, in agreement with renormalized perturbation theory, and the terms also contain an infinite series of all higher dimensional operators that are not renormalizable. Continuing slicing in this manner down to the scale of interest, the momentum slice integrations continuously transform the Lagrangian in a process called the renormalization group. It may seem odd that even though we started with a renormalizable Lagrangian, we generated all possible nonrenormalizable interactions, yet this is the heart of the physical meaning of renormalization itself. To understand this, consider how terms of various mass dimension change as we proceed to integrate out more and more momentum slices. A term with mass dimension d_i has a coefficient with mass dimension $4 - d_i$, in order to keep the action dimensionless. For any operator, the mass in the coefficient will naturally be of the order of cutoff scale Λ. Thus operators with $d_i < d$ become increasingly important as we integrate out momentum slices while operators with $d_i > d$ becomes less important. Operators of these types are referred to as relevant and irrelevant respectively [3, 22, 23]. Operators with $d_i = 4$, called marginal operators, require the effects of the higher order corrections to determine how the operator will evolve. We can now understand the physical origin of the divergences resulting from the original method - they were never truly part of the theory. We simply calculated with the "wrong" Lagrangian. In reality, whatever the form of the true Lagrangian at the cutoff scale, we will always be left with the relevant and some of the marginal operators at the low scale. The Standard Model is based on renormalizable interactions not because of some lucky circumstance, but because all of the irrelevant operators beyond the Standard Model decoupled near the cutoff of the theory; a scale presumably much higher than the scale of Standard Model interactions themselves.

In the preceding discussion, we tacitly assumed that the theory was governed by a free field fixed point (the requirement that the couplings were sufficiently weak). At the free field fixed point all the interactions vanish - all the tree level couplings and masses vanish - and the Lagrangian remains unchanged under the renormalization group flow. In general, places in coupling space where the theory remains unchanged under the momentum slice integrations are referred to as fixed points [3]. There may exist other fixed points in coupling space, including points that are strongly coupled such that higher order corrections become large and radically change the direction of the renormalization group flow. These effects may push the theory toward other non-free field fixed points. If these other fixed points are places where the theory becomes strongly coupled, the theory would

no longer have a perturbative description in terms of a Feynman diagram analysis. For reasons that are not currently understood, all field theories that are physically relevant are close to a free field theory fixed point in the ultraviolet or by a fixed point that reduces to the free fixed point in a certain limit.

1.4 Spontaneous Symmetry Breaking

Thus far, we have considered the properties of gauge theories with massless vector bosons. While we are free to write mass terms for scalar fields and fermions (provided that both chiralities transform under the same representation of the gauge group), gauge invariance forbids us from writing a mass term for the gauge fields. The term $A^\mu A_\mu$ is not a gauge invariant field bilinear. Although completely consistent for QED and QCD, where the photon and gluons are massless, it is an empirical fact that the vector bosons responsible for the weak force are massive and violate chirality - implying that the chiral parts of each fermion belong to a different representation of the gauge group. Furthermore, even if we decided to give up on a completely gauge invariant theory by adding a gauge field mass term by hand, we will find that the resulting physical longitudinal mode will in general render the theory unrenormalizable. These issues present us with a serious challenge if we wish to interpret the weak force as a gauge theory interacting with massive fermions.

Spontaneous symmetry breaking [24, 25, 26, 27] provides the solution to this problem by hiding the overall gauge symmetry and generating a mass term for the gauge bosons while preserving the renormalizablity of the theory. To understand how this works, consider a global, in general, non-Abelian symmetry group, G and some real scalar fields that belong to some representation,

$$\phi(x) = \begin{pmatrix} \phi_1(x) \\ \phi_2(x) \\ . \\ . \\ . \end{pmatrix} \tag{1.102}$$

Under an infinitesimal global transformation, we have,

$$\phi \rightarrow \phi - gT^a\Lambda^a\phi(x) \tag{1.103}$$

where $a = 1, ..., N$. Now, if the Lagrangian,

$$\mathcal{L}(\partial^\mu\phi, \phi) = \frac{1}{2}(\partial^\mu\phi)^T(\partial_\mu\phi) - V(\phi), \tag{1.104}$$

with some potential $V(\phi)$, remains invariant under eq.(1.103), then by Noether's theorem the current,

$$j^a_\mu = \pi^T_\mu(x) i T^a \phi(x) \tag{1.105}$$

with

$$\pi_\mu = \frac{\partial \mathcal{L}}{\partial(\partial^\mu \phi)} \tag{1.106}$$

must be conserved. The Euler-Largrange equations together with current conservation implies

$$\left(\frac{\partial \mathcal{L}}{\partial \phi}\right)^T i T^a \phi + \pi^T_\mu i T^a \partial^\mu \phi = 0. \tag{1.107}$$

Using the Lagrangian for the scalar fields and eq.(1.107), we obtain,

$$\left(\frac{\partial V}{\partial \phi}\right)^T T^a \phi = 0 \tag{1.108}$$

and this relation expresses the symmetry of the theory. Let us now suppose that $V(\phi)$ has a minimum at some $\phi \neq 0$ such that,

$$\langle 0|\phi|0\rangle = v \tag{1.109}$$

$$\left.\frac{\partial V}{\partial \phi}\right|_{\langle 0|\phi|0\rangle = v} = 0 \tag{1.110}$$

where $\langle 0|\phi|0\rangle$ denotes the ground state vacuum expectation value of the field operator. In general, the ground state defined by the vacuum expectation value will not remain invariant under the global symmetry transformation,

$$(1 - ig\Lambda^a T^a)v \neq v \tag{1.111}$$

implying that,

$$iT^a v \neq 0 \tag{1.112}$$

for some set of a. Shifting the scalar fields, $\tilde{\phi} = \phi - v$ so that,

$$\langle 0|\tilde{\phi}|0\rangle = 0 \tag{1.113}$$

the Lagrangian of eq.(1.104) becomes,

$$\mathcal{L} = \frac{1}{2}\left((\partial^\mu \tilde{\phi}_i)(\partial_\mu \tilde{\phi}_i) - \tilde{\phi}_i \tilde{\phi}_j \left.\frac{\partial^2 V}{\partial \phi_i \partial \phi_j}\right|_{\phi = v}\right) - V(v) + O(\tilde{\phi}^3). \tag{1.114}$$

We find that a mass matrix for the scalar fields appear,

$$M_{ij}^2 = \left.\frac{\partial^2 V}{\partial\phi_i \partial\phi_j}\right|_{\phi=v} \tag{1.115}$$

and that by differentiating eq.(1.108) we find that,

$$M_{ij}^2 iT^a v = 0 \tag{1.116}$$

for all a. However, in light of eq.(1.112), there must be at least one eigenvector with a zero eigenvalue, that is, there must be at least one massless linear combination. This is an important observation. If a theory has a ground state that is not invariant under the full symmetry group, a massless mode, referred to as a Goldston boson [28], will appear for each broken symmetry generator. More concretely, suppose that the ground state remains invariant under a subset of the generators of some group G, which generate some maximal subgroup H. In that case, we have,

$$T^a v = 0 \qquad (a = 1, ...M) \tag{1.117}$$

and

$$T^a v \neq 0 \qquad (a = M+1, ...N) \tag{1.118}$$

where the first M generators define H. This leaves us with $N - M$ massless modes which corresponding to $N - M$ Goldstone bosons. The vacuum expectation value has spontaneously broken the full global symmetry.

Promoting the global symmetry group, G, to a local gauge symmetry, we can use spontaneous symmetry breaking to provide mass terms for the gauge fields in a process called the Higgs mechanism [26, 27]. Again, if a scalar field (or fields) acquires a non-zero vacuum expectation value which minimizes the potential and leaves the ground state non-invariant, there will appear a massless Goldstone mode associated with each broken generator. However, in the local symmetry case, these Goldstone modes are not manifest - they are "eaten" by the gauge fields, and in so doing, supply a mass term along with a longitudinal degree of freedom for the gauge fields. Let us first explore how this mechanism works with an Abelian gauge symmetry. Consider the Lagrangian of scalar-electrodynamics,

$$\mathcal{L} = (D^\mu\phi)(D_\mu\phi^*) - \mu^2\phi\phi^* - \frac{1}{4}(\phi\phi^*)^2 - \frac{1}{4}F^{\mu\nu}F_{\mu\nu}. \tag{1.119}$$

For $\mu^2 > 0$ the potential has a minimum at $\langle 0|\phi|0\rangle = 0$ and the $U(1)$ gauge symmetry remains unbroken. We have the expected situation - a charged scalar field interacting

with a massless photon. Now, consider $\mu^2 < 0$. In this case, the potential no longer has a minimum at $\langle 0|\phi|0\rangle = 0$, but has a ring of minima located at,

$$\langle 0|\phi|0\rangle = \frac{1}{2}ve^{i\delta} \tag{1.120}$$

where δ is an arbitrary phase. Let us re-write the covariant derivative of eq.(1.119) with the shifted field,

$$\tilde{\phi} = \phi - \frac{1}{\sqrt{2}}ve^{i\delta}, \tag{1.121}$$

$$D_\mu\phi = \frac{1}{\sqrt{2}}e^{i\delta}[\partial_\mu\tilde{\phi}_1 + i(\partial_\mu\tilde{\phi}_2 + qvA_\mu) + iqA_\mu(\tilde{\phi}_1 + i\tilde{\phi}_2)], \tag{1.122}$$

where $\tilde{\phi}_1$ and $\tilde{\phi}_2$ are the real and imaginary parts of the shifted complex scalar respectively. Notice how A_μ and $\tilde{\phi}_2$ enter in eq.(1.122). Apart from the interaction term, $\tilde{\phi}_2$ and A_μ enter in the combination,

$$A'_\mu = A_\mu + \frac{1}{qv}\partial_\mu\tilde{\phi}. \tag{1.123}$$

We see that the mode $\tilde{\phi}_2$ and the gauge field mix and, if we expand out eq.(1.119) with the shifted fields, we find that the gauge field, A'_μ, acquires a mass $m = qv$. The mixing has provide the gauge field with a longitudinal degree of freedom as can readily be seen in eq.(1.123) upon converting to momentum space. Note that in order for the gauge field to acquire a mass, the scalar field had to gain a non-zero vacuum expectation value and be coupled to the gauge field itself.

It seems as though the field $\tilde{\phi}_2$ is not physical in the sense that it has become absorbed by the gauge field A'_μ. There exists a particular gauge that makes this observation apparent - a gauge choice with gauge parameter $\Lambda(x)$ as a function of $\tilde{\phi}_2$. Under any gauge transformation we have, in terms of the shifted fields,

$$\begin{aligned} \phi \to \phi' &= e^{-iq\Lambda(x)}\phi \\ &= \frac{1}{\sqrt{2}}(v + \tilde{\phi}'_1 + i\tilde{\phi}'_2)e^{i\delta}. \end{aligned} \tag{1.124}$$

Choosing,

$$q\Lambda(x) = \arctan\frac{\tilde{\phi}_2}{v + \tilde{\phi}_1}, \tag{1.125}$$

$\tilde{\phi}'_2$ disappears, i.e. $\tilde{\phi}'_2 = 0$. Re-writing the gauge transformed and shifted field $\tilde{\phi}_1$ as H, we find

$$\phi' = \frac{1}{\sqrt{2}}(v + H) \tag{1.126}$$

and therefore the covariant derivative of eq.(1.122) becomes,

$$(D_\mu\phi)' = \frac{1}{\sqrt{2}}e^{i\delta}(\partial_\mu H + igvA'_\mu + iqA'_\mu H) \tag{1.127}$$

where the gauge field A'_μ is the field A_μ transformed according to eq.(1.125). Using these results, we can re-write eq.(1.119) in this gauge,

$$\begin{aligned}\mathcal{L} &= \frac{1}{2}(\partial_\mu H)(\partial^\mu H) + \frac{1}{2}q^2 A'_\mu A'^\mu (v+H)^2 \\ &\quad -\frac{1}{2}\mu^2(v+H)^2 - \frac{\lambda}{16}(v+H)^4 - \frac{1}{4}F'^{\mu\nu}F'_{\mu\nu}.\end{aligned} \tag{1.128}$$

The gauge field's mass term results from absorbing the scalar degree of freedom $\tilde{\phi}_2$. We are left with one physical massive scalar H, the Higgs scalar, and a massive gauge field A'_μ. Note that the total number of degrees of freedom remain the same both before and after spontaneous symmetry breaking. Initially we had four degrees of freedom - a massless gauge field with two physical transverse degrees of freedom and a massive complex scalar field with two degrees of freedom. After spontaneous symmetry breaking, again we have four degrees of freedom - one massive gauge field with one longitudinal and two transverse and degrees of freedom, and a massive real scalar field with one degree of freedom.

The renormalizability of theories with spontaneous symmetry breaking is not an obvious or trivial point [8]. The gauge that we have chosen above that explicity removes $\tilde{\phi}_2$ from the theory, called the unitary gauge since only actual physical particles appear, is not manifestly renormalizable. In order to show that renormalizablity has not been lost, it is necessary to use a more general class of gauge choices called the R_ξ gauges (for more details see [3]). The R_ξ gauges are a specific gauge choice and there exists a particularly useful one, called the 't Hooft gauge. The gauge fixing part of the Lagrangian for the Abelian case under discusson in this gauge becomes,

$$\mathcal{L}_{GF} = -\frac{1}{2\xi}(\partial_\mu A^\mu - \xi q v\tilde{\phi}_2). \tag{1.129}$$

While the 't Hooft gauge is not manifestly unitary, (the unphysical Goldstone mode now propagates), it can be shown that the theory is manifestly renormalizable.

In order to build a realistic theory of the weak interactions, we will need to extend the Higgs mechanism to the non-Abelian case. It is useful to sketch how the argument follows. Recall that the covariant derivative for a non-Abelian theory is,

$$D_\mu = \partial_\mu + igT^a A^a_\mu \tag{1.130}$$

where T^a $(a = 1, ..., N)$ are the generators of the gauge group (Lie algebra) and are represented by $n \times n$ dimensional matrices corresponding to the representation of the matter multiplets. The Lagrangian for N scalar fields interacting with a non-Abelian gauge theory is,

$$\mathcal{L} = \frac{1}{2}(D^\mu\phi)^T(D_\mu\phi) - V(\phi) - \frac{1}{4}F_a^{\mu\nu}F^a_{\mu\nu} \tag{1.131}$$

where $V(\phi)$ is the scalar potential and contains all of the renormalizable gauge invariant self interactions, including the scalar mass term, and satisfies eq.(1.108). (It is assumed that ϕ is a column vector containing the n scalar fields.) As before, the gauge symmetry becomes spontaneously broken when some or all of the scalar fields in the multiplet acquire a non-zero vacuum expectation value. Writing the first term of eq.(1.131) with the shifted fields, $\tilde{\phi} = \phi - v$, we have

$$(D^\mu\phi)^T(D_\mu\phi) = (\partial^\mu\tilde{\phi})^T(\partial_\mu\tilde{\phi}) + 2g(\partial^\mu\tilde{\phi})^T iT^a v A^{a\mu} + g^2 A^a_\mu A^{b\mu} v^T T^a T^b v + ... \tag{1.132}$$

As in the global case, there will be $N - M$ Goldstone bosons corresponding to $\tilde{\phi}^T iT^a v$ with $a = M + 1, ..., N$. As a result, we are left with $n - N + M$ physical scalars. We see that these modes mix with the gauge fields, A^a_μ, and moving to the unitary gauge, we can arrange, $\tilde{\phi}'^T iT^a v = 0$ for $a = M + 1, ..., N$. This is the non-Abelian generalization of eq.(1.125). Clearly, the last term of eq.(1.132) behaves as a mass term for the gauge fields, allowing us to write

$$(M_A^2)^{ab} = g^2 v^T T^a T^b v \qquad (a, b = 1, ..., N). \tag{1.133}$$

The sub-matrix $(M_A^2)^{ab}$ $a, b = 1, ..., M$ vanishes since the generators in this range satisfy eq.(1.117), implying that the unbroken subgroup's gauge bosons remain massless. The lower $(N - M) \times (N - M)$ sub-matrix, $(M_A^2)^{ab}$ $a, b = M + 1, ..., N$, is symmetric and positive definite and can therefore be diagonalized by an orthogonal transformation. The eigenvalues of this sub-matrix correspond to the masses of the left-over $N - M$ gauge bosons which acquired their mass by absorbing the massless Goldstone modes. Performing calculations beyond leading order requires us to use the R_ξ gauge class where the unphysical Goldstone modes propagate. Using the orthogonal matrix that diagonalizes the $(N - M) \times (N - M)$ sub-matrix, we may write the scalars in a basis where the physical Higgs scalars are separated from the Goldstone modes [4],

$$\mathcal{L}_{G-H} = \frac{1}{2}(\partial^\mu H^b)(\partial_\mu H^b) - \frac{1}{2}\sum_b (\mu^b)^2 H^b H^b + \frac{1}{2}(\partial^\mu G^a)(\partial_\mu G^a) - \frac{1}{2}\sum_a \xi(M^a)^2 G^a G^a \tag{1.134}$$

where $\tilde{\phi} = G + H$. As a result of the R_ξ gauge choice, the gauge fixing part of the

Lagrangian becomes more complicated, although it is straightforward (if not somewhat tedious) to write the ghost field couplings to the Goldstone modes, the physical Higgs scalars, and the gauge fields respectively [2, 3, 4].

Note that the selection of a non-trivial ground state minimum through the vacuum expectation of a scalar field chooses a specific direction in "group space". While this selection violates the underlying gauge symmetry, allowing gauge boson mass terms, the symmetry is merely hidden. There are other equally valid directions in group space that the scalar vacuum expectation could have selected. As an example, we saw explicitly in the Abelian case that there was a ring of degenerate minima, encoded by a phase, of which the vacuum expectation picks one. The theory is aware that the underlying gauge symmetry is only hidden and it is this awareness that preserves renormalizability.

While the Higgs mechanism provides a theoretical framework for understanding the massive gauge bosons of the weak interaction, we must address the implications of the empirical observation that the weak force violates parity. Consider the Lagrangian,

$$\mathcal{L} = \bar{\psi}_L \gamma^\mu (\partial_\mu + igT_L^a A_\mu^a)\psi_L + \bar{\psi}_R \gamma^\mu (\partial_\mu + igT_R^a A_\mu^a)\psi_R \tag{1.135}$$

where $\psi_{L,R} = \frac{1}{2}(1 \pm \gamma_5)\psi$ and each chiral component transforms under a different representation of the gauge group,

$$\begin{aligned} \psi_L &\rightarrow \exp\left(-igT_L^a \Lambda^a\right)\psi_L \\ \psi_R &\rightarrow \exp\left(-igT_R^a \Lambda^a\right)\psi_R. \end{aligned} \tag{1.136}$$

Under a parity transformation, $\psi \rightarrow \gamma_0 \psi$, we find that $\psi_L \rightarrow \gamma_0 \psi_R$ and $\psi_R \rightarrow \gamma_0 \psi_L$ which implies that the Lagrangian of eq.(1.135) is parity invariant if and only if $T_L^a = T_R^a$. Therefore, the parity violating weak interactions require that the chiral components of the fermions belong to different representations of the gauge group. This presents us with another problem. The fermion mass term, $m\bar{\psi}\psi$ mixes chiralities, implying that the fermion mass term remains gauge invariant if and only if $T_L^a = T_R^a$ - a parity invariant theory. It appears that the weak interactions demand only massless fermions - a prediction incongruent with empirical fact. (Recently, neutrino oscillations have been confirmed, which naturally imply neutrino mass. For the moment we will ignore this point and assume that neutrinos are massless. We will return to a proper discussion of neutrino mass in chapter 3.) We may overcome this difficulty by once again appealing to the Higgs mechanism. Consider a general Yukawa type interaction of N real scalar fields with fermions,

$$\mathcal{L}_Y = \bar{\psi}_L Y_p \psi_R \phi_p + \bar{\psi}_R Y_p^\dagger \psi_L \phi_p \tag{1.137}$$

where ψ_L, ψ_R transform as eq.(1.136) and $p = 1, ..., N$. The scalar fields transform under

some representation of the gauge group as,

$$\phi \rightarrow \exp\left(-igT_{\phi}^{a}\Lambda^{a}\right)\phi. \tag{1.138}$$

Once spontaneous symmetry breaking occurs, the scalar fields are shifted by the vacuum expectation values leading to,

$$\mathcal{L}_{Y} = \bar{\psi}_{L}Y_{p}\psi_{R}(v+\tilde{\phi}_{p}) + \bar{\psi}_{R}Y_{p}^{\dagger}\psi_{L}(v+\tilde{\phi}_{p}). \tag{1.139}$$

We see that a mass term for the fermions emerges, namely, $Y_{p}v = M_{F}$.

Bibliography

[1] H. Weyl, Z. Phys. **56**, 330 (1929).

[2] E. S. Abers and B. W. Lee, Phys. Rept. **9**, 1 (1973).

[3] M. E. Peskin and D. V. Schroeder, *An Introduction to Quantum Field Theory* (Perseus Books, Cambridge, Massachusetts, 1995).

[4] D. Bailin and A. Love, *Introduction to Gauge Field Theory*, revised edition ed. (Institute of Physics Publishing, Bristol, UK, 1993).

[5] P. Ramond, *Field Theory: A Modern Primer*, 2nd ed. (Perseus Publishing, Cambridge, Massachusetts, 1990).

[6] T.-P. Cheng and L.-F. Li, *Gauge Theory of Elementary Particle Physics* (Oxford University Press, New York, New York, 1984).

[7] G. 't Hooft, Nucl. Phys. **B33**, 173 (1971).

[8] G. 't Hooft, Nucl. Phys. **B35**, 167 (1971).

[9] G. 't Hooft and M. J. G. Veltman, Nucl. Phys. **B44**, 189 (1972).

[10] S. Weinberg, *Gravitation and Cosmology* (John Wiley and Sons, New York, New York, 1972).

[11] T. Eguchi, P. B. Gilkey, and A. J. Hanson, Phys. Rept. **66**, 213 (1980).

[12] M. Nakahara, *Geometry, Topology and Physics* (Institute of Physics Publishing, New York, New York, 1995).

[13] R. P. Feynman, Acta Phys. Polon. **24**, 697 (1963).

[14] B. S. DeWitt, Phys. Rev. Lett. **12**, 742 (1964).

[15] L. D. Faddeev and V. N. Popov, Phys. Lett. **B25**, 29 (1967).

[16] J. C. Ward, Phys. Rev. **78**, 182 (1950).

[17] Y. Takahashi, Nuovo Cim. **6**, 371 (1957).

[18] J. C. Taylor, Nucl. Phys. **B33**, 436 (1971).

[19] A. A. Slavnov, Theor. Math. Phys. **10**, 99 (1972).

[20] C. Becchi, A. Rouet, and R. Stora, Phys. Lett. **B52**, 344 (1974).

[21] Itzykson and Zuber, *Introduction to Quantum Field Theory* (McGraw-Hill, New York, New York, 1980).

[22] K. G. Wilson and J. B. Kogut, Phys. Rept. **12**, 75 (1974).

[23] J. Polchinski, hep-ph/9210046 (1992).

[24] F. Englert and R. Brout, Phys. Rev. Lett. **13**, 321 (1964).

[25] G. S. Guralnik, C. R. Hagen, and T. W. B. Kibble, Phys. Rev. Lett. **13**, 585 (1964).

[26] P. W. Higgs, Phys. Lett. **12**, 132 (1964).

[27] P. W. Higgs, Phys. Rev. **145**, 1156 (1966).

[28] J. Goldstone, A. Salam, and S. Weinberg, Phys. Rev. **127**, 965 (1962).

Chapter 2

Supersymmetry for Model Building

2.1 Naturalness and the Standard Model

While the Standard Model, based on the spontaneously broken gauge theory $SU(3)_c \times SU(2)_L \times U(1)_Y \rightarrow SU(3)_c \times U(1)_{EM}$, successfully describes fundamental particle interactions at laboratory energies, the Standard Model must nevertheless provide an incomplete description of nature. In the first instance, the Standard Model does not include a quantum description gravity, which, at the very least, will be necessary for a complete picture of physics near Planck scale, $M_{Pl} \sim 2 \times 10^{18}$eV. Yet, as we will see, there exist compelling reasons [1, 2, 3] to believe that the Standard Model will break down at energy scales well below the gravitational scale. Furthermore, the Standard Model contains 19 free parameters that require laboratory measurement to fix. While the consistency of thousands of observations [4] with these 19 parameters presents a huge success for the Standard Model, it is widely believed that there must be some underlying relationships that explain the parameter set's origin.

The Higgs mechanism [5, 6], used to break $SU(2)_L \times U(1)_Y$ down to $U(1)_{EM}$, requires a fundamental scalar - the Higgs particle - with a mass of ~ 100 GeV. In principle, this presents no problem for the Standard Model. The Higgs particle mass is an input parameter and the theory retains renormalizabilty and predictability as outlined in the previous chapter. However, the renormalization group flow of scalar fields tends to push scalar masses towards the highest mass scale possible in the theory, namely, the field theory's cutoff. In the case of the Standard Model, the cutoff is presumably well above the electroweak unification scale. Heuristically, we can understand the poor ultra-violet behaviour of massive scalar fields by considering the self energy diagrams of Figure (2.1).

If we impose a UV cutoff of Λ (interpreted as the scale where new physics appears),

Figure 2.1: Feynman diagrams that contribute quadratic divergences to the Higgs mass.

we find that the scalar self energy diagrams of figure 2.1 depend on the cutoff through Λ^2, i.e. a quadratic divergence develops. On the other hand, fermion and gauge boson self energy corrections do not depend on Λ in this manner. We see that the scalar self energy graphs provide a large radiative correction to the scalar mass. Therefore, in order for a scalar to appear at the low scale after renormalization group running with a mass much less than the cutoff requires delicate and somewhat bizarre cancellations. In the Standard Model, a light Higgs mass can be achieved by fine tuning at each order in perturbation (to one part in 10^{28}), a theoretically unsatisfactory situation. Naturally, the Higgs mass should be $\sim \Lambda^2$. Embarrassingly, the Standard Model contains a relevant operator that fails to explain its small size - the naturalness problem of high energy physics. We can understand this situation from a slightly different angle. If we add a fermion mass term to a model Lagrangian (e.g. massless QED), the mass term reduces the symmetry of the theory by removing the ability to perform independent chiral rotation on the fermion fields. As a result, radiative corrections shift the fermion masses by a small amount as compared to other scales in the theory. In general, operators that reduce the symmetry of a theory tend to behave well under renormalization group flow [3]. Scalar mass terms, on the other hand, in general do not violate any symmetries and therefore the radiative corrections shift the scalar masses by a large factor, naturally of the order of the cutoff scale.

To escape the difficulties of fundamental scalars, strongly coupled models such as technicolour [7, 8, 9] have been suggested. In technicolour models, the Standard Model Higgs is no longer considered a fundamental scalar, but instead consists of a strongly coupled bound state of techni-fermions. Since technicolour models do not contain fundamental scalars, they elude the naturalness problem and the scale of new physics is not much greater than Higgs mass itself. While such models are appealing, technicolour is plagued with its own set of problems [10].

Alternatively, the naturalness problem has a solution through a symmetry principle that maintains a weakly coupled theory - supersymmetry [11, 12, 13, 14, 15, 16, 17]. The bizarre cancellations previously discussed are easily understood as the result of

supersymmetric contributions. Supersymmetry demands that for every scalar (fermion) there exists a fermionic (scalar) super-partner with the same mass. Roughly speaking, the closed loop fermionic contributions to the scalar mass cancel against the scalar loop quadratic divergences. Since we have not observed super-partners in nature, (at least not yet!) supersymmetry must be broken. Broken supersymmetry will partially cancel the quadratic divergences resulting in a light Higgs mass that can naturally and easily be understood.

2.2 The Supersymmetry Algebra

Consider the Poincare Algebra that encodes Lorentz transformations and local spacetime translations,

$$[P^\lambda, P^\mu] = 0 \tag{2.1}$$

$$[M^{\mu\nu}, P^\lambda] = i\left(\eta^{\nu\lambda}P^\mu - \eta^{\mu\lambda}P^\nu\right) \tag{2.2}$$

$$[M^{\mu\nu}, M^{\rho\sigma}] = i\left(\eta^{\nu\rho}M^{\mu\sigma} + \eta^{\mu\sigma}M^{\nu\rho} - \eta^{\mu\rho}M^{\nu\sigma} - \eta^{\nu\sigma}M^{\mu\rho}\right). \tag{2.3}$$

The Coleman-Mandula theorem [18] states that in any four dimensional Lorentz-invariant theory these generators, along with currents associated with Lorentz invariant quantum numbers generated by internal symmetries, are the only conserved quantities that transform as tensors. While this theorem places strong restrictions on the construction of new conserved quantities, the Coleman-Mandula theorem does not forbid conserved charges that transform as spinors. Consider a generator, Q, that carries one-half unit of spin. Using the two component Weyl spinors and the Van der Waerden notation (see Appendix I), the Jacobi identity

$$[P^\mu, [P^\nu, Q_\alpha]] + [P^\nu, [Q_\alpha, P^\mu]] + [Q_\alpha, [P^\nu, P^\mu]] = 0 \tag{2.4}$$

implies,

$$\begin{aligned} [P^\mu, Q_\alpha] &= 0 \\ [P^\mu, \bar{Q}^{\dot{\alpha}}] &= 0. \end{aligned} \tag{2.5}$$

Performing an infinitesimal Lorentz transformation on Q_α, we find that,

$$[M^{\mu\nu}, Q_\alpha] = -i\left(\sigma^{\mu\nu}\right)_\alpha{}^\beta Q_\beta \tag{2.6}$$

$$[M^{\mu\nu}, \bar{Q}^{\dot{\alpha}}] = -i\left(\bar{\sigma}^{\mu\nu}\right)^{\dot{\alpha}}{}_{\dot{\beta}}\bar{Q}^{\dot{\beta}}. \tag{2.7}$$

The spinorial generators obey anti-commutator relationships, as they are fermionic, and the anti-commutator itself is therefore bosonic. The only possibilities for the anti-commutators are,

$$\{Q_\alpha, Q^\beta\} = s\,(\sigma^{\mu\nu})_\alpha{}^\beta\, M_{\mu\nu} \tag{2.8}$$

$$\{Q_\alpha, \bar{Q}_{\dot{\alpha}}\} = t\,(\sigma^\mu)_{\alpha\dot{\beta}}\, P_\mu. \tag{2.9}$$

where s and t are undetermined constants. We already learned from eq.(2.5) that P_μ commutes with all Q and $\bar{Q}$. Therefore, P^μ must also commute with the anti-commutators and since P^μ does not commute with $M^{\mu\nu}$, s must necessarily vanish. On the other hand, t remains an undetermined positive number and the usual convention in the literature fixes $t = 2$,

$$\{Q_\alpha, \bar{Q}_{\dot{\alpha}}\} = 2\,(\sigma^\mu)_{\alpha\dot{\beta}}\, P_\mu. \tag{2.10}$$

Furthermore, there exists an important corollary of the supersymmetry algebra. Since, by Appendix A we have $\mathrm{Tr}\,(\sigma^\mu\bar{\sigma}^\nu) = 2\eta^{\mu\nu}$, eq.(2.10) implies

$$(\bar{\sigma}^\mu)^{\dot{\beta}\alpha}\,\{Q_\alpha, \bar{Q}_{\dot{\beta}}\} = 4P^\mu. \tag{2.11}$$

Consequently, the Hamiltonian is positive semi-definite, since for $\nu = 0$,

$$P^0 = H = \frac{1}{4}\left(Q_1\bar{Q}_{\dot{1}} + \bar{Q}_{\dot{1}}Q_1 + Q_2\bar{Q}_{\dot{2}} + \bar{Q}_{\dot{2}}Q_2\right) \geq 0 \tag{2.12}$$

This result tells us that supersymmetric theories possess a well defined vacuum bounded below by zero. Furthermore, eq.(2.12) implies that if a supersymmetric vacuum state exists, it is at the global minimum of the effective potential satisfying $E_{\mathrm{vac}} = \langle 0|\, H\, |0\rangle = 0$. This is in contrast to non-supersymmetric theories where the symmetric state is not necessarily the ground state. We will explore the implications of eq.(2.12) further when we discuss the spontaneous breaking of supersymmetry.

Another important consequence of the supersymmetry algebra is the existence of an equal number of fermionic and bosonic fields in a given supermultiplet [16, 17]. Let us see how this emerges. First, observe that Q, $\bar{Q}$ transform a bosonic state into a fermionic one, and visa versa. Two states are said to inhabit the same irreducible supermultiplet if they are proportional to one another through some combination of the Q and $\bar{Q}$ operators. In addition, since P^μ, and therefore P^2, commutes with each of Q and $\bar{Q}$ each state shares the same eigenvalue of P^2 - the states are mass degenerate. In passing, we note that the generators Q and $\bar{Q}$ also commute with any gauge group symmetry generator and thus each member of the supermultiplet has the same gauge charge. According to the spin-statistics theorem [19], the operator $(-1)^{2s}$ (where s is the spin angular momentum) has

eigenvalues $+1$ and -1 acting on a bosonic and fermionic state respectively. Since Q and $\bar{Q}$ change fermion number by one unit, each of these operators must anti-commute with $(-1)^{2s}$. Let us now consider a set of supermultiplet states, $|k\rangle$, with the same eigenvalue $p^\mu \neq 0$ of the operator P^μ. We can write,

$$\begin{aligned}
\sum_k \langle k|(-1)^{2s} P^\mu |k\rangle &= p^\mu \mathrm{Tr}\{(-1)^{2s}\} && (2.13)\\
&= \sum_k \langle k|(-1)^{2s} Q\bar{Q}|k\rangle + \sum_k \sum_l \langle k|(-1)^{2s}\bar{Q}|l\rangle\langle l|Q|k\rangle \\
&= \sum_k \langle k|(-1)^{2s} Q\bar{Q}|k\rangle + \sum_l \langle l|Q(-1)^{2s}\bar{Q}|l\rangle && (2.14)\\
&= \sum_k \langle k|(-1)^{2s} Q\bar{Q}|k\rangle - \sum_l \langle l|(-1)^{2s} Q\bar{Q}|l\rangle && (2.15)\\
&= 0 && (2.16)
\end{aligned}$$

where the anti-commutation of $(-1)^{2s}$ with Q and $\bar{Q}$, and the completion of states, $\sum_l |l\rangle\langle l|$, was used. Since the trace over $(-1)^{2s}$ in eq.(2.13) vanishes, there must be an equal number of fermions and bosons in the supermultiplet.

Thus far, we have only considered simple supersymmetry - an algebra with one spinorial generator along with its hermitian conjugate. (Also called $N = 1$ supersymmetry). We may also construct other supersymmetry algebras, called extended supersymmetry [20], that contain more than one spinorial generator. Consider a set of N supersymmetry generators Q_α^A, where A labels some internal symmetry group, with the usual commutation and anti-commutation relationship

$$\begin{aligned}
[P^\mu, Q_\alpha{}^A] &= 0 && (2.17)\\
[M^{\mu\nu}, Q_\alpha{}^A] &= -i\,(\sigma^{\mu\nu})_\alpha{}^\beta\, Q_\beta{}^A && (2.18)\\
[M^{\mu\nu}, \bar{Q}^{\dot{\alpha}}{}_A] &= -i\,(\bar{\sigma}^{\mu\nu})^{\dot{\alpha}}{}_{\dot{\beta}}\, \bar{Q}^{\dot{\beta}}{}_A. && (2.19)
\end{aligned}$$

The hermitian generators of the internal symmetry group obey the algebra,

$$[T^r, T^s] = i f^{rst} T^t \qquad (2.20)$$

such that,

$$\begin{aligned}
[T^r, Q_\alpha{}^A] &= -(T^r)^A{}_C Q_\alpha{}^C && (2.21)\\
[T^r, \bar{Q}_{\dot{\alpha}A}] &= \bar{Q}_{\dot{\alpha}C}(T^r)^C{}_A && (2.22)\\
[T^r, P^\mu] &= [T^r, M^{\mu\nu}] = 0 && (2.23)
\end{aligned}$$

where T^r inhabits a specific representation of the group and it can be shown that the anti-commutator has the form,

$$\{Q^A{}_\alpha, \bar{Q}_{\dot{\beta}B}\} = 2\delta^A_B \sigma^\mu_{\alpha\dot{\beta}} P_\mu. \tag{2.24}$$

As a result of internal symmetry, it is no longer necessary that $\{Q, Q\} = 0$. In general, we have,

$$\{Q_\alpha{}^A, Q_\beta{}^B\} = \epsilon_{\alpha\beta} Z^{AB} \tag{2.25}$$

where Z^{AB}, called central charges, have the property $Z^{AB} = -Z^{BA}$, and commute with all the spinorial generators, all the internal symmetry generators and themselves. Furthermore, the extended supersymmetry enlarges the particle content of the supermultiplets. While extended supersymmetry has a rich structure, it is unlikely to have any direct application to low energy phenomenology. In supersymmetry algebras with $N \geq 2$, it can be shown [20] that supermultipets containing helicity $\frac{1}{2}$ are TCP-self-conjugate and hence are automatically non-chiral. Since the weak interaction is realized differently between left and right chiral states, it appears that only $N = 1$ supersymmetry is suitable for embedding the Standard Model.

Finally, we should note that the supersymmetry algebras form Super Algebras - algebras that contain both commutation and anti-commutation relations. It has been shown [21] that these Super Algebras of symmetries of the S-matrix are the only extensions of the Poincare group that are consistent with relativistic quantum mechanics. In some sense, it would be remarkable if nature was unaware of this amazing fact.

2.3 Superfields

Since the supersymmetry generators are spinorial, an infinitesimal supersymmetry transformation can be characterized as,

$$U(\xi) = 1 - i(\xi^\alpha Q_\alpha + \bar{\xi}_{\dot{\alpha}} \bar{Q}^{\dot{\alpha}}) \tag{2.26}$$

where ξ and $\bar{\xi}$ are anti-commuting complex Grassmann parameters. Using the Grassmann algebra of $\xi, \bar{\xi}$, we may write the supersymmetry algebra entirely as commutators,

$$[P^\mu, \xi Q] = [P^\mu, \bar{\xi}\bar{Q}] = 0$$

$$[M^{\mu\nu}, \xi Q] = -i\,(\xi \sigma^{\mu\nu} Q) \tag{2.27}$$

$$[M^{\mu\nu}, \bar{\xi}\bar{Q}] = -i\,(\bar{\xi}\bar{\sigma}^{\mu\nu}\bar{Q}) \tag{2.28}$$

$$[\xi Q, \eta Q] = [\bar{\xi}\bar{Q}, \bar{\eta}\bar{Q}] = 0 \tag{2.29}$$

$$[\xi Q, \bar{\eta}\bar{Q}] = 2\left(\xi\sigma^{\mu}\bar{\eta}\right) P_{\mu} \tag{2.30}$$

with independent Grassmann parameters, ξ and η. The introduction of the Grassmann variables facilitates the construction of supersymmetric field theories and, in particular, allows us to readily find an explicit representation of the spinorial generators. A finite supersymmetry transformation, using arbitrary Grassmann parameters θ and $\bar{\theta}$ now reads

$$S\left(x^{\mu}, \theta, \bar{\theta}\right) = \exp\left[i\left(\theta Q + \bar{\theta}\bar{Q} - x^{\mu}P_{\mu}\right)\right]. \tag{2.31}$$

Two successive supersymmetry transformations become,

$$S\left(x^{\mu}, \theta, \bar{\theta}\right) S\left(a^{\mu}, \xi, \bar{\xi}\right) = S'\left(x^{\mu} + a^{\mu} - i\xi\sigma^{\mu}\bar{\theta} + i\theta\sigma^{\mu}\bar{\xi}, \theta + \xi, \bar{\theta} + \bar{\xi}\right). \tag{2.32}$$

where the Baker-Campbell-Hausdorff formula, eq.(1.40), has been applied. Note that since the parameters Grassmann parameters θ and ξ imply that terms of the form $(\theta)^3$ and $(\xi)^3$ vanish, therefore the Baker-Campbell-Hausdorff formula terminates after the first commutator. The space of Grassmann parameters together with spacetime coordinates, x^{μ}, that tracks the effects of the spinorial generators is referred to as superspace [22, 23] and the functions $S\left(x^{\mu}, \theta, \bar{\theta}\right)$ are called superfields. Upon expanding eq.(2.32) we find,

$$\begin{aligned} &S\left(x^{\mu} + a^{\mu} - i\xi\sigma^{\mu}\bar{\theta} + i\theta\sigma^{\mu}\bar{\xi}, \theta + \xi, \bar{\theta} + \bar{\xi}\right) \\ &= S\left(x^{\mu}, \theta, \bar{\theta}\right) + \left(a^{\mu} - i\xi\sigma^{\mu}\bar{\theta} + i\theta\sigma^{\mu}\bar{\xi}\right)\frac{\partial S}{\partial x^{\mu}} + \xi^{\alpha}\frac{\partial S}{\partial\theta^{\alpha}} + \bar{\xi}_{\dot{\alpha}}\frac{\partial S}{\partial\bar{\theta}_{\dot{\alpha}}} \end{aligned} \tag{2.33}$$

implying that the generators have the representation,

$$P_{\mu} = i\partial_{\mu} \tag{2.34}$$

$$iQ_{\alpha} = \frac{\partial}{\partial\theta^{\alpha}} - i\sigma^{\mu}_{\alpha\dot{\alpha}}\bar{\theta}^{\dot{\alpha}}\partial_{\mu} \tag{2.35}$$

$$i\bar{Q}_{\dot{\alpha}} = -\frac{\partial}{\partial\bar{\theta}^{\dot{\alpha}}} + i\theta^{\alpha}\sigma^{\mu}_{\alpha\dot{\alpha}}\partial_{\mu}. \tag{2.36}$$

It is straightforward to check that the representation obeys the supersymmetry algebra. Fermionic derivatives can also be constructed that anti-commute with all the supersymmetry generators,

$$D_{\alpha} = \frac{\partial}{\partial\theta^{\alpha}} + i\sigma^{\mu}_{\alpha\dot{\alpha}}\bar{\theta}^{\dot{\alpha}}\partial_{\mu} \tag{2.37}$$

$$\bar{D}_{\dot{\alpha}} = -\frac{\partial}{\partial\bar{\theta}^{\dot{\alpha}}} - i\theta^{\alpha}\sigma^{\mu}_{\alpha\dot{\alpha}}\partial_{\mu} \tag{2.38}$$

and

$$\{D_\alpha, \bar{D}_{\dot{\alpha}}\} = 2i(\sigma^\mu)_{\alpha\dot{\alpha}}\partial_\mu \tag{2.39}$$

$$\{D_\alpha, D_\beta\} = \{\bar{D}_{\dot{\alpha}}, \bar{D}_{\dot{\beta}}\} = 0. \tag{2.40}$$

Since the operators D and $\bar{D}$ commute with the combinations ξQ and $\bar{\xi}\bar{Q}$, which appear with any supersymmetry transformation (see eq.(2.31)), the fermionic derivatives behave covariantly and as such, they may be employed to impose covariant constraints on superfields. Superfields that obey the covariant condition

$$\bar{D}_{\dot{\alpha}}\Phi = 0, \tag{2.41}$$

called left chiral superfields, play an important role in realistic supersymmetric field theories by providing matter multiplets. Right chiral superfields obey

$$D_\alpha\Phi^\dagger = 0. \tag{2.42}$$

Let us begin by expanding the superfield Φ in light of eq.(2.41). Notice that any superfield that obeys this covariant condition may be regarded as a function of θ and $y^\mu = x^\mu + i\theta\sigma^\mu\bar{\theta}$ since,

$$\bar{D}_{\dot{\alpha}}\theta = \bar{D}_{\dot{\alpha}}y^\mu = 0. \tag{2.43}$$

Thus, we may write $\Phi = \Phi(y^\mu, \theta)$ such that,

$$\Phi(y^\mu, \theta) = \phi(y) + \sqrt{2}\theta\psi(y) + \theta\theta F(y) \tag{2.44}$$

where ψ is a fermionic field, and ϕ and F are complex scalar fields. Substituting $y^\mu = x^\mu + i\theta\sigma^\mu\bar{\theta}$ into the above expansion, we find,

$$\Phi(x^\mu, \theta, \bar{\theta}) = \phi + \sqrt{2}\theta\psi + \theta\theta F + i\partial_\mu\phi\theta\sigma^\mu\bar{\theta} - \frac{i}{\sqrt{2}}\theta\theta\partial_\mu\psi\sigma^\mu\bar{\theta} - \frac{1}{4}\partial_\mu\partial^\mu\phi\theta\theta\bar{\theta}\bar{\theta}. \tag{2.45}$$

Using the explicit representation of the supersymmetry algebra in eq.(2.34) and eq.(2.36), we see that

$$\delta\Phi = i(\xi Q + \bar{\xi}\bar{Q})\Phi \tag{2.46}$$

which implies the supersymmetry transformations

$$\delta\phi = \sqrt{2}\xi\psi \tag{2.47}$$

$$\delta\psi = \sqrt{2}\xi F - \sqrt{2}\partial_\mu\phi\sigma^\mu\bar{\xi} \tag{2.48}$$

$$\delta F = i\sqrt{2}\partial_\mu\psi\sigma^\mu\bar{\xi}. \tag{2.49}$$

Observe that the highest dimensional field, F transforms as a total derivative. That F transforms in this manner will be crucial in constructing supersymmetric field theories.

The field content of chiral superfields consist of fields of spin 0 and $\frac{1}{2}$ which suggests their use as matter multiplets for realistic field theories. In order to proceed in the construction of a supersymmetric field theory, we will also need a superfield that can accommodate the spin 1 fields of gauge theories. Such a superfield exists - the vector superfield. The vector superfield satisfies the reality condition,

$$V = V^\dagger. \tag{2.50}$$

and the component field expansion of V reads [20]

$$\begin{aligned} V(x^\mu, \theta, \bar{\theta}) &= C(x) + i\theta\chi - i\bar{\theta}\bar{\chi} + \frac{i}{2}\theta\theta\,(M + iN) - \frac{i}{2}\bar{\theta}\bar{\theta}\,(M - iN) \\ &\quad + \bar{\theta}\bar{\sigma}^\mu\theta V_\mu + i\theta\theta\bar{\theta}\left(\bar{\lambda} + \frac{1}{2}\bar{\sigma}^\mu\partial_\mu\chi\right) - i\bar{\theta}\bar{\theta}\theta\left(\lambda + \frac{i}{2}\sigma^\mu\partial_\mu\bar{\chi}\right) \\ &\quad + \frac{1}{2}\theta\theta\bar{\theta}\bar{\theta}\left(D - \frac{1}{2}\partial_\mu\partial^\mu C\right) \end{aligned} \tag{2.51}$$

where C, M, N, D are scalar fields, χ, λ are fermionic fields, and V_μ is a vector field. Writing the vector superfield in this form allows us to extract each component field by applying various combinations of the fermionic covariant derivatives to the vector superfield and evaluating at $\theta = \bar{\theta} = 0$. For example,

$$V|_{\theta,\bar{\theta}=0} = C \quad D_\alpha V|_{\theta,\bar{\theta}=0} = i\chi_\alpha \quad \bar{D}_{\dot{\alpha}}\bar{D}^{\dot{\alpha}}D_\alpha V|_{\theta,\bar{\theta}=0} = 4i\lambda_\alpha \quad \text{etc.} \tag{2.52}$$

As with the chiral superfield, we can determine the transformation properties of each component field by applying a supersymmetry transformation to the whole superfield, namely, $\delta_\xi = i(\xi Q + \bar{\xi}\bar{Q})V$. The details can be found in [17, 20]. However, we should note that once again the highest dimension field, in this case D, transforms as a total derivative,

$$\delta D = \partial_\mu\left(-\xi\sigma^\mu\bar{\lambda} + \lambda\sigma^\mu\bar{\xi}\right). \tag{2.53}$$

Having examined the field content of both the chiral and vector superfields, let us consider the product of chiral superfields. We will find upon expansion that $\Phi_i\Phi_j$ and $\Phi_i\Phi_j\Phi_k$ are also chiral superfields and that the combination $\Phi_i^\dagger\Phi_j$ is a vector superfield. Recall that the highest dimensionful field of both the chiral and vector superfields transform as a total derivative. This suggests that we can construct the Lagrangian,

$$\mathcal{L} = \sum_i \left[\Phi_i^\dagger\Phi_i\right]_D + \left([W(\Phi)]_F + \text{h.c.}\right) \tag{2.54}$$

where the subscripts F and D refer to the $\theta\theta$ and $\bar{\theta}\bar{\theta}\theta\theta$ terms of the superfield products. Renormalizability ensures that the holomorphic superpotential, $W(\Phi)$, (*i.e.* W only contains left chiral superfield) does not contain terms higher than Φ^3. Expanding each product, we will learn that the D term part contains all the kinetic terms of the theory and the F term of the superpotential contains all the mass terms and couplings to matter. Furthermore, the component bosonic fields $F(x)$ and $D(x)$ that are contained in the superfield expansions (see eq.(2.45) and eq.(2.51)) are auxiliary fields (i.e. they do not propagate) and as such they can be eliminated through the equations of motion [17, 20]:

$$F_i^\dagger = -\frac{\partial W}{\partial \phi_i} \tag{2.55}$$

$$D^a = -\sum_i g\phi_i^\dagger T_i^a \phi_i. \tag{2.56}$$

The derivative acting on W in eq.(2.55) is with respect to ϕ once $W(\Phi) \to W(\phi)$. In eq.(2.56), T^a refers to the generators of the gauge group in the representation, R, of the matter multiplets and g is the gauge field coupling. We will discuss supersymmetric gauge theories shortly. Most importantly, the tree-level potential [17, 20, 24] can be constructed from eq.(2.55) and eq.(2.56),

$$V(\phi_i) = \sum_i \left|\frac{\partial W}{\partial \phi_i}\right|^2 + \frac{1}{2}g^2 \sum_a \left(\sum_i \phi_i^\dagger T_i^a \phi_i\right)^2. \tag{2.57}$$

- supersymmetric theories generate their own potentials.

Note that we can also write the Lagrangian of eq.(2.54) with the use of superspace variables, $\theta, \bar{\theta}$. The Grassmann variables form a calculus with the properties [20],

$$\int d\theta^\alpha = \int d\bar{\theta}^{\dot{\alpha}} = 0 \tag{2.58}$$

$$\int d\theta^\alpha \, \theta^\alpha = \int d\bar{\theta}^{\dot{\alpha}} \, \theta^{\dot{\alpha}} = 1. \tag{2.59}$$

Multiple integrals can also be defined with the measure,

$$d^2\theta = -\frac{1}{4} d\theta^\alpha d\theta_\alpha \tag{2.60}$$

$$d^2\bar{\theta} = -\frac{1}{4} d\bar{\theta}_{\dot{\alpha}} d\bar{\theta}^{\dot{\alpha}} \tag{2.61}$$

such that $d^4\theta = d^2\bar{\theta}d^2\theta$. Using the properties of the Grassmann calculus, we find that

the supersymmetric Lagrangian can be written as,

$$\mathcal{L} = \int d^4\theta \sum_i \Phi_i^\dagger \Phi_i + \left(\int d^2\theta \, W(\Phi) + \text{h.c.} \right) \tag{2.62}$$

since the integrals project out the appropriate D and F terms. Writing the Lagrangian in this form reveals an important property of supersymmetric theories. It can be shown [25, 26] that radiative corrections to the effective action can always be written as a single superspace integration over $d^4\theta$ with no superspace delta functions. Since the superpotential part of the Lagrangian in eq.(2.62) can only be written as an integral over $d^4\theta$ by introducing delta functions, the superpotential does not receive any direct renormalization. However, the D term part is subject to renormalization as this term is purely an integral over $d^4\theta$. Since the D term part contains the kinetic terms of the Lagrangian, all renormalization effects in the theory are the result of wavefunction renormalizations - coupling constants and masses receive no direct renormalization in concordance with the no-renormalization theorems [25, 26].

To gain an appreciation of the supersymmetric Lagrangian eq.(2.54), let us construct supersymmetric QED. We will follow this example with a discussion of its extension to the non-Abelian case. Recall that a $U(1)$ gauge transformation acts on a vector field as, $V^\mu \to V^\mu + \partial^\mu \Lambda(x)$ where $\Lambda(x)$ is an arbitrary local gauge parameter. We can construct an appropriate transformation for the vector superfield by considering the term $i(\Phi - \Phi^\dagger)$. By construction, this new term satisfies the reality condition and therefore serves as a vector superfield. Expanding out in component fields, we find that the vector field in $\Phi - \Phi^\dagger$ can be identified as $V^\mu = -\partial^\mu(\phi + \phi^\dagger)$. Notice that this term appears not unlike a $U(1)$ gauge transformation. Furthermore, each of C, M, N, χ of eq.(2.51) can be identified through various combinations of the component fields of $\Phi - \Phi^\dagger$. In light of these observations, it was suggested that a $U(1)$ gauge transformation of a vector superfield may be written as,

$$V\left(x, \theta, \bar{\theta}\right) \to V\left(x, \theta, \bar{\theta}\right) + i\left[\Phi(x, \theta, \bar{\theta}) - \Phi^\dagger(x, \theta, \bar{\theta})\right]. \tag{2.63}$$

Not all the component fields of $\Phi - \Phi^\dagger$ are physical, but can be gauged away while leaving the effective gauge parameter, $\phi + \phi^\dagger$, independent. The particularly useful gauge choice, called the Wess-Zumino gauge [15],

$$V_{\text{WZ}}\left(x, \theta, \bar{\theta}\right) = \theta\sigma^\mu\bar{\theta}V_\mu(x) + i\theta\theta\bar{\theta}\bar{\lambda}(x) - \bar{\theta}\bar{\theta}\theta\lambda(x) + \frac{1}{2}\theta\theta\bar{\theta}\bar{\theta}D(x) \tag{2.64}$$

removes the extraneous degrees of freedom. In this gauge, the field content of the supersymmetric representation consists of a spinor field, $\lambda(x)$, a vector field, $V_\mu(x)$, and an

auxiliary mass dimension two field, $D(x)$. Since the lowest dimensional gauge covariant field is the spinor λ, this suggests that the gauge field strength can be constructed from a chiral superfield. It can be shown [17, 20] that the chiral superfield,

$$W_\alpha = \bar{D}^2 D_\alpha V \tag{2.65}$$

may be used to construct the gauge covariant field strength. Writing W_α in component fields in terms of $y^\mu = x^\mu + i\theta\sigma^\mu\bar{\theta}$, we have

$$W_\alpha = 4i\lambda_\alpha(y) - \left(4\delta_\alpha{}^\beta D(y) + 2i\left(\sigma^\mu\bar{\sigma}^\nu\right)_\alpha{}^\beta V_{\mu\nu}\right)\theta_\beta + 4\theta^2(\sigma^\mu)_{\alpha\dot{\alpha}}\partial_\mu\bar{\lambda}^{\dot{\alpha}} \tag{2.66}$$

where $V_{\mu\nu} = \partial_\mu V_\nu - \partial_\nu V_\mu$. The gauge field kinetic term becomes up to a total divergence,

$$\frac{1}{32}\left(W^\alpha W_\alpha\right) = -\frac{1}{4}V^{\mu\nu}V_{\mu\nu} + i\lambda\sigma^\mu\partial_\mu\bar{\lambda} + \frac{1}{2}D^2. \tag{2.67}$$

Notice that λ, called the gaugino, serves as the super-partner of the gauge field, V_μ.

All that remains is to couple the vector superfield to the matter chiral superfields. We will need both left and right chiralities to construct the massive fermions of QED, which suggests the need for two chiral superfields. Consider the objects,

$$S = \frac{1}{\sqrt{2}}\left(\Phi_1 + i\Phi_2\right) \tag{2.68}$$

$$T = \frac{1}{\sqrt{2}}\left(\Phi_1 - i\Phi_2\right) \tag{2.69}$$

Given that the vector superfield transforms as $V \to \Lambda - \Lambda^\dagger$, where Λ is an arbitrary chiral superfield, it can be shown [17, 20] that the objects $S^\dagger \exp(2qV)\, S$ and $T^\dagger \exp(-2qV)\, T$ are gauge invariant. Putting all this together and using eq.(2.54), we can finally write the Lagrangian for the supersymmetric $U(1)$ gauge theory,

$$\mathcal{L} = \frac{1}{32}\left(W^\alpha W_\alpha\right)_F + \left(S^\dagger \exp(2qV)\, S + T^\dagger \exp(-2qV)\, T\right)_D + m\left(ST + S^\dagger T^\dagger\right)_F \tag{2.70}$$

Expanding in the Wess-Zumino gauge, we can write eq.(2.70) in terms of the physical component fields and infer the Feynman rules for the theory.

Suffice it to say, the non-Abelian case is somewhat more involved; however the same methods are employed. The chiral superfield that serves to construct the gauge field strength becomes [17, 20],

$$\begin{aligned} W_\alpha^a &= 4i\lambda_\alpha^a(y) - \left(4\delta_\alpha^\beta D^a(y) + 2i\left(\sigma^\mu\bar{\sigma}^\nu\right)_\alpha{}^\beta V_{\mu\nu}^a(y)\right)\theta_\beta \\ &\quad + 4\theta^2(\sigma^\mu)_{\alpha\dot{\alpha}} D_\mu \lambda^{a\dot{\alpha}}(y) \end{aligned} \tag{2.71}$$

where a is the gauge group index and,

$$V^a_{\mu\nu} = \partial_\mu V_\nu - \partial_\nu V_\mu - g f^{abc} V^b_\mu V^c_\nu. \tag{2.72}$$

Using supersymmetric QED as an example, it can be shown [17, 20] that the objects $S^\dagger \exp(2igT^aV^a)S$ and $T^\dagger \exp(-2igT^aV^a)T$ are gauge invariant quantities. Assembling the parts, the non-Abelian supersymmetric Lagrangian becomes,

$$\mathcal{L} = \frac{1}{64}\left(W^a_\alpha W^{a\alpha}\right)_F + \left(S^\dagger \exp\left(2igT^aV^a\right) S + T^\dagger \exp\left(-2igT^aV^a\right) T\right)_D + \left(W(S,T) + \text{h.c}\right)_F \tag{2.73}$$

for some general gauge invariant superpotential, W.

2.4 A Cursory View of Spontaneous Supersymmetry Breaking

Since we do not observe super-partners of Standard Model particles, supersymmetry cannot be an exact symmetry of the low energy description of Nature. As such, we will assume that supersymmetry spontaneously breaks leaving the vacuum state non-invariant under a supersymmetry transformation, i.e.

$$Q_\alpha|0\rangle \neq 0. \tag{2.74}$$

We already observed that the supersymmetric ground state is the global minimum of the effective potential and must satisfy $E_{\text{vac}} = 0$. Supersymmetry becomes broken if $E_{\text{vac}} \neq 0$ and the positive semi-definite Hamiltonian implies the vacuum energy must become positive. Lifting the vacuum energy from zero, and thereby spontaneously breaking supersymmetry, can be accomplished by allowing certain fields to acquire non-zero vacuum expectation values that are not invariant under supersymmetry transformations [27]. A quick inventory of the fields at our disposal reveals that,

$$\langle 0|\{Q,\psi\}|0\rangle = \langle 0|\delta\psi|0\rangle \sim \langle 0|F|0\rangle \tag{2.75}$$

$$\langle 0|\{Q,\lambda\}|0\rangle = \langle 0|\delta\lambda|0\rangle \sim \langle 0|D|0\rangle \tag{2.76}$$

as the only candidate fields that can gain a vacuum expectation value without breaking Lorentz invariance. Thus, supersymmetry becomes spontaneously broken if and only if the auxiliary fields acquire a non-zero vacuum expectation value. Furthermore, in accordance with Goldstone's theorem, the fermionic partner of the field that receives a vacuum expectation value must be massless and can be identified as a Goldstone fermion.

Let us explore supersymmetry breaking with a couple of examples. First, consider the superpotential (the O'Raifeartaigh model) [27, 28],

$$W(\Phi_1, \Phi_2, \Phi_3) = \lambda\Phi_1 \left(\Phi_3^2 - M^2\right) + \mu\Phi_2\Phi_3 \tag{2.77}$$

with the Lagrangian,

$$\mathcal{L} = [\Phi_1\Phi_1^\dagger]_D + [\Phi_2\Phi_2^\dagger]_D + [\Phi_3\Phi_3^\dagger]_D + [W(\Phi_1, \Phi_2, \Phi_3) + \text{h.c.}]_F . \tag{2.78}$$

In this case, the tree-level potential is given by,

$$V = \sum_i F_i F_i^\dagger = \left|\frac{\partial W}{\partial \phi_i}\right|^2 \tag{2.79}$$

with,

$$F_1^\dagger = -\lambda(\phi_3^2 - M^2) \tag{2.80}$$

$$F_2^\dagger = -\mu\phi_3 \tag{2.81}$$

$$F_3^\dagger = -2\lambda\phi_1\phi_3 + \mu\phi_2. \tag{2.82}$$

so that,

$$V = \lambda^2|\phi_3^2 - M^2|^2 + \mu^2|\phi_3|^2 + |\mu\phi_2 + 2\lambda\phi_1\phi_3|^2. \tag{2.83}$$

Clearly, a solution with all of F_1, F_2, F_3 vanishing does not exist which implies that supersymmetry must be spontaneously broken. Since only F terms are involved, breaking supersymmetry in this manner is referred to as F-term breaking. Taking $M^2 < \mu^2/2\lambda^2$, the global minimum of the tree level potential in eq.(2.83) occurs at $\langle\phi_2\rangle = \langle\phi_3\rangle = 0$ and with $\langle\phi_1\rangle$ undetermined - *i.e.* the potential has a flat direction indicating a vacuum degeneracy. Expanding out the component fields of this model, we will find that the fermionic mass sector appears as,

$$\mathcal{L}^F_{mass} = -(\mu\psi_2\psi_3 + \lambda\langle\phi_1\rangle\psi_3^2 + \text{h.c.}). \tag{2.84}$$

and we see that ψ_1 is left massless as anticipated by Goldstone's theorem [29]. Decomposing ϕ_3 as

$$\phi_3 = \frac{1}{\sqrt{2}}(a + ib) \tag{2.85}$$

the bosonic mass sector can be re-written,

$$\mathcal{L}^B_m = -\frac{1}{2}(\mu^2 - 2\lambda^2M^2)a^2 - \frac{1}{2}(\mu^2 + 2\lambda^2M^2)b^2 - \mu^2\phi_2^\dagger\phi_2 \tag{2.86}$$

indicating that,

$$m_a^2 = \mu^2 - 2\lambda^2 M^2 \tag{2.87}$$

$$m_b^2 = \mu^2 + 2\lambda^2 M^2 \tag{2.88}$$

while ϕ_1 remains massless. We find that both ϕ_1 and ϕ_2 remain mass degenerate with their respective superpartners even though supersymmetry has been broken. The effects of the spontaneously broken supersymmetry are revealed through the splittings of the masses of a and b from the mass of their super-partner, ψ_3. The peculiarity of this situation results from the fact that only the superfield Φ_3 couples to the superfield Φ_1 which ultimately contains the Goldstone fermion. Note that, while the masses of a and b are split from ψ_3, we have the following relationship:

$$m_a + m_b = 2\mu^2 = 2m_{\psi_3}^2. \tag{2.89}$$

This results holds in general [30],

$$\mathrm{STr}\,\mathcal{M}^2 = \sum_J (-1)^{2J}(2J+1)m_J^2 = 0 \tag{2.90}$$

where STr is called the supertrace and J refers to the spin of each particle. There exists one exception to this relationship, D-term supersymmetry breaking [31], which we now examine.

Let us now examine the case where the D field acquires a vacuum expectation value in the absence of F-term supersymmetry breaking. To begin, we need to consider the supersymmetric $U(1)$ gauge theory since we can add the gauge invariant term $[2\xi V]_D$ to the Lagrangian,

$$\mathcal{L} = \frac{1}{32}\left[W^\alpha W_\alpha\right]_F + \left[S^\dagger \exp(2qV)S + 2\xi V\right]_D. \tag{2.91}$$

This simple Lagrangian gives, through its equations of motion,

$$F^\dagger = 0 \tag{2.92}$$

$$D + \xi + q\xi\phi^\dagger\phi = 0. \tag{2.93}$$

Writing out the component fields, we will find that the tree-level potential becomes,

$$V = \frac{1}{2}D^2 = \frac{1}{2}\left|\xi + q\phi^\dagger\phi\right|^2. \tag{2.94}$$

There are two cases to consider here: $\xi q < 0$ and $\xi q > 0$. The first case implies the possibility that D^2 can vanish, namely, $\langle\phi^\dagger\phi\rangle = -\frac{\xi}{e}$. This situation leaves supersym-

metry unbroken, but breaks the $U(1)$ gauge symmetry instead. We obtain a massive gauge boson as well as a massive scalar - the "Higgs particle" - degenerate in mass the with gauge boson. Since supersymmetry is left unbroken, there must also be two Weyl fermions with the same mass as the gauge boson and the scalar field. Indeed, the two fermion degrees of freedom exist and they mix to form a Dirac fermion with the appropriate degenerate mass. This is the generalization of the Higgs mechanism to the supersymmetric case. Case two excludes the solution $D^2 = 0$ and thereby breaks supersymmetry. The minimum of the potential now occurs at $< \phi >= 0$, $D = -\xi$ and therefore the vacuum energy becomes, $E_{\text{vac}} = \frac{1}{2}\xi^2$. In this case, the $U(1)$ gauge symmetry remains unbroken and thus V^μ remain massless. The field λ also remains massless, and is interpretation as the Goldstone fermion, or Goldstino, associated with the breaking of the global supersymmetry. However, the two real scalar fields that compose ϕ receive a mass as the result of its coupling to the Goldstino,

$$m_\phi^2 = q\xi \tag{2.95}$$

while their fermionic partner ψ remains massless. Notice that the mass shift for each real scalar is in the same direction, unlike the situation with F-term breaking. This observation modifies eq.(2.90) to,

$$\text{STr}\mathcal{M}^2 = 2\text{Tr}\, Q\langle D\rangle \tag{2.96}$$

where Q is the charge matrix and $\langle D\rangle$ is the vacuum expectation value of the auxiliary D field. In practice supersymmetry breaking may be achieved through a combination of both F-term and D-term methods.

One other general aspect of supersymmetry breaking is worth mentioning. There is no reason to believe that supersymmetry remains a global symmetry. If we allow supersymmetry to become a local symmetry, we notice that since $\{Q, \bar{Q}\}$ depends on P^μ, the local theory becomes a theory of local spacetime coordinate transformations - *i.e.* a theory of gravity. Local supersymmetry is therefore referred to as supergravity [32, 33, 34]. Although the theory is not renormalizable, supergravity can provide us with generalizations of F-term and D-term supersymmetry breaking. In this case, the superpartner of the graviton, the gravitino, acquires a mass through supergravity breaking [35] by absorbing a Goldstino in much the same way that gauge fields acquire their mass by absorbing a Goldstone boson. It is not our intent to explore the details of supergravity theories or supergravity breaking mechanisms (the super-Higgs mechanisms [35]) or their alternatives. This would lead us too far from our immediate goals. However, it is important to note that in supergravity theories, it is possible to break supersymmetry

with a vanishing vacuum energy - completely unlike the global case. In fact, we may tune the vacuum energy to any value. Although we are free to fine tune supergravity theories, they do not provide us with an explanation for the small cosmological constant. If we break supersymmetry supergravitationally, with minimal assumptions (*i.e.* assuming minimal kinetic terms in the Kahler potential), while arranging for a vanishing cosmological constant [17, 20], we arrive at a simple relationship [36] involving the mass of the gravitino, $m_{3/2}$, the scale of supersymmetry breaking, M_s, and the Planck mass, M_{Pl},

$$m_{\frac{3}{2}} = \frac{M_s^2}{\sqrt{3}M_{Pl}}. \tag{2.97}$$

Since $m_{3/2}$ represents the mass splittings in the supergravity multiplet, it is possible that splitting may be very small compared to the scale of supersymmetry breaking. If low energy supersymmetry exists with supergravity mediated supersymmetry breaking, $m_{3/2}$ should be $\sim$ 1TeV in order to stabilize the gauge hierarchy problem.

There exists a variety of supergravity inspired supersymmetry breaking models. Perhaps one of the most compelling reasons for using such methods is that naturally the resulting supersymmetry breaking occurs in a flavour diagonal manner - gravity is ignorant of flavour. This desired property naturally explains the supression of flavour changing neutral currents in supersymmetric extensions of the Standard Model.

While supergravity provides a successful framework for breaking supersymmetry, there exist other methods such as gauge-mediated supersymmetry [37] breaking, anomaly-mediated supersymmetry breaking [38, 39, 40], and variations along this theme including various forms of strongly interacting physics.

2.5 The Minimal Supersymmetric Standard Model

It is relatively straightforward, if not somewhat tedious, to construct a suitable supersymmetric extension of the Standard Model (for example see [41, 24]). To begin, observe that the quarks and leptons of the Standard Model can be considered component fields of chiral supermultiplets. Since the weak interactions require different representations for the left-handed and right-handed chiralities of the fermions of the Standard Model, we will require two types of chiral superfields. Recall that the holomorphicity of the superpotential demands that the superpotential consists only of left-handed chiral superfields. Therefore, let us adopt the following notation. First, let $\mathbf{L}^a = (L_1^a, L_2^a, L_3^a)^T$ denote a generation space column vector, of left-handed chiral superfields that transform as $SU(2)$ doublets, where $a = 1, 2$ represent $SU(2)$ indices. The superfield $\mathbf{L}$ contains the $SU(2)$ lepton doublets of the Standard Model plus the scalar $SU(2)$ doublet superpartners (sleptons), which will be denoted as $\tilde{L}$. Second, let us denote the conjugate

$SU(2)$ singlet chiral superfield, that transforms left handed, as $\mathbf{E} = (E_1, E_2, E_3)$, *i.e.* a row vector in generation space. The superpartner of $\mathbf{E}$ will be denoted as $\tilde{\mathbf{E}}$. In the same way, we define $\mathbf{Q}^a$, $\mathbf{U}$, and $\mathbf{D}$ to denote the quark $SU(2)$ doublet chiral superfield, the conjugate $SU(2)$ singlet up-like quark chiral superfield, and the conjugate $SU(2)$ singlet down-like quark chiral superfield respectively. The quark superpartners (squarks) will be denoted as $\tilde{\mathbf{Q}}, \tilde{\mathbf{U}}, \tilde{\mathbf{D}}$.

The supersymmetric extension of the Higgs sector is less obvious. The Standard Model contains only one Higgs doublet and uses its complex conjugate to couple with the up-like quarks such that the electroweak quantum numbers match. As the superpotential must be holomorphic, we can no longer employ the complex conjugate of the Higgs doublet. At the very least, a supersymmetric Standard Model will require a second Higgs doublet that couples to the up-like quarks separate from the Higgs doublet that couples to the leptons and down-like quarks. Thus, we will need two distinct chiral superfields, one for the up-like quark sector, H_u, and another for the leptons and the down-like quark sector, H_d. The Higgs chiral superfields contain the Higgs scalars and their fermionic super-partners, the Higgsinos. It is possible that the Higgs sector could be more complicated, containing many more Higgs multiplets than just one extra doublet, however, we will take the minimal path by adding just one extra doublet.

Let us tentatively write the superpotential for a supersymmetric Standard Model by simply promoting the fields of the Standard Model Yukawa sector, along with the new Higgs superfields, to their chiral superfield counter-parts,

$$W_{\text{MSSM}} = \epsilon_{ab} H_d^a \mathbf{E} \mathbf{Y}_{\text{E}} \mathbf{L}^b + \epsilon_{ab} H_d^a \mathbf{D} \mathbf{Y}_{\text{D}} \mathbf{Q}^b + \epsilon_{ab} H_u^a \mathbf{U} \mathbf{Y}_{\text{U}} \mathbf{Q}^b \tag{2.98}$$

where matrix multiplication over generation space is understood. Just as in the Standard Model, we can make field re-definitions such that the lepton and down-like quark Yukawa couplings are flavour diagonal leaving the CKM matrix in the up-like quark sector after an Iwasawa decomposition. However, as it stands, the superpotential of eq.(2.98) cannot describe nature. Let us examine this superpotential in more detail. In addition to lepton number, baryon number, and hypercharge charge number, the superpotential possesses an underlying Peccei-Quinn symmetry [24]. Since only weak iso-spinors carry the Peccei-Quinn symmetry, the Peccei-Quinn symmetry will break through electroweak symmetry breaking, resulting in a light axion. Since axions have not been observed, this presents a problem for the superpotential of eq.(2.98). Furthermore, there exists another symmetry, associated with a global $U(1)$ transformation of the Grassmann superfields themselves. If under the transformation, $\theta \to e^{i\alpha}\theta$ the chiral superfields transform as $\Phi \to e^{iR\alpha}\Phi$ such that $W \to e^{2i\alpha}W$, the theory then possesses an R-symmetry. The superpotential of eq.(2.98) is R-invariant with $\Phi \to e^{i2\alpha/3}\Phi$, where Φ represents any

chiral superfield of the superpotential. R-symmetry implies massless gauginos, which presents a phenomenological problem as gauginos have certainly not been observed. Thus, the candidate superpotential of eq.(2.98) requires augmentation to ameliorate these problems.

Introducing the superpotential term $\mu\epsilon_{ab}H_u^a H_d^b$, which gives a common mass to the Higgs, helps solve these issues. Notice that this mass term does not violate supersymmetry or electroweak symmetry, but it does break both the Peccei-Quinn and R-symmetries, leaving an R' symmetry. Once the gauginos become massive from supersymmetry breaking effects, the R' symmetry is further reduced to a conserved R-parity. It can be shown that R-parity, expressible in terms of lepton number, baryon number, and spin, namely $R = (-1)^{3(B-L)+2S}$, implies that superpartners are R-parity odd while Standard Model particles are R-parity even. In addition, R-parity points to the absolute stability of the lightest supersymmetric particle (LSP). This observation has far reaching consequences in cosmology and may explain the presence of dark matter. Furthermore, R-parity constrains the form of the superpotential by forbidding operators such as DDU, QDL, LLE, and LH_u. These terms would mediate Standard Model forbidden processes, such as lepton and baryon number violation, at levels inconsistent with observation - unless the couplings involved were arranged (perhaps through some other exotic physics) to be very small. Since R-parity only permits terms in the superpotential that conserve lepton and quark number, while at the same time providing a dark matter candidate, and since we have already restricted ourselves to one extra Higgs doublet within the confines of $N = 1$ supersymmetry, the model under discussion is called the Minimal Supersymmetric Standard Model (MSSM).

Unfortunately, while the μ term goes a long way toward creating a more realistic superpotential, the μ term is a relevant operator that has no symmetry restriction. Thus, in principle, μ could have an arbitrarily large mass, inconsistent with the electroweak symmetry breaking scale. As a result, the μ parameter requires a fine tuning. Presumably, unknown dynamics at a scale higher than the MSSM sets the mass of the μ term. However, while a fine tuning is necessary, it is only required once, unlike the Standard Model Higgs mass. Supersymmetry then guarantees quantum mechanical stability of the theory. The new and improved superpotential for the MSSM has the form,

$$W_{\text{MSSM}} = \epsilon_{ab}H_d^a \mathbf{E}\mathbf{Y}_{\text{E}}\mathbf{L}^b + \epsilon_{ab}H_d^a \mathbf{D}\mathbf{Y}_{\text{D}}\mathbf{Q}^b + \epsilon_{ab}H_u^a \mathbf{U}\mathbf{Y}_{\text{U}}\mathbf{Q}^b + \mu\epsilon_{ab}H_u^a H_d^b \qquad (2.99)$$

The gauge interactions of the Standard Model can be made supersymmetric straightforwardly by using the techniques of the previous section. As we pointed out, supersym-

metric theories generate their own potential. In the MSSM, the potential becomes,

$$V = \sum_{i=H_u,H_d,\mathbf{L},\mathbf{Q},\mathbf{E},\mathbf{U},\mathbf{D}} F_i^\dagger F_i + \frac{1}{2}\left(D^2 + D^a D^a + D^A D^A\right) \tag{2.100}$$

where a and A refer to the electroweak $SU(2)$ index, and strong $SU(3)$ index respectively, and D^2 is the D-term associated with $U(1)$ hypercharge. At the electroweak minimum, where the electroweak symmetry becomes broken, and with all other scalar fields set to zero, we find that eq.(2.100) implies,

$$D = \frac{1}{4} g_1 \left(|v_u|^2 - |v_d|^2\right) \tag{2.101}$$

$$D^{(3)} = -\frac{1}{4} g_2 \left(|v_u|^2 - |v_d|^2\right) \tag{2.102}$$

$$F_{H_u} = \frac{1}{\sqrt{2}} \mu v_d \,(0,\ i)^T \tag{2.103}$$

$$F_{H_d} = \frac{1}{\sqrt{2}} \mu v_u \,(i,\ 0)^T \tag{2.104}$$

where v_u, v_d correspond to the vacuum expectation values of the up-like and down-like Higgs. We see that the electroweak minimum is not at the supersymmetry preserving minimum of the potential. The μ term once again plays an important role. In the absence of the μ term, the F-terms above vanish and the theory develops an infinite number of degenerate supersymmetry preserving minima with vanishing D-terms along $|v_u| = |v_d|$. The μ term prevents this possibility by lifting the vacuum degeneracy - only with $|v_d| = |v_u| = 0$ does the potential sit at the supersymmetry preserving minimum. However, this condition leaves the electroweak symmetry and supersymmetry unbroken, which is phenomenologically unacceptable. Thus, as it stands, the MSSM offers no explanation for electroweak or supersymmetry breaking and therefore the MSSM requires extension.

Fortunately, it is unnecessary to know the exact method by which supersymmetry breaks. Supersymmetry breaking can be encoded through a series of soft terms - supersymmetry breaking interactions of dimension two and three (see for example [24]). Again, we must appeal to some unknown physics at some high scale to explain the origin of these soft terms. The soft supersymmetry breaking Lagrangian is given by,

$$\begin{aligned}
\mathcal{L}_{\text{breaking}} \;=\; & -\delta_{\alpha\beta}\tilde{\mathbf{L}}^{\alpha\dagger}\mathbf{m}^2_{\tilde{\mathbf{L}}}\tilde{\mathbf{L}}^{\beta} - \tilde{\mathbf{E}}\mathbf{m}^2_{\tilde{\mathbf{E}}}\tilde{\mathbf{E}}^{\dagger} \\
& -\delta_{\alpha\beta}\tilde{\mathbf{Q}}^{\alpha\dagger}\mathbf{m}^2_{\tilde{\mathbf{Q}}}\tilde{\mathbf{Q}}^{\beta} - \tilde{\mathbf{D}}\mathbf{m}^2_{\tilde{\mathbf{D}}}\tilde{\mathbf{D}}^{\dagger} - \tilde{\mathbf{U}}\mathbf{m}^2_{\tilde{\mathbf{U}}}\tilde{\mathbf{U}}^{\dagger} \\
& -m^2_{\mathrm{H_d}}\delta_{\alpha\beta}H_{\mathrm{d}}^{\alpha *}H_{\mathrm{d}}^{\beta} - m^2_{\mathrm{H_u}}\delta_{\alpha\beta}H_{\mathrm{u}}^{\alpha *}H_{\mathrm{u}}^{\beta} \\
& + \left(-B\mu\epsilon_{\alpha\beta}H_{\mathrm{d}}^{\alpha}H_{\mathrm{u}}^{\beta} \;+\; \text{c. c.}\right)
\end{aligned}$$

$$+\left(-\epsilon_{\alpha\beta}H_d^\alpha \tilde{\mathbf{E}}\mathbf{A}_E\tilde{\mathbf{L}}^\beta + \text{c. c.}\right)$$
$$+\left(-\epsilon_{\alpha\beta}H_d^\alpha \tilde{\mathbf{D}}\mathbf{A}_D\tilde{\mathbf{Q}}^\beta - \epsilon_{\alpha\beta}H_u^\alpha \tilde{\mathbf{U}}\mathbf{A}_U\tilde{\mathbf{Q}}^\beta + \text{c. c.}\right)$$
$$+\left(-\frac{1}{2}M_1\tilde{B}\tilde{B} - \frac{1}{2}M_2\tilde{W}^a\tilde{W}^a - \frac{1}{2}M_3\tilde{G}^b\tilde{G}^b + \text{c. c.}\right) \quad (2.105)$$

where $\tilde{B}$ denotes electroweak U(1) gaugino field; $\tilde{W}^a$, $a = 1, 2, 3$, denote electroweak SU(2) gaugino fields; $\tilde{G}^b$, $b = 1, ..., 8$, denote strong interaction, SU(3), gaugino fields; $\mathbf{m}_{\tilde{L}}^2$, $\mathbf{m}_{\tilde{E}}^2$, $\mathbf{m}_{\tilde{Q}}^2$, $\mathbf{m}_{\tilde{D}}^2$, $\mathbf{m}_{\tilde{U}}^2$, B, $\mathbf{A}_E$, $\mathbf{A}_D$-$\mathbf{A}_U$, $m_{H_d}^2$, $m_{H_u}^2$, M_1, M_2, M_3 are the supersymmetry breaking parameters.

At this point let us examine the Higgs sector and the implications of massive gauginos that results from the eq.(2.105). With the use of the soft supersymmetry breaking Lagrangian, the Higgs potential now appears as,

$$V_{\text{Higgs}} = \sum_{i=u,d}\left(\mu^2 + m_{H_i}^2\right)\left(H_i^0\right)^2 - B\mu H_u^0 H_d^0 + \text{c.c} + \frac{1}{8}(g_1^2+g_2^2)\left(\left(H_u^0\right)^2 - \left(H_d^o\right)^2\right)^2 \quad (2.106)$$

Unlike the Standard Model, where the quartic Higgs coupling is an input parameter, we see that the MSSM dictates the quartic coupling in terms of the gauge couplings g_1 and g_2. Furthermore, the physical Higgs fields form CP eigenstates [41], leaving us with two charged Higgs, H^+, H^- a CP-odd neutral Higgs scalar, A, and two CP-even Higgs scalars, h and H. The up and down like Higgs vacuum expectation values that sit at the electroweak symmetry breaking minimum of the Higgs potential are constrained by the Fermi constant such that,

$$v_u^2 + v_d^2 = \frac{G_F}{2} \quad (2.107)$$

with their ratio defined by,

$$\tan\beta = \frac{v_u}{v_d}. \quad (2.108)$$

In addition, the electroweak breaking minimization implies the relations

$$\mu^2 + m_{H_u}^2 - B\mu\cot\beta = \frac{1}{2}m_Z^2\cos 2\beta \quad (2.109)$$

$$\mu^2 + m_{H_d}^2 - B\mu\tan\beta = \frac{1}{2}m_Z^2\cos 2\beta \quad (2.110)$$

which may be used to eliminate the B term from the soft supersymmetry breaking Lagrangian, resulting in the tree-level expression for μ^2,

$$\mu^2 = -\frac{1}{2}m_Z^2 - \frac{m_{H_d}^2 - m_{H_u}^2\tan^2\beta}{1-\tan^2\beta}. \quad (2.111)$$

Evaluating the Higgs potential around the electroweak breaking minimum we find a

tree-level constraint on the mass the lightest Higgs scalar, h, namely,

$$m_h^2 = m_Z^2 \cos^2 2\beta - m_A^2 \left(\frac{m_z}{m_A}\right)^4 (2 - \sin^2 2\beta) + ... \tag{2.112}$$

where m_Z and m_A are the masses of the Z^0 gauge boson and the CP-odd Higgs scalar respectively. Notice that the constraint eq.(2.112) indicates that the lightest Higgs is lighter than the Z^0 mass. This is a rather embarrassing prediction since the empirical constraint on the lightest Higgs scalar points to $m_h \geq 114$GeV [4]. However, the estimate of eq.(2.112) gives only a tree-level constraint. The non-triviality of the top quark loop corrections (the top Yukawa is not small) dramatically raises the mass bound on m_h, comfortably placing the mass of m_h above the Z^0 mass. However, the bound cannot be stretched to arbitrarily high energies and the MSSM prefers a relatively light Higgs have a mass $\lesssim 130$ GeV - a tantalizing prospect for the LHC and Tevatron.

In addition to the new scalar particles that form the superpartners of the Standard Model fermions, the MSSM also introduces new fermions, namely, the Higgsinos, $\tilde{H}_u^+$, $\tilde{H}_d^-$, $\tilde{H}_u^0$ $\tilde{H}_d^0$, the weak gauginos, $\tilde{W}^\pm$, $\tilde{W}^0$, $\tilde{B}$, and the strong gauginos, called gluinos, $\tilde{g}$. The weak sector gauginos and Higgsinos mix after electroweak symmetry breaking. In particular, after the Higgs scalars acquire their vacuum expectation values, we can write the mass term for the charged Higgsinos and charged Winos of the MSSM Lagrangian as,

$$\mathcal{L} = -\left(\tilde{W}^+ \; \tilde{H}_u^+\right) \mathbf{M_C} \begin{pmatrix} \tilde{W}^- \\ \tilde{H}_d^- \end{pmatrix} + \text{c. c.} \tag{2.113}$$

with the mass matrix,

$$\mathbf{M_C} = \begin{pmatrix} M_2 & \sqrt{2} m_W \cos\beta \\ \sqrt{2} m_W \sin\beta & \mu \end{pmatrix}. \tag{2.114}$$

By diagonalizing the mass matrix $\mathbf{M_C}$, we can re-express the Lagrangian in the mass eigenbasis, namely,

$$\begin{pmatrix} \tilde{\chi}_1^- \\ \tilde{\chi}_2^- \end{pmatrix} = \mathbf{O_L} \begin{pmatrix} \tilde{W}^- \\ \tilde{H}_d^- \end{pmatrix}, \qquad \begin{pmatrix} \tilde{\chi}_1^+ \\ \tilde{\chi}_2^+ \end{pmatrix} = \mathbf{O_R} \begin{pmatrix} \tilde{W}^+ \\ \tilde{H}_u^+ \end{pmatrix} \tag{2.115}$$

with

$$\mathbf{M_C} = \mathbf{O_R^T} \text{diag}\left(M_{\tilde{\chi}_1^-}, M_{\tilde{\chi}_2^-}\right) \mathbf{O_L}. \tag{2.116}$$

The mass eigenstate fields $\chi_{1,2}^\pm$ are referred to as charginos and the real orthogonal matrices $\mathbf{O_R}$ and $\mathbf{O_L}$ are chosen such that the mass eigenvalues $M_{\tilde{\chi}_1^-}$, $M_{\tilde{\chi}_2^-}$ are positive.

Therefore, the mass term becomes,

$$\mathcal{L} = -M_{\tilde{\chi}_1^-}\tilde{\chi}_1^+\tilde{\chi}_1^- - M_{\tilde{\chi}_2^-}\tilde{\chi}_2^+\tilde{\chi}_2^- + \text{c. c.}. \tag{2.117}$$

A similar situation arises with the weak neutral fermions after electroweak symmetry breaking. The four neutral fermionic fields, $\tilde{H}_u^0$, $\tilde{H}_d^0$, $\tilde{B}$, and $\tilde{W}^0$ mix to form four mass eigenstates called neutralinos, $\tilde{\chi}_1^0$, $\tilde{\chi}_2^0$, $\tilde{\chi}_3^0$, $\tilde{\chi}_4^0$. The neutralino mass Lagrangian is given by

$$\mathcal{L} = -\left(\tilde{B}\,\tilde{W}^3\,\tilde{H}_{\rm d}^0\,\tilde{H}_{\rm u}^0\right)\mathbf{M}_{\rm ne}\begin{pmatrix}\tilde{B}\\ \tilde{W}^3\\ \tilde{H}_{\rm d}^0\\ \tilde{H}_{\rm u}^0\end{pmatrix} + \text{c. c.} \tag{2.118}$$

where

$$\mathbf{M}_{\rm ne} = \begin{pmatrix} M_1 & 0 & -m_{\rm Z}\cos\beta\sin\theta_{\rm W} & m_{\rm Z}\sin\beta\sin\theta_{\rm W}\\ 0 & M_2 & m_{\rm Z}\cos\beta\cos\theta_{\rm W} & -m_{\rm Z}\sin\beta\cos\theta_{\rm W}\\ -m_{\rm Z}\cos\beta\sin\theta_{\rm W} & m_{\rm Z}\cos\beta\cos\theta_{\rm W} & 0 & -\mu\\ m_{\rm Z}\sin\beta\sin\theta_{\rm W} & -m_{\rm Z}\sin\beta\cos\theta_{\rm W} & -\mu & 0\end{pmatrix}. \tag{2.119}$$

An orthonormal rotation leads to the mass eigenstates,

$$\begin{pmatrix}\tilde{\chi}_1^0\\ \tilde{\chi}_2^0\\ \tilde{\chi}_3^0\\ \tilde{\chi}_4^0\end{pmatrix} = \mathbf{O}_{\rm ne}\begin{pmatrix}\tilde{B}\\ \tilde{W}^3\\ \tilde{H}_{\rm d}^0\\ \tilde{H}_{\rm u}^0\end{pmatrix} \tag{2.120}$$

where $\mathbf{O}_{\rm ne}$ is a real, orthogonal matrix. Decomposing the mass matrix in terms of real mass eigenvalues, $M_{\tilde{\chi}_a^0}$, $a = 1,2,3,4$ we obtain,

$$\mathbf{M}_{\rm ne} = \mathbf{O}_{\rm ne}^{\rm T}\text{diag}\left(M_{\tilde{\chi}_1^0}\,M_{\tilde{\chi}_2^0}\,M_{\tilde{\chi}_3^0}\,M_{\tilde{\chi}_4^0}\right)\mathbf{O}_{\rm ne}, \tag{2.121}$$

which allows us to write the mass term Lagrangian,

$$\mathcal{L} = -\frac{1}{2}\sum_{a=1}^{4} M_{\tilde{\chi}_a^0}\tilde{\chi}_a^0\tilde{\chi}_a^0. \tag{2.122}$$

Finally, we come to the squark and slepton sector. Recall that for each lepton and quark in the Standard Model there exist two complex scalar fields associated with the two chiral components. Observing the structure of the superpotential and soft supersymmetry breaking terms respectively, we can schematically write the scalar mass squared

matrix for the squarks and sleptons (denoted as $\tilde{f}$) as,

$$\left(\tilde{f}_L^* \; \tilde{f}_R^*\right) \mathbf{M}_S^2 \begin{pmatrix} \tilde{f}_L \\ \tilde{f}_R \end{pmatrix} \tag{2.123}$$

where,

$$\mathbf{M}_S^2 = \begin{pmatrix} \tilde{m}^2_{\tilde{L},\tilde{Q}} + m_f^2 + \Delta_{\tilde{L},\tilde{Q}} & F^\dagger(m_f, \mu, \tan\beta, A) \\ F(m_f, \mu, \tan\beta, A) & \tilde{m}^2_{\tilde{E},\tilde{U},\tilde{D}} + m_f^2 + \Delta_{\tilde{E},\tilde{U}\tilde{D}} \end{pmatrix}. \tag{2.124}$$

The terms $\Delta_{\tilde{L},\tilde{Q}}$ and $\Delta_{\tilde{E},\tilde{U}\tilde{D}}$ arise from D-term contributions and depend on the third component of isospin as well as hypercharge. The function $F(m_f, \mu, \tan\beta, A)$ results from F-term contributions as well as from A-terms in the soft supersymmetry breaking potential. The full slepton mass matrix for all generations reads,

$$M^2_{\text{slepton}} = \begin{pmatrix} \mathbf{m}^2_{\text{LL}} & \mathbf{m}^{2\dagger}_{\text{RL}} \\ \mathbf{m}^2_{\text{RL}} & \mathbf{m}^2_{\text{RR}} \end{pmatrix} \tag{2.125}$$

where,

$$\mathbf{m}^2_{\text{LL}} = \mathbf{m}_{\text{l}}^2 + \mathbf{m}^2_{\tilde{\text{L}}} + m_Z^2 \cos 2\beta \left(\sin^2\theta_W - \frac{1}{2}\right) \cdot \mathbf{I}, \tag{2.126}$$

$$\mathbf{m}^2_{\text{RR}} = \mathbf{m}_{\text{l}}^2 + \mathbf{m}^2_{\tilde{\text{E}}} - m_Z^2 \cos 2\beta \sin^2\theta_W \cdot \mathbf{I}, \tag{2.127}$$

$$\mathbf{m}^2_{\text{RL}} = -\mu \mathbf{m}_{\text{l}} \tan\beta + \frac{v\cos\beta}{\sqrt{2}} \mathbf{A}_{\text{E}} \tag{2.128}$$

with

$$\mathbf{m}_{\text{l}} = \text{diag}\left(m_{\text{l}_1}\; m_{\text{l}_2}\; m_{\text{l}_3}\right), \tag{2.129}$$

and m_{l_1}, m_{l_2}, m_{l_3} are electron, muon, and tau masses respectively. The squarks follow analogously. The above Lagrangian written in terms of mass eigenstates $\tilde{f}_1, ..., \tilde{f}_6$ (six complex scalar fields, two for each generation) becomes,

$$\mathcal{L} = -\sum_{b=1}^{6} m^2_{\tilde{f}_b} \tilde{f}_b^* \tilde{f}_b \tag{2.130}$$

with

$$\begin{pmatrix} \tilde{f}_1 \\ \tilde{f}_2 \\ \tilde{f}_3 \\ \tilde{f}_4 \\ \tilde{f}_5 \\ \tilde{f}_6 \end{pmatrix} = \mathbf{U}_{\tilde{\text{f}}} \begin{pmatrix} \tilde{e}_1 \\ \tilde{e}_2 \\ \tilde{e}_3 \\ \tilde{E}_1^* \\ \tilde{E}_2^* \\ \tilde{E}_3^* \end{pmatrix}, \tag{2.131}$$

and $\mathbf{U}_{\tilde{\mathbf{f}}}$ is a complex unitary matrix defined by,

$$\begin{pmatrix} \mathbf{m}^2_{\mathrm{LL}} & \mathbf{m}^{2\dagger}_{\mathrm{RL}} \\ \mathbf{m}^2_{\mathrm{RL}} & \mathbf{m}^2_{\mathrm{RR}} \end{pmatrix} = \mathbf{U}^{\dagger}_{\tilde{\mathbf{f}}} \mathrm{diag}\left(m^2_{\tilde{f}_1}\ m^2_{\tilde{f}_2}\ m^2_{\tilde{f}_3}\ m^2_{\tilde{f}_4}\ m^2_{\tilde{f}_5}\ m^2_{\tilde{f}_6}\right) \mathbf{U}_{\tilde{\mathbf{f}}}. \tag{2.132}$$

As we noted in section 2.3, the no-renormalization theorems guarantee better UV behaviour of supersymmetric theories as compared to their non-supersymmetric counterparts. In $N = 1$ supersymmetry, wavefunction renormalization effects contribute and therefore the couplings of the MSSM are subject to renormalization group flow. A complete list of the renormalization group equations for the MSSM appears in Appendix III. As we will see, these corrections have profound phenomenological consequences. We have already noted that important quantum loop corrections push the mass of the lightest Higgs particle to acceptable levels. Most suggestively, consistent gauge coupling constant unification can be achieved with the MSSM. In the MSSM, the renormalization group equations for the U(1) hypercharge coupling constant, g_1, the weak SU(2) coupling constant, g_2, the strong SU(3) coupling constant g_3, expressed through $\alpha_i = g_i/4\pi$ read [20, 21]

$$M\frac{d\alpha_i}{dM} = -\frac{b_i}{2\pi}\alpha_i^2 + \mathcal{O}(\alpha_i^3) \tag{2.133}$$

where in general,

$$b = \frac{11}{3}C_1(G) + \frac{2}{3}\sum_R C_2(R) - \frac{1}{3}\sum_S C_2(S). \tag{2.134}$$

The group factors $C_1(G)$ and $C_2(R,S)$ are defined by,

$$C_1(G)\delta^{ab} = f^{acd}f^{bcd} \tag{2.135}$$

$$C_2(R,S)\delta^{ab} = \mathrm{Tr}(T^a_{R,S}T^b_{R,S}) \tag{2.136}$$

where R and S denote the representation of the Weyl fermions and scalars under the gauge group G respectively. For the MSSM (with two Higgs doublets), we have,

$$b_1 = -10;\ b_2 = -1;\ b_3 = 3. \tag{2.137}$$

Integrating eq.(2.133) between M_{Z} and the unification scale M_{GUT} we find,

$$\alpha_i^{-1}(M_{\mathrm{Z}}) - \alpha_i^{-1}(M_{\mathrm{GUT}}) = -\frac{b_i}{2\pi}\ln\frac{M_{\mathrm{GUT}}}{M_{\mathrm{Z}}} \tag{2.138}$$

with,

$$\frac{5}{3}\alpha_1(M_{\mathrm{GUT}}) = \alpha_2(M_{\mathrm{GUT}}) = \alpha_3(M_{\mathrm{GUT}}) = \alpha_{\mathrm{GUT}}(M_{\mathrm{GUT}}) \tag{2.139}$$

(the factor of 5/3 properly normalizes the hypercharge coupling to the unification cou-

pling constant, see chapter 3 for details). Using eq.(2.138), we can eliminate $\alpha_{GUT}(M_{GUT})$ and $\ln M_{GUT}/M_Z$ from the system of equations yielding,

$$\sin^2\theta_W(M_Z) = \frac{1}{15}\left(3 + 7\frac{\alpha_{em}(M_Z)}{\alpha_3(M_Z)}\right) = 0.234 \tag{2.140}$$

where the initial conditions [4] $\alpha_{em}^{-1}(M_Z) = 128.8$ and $\alpha_3(M_Z) = 0.108$ have been used. The predicted value of $\sin^2\theta_W$ from eq.(2.140) fits the measured value, [4], remarkably well. Furthermore, using the measured value of M_Z together with eq.(2.138) yields the unification scale $M_{GUT} \approx 1.5 \times 10^{16}$GeV, two orders of magnitude below the reduced Plank mass. We will comment more on unification issues in chapter 4.

The running of the soft supersymmetry breaking Lagrangian and the superpotential are of particular phenomenological importance. A priori, the parameters of the superpotential and the soft supersymmetry breaking Lagrangian are unfixed in so far as they reproduce the known masses and couplings of the Standard Model. This leaves a huge parameter space consisting of undetermined scalar masses with undetermined phases, an unknown Higgs vacuum expectation value ratio, $\tan\beta$, a large parameter range with undetermined sign for the μ parameter, undetermined gaugino masses along with undetermined trilinear A-terms. In addition there exists the problem of supersymmetric flat directions, or moduli problems, which present certain cosmological challenges (for review see [42]). It appears that the MSSM has created more problems than it solves as the number of free parameters has jumped significantly from the Standard Model set. However, the MSSM cannot be a final theory of nature and presumably the question concerning the origin of the MSSM parameter set will be answered by some unknown high scale physics. Empirically, the squark and slepton mass matrices must be nearly diagonal and nearly degenerate so that flavour changing neutral current processes remain suppressed and presicion electroweak fits are not upset. Furthermore the superpartners must be sufficiently massive to have escaped detection. As a result, the following simplifying assumptions have been suggested:

- The squark and slepton masses matrices are proportional to the identity giving all the squarks and sleptons a universal scalar mass, m_0
- All gaugino masses are degenerate with a universal gaugino mass, $m_{1/2}$
- The trilinear A-terms are proportional to the Yukawa matrices with universal A-parameter, A_0

These assumptions dramatically reduce the number of free parameters but the conditions must be imposed at some initial scale - the scale where supersymmetry breaks.

As discussed in the previous section, there are a variety of methods for breaking supersymmetry and the method employed will determine the initial conditions for the RGEs. For the remainder of the discussion, we will restrict to the generic (and perhaps most popular) minimal supergravity method - mSUGRA. In the mSUGRA scenario, the simplifying assumptions are imposed at or near the unification scale. The parameters of the MSSM are then evolved via the renormalization group equations from the high scale to the electroweak scale. The simplifying mSUGRA assumptions are codified at the high scale as,

$$\mathbf{m}_{\tilde{L}}^2 = \mathbf{m}_{\tilde{E}}^2 = \mathbf{m}_{\tilde{Q}}^2 = \mathbf{m}_{\tilde{D}}^2 = \mathbf{m}_{\tilde{U}}^2 = m_0^2 \cdot \mathbf{I}, \tag{2.141}$$

$$m_{H_d}^2 = m_{H_u}^2 = m_0^2, \tag{2.142}$$

$$\mathbf{A_E} = \mathbf{A_D} = \mathbf{A_U} = \mathbf{A_0}, \tag{2.143}$$

$$M_1 = M_2 = M_3 = m_{1/2} \tag{2.144}$$

where m_0 and $m_{1/2}$ denote the universal scalar mass and the universal gaugino mass respectively ($\mathbf{I}$ is the 3×3 unit matrix). As we will learn in Part II, the running of these parameters can lead to the emergence of flavour changing neutral current processes which have testable laboratory consequences. Remarkably, the renormalization group running of the MSSM parameter set can also trigger electroweak symmetry breaking under rather roboust initial conditions [43, 44, 45]. Running from the unification scale, the up-like Higgs mass, $m_{H_u}^2$, becomes negative through contributions from the large top Yukawa coupling. Interestingly, only $m_{H_u}^2$ turns negative, leaving all the sleptons and squarks (mass)^2 positive thereby avoiding the embarrassing prediction of the spontaneous breakdown of colour or electric charge.

Bibliography

[1] E. Gildener and S. Weinberg, Phys. Rev. **D13**, 3333 (1976).

[2] E. Gildener, Phys. Rev. **D14**, 1667 (1976).

[3] G. 't Hooft, , lecture given at Cargese Summer Inst., Cargese, France, Aug 26 - Sep 8, 1979.

[4] S. Eidelman *et al.*, Phys. Lett. **B592**, 1 (2004).

[5] P. W. Higgs, Phys. Lett. **12**, 132 (1964).

[6] P. W. Higgs, Phys. Rev. **145**, 1156 (1966).

[7] L. Susskind, Phys. Rev. **D20**, 2610 (1979).

[8] S. Weinberg, Phys. Rev. **D19**, 1277 (1979).

[9] M. E. Peskin, , contributed to Proc. of 10th Int. Symp. on Lepton and Photon Interactions at High Energy, Bonn, West Germany, Aug 24-29, 1981.

[10] S. Dimopoulos and J. R. Ellis, Nucl. Phys. **B182**, 505 (1982).

[11] Y. A. Golfand and E. P. Likhtman, JETP Lett. **13**, 323 (1971).

[12] D. V. Volkov and V. P. Akulov, Phys. Lett. **B46**, 109 (1973).

[13] J. Wess and B. Zumino, Nucl. Phys. **B70**, 39 (1974).

[14] S. Ferrara, J. Wess, and B. Zumino, Phys. Lett. **B51**, 239 (1974).

[15] J. Wess and B. Zumino, Nucl. Phys. **B78**, 1 (1974).

[16] S. P. Martin, hep-ph/9709356 (1997).

[17] H. P. Nilles, Phys. Rept. **110**, 1 (1984).

[18] S. R. Coleman and J. Mandula, Phys. Rev. **159**, 1251 (1967).

[19] R. F. Streater and A. S. Wightman, *PCT, Spin and Statistics, and All That* (Addison-Wesley, New York, 1989).

[20] D. Bailin and A. Love, *Supersymmetric Gauge Field Theory and String Theory* (Institute of Physics Publishing, Bristol, UK, 1994).

[21] R. Haag, J. T. Lopuszanski, and M. Sohnius, Nucl. Phys. **B88**, 257 (1975).

[22] A. Salam and J. Strathdee, Nucl. Phys. **B76**, 477 (1974).

[23] S. Ferrara and B. Zumino, Nucl. Phys. **B79**, 413 (1974).

[24] P. Ramond, *Journeys Beyond the Standard Model* (Perseus Books, Cambridge Massachusetts, 1999).

[25] J. Iliopoulos and B. Zumino, Nucl. Phys. **B76**, 310 (1974).

[26] M. T. Grisaru, W. Siegel, and M. Rocek, Nucl. Phys. **B159**, 429 (1979).

[27] P. Fayet, Phys. Lett. **B58**, 67 (1975).

[28] L. O'Raifeartaigh, Nucl. Phys. **B96**, 331 (1975).

[29] P. Fayet and J. Iliopoulos, Phys. Lett. **B51**, 461 (1974).

[30] S. Ferrara, L. Girardello, and F. Palumbo, Phys. Rev. **D20**, 403 (1979).

[31] P. Fayet, Nucl. Phys. **B90**, 104 (1975).

[32] D. Z. Freedman, P. van Nieuwenhuizen, and S. Ferrara, Phys. Rev. **D13**, 3214 (1976).

[33] D. Z. Freedman and P. van Nieuwenhuizen, Phys. Rev. **D14**, 912 (1976).

[34] S. Deser and B. Zumino, Phys. Lett. **B62**, 335 (1976).

[35] E. Cremmer *et al.*, Phys. Lett. **B79**, 231 (1978).

[36] S. Deser and B. Zumino, Phys. Rev. Lett. **38**, 1433 (1977).

[37] M. Dine and A. E. Nelson, Phys. Rev. **D48**, 1277 (1993).

[38] M. Dine, N. Seiberg, and E. Witten, Nucl. Phys. **B289**, 589 (1987).

[39] L. Randall and R. Sundrum, Nucl. Phys. **B557**, 79 (1999).

[40] G. F. Giudice, M. A. Luty, H. Murayama, and R. Rattazzi, JHEP **12**, 027 (1998).

[41] H. E. Haber and G. L. Kane, Phys. Rept. **117**, 75 (1985).

[42] K. Enqvist and A. Mazumdar, Phys. Rept. **380**, 99 (2003).

[43] K. Inoue, A. Kakuto, H. Komatsu, and S. Takeshita, Prog. Theor. Phys. **68**, 927 (1982).

[44] L. E. Ibanez and G. G. Ross, Phys. Lett. **B110**, 215 (1982).

[45] L. Alvarez-Gaume, M. Claudson, and M. B. Wise, Nucl. Phys. **B207**, 96 (1982).

Chapter 3

Neutrino Mass and a Grand Unification Primer

3.1 The Lepton Sector of the Standard Model

As the only potentially exactly massless fermions of the Standard Model, neutrinos occupy a special place in the low energy description of nature. Furthermore, neutrinos carry no colour or electric charge. For these reasons, let us consider the leptonic structure of the Standard Model in detail.

It can be shown (see [1, 2] for example) that the leptons enter the charged weak interaction through the currents,

$$J_\mu^{lep}(x) = \sum_{i=e,\mu,\tau} \bar{e}_i(x)\gamma_\mu(1-\gamma_5)\nu_i(x) \tag{3.1}$$

$$J_\mu^{lep\dagger}(x) = \sum_{i=e,\mu,\tau} \bar{\nu}_i(x)\gamma_\mu(1-\gamma_5)e_i(x) \tag{3.2}$$

where the index i denotes lepton flavour and the fields $e(x)$ and $\nu(x)$ represent the charged lepton and neutrino respectively. Re-writing the currents of eq.(3.1) and eq.(3.2) using the projection operators, $P_L = \frac{1}{2}(1-\gamma_5)$ and $P_R = \frac{1}{2}(1+\gamma_5)$, we obtain,

$$\frac{1}{2}L_\mu = \sum_i \bar{e}_{iL}\gamma_\mu\nu_{iL} \tag{3.3}$$

$$\frac{1}{2}L_\mu^\dagger = \sum_i \bar{\nu}_{iL}\gamma_\mu e_{iL}. \tag{3.4}$$

The Lorentz covariant objects L_μ and $L_\mu^\dagger$ have the form of $SU(2)$ raising and lowering operators which can be made manifest by placing the neutrino and the charged lepton

into an $SU(2)$ doublet,

$$L_i = \begin{pmatrix} \nu_{Li} \\ e_{Li} \end{pmatrix} \tag{3.5}$$

implying the $SU(2)$ generators,

$$T^j_\mu = \frac{1}{2}\sum_i \bar{L}_i \gamma_\mu \tau^j L_i. \tag{3.6}$$

The charged weak currents may now be written as,

$$\frac{1}{2}J^{lep}_\mu = T^1_\mu - iT^2_\mu \tag{3.7}$$

$$\frac{1}{2}J^{lep\dagger}_\mu = T^1_\mu + iT^2_\mu. \tag{3.8}$$

While the $SU(2)$ generators permit the construction of the charged weak leptonic currents (now with the inclusion of a neutral component), they cannot by themselves account for the electromagnetic current,

$$J^{em}_\mu = \sum_i \bar{e}\gamma_\mu e. \tag{3.9}$$

This observation suggests the enlargement of the $SU(2)$ group. The simplest choice (and the empirically correct one) is the extension $SU(2)\times U(1)$ [3, 4]. The $U(1)$ current reads,

$$\frac{1}{2}J^Y_\mu = \sum_i \left(Y_{L_i}\bar{L}_i\gamma_\mu L_i + Y_{e_{iR}}\bar{e}_{iR}\gamma_\mu e_{iR}\right) \tag{3.10}$$

where the right-handed component of the charged leptons, e_{iR} transform as $SU(2)$ singlets. The as yet undetermined coefficients Y are referred to as hypercharge. Notice the absence of ν_{iR} which, within the confines of the Standard Model, does not exist. Using J^{lep}_μ and J^Y_μ, the electromagnetic current can be written as,

$$J^{em}_\mu = T^3_\mu + \frac{1}{2}Y_\mu \tag{3.11}$$

implying the relation, $Q_{em} = T_3 + \frac{1}{2}Y$, between electric charge and hypercharge (T_3 denotes the eigenvalue of the third component). It is straightforward to see that $Y_{L_i} = -1$ and $Y_{e_{iR}} = -2$. Thus, the leptonic part of the Standard Model with the inclusion of the $SU(2)_L \times U(1)_Y$ gauge bosons, and in the absence of fermion masses reads (the subscript L on the $SU(2)$ gauge group denotes that the weak interaction couples only to

left-handed fields and the subscript Y refers to the $U(1)$ hypercharge gauge group),

$$\mathcal{L}_{lep} = \sum_i \left(\bar{L}_i i\gamma^\mu D_\mu L_i + \bar{e}_{iR} i\gamma^\mu D_\mu e_{iR}\right) - \frac{1}{4} W^a_{\mu\nu} W^{a\mu\nu} - \frac{1}{4} B_{\mu\nu} B^{\mu\nu} \tag{3.12}$$

where

$$D_\mu L_i = (\partial_\mu + ig\frac{1}{2}\tau^a W^a_\mu - ig'\frac{Y_{L_i}}{2} B_\mu) L_i \tag{3.13}$$

$$D_\mu e_{iR} = (\partial_\mu - ig'\frac{Y_{e_{iR}}}{2} B_\mu) e_{iR} \tag{3.14}$$

$$W^a_{\mu\nu} = \partial_\mu W^a_\nu - \partial_\nu W^a_\mu - g\epsilon^{abc} W^b_\mu W^c_\nu \tag{3.15}$$

$$B_{\mu\nu} = \partial_\mu B_\nu - \partial_\nu B_\mu \tag{3.16}$$

The physical gauge bosons - the photon, A_μ, the $W^\pm_\mu$, and the Z^0_μ - are formed from linear combinations of $W^{1,2,3}_\mu$ and B_μ, namely,

$$W^\pm_\mu = \frac{1}{\sqrt{2}} (W^1_\mu \pm i W^2_\mu) \tag{3.17}$$

$$Z^0_\mu = -\sin\theta_W B_\mu + \cos\theta_W W^3_\mu \tag{3.18}$$

$$A_\mu = \cos\theta_W B_\mu + \sin\theta_W W^3_\mu \tag{3.19}$$

with

$$g \sin\theta_W = g' \cos\theta_W = e. \tag{3.20}$$

As discussed in chapter 1, a Dirac fermion mass term of the form $m\bar{\psi}\psi = m(\bar{\psi}_L\psi_R + \bar{\psi}_R\psi_L)$ cannot be written if the individual chiral components transform differently under some gauge group; i.e. the term is not gauge invariant. Since the charged leptons and the weak gauge bosons have mass, the gauge group $SU(2)_L \times U(1)_Y$ must be spontaneously broken, presumably via the Higgs mechanism. In addition to providing the gauge fields with mass, the Higgs scalar, belonging to an $SU(2)$ doublet, can also be coupled to the lepton fields,

$$\mathcal{L}_{\text{Lepton-Yukawa}} = \epsilon_{\alpha\beta} Y^{lep}_{ij} \bar{L}^\alpha_i e_{jR} H^\beta. \tag{3.21}$$

where $\epsilon_{\alpha\beta}$, the totally anti-symmetric symbol, transforms as an $SU(2)$ tensor. Once the Higgs field gains its vacuum expectation value,

$$H = \begin{pmatrix} 0 \\ \frac{1}{\sqrt{2}}(v + h(x)) \end{pmatrix} \tag{3.22}$$

the Lagrangian eq.(3.21) provides a mass-term for the charged leptons, namely,

$$\mathcal{L}_{\text{Lepton-Mass-Term}} = \frac{v}{\sqrt{2}} Y^{lep}_{ij} \bar{e}_{iL} e_{jR} + \text{h.c.} \tag{3.23}$$

while leaving the neutrino massless due to the absence of a ν_R field. Since the neutrinos are massless by construction, and hence degenerate, we can perform an unphysical bi-unitary transformation on the lepton fields, diagonalizing the Yukawa matrix without loss of generality,

$$\mathcal{L}_{\text{Lepton-Mass-Term}} \rightarrow \frac{v}{\sqrt{2}} \sum_i \left(Y^{lep}_{\text{diag}}\right)_{ii} \bar{e}_{iL} e_{iR} = M_{ii} \bar{e}_{iL} e_{iR}. \tag{3.24}$$

The massless neutrinos render no difference between the gauge and mass eigenstates. Therefore, in the Standard Model lepton sector, no non-trivial mixing angles or CP violating phases can exist; unlike the quark sector where all six quark flavours have mass. Moreover, the lepton mass term Lagrangian remains invariant under three global phase transformations - one for each family,

$$L_i \rightarrow e^{i\alpha_i} L_i \;\; ; \;\; e_{iR} \rightarrow e^{i\alpha_i} e_{iR}. \tag{3.25}$$

The Standard Model conserves this phase, interpreted as lepton number, in all perturbative processes.

3.2 Patterns of Neutrino Mass

Thus far we have considered the Standard Model with massless neutrinos. The absence of a right-handed neutrino prevented us from writing Yukawa couplings to the Higgs scalar, generating a Dirac mass term. However, the neutrino holds a special place in particle theory in that the neutrino carries no conserved charge (other than global phase rotation associated with lepton number). This property allows us to construct another type of mass term - the Majorana mass [5]. Let us explore how such a mass term arises. Working in the four component spinor formalism, we adopt the conventions,

$$\begin{aligned} \psi^c &= C\bar{\psi}^T = C\gamma^0\psi^*, \qquad \bar{\psi}^c = \psi^T C \\ \psi_L &= \tfrac{1}{2}(1-\gamma^5)\psi, \qquad \psi_R = \tfrac{1}{2}(1+\gamma^5)\psi. \end{aligned} \tag{3.26}$$

such that

$$\psi = \psi_L + \psi_R \tag{3.27}$$

and where the charge conjugation matrix is defined as $C = -i\gamma^0\gamma^2$. Translating to the two component Van der Warden notation (see Appendix I) we have the translation dictionary,

$$\psi = \begin{pmatrix} \xi_\alpha \\ \bar{\chi}^{\dot{\beta}} \end{pmatrix}; \psi^c = \begin{pmatrix} i\sigma^2(\bar{\chi}^{\dot{\beta}})^* \\ -i\sigma^2(\xi_\alpha)^* \end{pmatrix} = \begin{pmatrix} \chi_\beta \\ \bar{\xi}^{\dot{\alpha}} \end{pmatrix}. \tag{3.28}$$

Also we adopt the notation,

$$\begin{aligned} (\psi_L)^c &= \frac{1}{2}(1+\gamma^5)\psi^c = (\psi^c)_R \equiv \psi^c_R \\ (\psi^c)_L &= \frac{1}{2}(1-\gamma^5)\psi^c = (\psi_R)^c \equiv \psi^c_L. \end{aligned} \tag{3.29}$$

Recall that the Dirac mass term mixes chiralities,

$$\mathcal{L}_{\text{Dirac}} = m_D(\bar{\psi}_L\psi_R + \text{h.c.}) = \frac{m_D}{2}(\bar{\psi}_L\psi_R + \overline{(\psi_L)^c}(\psi_R)^c + \text{h.c.}) = m_D\bar{\psi}\psi \tag{3.30}$$

and as such, only the Dirac mass term provides mass for fermions that carry a conserved $U(1)$ quantity such as electric charge. On the other hand, we can construct other Lorentz invariant mass terms, Majorana masses,

$$\mathcal{L}_{\text{Majorana-T}} = \frac{m_T}{2}\{\overline{(\psi_L)^c}\psi_L + \text{h.c}\} \tag{3.31}$$

$$\mathcal{L}_{\text{Majorana-S}} = \frac{m_S}{2}\{\overline{(\psi_R)^c}\psi_R + \text{h.c.}\} \tag{3.32}$$

We are now in a position to write the most general mass term for a fermionic field - the combined Dirac-Majorana mass,

$$\begin{aligned} \mathcal{L}_{\text{Dirac-Majorana}} &= \frac{1}{2}\left[m_T\overline{(\psi_L)^c}\psi_L + m_S\overline{(\psi_R)^c}\psi_R + m_D(\bar{\psi}_L\psi_R + \overline{(\psi_L)^c}(\psi_R)^c) + \text{h.c}\right] \\ &= \frac{1}{2}\begin{pmatrix} \overline{(\psi_L)^c} & \bar{\psi}_R \end{pmatrix}\begin{pmatrix} m_T & m_D \\ m_D & m_S \end{pmatrix}\begin{pmatrix} \psi_L \\ (\psi_R)^c \end{pmatrix} + \text{h.c.} \end{aligned} \tag{3.33}$$

Diagonalizing this matrix leads to the mass eigenstates. The subscripts on the mass terms require an explanation. The mass term m_D refers to a Dirac mass term, which, by its nature, also conserves $U(1)$ quantum numbers. As we have seen, the Standard Model accommodates such masses by employing a doublet Higgs field with Yukawa couplings to the charged leptons (and quarks). The other terms, m_T and m_S, are Majorana mass terms and transform as an $SU(2)_L$ triplet and an $SU(2)_L$ singlet respectively. It is obvious that both of these mass terms cannot carry a conserved $U(1)$ charge, and, as a

result, these terms violate lepton number by two units. More succinctly, we have

$$L = \begin{pmatrix} \nu_L \\ e_L \end{pmatrix} \sim (\mathbf{2}, -1) \; ; \; e_R \sim (\mathbf{1}, -2) \tag{3.34}$$

implying that,

$$\begin{aligned} \bar{L}e_R &\sim (\mathbf{2}, 1) \times (\mathbf{1}, -2) = (\mathbf{2}, -1) \\ \bar{L}L &\sim (\mathbf{2}, -1) \times (\mathbf{1}, -1) = (\mathbf{1}, -2) + (\mathbf{3}, -2) \end{aligned} \tag{3.35}$$

where the bold face index refers to the lepton field's $SU(2)$ representation and the last index refers to the lepton field's hypercharge.

We now have several options avaliable for constructing neutrino mass terms. Let us consider the simplest case: adding a right-handed neutrino (neutrino singlet), ν_R, to the Standard Model, allowing us to construct the usual Dirac mass term involving Yukawa couplings to the doublet Higgs field,

$$\mathcal{L}_{\text{Dirac-Mass}} = Y_{ij}\delta_{\alpha\beta}\bar{L}_i^{\alpha}H^{*\beta}\nu_{jR} + \text{h.c.} \tag{3.36}$$

(where $i\sigma^2 H^* \sim (\mathbf{2}, -1)$ has been used). If we include only this term for neutrino mass, we immediately encounter a naturalness problem. Phenomenologically, neutrino masses must be in the eV range (for a detailed account see [6]), which would require a Yukawa coupling on the order of $\sim 10^{-11}$ once the Higgs doublet acquires its vacuum expectation value. Such small Yukawa couplings most probably point to an incomplete picture of the underlying theory and, at the very least, implies a theoretically unsatisfying situation. This leaves us with essentially three choices for constructing neutrino mass:

- Extend the Higgs sector
- Extend the lepton sector mass terms
- Extend both the lepton mass terms and the Higgs sector

We have already observed that the Majorana mass term $m_T\overline{(\nu_L)^c}\nu_L$ transforms as an $SU(2)$ triplet. Thus, we may construct a Majorana mass by extending the Standard Model Higgs sector by including a triplet Higgs, $\mathbf{H} \sim (\mathbf{3}, 2)$ (for example see [7]),

$$\tau \cdot \mathbf{H} = \begin{pmatrix} H^+ & \sqrt{2}H^{++} \\ \sqrt{2}H^0 & -H^+ \end{pmatrix}. \tag{3.37}$$

The gauge invariant Yukawa couplings that induce the neutrino mass terms once the

neutral component of **H** acquires a vacuum expectation read,

$$\mathcal{L}_{\text{Triplet-Mass}} = \mathbf{Y}\overline{(L^{\alpha})^{c}}L^{\beta}\mathbf{H}(\epsilon\tau)_{\alpha\beta} + \text{h.c.} \tag{3.38}$$

where the flavour indices have been suppressed and $(\epsilon\tau)_{\alpha\beta}$ is totally symmetric. Again, we are confronted with phenomenological problems with this scenario. The triplet Higgs vacuum expectation contributes to the ρ parameter [7],

$$\rho = \left(\frac{M_W}{M_Z \cos\theta_W}\right)^2 = 1 - 2\frac{v_T^2}{v_D^2} + \mathcal{O}\left(\frac{v_T^4}{v_D^4}\right) + \text{radiative corrections} \tag{3.39}$$

where v_T and v_D refer to the triplet and doublet Higgs vacuum expectation values respectively. Since experimentally the ρ parameter is well known ($\rho_{exp} = 1.00412 \pm 0.00124$) and $v_D \sim 200$ GeV, the triplet Higgs vacuum expectation value is highly constrained, namely $v_H \lesssim 1$ GeV. Assuming that v_H saturates this bound (otherwise we encounter another naturalness problem in explaining the small ratio v_H/v_D) the required Yukawa couplings still remain tiny, $Y \sim 10^{-9}$. Again, the solution appears theoretically unsatisfying.

This leads us to perhaps the most elegant and natural method for providing neutrinos with small mass terms: the see-saw mechanism [8, 9]. It its minimal form, this scenario only extends the lepton sector physics by including a neutrino singlet Majorana mass m_S while leaving m_T absent. Since the neutrino singlet lacks any Standard Model quantum numbers, its Majorana mass, $m_S\bar{\nu}_R^c\nu_R$, is unconstrained and should naturally be near the cutoff of the quantum field theory, presumably $m_S \sim M_{\text{GUT}} \sim 10^{16}$GeV. In this case the Yukawa coupling becomes,

$$\mathcal{L}_{\text{see-saw}} = \mathbf{Y}^N\delta_{\alpha\beta}\bar{L}^{\alpha}H^{*\beta}\nu_R + m_S\overline{(\nu_R)^c}\nu_R + \text{h.c.} \tag{3.40}$$

where again, flavour indices have been suppressed. Once the doublet Higgs acquires a vacuum expectation value, we may re-write this expression as

$$\mathcal{L}_{see-saw} = \frac{1}{2}\left[\begin{pmatrix} \overline{(\nu_L)^c} & \bar{\nu}_R \end{pmatrix}\begin{pmatrix} 0 & \mathbf{m}_D^T \\ \mathbf{m}_D & \mathbf{m}_S \end{pmatrix}\begin{pmatrix} \nu_L \\ (\nu_R)^c \end{pmatrix} + \text{h.c.}\right] \tag{3.41}$$

where $\mathbf{m}_D = v_D(\mathbf{Y})$. Assuming that $m_D \sim m_{\text{lepton}}$ and that $m_S \sim M_{\text{GUT}}$, diagonalizing the matrix in eq.(3.41) will provide the left-handed neutrinos with tiny Majorana masses,

$$\mathbf{m}_\nu = \mathbf{m}_D^T\mathbf{m}_s^{-1}\mathbf{m}_D. \tag{3.42}$$

Strictly speaking, ν_L is not a mass eigenstate. However, considering the large discrepancy between the eigenvalues in the mass matrix eq.(3.42), ν_L closely approximates the

mass eigenstate. The see-saw mechanism also fits nicely with supersymmetry. Supersymmetry provides, perhaps, the most natural framework for the see-saw mechanism as the introduction of a heavy neutrino singlet only compounds the hierarchy problem of the Standard Model. Using the notation of chapter 2, the neutrino singlet extension of the MSSM lepton sector reads

$$\begin{aligned} W_{\text{MSSM-RN}} &= \epsilon_{ab} H_d^a \mathbf{E} \mathbf{Y}_{\text{E}} \mathbf{L}^b + \epsilon_{ab} H_d^a \mathbf{D} \mathbf{Y}_{\text{D}} \mathbf{Q}^b + \mathbf{Y}_\nu \epsilon_{ab} H_u^a \mathbf{N} \mathbf{L}^b \\ &\quad + \epsilon_{ab} H_u^a \mathbf{U} \mathbf{Y}_{\text{U}} \mathbf{Q}^b + \mu \epsilon_{ab} H_u^a H_d^b + \frac{1}{2} \mathcal{M} \mathbf{N} \mathbf{N} \end{aligned} \tag{3.43}$$

with the addition terms in the soft supersymmetry breaking Lagrangian displayed in Appendix III. As in the non-supersymmetric counter part, the light neutrinos acquire their mass once the heavy neutrino singlets are integrated out and once Higgses acquire their vacuum expectation values.

It should be acknowledged that there exists other methods that induce a neutrino mass term. Examples include scalar see-saw mechanisms, further extensions of the Higgs sector, Majoron models that spontaneously break lepton number, and models with radiatively induced neutrino mass (see [6] for an exhaustive treatment). Regardless of the underlying UV complete theory involved, from the point of view of the Standard Model, the effective Majorana neutrino mass term appears as the dimension five operator,

$$\mathcal{L}_{eff} = \frac{f}{\Lambda} LLHH + \text{h.c.} \tag{3.44}$$

where f is a dimensionless constant assumed to be of order one, and Λ is the scale of new physics (flavour and $SU(2)$ indices have been suppressed). In the effective field theory framework, we should eventually expect such an operator to arise as no gauge symmetry forbids it. Since this dimension five operator first appears beyond the renormalizable dimension four interactions of the Standard Model, we might naively expect that the discovery of neutrino mass should be the first signal of physics beyond the Standard Model. In addition to the direct consequences of neutrino mass (such as neutrino oscillations, which we discuss in the next section), neutrino mass can also induce other operators that violate lepton flavour. If the neutrino masses are non-degenerate with non-trivial mixings, diagrams of the form shown in Figure (3.1) give rise to the lepton flavour violating (LFV) interaction $\mu \to e, \gamma$. Neutrino mass also allows other Standard Model forbidden processes such as $\tau \to \mu, \gamma$, $\tau \to e, \gamma$, and neutrinoless double beta decay (see [6] for more processes and further details). The process $\mu \to e, \gamma$, considered in Figure(3.1), where we augment the Standard Model by including neutrino mass and where we assume that the neutrino masses are on the order of an eV, leads to the hopelessly unobservable

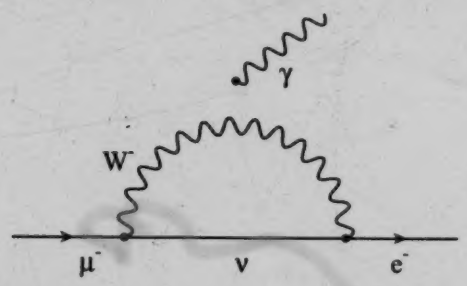

Figure 3.1: Feynman diagrams that contribute to the process $\mu \to e\gamma$.

branching ratio [10, 11, 12],

$$B(\mu \to e\gamma) = \frac{\Gamma(\mu \to e\gamma)}{\Gamma(\mu \to e\nu\bar{\nu})} = \frac{3G_F}{\sqrt{2}(32\pi)} \left(\sum_i U_{ei}^* U_{\mu i} (m_i^2/M_W^2) \right)^2 \lesssim 10^{-40}. \quad (3.45)$$

As we will see in Part II, the situation for $\mu \to e\gamma$ changes drastically in the context of supersymmetry.

3.3 Neutrino Oscillations: Experimental Evidence for Neutrino Mass

At present, the solar neutrino, and atmospheric neutrino, deficit observations coupled with confirmation from reactor, and accelerator, experiments provide the only direct evidence for physics beyond the Standard Model [13, 14, 15, 16, 17, 18, 19, 20, 21, 22, 23, 24, 25, 26, 27]. These observations imply that neutrinos oscillate between flavour states providing convincing evidence of neutrino mass. As we noted in section 1, no non-trivial mixing angles or CP violating phases exist within the lepton sector of the Standard Model - all three neutrinos have vanishing mass. If we consider the possibility of non-degenerate massive neutrinos, the weak eigenstates and the gauge eigenstates no longer align. Thus we expect the appearance of a non-trivial CKM-like matrix, called the Pontecorvo-Maki-Nakagawa-Sakata (PMNS) matrix [28, 29], in the lepton sector. As a consequence, the principles of quantum mechanics tell us that a neutrino prepared in a gauge eigenstate is a superposition of the neutrino's mass eigenstates. Thus, neutrinos may oscillate between different flavours [28, 29, 30]. Let us explore this phenomenon in more detail. In the vacuum the time dependence of a neutrino flavour state may be

written as,

$$|\nu^\alpha(t)\rangle = \sum_i U_{\alpha i} \exp(-iE_i t)\,|\nu^i\rangle \tag{3.46}$$

where α and i refer to the flavour state and the mass eigenstate respectively and the unitary matrix U connects these states. The transition amplitude reads,

$$\langle\nu^\beta|\nu^\alpha\rangle_t = \sum_i U_{\alpha i} U^\dagger_{i\beta} \exp(-iE_i t) \tag{3.47}$$

and assuming small neutrino masses ($|\mathbf{p}| \gg m_i$), we can make the approximation

$$E_i = \sqrt{p^2 + m_i^2} \approx p + \frac{m_i^2}{2E}. \tag{3.48}$$

For illustrative purposes, let us consider only two generations. With the aid of eq.(3.47), we may write

$$|\nu^\alpha(t)\rangle \approx e^{-ipt} U \begin{pmatrix} 1 - i\frac{m_1^2}{2E}t & 0 \\ 0 & 1 - i\frac{m_2^2}{2E}t \end{pmatrix} U^\dagger |\nu^\beta\rangle \tag{3.49}$$

where the state $|\nu^\beta\rangle$ is prepared at some initial time. In light of $U^\dagger m^\dagger m U = m^2_{diag}$, we obtain

$$|\nu^\alpha(t)\rangle \approx e^{-ipt} \left[\exp\left(-i\frac{m^\dagger m}{2E}t\right)\right]_{\alpha\beta} |\nu^\beta\rangle \tag{3.50}$$

which, up to a phase, reduces to the Schrodinger equation,

$$i\frac{d}{dt}|\nu^\alpha(t)\rangle \approx \frac{m^\dagger m}{2E}|\nu^\alpha\rangle. \tag{3.51}$$

We should note that, since the expressions contain $m^\dagger m$ and not $m^T m$, a neutrino oscillation experiment cannot distinguish between Dirac and Majorana mass terms. Oscillation experiments only imply masses and mixings. In the two generation case we may take

$$U = \begin{pmatrix} \cos\theta & \sin\theta \\ -\sin\theta & \cos\theta \end{pmatrix} \tag{3.52}$$

without loss of generality. Using this expression for U we have,

$$\begin{aligned} U m^2_{diag} U^\dagger &= \begin{pmatrix} m_1^2\cos^2\theta + m_2^2\sin^2\theta & \frac{1}{2}(m_2^2 - m_1^2)\sin 2\theta \\ \frac{1}{2}(m_2^2 - m_1^2)\sin 2\theta & m_1^2\sin^2\theta + m_2^2\cos^2\theta \end{pmatrix} \\ &= \frac{m_1^2 + m_2^2}{2} + \frac{\Delta m^2}{2}\begin{pmatrix} -\cos\theta & \sin 2\theta \\ \sin 2\theta & \cos\theta \end{pmatrix}. \end{aligned} \tag{3.53}$$

where $\Delta m^2 = m_2^2 - m_1^2$. This allows us to re-write eq.(3.50) as,

$$|\nu(t)^\alpha\rangle = \exp\left\{-i\left(p + \frac{m_1^2 + m_2^2}{4E}t\right)\right\}\left[\exp\left(-i\frac{\Delta m^2}{4E}\tau^a r^a t\right)\right]_{\alpha\beta}|\nu^\beta\rangle \tag{3.54}$$

where τ^a are the Pauli matrices and $r^a = (\sin 2\theta, 0, -\cos 2\theta)$. Finally, we find, up to irrelevant phase factors,

$$|\nu(t)^\alpha\rangle = \begin{pmatrix} \cos\frac{\Delta m^2}{4E}t - i\sin\frac{\Delta m^2}{4E}t\cos 2\theta & -i\sin\frac{\Delta m^2}{4E}t\sin 2\theta \\ -i\sin\frac{\Delta m^2}{4E}t\sin 2\theta & \cos\frac{\Delta m^2}{4E}t + i\sin\frac{\Delta m^2}{4E}t\cos 2\theta \end{pmatrix}|\nu^\beta\rangle. \tag{3.55}$$

Denoting the electron flavour state as $(1,0)^T$ and the muon flavour state as $(0,1)^T$, we find

$$\langle\nu^e|\nu^e\rangle_t = \cos\frac{\Delta m^2}{4E}t - i\sin\frac{\Delta m^2}{4E}t\cos 2\theta \tag{3.56}$$

leading to the transition probabilities,

$$\begin{aligned} P_{\nu_e\to\nu_e} &= |\langle\nu^e|\nu^e\rangle|^2 = 1 - \sin^2\theta\sin^2\frac{\Delta m^2}{4E}t \\ P_{\nu_e\to\nu_\mu} &= \sin^2 2\theta\sin^2\frac{\Delta m^2}{4E}t. \end{aligned} \tag{3.57}$$

In the case of N generations, the transition probability reads,

$$P_{\nu_e\to\nu_e} = 1 - \sum_{i,j} 4\,|U_{ei}|^2\,|U_{ej}|^2\sin^2\frac{\Delta m_{ij}^2}{4E}t \tag{3.58}$$

and in the case of three generations an Iwasawa decomposition in general leads to the introduction of two additional CP violating phases (for review see [31]). Taking $c = 1$, the length defined by

$$L_0 = \pi\frac{4E}{\Delta m^2}, \tag{3.59}$$

called the oscillation length, allows us to re-write the transition probability as,

$$P_{\nu_e\to\nu_e} = 1 - \sin^2 2\theta\sin^2\left(\pi\frac{x}{L_0}\right) \tag{3.60}$$

where $x = t$ defines the distance from the source generating the neutrino flux. For $x \gg L_0$ the sine-squared function averages to one half, leading to,

$$P_{\nu_e\to\nu_e} = 1 - \frac{1}{2}\sin^2 2\theta. \tag{3.61}$$

At this point we should bear in mind that the oscillation effect inherently results

from the superposition principle of quantum mechanics. As such, the appropriate treatment should include a derivation of the oscillation phenomena within the wave-packet formalism [32, 33]. However, the more rigorous treatment leads to the same results. Importantly, remember that if the energy and momentum are measured with sufficient accuracy, the transition between neutrino states cannot occur. Let us expand on this point. If the error in $m_\nu = \sqrt{E_\nu^2 - |\mathbf{p}_\nu|^2}$, δm_ν, is smaller than the mass splitting Δm_ν, then $|\mathbf{p}_\nu|$ must be measured with an accuracy of $\delta|\mathbf{p}_\nu|$ such that,

$$\Delta m^2 \gg \delta m_\nu^2 = \frac{\partial m_\nu}{\partial(|\mathbf{p}_\nu|)}\delta|\mathbf{p}_\nu| = 2|\mathbf{p}_\nu|\delta|\mathbf{p}_\nu|. \tag{3.62}$$

By the uncertainty principle, the position becomes undetermined on the order of $(\delta x)(\delta|\mathbf{p}_\nu|) > h/2\pi$ which implies (taking $h/2\pi = 1$)

$$\delta x > \frac{2|\mathbf{p}_\nu|}{\Delta m^2} = \frac{L_0}{2\pi}. \tag{3.63}$$

In this case, the position becomes undetermined on the order of the oscillation length and thus the oscillation pattern vanishes. Instead, the oscillation phenomenon reduces to eq.(3.61) which simply indicates that either of the mass eigenstates selected by the observation is the incoherent sum of the two weak eigenstates. The loss of the oscillation pattern also occurs if the origin of the beam is sufficiently localized and again leads to eq.(3.61).

Thus far, we have discussed neutrino oscillations in vacua, however, matter effects also play a role in the neutrino oscillation phenomenon. At tree level, in matter, ν^e interacts via both the charged and neutral currents while ν^μ and ν^τ interact exclusively through the neutral current [34]. This difference in the interaction type alters the effective Hamiltonian, leading to a coherent effect, called the MSW effect [34, 35, 36, 37], which may radically alter the oscillation pattern. Let us examine the MSW effect in more detail.

Due to the extra contributions that ν^e receives from interacting with electrons in matter relative to the other neutrino flavours, the Schrodinger equation becomes (again assuming two generations for illustrative purposes),

$$i\frac{d}{dt}\begin{pmatrix}\nu^e\\ \nu^\mu\end{pmatrix} = \begin{pmatrix} -\frac{\Delta m^2}{4E}\cos 2\theta + \sqrt{2}G_F n_e & \frac{\Delta m^2}{4E}\sin 2\theta \\ \frac{\Delta m^2}{4E}\sin 2\theta & \frac{\Delta m^2}{4E}\cos 2\theta \end{pmatrix}\begin{pmatrix}\nu^e\\ \nu^\mu\end{pmatrix} \tag{3.64}$$

where the term $\sqrt{2}G_F n_e$ modifies the original effective Hamiltonian, where n_e denotes the electron number density in matter and where G_F refers to the Fermi constant.

Diagonalizing the Hamiltonian,

$$\begin{pmatrix} \nu^e \\ \nu^\mu \end{pmatrix} = \begin{pmatrix} \cos\tilde{\theta} & \sin\tilde{\theta} \\ -\sin\tilde{\theta} & \cos\tilde{\theta} \end{pmatrix} \begin{pmatrix} \tilde{\nu}^1 \\ \tilde{\nu}^2 \end{pmatrix}, \tag{3.65}$$

where $\tilde{\nu}^{1,2}$ denote energy eigenstates in matter, we obtain

$$\cos 2\tilde{\theta} = \frac{-2\sqrt{2}EG_F n_e/\Delta m^2 + \cos 2\theta}{\sqrt{\left(-2\sqrt{2}EG_F n_e/\Delta m^2 - \cos 2\theta\right)^2 + \sin^2 2\theta}} \tag{3.66}$$

$$\sin 2\tilde{\theta} = \frac{\sin 2\theta}{\sqrt{\left(-2\sqrt{2}EG_F n_e/\Delta m^2 - \cos 2\theta\right)^2 + \sin^2 2\theta}}. \tag{3.67}$$

with energy eigenvalues,

$$\tilde{m}^2_{1,2} = \frac{\sqrt{2}EG_F n_e}{2} \mp \frac{1}{2}\sqrt{(\sqrt{2}EG_F n_e - \Delta m^2\cos 2\theta)^2 + (\Delta m^2)^2 \sin^2 2\theta}. \tag{3.68}$$

Furthermore, the oscillation length in matter reads,

$$\tilde{L}_0 = \frac{4\pi E}{\tilde{m}^2_2 - \tilde{m}^2_1} = \frac{4\pi E}{\Delta m^2} \frac{1}{\left[\left(\sqrt{2}EG_F n_e/\Delta m^2 - \cos 2\theta\right)^2 + \sin^2 2\theta\right]^{\frac{1}{2}}} \tag{3.69}$$

which becomes much shorter than the oscillation length in vacua, L_0, as n_e becomes large. Notice that a resonance behaviour appears in eq.(3.67) when $\sqrt{2}EG_F n_e/\Delta m^2$ approaches $\cos 2\theta$ causing $\sin 2\tilde{\theta}$ to approach unity (i.e. $\tilde{\theta} = \pi/4$) regardless of the value of θ. We can re-state the resonance condition in terms of a critical electron number density,

$$n_e^{crit} = \frac{1}{2\sqrt{2}G_F}\frac{\Delta m^2}{E}\cos 2\theta. \tag{3.70}$$

At the critical density, the two neutrinos mix maximally. The MSW effect is particularly relevant to the study of solar neutrinos as the current favoured solution to the combined solar, atmospheric, and reactor neutrino deficit observations is the LMA (Large Mixing Angle)-MSW solution [38, 39]. In this scenario, a region exists inside the sun where $n_e = n_e^{crit}$, causing the MSW effects as the solar neutrino flux emerges. In addition, there are also subtle effects governing the conversion process that depend on the width of the resonance region (and hence the sun's density profile) as compared to the oscillation length. Detailed analysis of these effects can be found in [6] and references therein. The combined data also suggests that the mixing angles of the PMNS matrix are large (unlike the CKM matrix of the quark sector). Furthermore, the MSW effect may also play a small role with neutrino flux passing through the earth, appearing as a diurnal

asymmetry for the solar neutrinos.

3.4 The Prototype GUT: $SU(5)$

While the Standard Model has proven to be an excellent description of low energy particle interactions (energies up to ~ 100 GeV), the framework leaves us with some unsettling issues. As already discussed in chapter 2, the Standard Model suffers from a hierarchy problem, for which supersymmetry provides a natural solution. However, there are a number of other curious puzzles. One is that the fermion content is spread out among five different representations of the Standard Model gauge groups $SU(3)_c \times SU(2)_L \times U(1)_Y$, namely,

$$f_L = N_G \left[\left(\mathbf{3}, \mathbf{2}, \frac{1}{3} \right) + \left(\bar{\mathbf{3}}, \mathbf{1}, -\frac{4}{3} \right) + \left(\bar{\mathbf{3}}, \mathbf{1}, \frac{2}{3} \right) + (\mathbf{1}, \mathbf{2}, -1) + (\mathbf{1}, \mathbf{1}, 1) \right] \tag{3.71}$$

where the first two entries refer to the multiplicities of the $SU(3)_c$ and $SU(2)_L$ groups respectively, the last entry refers to the hypercharge assignment, and N_G refers to the number of generations. The Standard Model provides no explanation for charge quantization (the $U(1)_Y$ quantum numbers are assigned by hand), nor the relative ratio between the strong and the electromagnetic coupling constants, nor the fortuitous and somewhat magical anomaly cancellation that occurs generation by generation [40]. Further to these issues, the Standard Model contains 19 free parameters that must be determined by observation. In light of the recently confirmed observation of neutrino oscillations [13, 14, 15, 16, 17, 18, 19, 20, 21, 22, 23, 24, 25, 26, 27], it appears that, at the very least, the Standard Model must be amended with additional particle content and probably with a new energy scale. These are only some of the curious issues that beg for a more complete explanation.

A unified framework with a universal coupling constant exists if we embed the Standard Model into a semi-simple gauge group (or possibly the product of identical simple groups with the same coupling constant) of at least rank four (for reviews see [41, 42]). That is, since the Standard Model contains four mutually diagonalizable generators, we require a gauge group with at least four mutually commuting generators. If we wish to avoid vector-like theories that introduce heavy mirror fermions, we will also require a Lie group that admits complex representations since $f_L \neq f_R$. Perhaps the simplest group that fulfills these basic requirements is the semi-simple Lie group $SU(5)$ [43]. Let us explore to what extent $SU(5)$ may address the shortcomings of the Standard Model.

First we note that the fermions of the Standard Model can be assigned to representations of $SU(5)$. Since the $SU(3)_c \times SU(2)_L$ content of the $\mathbf{5}$, $\bar{\mathbf{5}}$ and the $\mathbf{10}$ of $SU(5)$

breaks down as,

$$\mathbf{5} = (\mathbf{3},\mathbf{1}) + (\mathbf{1},\mathbf{2}) \tag{3.72}$$

$$\bar{\mathbf{5}} = (\bar{\mathbf{3}},\mathbf{1}) + (\mathbf{1},\mathbf{2}) \tag{3.73}$$

$$\mathbf{10} = (\bar{\mathbf{3}},\mathbf{1}) + (\mathbf{3},\mathbf{2}) + (\mathbf{1},\mathbf{2}) \tag{3.74}$$

we see that these representations can hold all fifteen two component left-handed Weyl fermions of eq.(3.71). In particular, we have,

$$\bar{\mathbf{5}} : (\psi^i)_L = \begin{pmatrix} d_L^{c1} \\ d_L^{c2} \\ d_L^{c3} \\ e_L \\ \nu_L^e \end{pmatrix} \tag{3.75}$$

(where the indices on the quark fields refer to $SU(3)$ colour) and

$$\mathbf{10} : (\chi_{ij})_L = \frac{1}{\sqrt{2}} \begin{pmatrix} 0 & u_L^{c3} & -u_L^{c2} & u_{1L} & d_{1L} \\ -u_L^{c3} & 0 & u_L^{c1} & u_{2L} & d_{2L} \\ u_L^{c2} & -u_L^{c1} & 0 & u_{3L} & d_{3L} \\ -u_{1L} & -u_{2L} & -u_{3L} & 0 & e_L^c \\ -d_{1L} & -d_{2L} & -d_{3L} & -e_L^c & 0 \end{pmatrix}. \tag{3.76}$$

The $SU(5)$ tensors ψ_i, χ_{ij} have been introduced with the upper and lower components distinguishing each representation from its complex conjugate. For more details on group theory and Lie algebras for particle physics see [44, 45].

Given that we have decided on the fermion representations in $SU(5)$, at this point we must address anomaly cancellation. As the Standard Model is a chiral gauge theory, the axial-vector current can couple with two gauge bosons at the one loop level through triangle diagrams [46, 47]. These diagrams threaten current conservation, a prerequisite for renormalizable gauge theories, and moreover, these diagrams violate the Ward identities associated with the amplitude for the process. In fact, the anomaly associated with any chiral gauge theory can be stated (see [44, 45]) in terms of the generators of the gauge group in the representation of the fermions,

$$\mathrm{Tr}\left(\{T^a(R), T^b(R)\}T^c(R)\right) = \frac{1}{2}A(R)d^{abc} \tag{3.77}$$

where d^{abc} is an invariant tensor defined by,

$$\frac{1}{2}\{T^a, T^b\} = d^{abc}T^c. \tag{3.78}$$

In order for the gauge anomaly to vanish, and hence preserve renormalizability, the fermion representations must be chosen such that $\sum_R A(R) = 0$ or the gauge group itself must have $A(R) = 0$ for all R. The Standard Model accomplishes anomaly cancellation, generation by generation, through the peculiarities of the weak quantum number assignments [40, 48]. In $SU(5)$, anomaly cancellation occurs since $A(\bar{\mathbf{5}}) + A(\mathbf{10}) = 0$. Just as in the Standard Model, anomaly cancellation in $SU(5)$ occurs due to the specifics of the fermion representations. While the $SU(5)$ GUT reduces the number of representations required for the fermions as compared to the Standard Model, $SU(5)$ offers no essential further insight as to the origin of anomaly cancellation.

As noted in Chapter 1, the gauge fields must belong to the adjoint representation of the gauge group, which in the $SU(5)$ case is $5^2 - 1 = 24$ dimensional. The **24** adjoint representation of $SU(5)$ breaks down under $SU(3)_c \times SU(2)_L$ as,

$$\mathbf{24} : (A^i_j) = (\mathbf{8},\mathbf{1}) + (\mathbf{1},\mathbf{3}) + (\mathbf{1},\mathbf{1}) + (\mathbf{3},\mathbf{2}) + (\bar{\mathbf{3}},\mathbf{2}). \tag{3.79}$$

We immediately identify $(\mathbf{8},\mathbf{1})$, $(\mathbf{1},\mathbf{3})$, and $(\mathbf{1},\mathbf{1})$ with the gauge bosons of the Standard Models - namely, the $SU(3)_c$ gluons, the $SU(2)_L$ vector fields $\mathbf{W}$, and the $U(1)_Y$ B-field. This leaves us with twelve remaining gauges fields that belong to the $(\mathbf{3},\mathbf{2})$ and the $(\bar{\mathbf{3}},\mathbf{2})$,

$$A^j_\alpha = (X_\alpha, Y_\alpha) \tag{3.80}$$

$$A^\alpha_j = (X^\alpha, Y^\alpha)^T \tag{3.81}$$

where the Latin and Greek indices refer to $SU(2)_L$ and $SU(3)_c$ components respectively. We will discuss these additional gauge fields in a moment.

The simple gauge group $SU(5)$ offers a simple explanation for electric charge quantization. Since electric charge is an additive quantum number, the charge operator, Q, must be some linear combination of the diagonal generators of $SU(5)$. In particular, since

$$Q = T_3 + \frac{Y}{2} \tag{3.82}$$

is the charge operator of the Standard Model, we require a linear combination of the diagonal generators of $SU(5)$ that belong to the $SU(2)_L$ and $U(1)$ subgroups, namely,

$$Q = \frac{1}{2}(T_3 + cT_0). \tag{3.83}$$

with the $SU(5)$ generators T_3 and T_0 defined by,

$$T_3 = \text{diag}(0,0,0,1,-1) \tag{3.84}$$

$$T_0 = \frac{1}{\sqrt{15}}\text{diag}(-2,-2,-2,3,3) \tag{3.85}$$

and c of eq.(3.83) is a normalization constant that maps T_0 to Y. A priori the commutation relations, $[T_a/2, T_b/2] = if_{abc}T_c/2$, fix the normalization of the $SU(5)$ generators and this normalization does not correspond to the normalization of Standard Model hypercharge. By examining the charges of the fermions of the $\mathbf{5}$, clearly $c = -\sqrt{(5/3)}$. Since the charge operator of $SU(5)$ contains discrete eigenvalues, charge automatically becomes quantized. Specifically, the charge operator in the fundamental representation reads,

$$Q = \text{diag}\left(-\frac{1}{3}, -\frac{1}{3}, -\frac{1}{3}, 1, 0\right). \tag{3.86}$$

Determining the charges of other representations becomes straightforward by recognizing that any $SU(5)$ tensor $\psi^{ij\ldots}_{kl\ldots}$ shares the same quantum numbers as $\psi^i\psi^j\psi_k\psi_l\ldots$. Thus, for the adjoint representation we have,

$$Q(A^i_j) = Q_i - Q_j \tag{3.87}$$

which, when applied to the gauge fields of $SU(5)$ tells us that not only do the twelve additional gauge fields carry colour, but that they also carry fractional electric charge, $Q(X) = -4/3$ and $Q(Y) = -1/3$. These gauge bosons transform quarks into leptons and up-like quarks into down-like quarks (and vice-versa). Thus the X and Y bosons violate baryon number, B, and lepton number, L and for this reason, the X and Y bosons are often referred to as lepto-quarks. Various baryon and lepton number violating processes are induced by the new $SU(5)$ gauge bosons - including operators that give rise to nucleon decay [49, 50, 51]. As these exotic gauge bosons have not been observed, nor their baryon or lepton number violating induced processes, they must have acquired larger (presumably GUT scale) masses when $SU(5)$ spontaneously broke to the Standard Model. Incidentally, $SU(5)$ accidentally preserves the combination $B - L$, a point to which we will return to shortly.

Spontaneously breaking $SU(5)$ down to the Standard Model through the Higgs mechanism is an involved process. Let us consider breaking $SU(5)$ in stages (see [41, 42]) as, $SU(5) \to SU(3)_c \times SU(2)_L \times U(1)_Y \to SU(3)_c \times U(1)_{em}$. Since the initial breaking occurs at $M_{GUT} \sim 10^{16}$ GeV, it will be difficult to experimentally distinguish between particular Higgs manifestations - assuming that the GUT hypothesis is correct. However, let us briefly describe one, perhaps minimal, mechanism. Using an adjoint and

fundamental representation of Higgs scalars, namely, $\tilde{H}^i_j$ and H_i, it can be shown that,

$$SU(5) \rightarrow^{\langle \tilde{H} \rangle \sim M_{GUT}} SU(3)_c \times SU(2)_L \times U(1)_Y \rightarrow^{\langle H \rangle \sim \sqrt{G_F}} SU(3)_c \times U(1)_Y \quad (3.88)$$

with the Higgs potential,

$$V(\tilde{H}, H) = V(\tilde{H}) + V(H) + \lambda_4 \left(\mathrm{Tr}\tilde{H}^2\right)\left(H^\dagger H\right) + \lambda_5 \left(H^\dagger \tilde{H}^2 H\right) \quad (3.89)$$

where

$$V(\tilde{H}) = -m_1^2 \left(\mathrm{Tr}\tilde{H}^2\right) + \lambda_1 \left(\mathrm{Tr}\tilde{H}^2\right)^2 + \lambda_2 \left(\mathrm{Tr}\tilde{H}^4\right) \quad (3.90)$$

$$V(H) = -m_2^2 \left(H^\dagger H\right) + \lambda_3 \left(H^\dagger H\right)^2. \quad (3.91)$$

As we can see, the Higgs potential is already more complicated than the Standard Model and we have yet to discuss fermions. The adjoint of Higgs, $\tilde{H}$, provides the large masses for the X and Y gauge bosons by acquiring a vacuum expectation value while leaving the twelve Standard Model gauge bosons massless. The Standard Model weak gauge bosons acquire their mass through the vacuum expectation value of the $SU(2)$ doublet contained in the fundamental of Higgs and the cross terms in the Higgs potential ensures that the Higgs triplet of the fundamental obtains a large ($\sim M_{GUT}$) mass. Problematically, we have a huge disparity of mass scales, namely the difference between the adjoint Higgs vacuum expectation value and the weak scale vacuum expectation value in the fundamental Higgs. Quantum corrections drive the mass of the light Higgs mass toward the high scale, which requires a fine tuning to rectify. In fact, this is simply a reincarnation of the gauge hierarchy problem that we discussed in chapter 2. Again, perhaps the most natural solution is to embed the grand unified theory framework in supersymmetry. As we noted at the end of chapter 2, consistent coupling constant unification can be achieved bottom-up using the MSSM field content. Thus, we are naturally led to supersymmetric GUTs which have restrictive (and rich) low energy phenomenological predictions e.g. [52, 53] (for reviews [41, 42]).

Since the fermions of $SU(5)$ transform as $\bar{\mathbf{5}} + \mathbf{10}$, mass terms can be constructed by observing that,

$$\bar{\mathbf{5}} \times \mathbf{10} = \mathbf{5} + \overline{\mathbf{45}} \quad (3.92)$$

$$\mathbf{10} \times \mathbf{10} = \bar{\mathbf{5}} + \mathbf{45} + \mathbf{50} \quad (3.93)$$

$$\bar{\mathbf{5}} \times \bar{\mathbf{5}} = \overline{\mathbf{10}} + \overline{\mathbf{15}}. \quad (3.94)$$

Since these tensor products do not contain the singlet representation, fermion masses

must arise from spontaneous symmetry breaking just as in the Standard Model. Furthermore, the Higgs representations we have considered thus far, only H, which transforms as a fundamental, (i.e. $H \sim \mathbf{5}$) which contains the weak $SU(2)$ doublet is suitable for fermion mass construction. The adjoint representation, $\tilde{H}$, fortunately does not couple to the fermions as $\langle \tilde{H} \rangle$ would provide the fermions with unacceptable GUT scale masses. In non-minimal incarnations, we could also use a **45** of Higgses to construct fermion masses. The other possible representations are unsuitable since they lack a colour singlet direction. Thus, using the minimal Higgs content, may write the Yukawa sector symbolically as,

$$\mathcal{L}_{\text{Yukawa}} = Y_U \mathbf{10} \cdot \bar{\mathbf{5}} \cdot \bar{\mathbf{5}}_H + Y_D \mathbf{10} \cdot \mathbf{10} \cdot \mathbf{5_H} + \text{h.c.} \tag{3.95}$$

where all flavour and group indices have been suppressed. After symmetry breaking, the Yukawa Lagrangian predicts,

$$m_e = m_d \tag{3.96}$$

$$m_\mu = m_s \tag{3.97}$$

$$m_\tau = m_b \tag{3.98}$$

near the unification scale. These relations are subject to renormalization group flow which corrects these values at the weak scale. For example, after renormalization group running and assuming three generations, the last relation, $m_\tau = m_b$ becomes the approximately correct relation [54],

$$m_\tau(m_Z) \approx \frac{1}{2.2} m_b(m_Z). \tag{3.99}$$

The expressions for the lighter fermions are also corrected, but the predictions are less successful owing in part to non-perturbative effects that govern the lighter quark masses.

One of the motivating factors behind grand unification is a context for coupling constant unification which would explain the ratios between all the coupling constants of the Standard Model. In the $SU(5)$ GUT, the covariant derivative appears as

$$D_\mu = \partial_\mu + i g_5 A_\mu^a \frac{T^a}{2} \tag{3.100}$$

where g_5 represents the universal coupling constant such that,

$$g_5 = g_3 = g_2 = g_1. \tag{3.101}$$

In eq.(3.101) we identify g_3 as the strong coupling constant, g_2 as the weak coupling

constant, and $g_1 = \sqrt{5/3}g'$ with the $U(1)_Y$ hypercharge coupling constant g'. As we saw in detail in chapter 2, the renormalization group equations imply that each coupling scales logarithmically with energy, resulting in a unification scale of $\sim 10^{16}$ GeV. Presumably, the different renormalization group equations of section 2.5, describing separate trajectories for each coupling constant, result after the grand unified group, in this case $SU(5)$, spontaneously breaks and the heavy gauge bosons are integrated out. At the unification scale, it can be shown (see for example [41]) that the Weinberg angle is uniquely determined,

$$\sin^2\theta_w = \frac{g'^2}{g^2 + g'^2} = \frac{3}{8} \tag{3.102}$$

and its prediction at the low scale after renormalization group running becomes a test of the model. As we demonstrated in section 2.5, consistent unification is possible in a supersymmetric framework, which provides yet another motive for embedding the grand unified theories in supersymmetry.

Conspicuously, we have thus far ignored neutrino mass. As we learned in the previous sections, there now exists compelling evidence that neutrinos have mass. Let us explore how $SU(5)$ might accommodate this empirical fact. One option would be to look for an $I = 1$ Higgs field that can couple to the fermions, providing a Majorana mass term for the neutrinos. Unfortunately, in the minimal $SU(5)$ model under discussion, only the **24** contains an $I = 1$ Higgs field, and, as we have already learned, the adjoint of Higgs scalars does not couple to the fermions. Furthermore, we have already noted that $SU(5)$ conserves $B - L$ globally which prevents a Majorana mass term of the form $M_L\nu_L\nu_L$. However, we are free to add a neutrino singlet field, ν_R, by hand, placing the field in the **1** of $SU(5)$. A large gauge invariant Majorana mass term, $M_R\nu_R\nu_R$, could then be written down and the see-saw mechanism could then be employed to provide the ν_Ls with Majorana mass. While this procedure violates global $B - L$, we should naturally expect that eventually this accidental symmetry would be broken by higher dimensional operators. As $SU(5)$ provides no explanation for a right handed mass term, presumably the UV completion will also explain the violation of $B - L$. In a very real sense, neutrino mass implies physics beyond $SU(5)$ for GUT model building.

Let us briefly return to the subject of anomalies. We observed that the fermion representation of the Standard Model and $SU(5)$ preserved vector and axial-vector current conservation by canceling all the associated triangle diagrams. With just the Standard Model fermion content, other currents such as

$$j^\mu_B = \frac{1}{3}\sum\left(\bar{q}_L\gamma^\mu q_L + \bar{u}_R\gamma^\mu u_R + \bar{d}_R\gamma^\mu d_R\right) \tag{3.103}$$

$$j^\mu_L = \frac{1}{3}\sum\left(\bar{l}_L\gamma^\mu l_L + \bar{e}_R\gamma^\mu e_R\right) \tag{3.104}$$

as well as the combination j^{μ}_{B+L} are also also anomalous. The anomalies associated with these currents do not cancel. Fortunately, these anomalies are harmless since both B and L are global $U(1)$ symmetries (although there are various cosmological implications [55, 56, 57, 58]); the presence of the anomalies simply tells us that neither $U(1)_B$, $U(1)_L$ or $U(1)_{B+L}$ can be gauged. Thus if we wish to develop GUTs that naturally explain neutrino mass, we should look for groups that not only naturally accommodate a right-handed neutrino in a representation with the other fermions (*i.e.* without appealing to adding a singlet by hand), but we should also look for a gauge group that contains a $U(1)_{B-L}$ factor, such that when $U(1)_{B-L}$ breaks, the right-handed neutrino acquires a large Majorana mass.

3.5 A Larger Group for Model Building: $SO(10)$

As we alluded to in the previous section, neutrino mass suggests grand unification beyond $SU(5)$. If we also wish to include gauged $U(1)_{B-L}$, we will require a gauge group of at least rank five. Additionally, we will again require a group that admits complex representations and, given the nice features of $SU(5)$, it would also be useful to consider groups that contain $SU(5)$ as a subgroup. The orthogonal groups of the form $SO(4n+2)$ fit our prerequisites of which $SO(10)$ [59] is the smallest. It will be useful to decompose representations of $SO(10)$ under $SU(5) \times U(1)$, $SU(2)_L \times SU(2)_R \times SU(4)$, and $SU(3)_c \times SU(2)_L \times SU(2)_R \times U(1)$. Interestingly, the $SO(n)$ groups admit special representations called spinors (see [44, 45]). Perhaps the most familiar examples are the spinor representations of $SO(3)$ which has the same algebra as $SU(2)$. In the case of $SO(10)$, the sixteen dimensional spinor representation transforms under $SU(5)$ and $SU(3)_c \times SU(2)_L \times SU(2)_R$ respectively as,

$$\mathbf{16}_L = \bar{\mathbf{5}} + \mathbf{10} + \mathbf{1} \tag{3.105}$$

$$\mathbf{16}_L = (\mathbf{3},\mathbf{2},\mathbf{1}) + (\mathbf{1},\mathbf{2},\mathbf{1}) + (\bar{\mathbf{3}},\mathbf{1},\mathbf{2}) + (\mathbf{1},\mathbf{1},\mathbf{2})\,. \tag{3.106}$$

Thus we see that the **16** not only accommodates all the Standard Model fermions, but also a neutrino singlet which may be used with the see-saw mechanism once $SO(10)$ breaks. In fact, all the fermions of a single generation fit into one representation of $SO(10)$. Furthermore, $SO(10)$ is automatically anomaly free as $A(R) = 0$ for all R and hence provides a natural explanation for anomaly cancellation. The reduction of the number of fermion representations and automatic anomaly cancellation addresses two of the aesthetically unpleasing aspects of $SU(5)$.

As the **45** is the adjoint representation, $SO(10)$ predicts forty five gauge bosons.

Under $SU(3)_c \times SU(2)_L \times SU(2)_R$, the adjoint representation breaks down as,

$$\begin{aligned} \mathbf{45} &= (\mathbf{8},\mathbf{1},\mathbf{1}) + (\mathbf{1},\mathbf{3},\mathbf{1}) + (\mathbf{1},\mathbf{1},\mathbf{3}) + (\mathbf{1},\mathbf{1},\mathbf{1}) \\ &\quad + (\bar{\mathbf{3}},\mathbf{2},\mathbf{2}) + (\mathbf{3},\mathbf{2},\mathbf{2}) + (\mathbf{3},\mathbf{1},\mathbf{1}) + (\mathbf{3},\mathbf{1},\mathbf{1}) \end{aligned} \tag{3.107}$$

We identify the gluons with $(\mathbf{8},\mathbf{1},\mathbf{1})$, the electroweak gauge bosons ($W_L^{1,2,3}$) with $(\mathbf{1},\mathbf{3},\mathbf{1})$, the X and Y gauge bosons of the $SU(5)$ theory with $(\bar{\mathbf{3}},\mathbf{2},\mathbf{2})$ and $(\mathbf{3},\mathbf{2},\mathbf{2})$, and the new $SO(10)$ gauge bosons with $(\mathbf{1},\mathbf{1},\mathbf{3})$, $(\mathbf{1},\mathbf{1},\mathbf{1})$, $(\mathbf{3},\mathbf{1},\mathbf{1})$, and $(\bar{\mathbf{3}},\mathbf{1},\mathbf{1})$. Unlike $SU(5)$ or the Standard Model, the combination $B-L$ is now gauged and can be identified with $(\mathbf{1},\mathbf{1},\mathbf{1})$. Interestingly, we see the existence of $SU(2)_R$ gauge bosons, $W_R^{1,2,3}$, with $(\mathbf{1},\mathbf{1},\mathbf{3})$ and from eq.(3.106), the fermions also form doublets under $SU(2)_R$. Thus $SO(10)$ restores the left-right symmetry lacking in both $SU(5)$ and the Standard Model. Presumably, the right-handed $SU(2)_R$ bosons acquire large masses once $SO(10)$ breaks down to the Standard Model.

Symmetry breaking in $SO(10)$ is even more complicated than in $SU(5)$. There are a large number of symmetry breaking patterns that can eventually lead to the Standard Model. Depending on the symmetry breaking pattern and number of intermediate scales desired, Higgses in representations such as $\mathbf{10_H}$, $\mathbf{45_H}$, $\mathbf{16_H}$, $\mathbf{54_H}$, $\mathbf{126_H}$, or the $\mathbf{210_H}$ may be employed. As an example, the breaking pattern $SO(10) \to SU(3)_c \times SU(2)_L \times SU(2)_R \times U(1)_{B-L} \to SU(3)_c \times SU(2)_L \times U(1)_Y$ may be accomplished by using a $\mathbf{45_H}$ for the first stage, a $\mathbf{126_H}$ for the second stage, and finally a $\mathbf{10_H}$ for the last stage. However, only lower dimensional Higgs representations, i.e., representations no larger than the $\mathbf{54_H}$, are inspired by string theory and, phenomenologically, lower dimensional representations might be preferred. Often, the desired textures for the quark and lepton mass matrices serve as a guide for model building. In particular, model building with $SO(10)$ links the quark and lepton mass matrices in a non-trivial fashion. Generally, this leads to the challenging task of incorporating the small mixing angles of the CKM matrix with the observationally preferred large mixing angles of the PMNS matrix. Recently, progress has been made in this direction [60, 61, 62, 63, 64, 65, 66, 67, 68, 69, 70, 71] and as we shall see in Part II, some of these model classes also have deep implications for lepton flavour violation.

Bibliography

[1] H. Georgi, *Weak Interactions and Modern Particle Theory* (Benjamin/cummings, Menlo Park, 1984).

[2] D. Bailin and A. Love, *Introduction to Gauge Field Theory*, revised edition ed. (Institute of Physics Publishing, Bristol, UK, 1993).

[3] S. Weinberg, Phys. Rev. Lett. **19**, 1264 (1967).

[4] A. Salam, , originally printed in *Svartholm: Elementary Particle Theory, Proceedings Of The Nobel Symposium Held 1968 At Lerum, Sweden*, Stockholm 1968, 367-377.

[5] E. Majorana, Nuovo Cim. **14**, 171 (1937).

[6] Fukagita and Yanagida, *Neutrino*, revised edition ed. (Institute of Physics Publishing, Bristol, UK, 1993).

[7] T.-P. Cheng and L.-F. Li, *Gauge Theory of Elementary Particle Physics* (Oxford University Press, New York, New York, 1984).

[8] T. Yanagida, Proceedings of the Workshop on the Baryon Number of the Universe and Unified Theories, Tsukuba, Japan, 13-14 Feb 1979 .

[9] M. Gell-Mann, P. Ramond, and R. Slansky, Proceedings of the Supergravity Workshop, Stony Brook, N.Y., Sep. 27-29, 1979 .

[10] T.-P. Cheng and L.-F. Li, Phys. Rev. **D16**, 1425 (1977).

[11] W. J. Marciano and A. I. Sanda, Phys. Lett. **B67**, 303 (1977).

[12] S. M. Bilenky, S. T. Petcov, and B. Pontecorvo, Phys. Lett. **B67**, 309 (1977).

[13] R. Davis Jr, D. S. Harmer, and K. C. Hoffman, Phys. Rev. Lett. **20**, 1205 (1968).

[14] S. Fukuda *et al.*, Phys. Rev. Lett. **86**, 5651 (2001).

[15] S. Fukuda *et al.*, Phys. Rev. Lett. **85**, 3999 (2000).

[16] Y. Fukuda *et al.*, Phys. Lett. **B467**, 185 (1999).

[17] Q. R. Ahmad *et al.*, Phys. Rev. Lett. **87**, 071301 (2001).

[18] Q. R. Ahmad *et al.*, Phys. Rev. Lett. **89**, 011302 (2002).

[19] Q. R. Ahmad *et al.*, Phys. Rev. Lett. **89**, 011301 (2002).

[20] D. N. Abdurashitov *et al.*, Phys. Lett. **B328**, 234 (1994).

[21] J. N. Abdurashitov *et al.*, Phys. Rev. Lett. **83**, 4686 (1999).

[22] J. N. Abdurashitov *et al.*, J. Exp. Theor. Phys. **95**, 181 (2002).

[23] P. Anselmann *et al.*, Phys. Lett. **B285**, 390 (1992).

[24] P. Anselmann *et al.*, Phys. Lett. **B285**, 376 (1992).

[25] P. Anselmann *et al.*, Phys. Lett. **B357**, 237 (1995).

[26] K. Eguchi *et al.*, Phys. Rev. Lett. **92**, 071301 (2004).

[27] M. H. Ahn *et al.*, Phys. Rev. Lett. **90**, 041801 (2003).

[28] B. Pontecorvo, Sov. Phys. JETP **6**, 429 (1957).

[29] Z. Maki, M. Nakagawa, and S. Sakata, Prog. Theor. Phys. **28**, 870 (1962).

[30] V. N. Gribov and B. Pontecorvo, Phys. Lett. **B28**, 493 (1969).

[31] P. Ramond, *Journeys Beyond the Standard Model* (Perseus Publishing, Cambridge, Massachusetts, 1999).

[32] B. Kayser, Phys. Rev. **D24**, 110 (1981).

[33] C. Giunti, C. W. Kim, and U. W. Lee, Phys. Rev. **D44**, 3635 (1991).

[34] L. Wolfenstein, Phys. Rev. **D17**, 2369 (1978).

[35] S. P. Mikheev and A. Y. Smirnov, Nuovo Cim. **C9**, 17 (1986).

[36] S. P. Rosen and J. M. Gelb, Phys. Rev. **D34**, 969 (1986).

[37] S. J. Parke and T. P. Walker, Phys. Rev. Lett. **57**, 2322 (1986).

[38] H. A. Bethe, Phys. Rev. Lett. **56**, 1305 (1986).

[39] J. N. Bahcall, P. I. Krastev, and A. Y. Smirnov, Phys. Rev. **D58**, 096016 (1998).

[40] C. Bouchiat, J. Iliopoulos, and P. Meyer, Phys. Lett. **B38**, 519 (1972).

[41] G. G. Ross, *Grand Unified Theories* (Benjamin/Cummings Publishing Company Inc., Reading, Massachusetts, 1985).

[42] R. N. Mohapatra, hep-ph/9911272 (1999).

[43] H. Georgi and S. L. Glashow, Phys. Rev. Lett. **32**, 438 (1974).

[44] R. Slansky, Phys. Rept. **79**, 1 (1981).

[45] H. Georgi, *Lie Algebras in Particle Physics*, second edition ed. (Perseus Books, Reading, Massachustts, 1999).

[46] J. S. Bell and R. Jackiw, Nuovo Cim. **A60**, 47 (1969).

[47] S. L. Adler, Phys. Rev. **177**, 2426 (1969).

[48] S. L. Adler and W. A. Bardeen, Phys. Rev. **182**, 1517 (1969).

[49] S. Weinberg, Phys. Rev. Lett. **43**, 1566 (1979).

[50] F. Wilczek and A. Zee, Phys. Lett. **B88**, 311 (1979).

[51] F. Wilczek and A. Zee, Phys. Rev. Lett. **43**, 1571 (1979).

[52] N. Sakai and T. Yanagida, Nucl. Phys. **B197**, 533 (1982).

[53] S. Weinberg, Phys. Rev. **D26**, 287 (1982).

[54] A. J. Buras, J. R. Ellis, M. K. Gaillard, and D. V. Nanopoulos, Nucl. Phys. **B135**, 66 (1978).

[55] G. 't Hooft, Phys. Rev. Lett. **37**, 8 (1976).

[56] N. S. Manton, Phys. Rev. **D28**, 2019 (1983).

[57] F. R. Klinkhamer and N. S. Manton, Phys. Rev. **D30**, 2212 (1984).

[58] M. E. Shaposhnikov, Nucl. Phys. Proc. Suppl. **26**, 78 (1992).

[59] H. Fritzsch and P. Minkowski, Ann. Phys. **93**, 193 (1975).

[60] K. S. Babu and S. M. Barr, Phys. Lett. **B381**, 202 (1996).

[61] C. H. Albright and S. M. Barr, Phys. Rev. **D62**, 093008 (2000).

[62] C. H. Albright and S. M. Barr, Phys. Rev. **D64**, 073010 (2001).

[63] C. H. Albright and S. Geer, Phys. Lett. **B532**, 311 (2002).

[64] K. S. Babu, J. C. Pati, and F. Wilczek, Nucl. Phys. **B566**, 33 (2000).

[65] Z. Berezhiani and A. Rossi, Nucl. Phys. **B594**, 113 (2001).

[66] T. Blazek, S. Raby, and K. Tobe, Phys. Rev. **D62**, 055001 (2000).

[67] W. Buchmuller and D. Wyler, Phys. Lett. **B521**, 291 (2001).

[68] M.-C. Chen and K. T. Mahanthappa, Phys. Rev. **D65**, 053010 (2002).

[69] R. Kitano and Y. Mimura, Phys. Rev. **D63**, 016008 (2001).

[70] N. Maekawa, Prog. Theor. Phys. **106**, 401 (2001).

[71] G. G. Ross and L. Velasco-Sevilla, Nucl. Phys. **B653**, 3 (2003).

Part II

Constraints on Extensions of the Standard Model from Observations

There is a theory which states that if ever anybody discovers exactly what the Universe is for and why it is here, it will instantly disappear and be replaced by something even more bizarre and inexplicable.

There is another theory which states that this has already happened.

The Restaurant at the End of the Universe

Preamble

As the research community anticipates the start of the LHC project at CERN, models that extend the Standard Model are being tested by low energy observations. The low energy implications of hypothesized new interactions near the electroweak unification scale and the implications of new physics that addresses the origin of neutrino mass are currently of particular interest. Precision low energy observations provide a window into physics at high scales as a result of renormalization effects. From the low energy point of view, new interactions appear as non-renormalizable operators that point toward the scale where the theory requires ultra-violet completion. As an example, if the neutrino oscillation data is interpreted as evidence for Majorana neutrino mass, the mass operator involving Standard Model fields appears as the non-renormalizable operator

$$\frac{f}{\Lambda} LLHH. \tag{3.108}$$

Based on the current observational data neutrino masses are $\lesssim$ eV, which suggests a scale of new physics at $\Lambda \sim 10^{14}$ GeV - well beyond the reach of any current or proposed collider facility. The papers discussed in Part II examine the low energy consequences of energy scales where new physics is expected.

The gauge hierarchy problem outlined in Part I strongly suggests that new physics will appear in the TeV energy range. It is hoped that the underlying mechanism responsible for electroweak symmetry breaking will be discovered during the LHC program. Wide classes of theories that provide an ultra-violet completion of the Standard Model call for the existence of new scalar interactions. These scalar interactions may have indirect effects on low energy processes. Ambitiously, an experimental undertaking involving positron-neutrino correlation measurements of pure Fermi $0^+ \rightarrow 0^+$ super allowed transitions in β-decay of ^{32}Ar and ^{33}Ar was completed to search for the presence of new scalar interactions. As these experiments are difficult, the resulting limits on scalar interactions attained were substantially weaker than the already pre-exiting limits on new pseudo-scalar interactions. In light of these experiments, we show in chapter 4 that pion physics can provide an important testbed for new physics that violates chirality independent of whether it violates parity. We demonstrate, model independently, that new scalar interactions originating at scales near electroweak unification can affect the pion branching ratio by inducing pseudo-scalar interactions through renormalization group flow. Under rather robust assumptions, the experimental limits on induced the pseudo-scalar interactions dramatically improve upon the limits on underlying scalar interactions set from positron-neutrino correlation precision measurements of radioactive atoms.

Over the last five years the new experimental results in neutrino physics have be-

come a watershed for the high energy physics community. The confirmation of neutrino oscillations provides the only direct evidence for physics beyond the Standard Model. Much effort has been expended both experimentally and theoretically to gain a deeper understanding of the physics involved. As discussed in Part I, the see-saw mechanism provides the most elegant method for generating small neutrino masses. Naturally, supersymmetry dovetails with the neutrino see-saw, providing a plethora of opportunities for low energy observation. In particular, the supersymmetric see-saw with gravity mediated supersymmetry breaking predicts flavour violation and in particular the process $\mu \to e\gamma$. In addition, the MSSM also predicts the stability of the lightest supersymmetric particle (LSP) which may provide an explanation for dark matter. If the LSP composes the dark matter, as inferred from the precision observations of the cosmic background radiation (CMBR), the MSSM parameter space becomes highly constrained. As we find in chapter 5, the see-saw and MSSM parameter spaces will become even further reduced by the next generation of $\mu \to e\gamma$ experiments.

From a phenomenological perspective, it is an irresistible temptation to build models that attempt to explain the origin of the see-saw. The grand unified model supersymmetric $SO(10)$ provides a compelling framework. As discussed in Part I, $SO(10)$ contains a neutrino singlet in the **16** spinor representation along with all the fermions of the Standard Model. By imposing flavour symmetries, it is possible to construct realistic models that explain the origin of both the observed PMNS and CKM matrices. However, these models also predict lepton flavour violation. As we will learn in chapter 6 the level of LFV predicted in a certain class of popular supersymmetric $SO(10)$ models is dangerously close to the experimental limit, assuming MSSM parameters such that the LSP forms the dark matter.

Chapter 4

Constraints on Scalar Couplings from $\pi^{\pm} \to l\nu$

4.1 Introduction

While there is strong support for the $V - A$ form of the charged weak current, it is possible that new physics at or above the weak scale could give rise to scalar interactions that would compete with standard model processes. Examples of such possible physics include the exchange of extra Higgs multiplets which could enter the theory at scales from the Z mass upwards [1], leptoquarks which could be present at scales above 200 GeV [1], contact interactions from quark/lepton compositeness which could be present at the TeV scale [1], or strong gravitational interactions in TeV brane world models [1]. Recently, precision experiments [2, 3, 4] have searched for scalar interactions in β-decay, however, direct experimental constraints on scalar couplings still remain relatively weak as compared to the corresponding limits on pseudoscalar couplings [1, 5].

The precision of the limits on pseudoscalar couplings comes in part from the fact that the pion, a pseudoscalar meson, has a chirally suppressed decay $\pi^{\pm} \to l^{\pm}\nu_l$ which would be sensitive to new pseudoscalar interactions [6]. These pseudoscalar interactions would be detected by the failure of the standard model prediction [7] for the chiral suppression in the ratio of branching ratios $\frac{\Gamma(\pi^- \to e\bar{\nu})}{\Gamma(\pi^- \to \mu\bar{\nu})}$. It is the large chiral suppression factor, by the square of the electron-muon mass ratio, that allows such a powerful test of new physics that violates chirality and parity.

In the standard model, the leading contribution to pion decay occurs through tree level W exchange. At the quark level, this is the same process that is involved in the β-decay of a nucleon ignoring the spectator quarks. While the pion cannot decay through a scalar interaction, the pion can decay through induced pseudoscalar interactions generated from the electroweak renormalization of the scalar couplings. It is of considerable

interest to use limits on the induced pseudoscalar couplings to set indirect limits on the size of the underlying scalar interactions.

In the following sections we outline our methods and estimate the limits on the size of scalar couplings based on the indirect effects from charged pion decay. We use general operator techniques to obtain model independent results and we combine these results with data from pion decay and also muon capture, to constrain the scalar couplings indirectly. We also discuss some of the implications of these results and comment on prospects for future searches for scalar interactions.

4.2 Pion Physics and New Pseudoscalar Interactions

Consider constructing an effective Lagrangian and matrix element for the process $\pi^{\pm} \to l^{\pm}\nu_l$ in the presence of pseudoscalar interactions. We can set limits on the strength of the pseudoscalar interactions from their interference with tree level W exchange. Since the pion is a pseudoscalar, we can use the following relations for current matrix elements,

$$\begin{aligned}
&\langle 0\,|\bar{u}\gamma_\mu\gamma_5 d|\,\pi(p)\rangle = i\sqrt{2}f_\pi p_\mu \\
&\langle 0\,|\bar{u}\gamma_5 d|\,\pi(p)\rangle = i\sqrt{2}\tilde{f}_\pi = i\sqrt{2}\,\frac{f_\pi m_\pi^2}{m_u + m_d} \\
&\langle 0\,|\bar{u}\sigma^{\mu\nu}\gamma_5 d|\,\pi(p)\rangle = 0 \\
&\langle 0\,|\bar{u}\sigma^{\mu\nu} d|\,\pi(p)\rangle = 0,
\end{aligned} \tag{4.1}$$

where $f_\pi = 93$ MeV and $\tilde{f}_\pi = 1.8 \times 10^5$ MeV^2. The matrix element for the tree level W contribution can easily be constructed by using eq.(4.1), giving;

$$\mathcal{M}_{W^\pm} = G_F f_\pi \cos\theta_c [\bar{l}\gamma^\mu(1-\gamma_5)\nu_l] p_\mu, \tag{4.2}$$

where p_μ is the pion momentum and θ_c is the Cabibbo angle. A pseudoscalar contribution with left-handed neutrinos in the final state can be expressed as a four-fermi contact operator,

$$\mathcal{L}_P = -i\frac{\rho}{2\Lambda^2}[\bar{l}(1-\gamma_5)\nu_l][\bar{u}\gamma_5 d] \tag{4.3}$$

where ρ is the pseudoscalar coupling constant. This expression can be converted to a matrix element using eq.(4.1),

$$\mathcal{M}_P = \rho\frac{\tilde{f}_\pi}{\sqrt{2}\Lambda^2}[\bar{l}(1-\gamma_5)\nu_l]. \tag{4.4}$$

In the presence of a pseudoscalar interaction, the overall matrix element for the process $\pi^{\pm} \to l^{\pm}\nu_l$ is the coherent sum, $\mathcal{M}_P + \mathcal{M}_{W^{\pm}} = \mathcal{M}_l$.

$$\mathcal{M}_l = G_F f_\pi \cos\theta_c [\bar{l}\gamma^\mu(1-\gamma_5)\nu_l]p_\mu + \frac{\rho \tilde{f}_\pi}{\sqrt{2}\Lambda^2}[\bar{l}(1-\gamma_5)\nu_l] \tag{4.5}$$

Having constructed the matrix element, we can now estimate the ratio of branching ratios,

$$\frac{\Gamma(\pi^- \to e\nu_e)}{\Gamma(\pi^- \to \mu\nu_\mu)} = \frac{(m_\pi^2 - m_e^2)}{(m_\pi^2 - m_\mu^2)} \frac{\langle |M_{e\nu}|^2 \rangle}{\langle |M_{\mu\nu}|^2 \rangle}. \tag{4.6}$$

Summing over final states of the squared matrix element we have

$$\begin{aligned} \langle |\mathcal{M}_l|^2 \rangle &= 4G_f^2 f_\pi^2 \cos^2\theta_c m_l^2 (m_\pi^2 - m_l^2) + 8\frac{G_F \tilde{f}_\pi f_\pi \cos\theta_c \rho}{\sqrt{2}\Lambda^2} m_l (m_\pi^2 - m_l^2) \\ &\quad + 2\frac{\rho^2 \tilde{f}_\pi^2}{\Lambda^4}(m_\pi^2 - m_l^2). \end{aligned} \tag{4.7}$$

For simplicity we have assumed that the pseudoscalar coupling is real, however, in general ρ may be complex. The more general expression is obtained by making the following replacements,

$$\begin{aligned} \rho &\to \frac{\rho + \rho^*}{2} = \mathrm{Re}(\rho) \\ (\rho)^2 &\to |\rho|^2. \end{aligned} \tag{4.8}$$

We find that the branching ratio is given by

$$\frac{\Gamma(\pi^- \to e\nu_e)}{\Gamma(\pi^- \to \mu\nu_\mu)} = \frac{(m_\pi^2 - m_e^2)}{(m_\pi^2 - m_\mu^2)} \left[\frac{m_e^2(m_\pi^2 - m_e^2) + R_e}{m_\mu^2(m_\pi^2 - m_\mu^2) + R_\mu} \right], \tag{4.9}$$

where the $R_{e,\mu}$ functions are

$$R_{e,\mu} = \sqrt{2}\frac{\tilde{f}_\pi \mathrm{Re}(\rho)}{G_F f_\pi \Lambda^2 \cos\theta_c} m_{e,\mu}(m_\pi^2 - m_{e,\mu}^2) + \frac{|\rho|^2 \tilde{f}_\pi^2}{2 f_\pi^2 G_F^2 \Lambda^4 \cos^2\theta_c}(m_\pi^2 - m_{e,\mu}^2). \tag{4.10}$$

Thus far we have only discussed interactions with left-handed neutrinos in the final state. The inclusion of right-handed neutrinos requires a modification since pseudoscalar contributions to decays with right-handed neutrinos in the final state cannot interfere with the W exchange graph; hence the contributions to the rate add incoherently. With right-handed neutrinos, the expression for the matrix element becomes,

$$\mathcal{M}_P = \frac{\rho' \tilde{f}_\pi}{\sqrt{2}\Lambda^2}[\bar{l}(1+\gamma_5)\nu_l], \tag{4.11}$$

where ρ' is the pseudoscalar coupling involving right-handed neutrinos. Defining

$$T \equiv \frac{(m_\pi^2 - m_e^2)^2}{(m_\pi^2 - m_\mu^2)^2}\frac{m_e^2}{m_\mu^2} = 1.28 \times 10^{-4}, \tag{4.12}$$

we can express the branching ratio as

$$\frac{\Gamma(\pi^- \to e\nu_e)}{\Gamma(\pi^- \to \mu\nu_\mu)} = T\left(\frac{1 + \sqrt{2}\frac{\tilde{f}_\pi \mathrm{Re}(\rho_e)}{G_F\Lambda^2 f_\pi \cos\theta_c m_e} + \frac{|\rho_e|^2\tilde{f}_\pi^2}{2G_F^2\Lambda^4 f_\pi^2\cos^2\theta_c m_e^2} + \frac{|\rho'_e|^2\tilde{f}_\pi^2}{2G_F^2 f_\pi^2\Lambda^4\cos^2\theta_c m_e^2}}{1 + \sqrt{2}\frac{\tilde{f}_\pi \mathrm{Re}(\rho_\mu)}{G_F\Lambda^2 f_\pi \cos\theta_c m_\mu} + \frac{|\rho_\mu|^2\tilde{f}_\pi^2}{2G_F^2\Lambda^4 f_\pi^2\cos^2\theta_c m_\mu^2} + \frac{|\rho'_\mu|^2\tilde{f}_\pi^2}{2G_F^2\Lambda^4 f_\pi^2\cos^2\theta_c m_\mu^2}}\right), \tag{4.13}$$

If we assume either universal scalar couplings or else scalar couplings involving only the first generation, we obtain the following approximation for the ratio of decay widths,

$$\frac{\Gamma(\pi^- \to e\nu_e)}{\Gamma(\pi^- \to \mu\nu_\mu)} \approx T\left(1 + \sqrt{2}\frac{\tilde{f}_\pi \mathrm{Re}(\rho)}{G_F\Lambda^2 f_\pi \cos\theta_c m_e} + \frac{|\rho|^2\tilde{f}_\pi^2}{2G_F^2\Lambda^4 f_\pi^2\cos^2\theta_c m_e^2} + \frac{|\rho'|^2\tilde{f}_\pi^2}{2G_F^2\Lambda^4 f_\pi^2\cos^2\theta_c m_e^2}\right) \tag{4.14}$$

We will discuss the effects of more general generation dependence of the scalar couplings in section 4.6. The theoretical standard model calculation including radiative corrections is $\mathrm{Br}_{\mathrm{th}} = (1.2352 \pm .0005) \times 10^{-4}$ [7] and the measured experimental branching ratio is $\mathrm{Br}_{\mathrm{exp}} = (1.230 \pm .0040) \times 10^{-4}$ [1, 8, 9, 10]. Combining the experimental and theoretical uncertainties in quadrature, we can obtain a bound on the pseudoscalar couplings at 2σ,

$$-1.0\times10^{-2} \le \sqrt{2}\frac{\tilde{f}_\pi \mathrm{Re}(\rho)}{G_F\Lambda^2 f_\pi \cos\theta_c m_e} + \frac{|\rho|^2\tilde{f}_\pi^2}{2G_F^2\Lambda^4 f_\pi^2\cos^2\theta_c m_e^2} + \frac{|\rho'|^2\tilde{f}_\pi^2}{2G_F^2\Lambda^4 f_\pi^2\cos^2\theta_c m_e^2} \le 2.2\times10^{-3}. \tag{4.15}$$

4.3 Local Scalar Operator Analysis

Electroweak interactions can radiatively induce pseudoscalar operators from pure scalar interactions. Suppose that at some scale Λ there exists new physics that generates a purely scalar four-fermi interaction. It may be due to the exchange of fundamental scalars or it may be due to a variety of other physics such as compositeness, extra dimensions, leptoquarks, et cetera. Independent of the details of the new physics that generates the scalar interactions, they will appear as non-renormalizable four-fermi scalar contact operators below the scale Λ.

In order to facilitate power counting, the $\overline{\mathrm{MS}}$ scheme is most often used with effective field theory [11]. The $\overline{\mathrm{MS}}$ scheme (or any mass independent subtraction scheme)

presents the subtlety that heavy particles do not decouple in beta function calculations. That is, mass independent renormalization schemes do not satisfy the conditions of the Applequist-Carazzone theorem [11]. This is dealt with by simply integrating out the heavy fields by hand at their associated scale. Thus whether we analyze the effective interactions in a UV complete theory or in the effective theory, we will arrive at the same renormalization group running (up to threshold corrections) provided that we are only interested in results below Λ and only up to some finite power of $(\frac{1}{\Lambda})$.

We start by considering SU(2) $\times$ U(1) invariant four-fermion contact interactions that are generation independent and flavour diagonal (see figure 4.1 and figure 4.4). We will discuss the effects of generation dependence in section 4.6. We consider two types of scalar operators in order to facilitate comparison with the direct experimental constraints. Type A (O_A) have left-handed neutrinos in the final state while Type B (O_B) have right-handed (sterile) neutrinos. These interactions appear as extensions to the standard model Lagrangian involving non-renormalizable operators,

$$\mathcal{L}_{\text{scalar}} = \frac{s_A}{\Lambda^2} O_A + \frac{s_B}{\Lambda^2} O_B \tag{4.16}$$

where s_A and s_B are undetermined scalar couplings. From these interactions, electroweak radiative corrections (see figure 4.2 and figure 4.5) can in principle induce pseudoscalar interactions. We retain corrections up to order $\frac{1}{\Lambda^2}$ and from this analysis we extract the anomalous dimension matrix.

4.3.1 Type A Operator Analysis: O_A

The operators of Type A are as follows,

$$O_1 = [\bar{e}_R L][\bar{Q} d_R] \tag{4.17}$$

$$O_2 = [\bar{e}_R L][\bar{u}_R Q], \tag{4.18}$$

(where the SU(2) indices have been suppressed) such that the pure scalar interaction is

$$O_A = O_1 + O_2. \tag{4.19}$$

Since we are assuming that at the scale Λ there is a pure scalar interaction, we take O_1 and O_2 to enter the theory at the high scale with equal weight.

In calculating the anomalous dimension matrix a third operator is generated through renormalization: the operator $O' = [\bar{e}_R Q][\bar{u}_R L]$ mixes with the other two. However, in order to construct the matrix element for the pion decay amplitude, we need to rotate the operators to a basis that has a definite matrix element between the vacuum and the

Figure 4.1: $\mathcal{O}_1$ and $\mathcal{O}_2$, Type A contact interactions

Figure 4.2: Example of electroweak corrections to Type A contact interactions. All permutations are required including wavefunction renormalization; the vector bosons are the $W_{\mu}^{1,2,3}$ and B_{μ}.

on-shell pion state. This requires Fierz reordering,

$$O' = -\frac{1}{2}O_2 + (-\frac{1}{8})[\bar{e}_R\sigma_{\mu\nu}L][\bar{u}_R\sigma^{\mu\nu}Q] \tag{4.20}$$

where we define

$$O_3 \equiv (-\frac{1}{8})[\bar{e}_R\sigma_{\mu\nu}L][\bar{u}_R\sigma^{\mu\nu}Q]. \tag{4.21}$$

Note that $< 0|O_3|\pi(p) >= 0$. This leaves us with the following beta functions,

$$\mu\frac{\partial(\mathcal{O})}{\partial\mu} = \frac{1}{32\pi^2}\gamma\mathcal{O} \tag{4.22}$$

where,

$$\mathcal{O} = \begin{pmatrix} O_1 \\ O_2 \\ O_3 \end{pmatrix} \tag{4.23}$$

and

$$\gamma = \begin{bmatrix} 6g^2 + \frac{98}{9}g'^2 & 0 & 0 \\ 0 & 6g^2 + \frac{128}{9}g'^2 & 6g^2 + 10g'^2 \\ 0 & \frac{9}{2}g^2 + \frac{15}{2}g'^2 & 12g^2 + \frac{103}{9}g'^2 \end{bmatrix}. \tag{4.24}$$

The constants g' and g are the U(1) and SU(2) coupling constants, respectively. The

results of the numerical integration of the renormalization group equations are displayed in figure 4.3. O_1 and O_2 start out with equal amplitude at the scale Λ. They are then renormalized to the weak scale of roughly 100 GeV. In the first panel the x-axis indicates the starting scale Λ, i.e. the scale of new physics. The y-axis indicates the amount each operator is suppressed in running from the scale Λ to the weak scale. Each operator renormalizes differently and the splittings give rise to the pseudoscalar interaction. If the scale Λ is at or very near the weak scale then threshold effects become important, which we will discuss in the following section. The second panel plots the difference of O_1 and O_2 as a function of scale. This difference is proportional to the amount of pseudoscalar interaction induced.

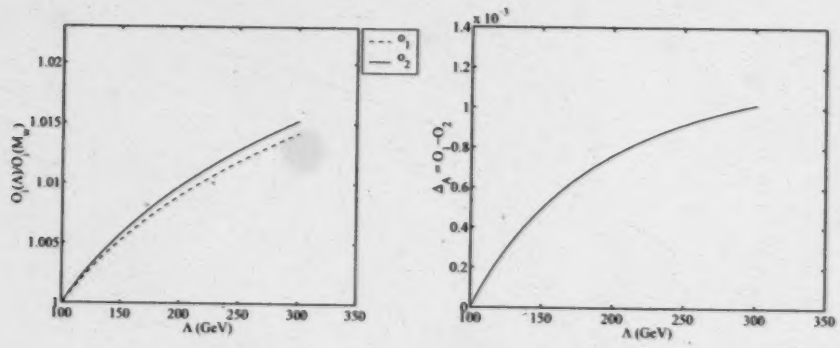

(a) (b)

Figure 4.3: Type A operator RGE analysis. Panel (a) shows how each operator evolves with scale. Panel (b) displays the induced pseudoscalar proportionality factor.

4.3.2 Type B Operator Analysis: O_B

The Type B operators are as follows,

$$O_1 = [\bar{L}\nu_R][\bar{Q}d_R] \tag{4.25}$$

$$O_2 = [\bar{L}\nu_R][\bar{u}_R Q] \tag{4.26}$$

(where the SU(2) indices have been suppressed) with

$$O_B = O_1 + O_2. \tag{4.27}$$

We assume that the interaction at the scale Λ is purely scalar as in the Type A scenario. Again operator mixing is present with a third induced operator, namely

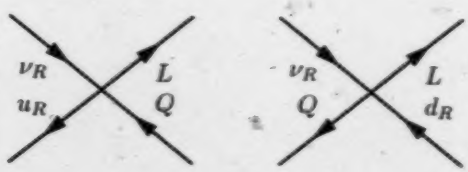

Figure 4.4: $\mathcal{O}_1$ and $\mathcal{O}_2$, Type B contact interactions

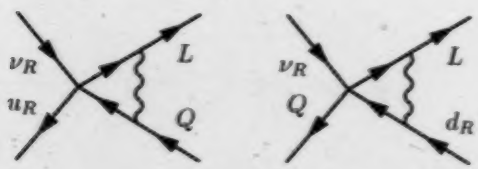

Figure 4.5: Example of electroweak corrections to Type B contact interactions. All permutations are required including wavefunction renormalization; the vector bosons are the $W_\mu^{1,2,3}$ and B_μ.

$O' = [\bar{L}d_R][\bar{Q}\nu_R]$ which must be rotated as before into the appropriate basis: $O' = -\frac{1}{2}O_2 + (-\frac{1}{8})[\bar{L}\sigma^{\mu\nu}\nu_R][\bar{Q}\sigma_{\mu\nu}d_R]$ where $O_3 = (-\frac{1}{8})[\bar{L}\sigma^{\mu\nu}\nu_R][\bar{Q}\sigma_{\mu\nu}d_R]$. We extract the following anomalous dimension matrix:

$$\mu\frac{\partial(\mathcal{O})}{\partial\mu} = \frac{1}{32\pi^2}\gamma\mathcal{O} \tag{4.28}$$

where,

$$\mathcal{O} = \begin{pmatrix} O_1 \\ O_2 \\ O_3 \end{pmatrix} \tag{4.29}$$

and

$$\gamma = \begin{bmatrix} 6g^2 + \frac{38}{9}g'^2 & 0 & 0 \\ 0 & 6g^2 + \frac{11}{9}g'^2 & 6g^2 - \frac{2}{3}g'^2 \\ 0 & \frac{9}{2}g^2 - \frac{1}{3}g'^2 & 12g^2 + \frac{34}{9}g'^2 \end{bmatrix}. \tag{4.30}$$

The results of the numerical integration of the renormalization group equations are displayed in figure 4.6. As we have seen before in section 4.3.1 the graphs in figure 4.6 illustrate the effects of renormalization on the operators O_1 and O_2 when they enter with the same amplitude at the scale Λ.

In both Type A and B scalar interactions we see that renormalization effects induce

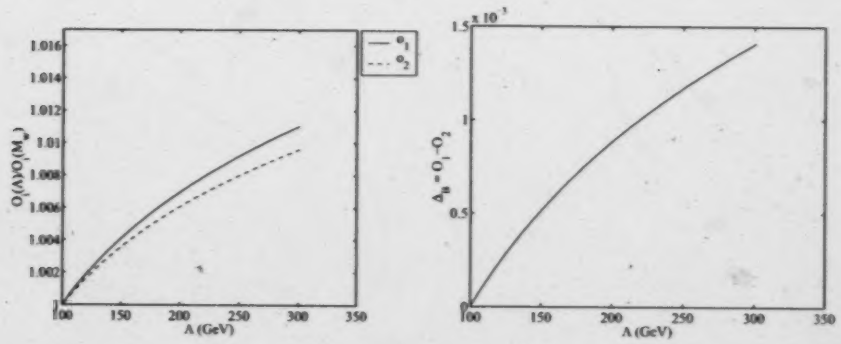

Figure 4.6: Type B operator RGE analysis. Panel (a) shows how each operator evolves with scale. Panel (b) displays the induced pseudoscalar proportionality factor.

a pseudoscalar interaction. The size of the pseudoscalar interaction depends on how far the scale Λ is from the weak scale. The larger the scale separation is, the larger the induced pseudoscalar proportionality factor becomes. The effective pseudoscalar couplings, which we denoted as ρ and ρ' in section 4.2 , are given by,

$$\begin{aligned} \rho &= s_A \Delta_A(\Lambda) \\ \rho' &= s_B \Delta_B(\Lambda) \end{aligned} \tag{4.31}$$

where Δ_A and Δ_B are the renormalization group factors induced from the running from the scale Λ down to the weak scale (Δ_A and Δ_B are plotted in the second panel of figure 4.3 and figure 4.6). The factors s_A and s_B are the undetermined scalar coupling constants introduced in eq.(4.16). Since the pseudoscalar is induced from a scalar interaction we are now in a position to place limits on the magnitude of the scalar coupling from pion physics; the scalar couplings s_A and s_B at the scale of the new physics Λ are now constrained by the requirement that ρ and ρ' satisfy eq.(4.15).

A comment on QCD corrections is in order. QCD is a parity invariant theory and therefore QCD corrections cannot induce a pseudoscalar interaction by themselves. In our analysis, the induced pseudoscalar arises from the difference of two operators that initially combined to give a purely scalar interaction and the QCD corrections will affect the two operators in the same way. The QCD corrections can only adjust this difference by an overall multiplicative factor. This is true for both operators of Type A and B. However, in section 4.5 we compare the direct experimental constraints on scalar couplings from β decay to the indirect constraints on the renormalization induced pseu-

doscalar interactions from pion decay. Since the same scalar operators are involved in both processes, the QCD effects are the same for each case and therefore will cancel in a comparison of the relative strengths of the limits from the two processes. The largest part of the QCD renormalization of the scalar operators (and hence of their weak interaction induced pseudoscalar difference) will come from the QCD induced running from the weak scale down to the chiral symmetry breaking scale, of order $4\pi f_\pi \approx 1\text{GeV}$ [12], where we take the pion decay matrix element using PCAC. The correction to each of the operators can be computed through the QCD renormalization group running of these operators,

$$\begin{aligned} O_{A,B}(1\,\text{GeV}) &= \left(\frac{\alpha_s(1\,\text{GeV}^2)}{\alpha_s(M_W^2)}\right)^{4/21} O_{A,B}(M_w) \\ &\approx 1.3\, O_{A,B}(M_w) \end{aligned} \tag{4.32}$$

for $\Lambda_{QCD} = 200\,\text{MeV}$. The induced pseudoscalar, which is proportional to $\Delta_{A,B}$, will be enhanced by this factor of 1.3.

4.4 Pseudoscalar Interactions From Threshold Effects

A limitation of the renormalization group operator analysis of the last section is its inapplicability if the scale of new physics is at or very near the electroweak scale. In this case, threshold effects become the dominate contribution. To estimate the threshold effects, we consider a toy model where a VEVless scalar doublet is added to the standard model. Indeed it is only for the exchange of a scalar doublet that we need to consider a possible scale for new physics near the electroweak scale. For leptoquarks, compositeness, and extra dimensional gravity, direct experimental constraints imply [1] that the scale Λ of new physics is sufficiently above the electroweak scale that RGE running dominates threshold effects. In principle, the addition of a VEVless scalar doublet can lead to both scalar and pseudoscalar interactions in the tree level Lagrangian. Since pseudoscalar interactions are directly constrained by tree level contributions to pion decay and we are presently interested in limits on pure scalar interactions, we arrange the couplings such that only scalar interactions arise at the scale of new physics,

$$\mathcal{L} = (\lambda)\bar{L}e_R S + (\lambda')\bar{Q}d_R S - (\lambda')\bar{Q}u_R\tilde{S} + \text{h.c.} \tag{4.33}$$

where, λ and λ' are the scalar couplings to the quarks and leptons respectively, and $\tilde{S} = i\sigma^2 S$. In this working example, the scalar interactions have the property that they couple in a universal and flavour diagonal manner with undetermined scalar couplings to quarks and leptons. It is the charged scalar couplings that the β-decay ex-

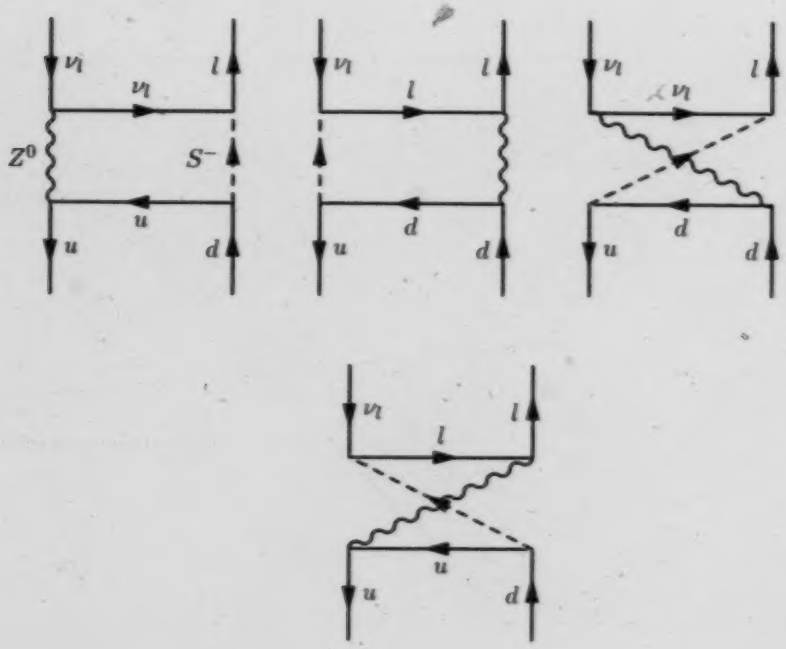

Figure 4.7: Dressed Z^0 exchange diagrams.

periments constrain directly. The pseudoscalar interaction can potentially be induced at one loop through three classes of diagrams: scalar-dressed Z exchange box diagrams, scalar-dressed W exchange box diagrams and radiative corrections to the quark vertex (see figure 4.7, figure 4.8 and figure 4.9). The weak interactions do not respect parity and the scalar interactions change chirality, thus diagrams of this form can potentially induce a pseudoscalar interaction. To estimate the effect of the scalar on the branching ratio, we will make the approximation that the quarks are massless and ignore external momenta. Box diagrams that involve the Higgs or the Goldstone modes can be ignored since the couplings are mass proportional and hence their contribution is small.

By explicit calculation we can show that while both the dressed W and Z exchange box diagrams give non-zero amplitudes, their tensor structure is such that after taking the matrix element between the pion and the vacuum they give vanishing contributions. In the vertex correction class of diagrams we are dealing with primitively divergent graphs (see figure 4.9). In order to obtain a conservative estimate of the induced pseudoscalar arising already from threshold effects, we can regulate the loop diagrams by cutting off the loop momentum at the weak scale and integrate from 0 to M_Z. Cutting off the loop

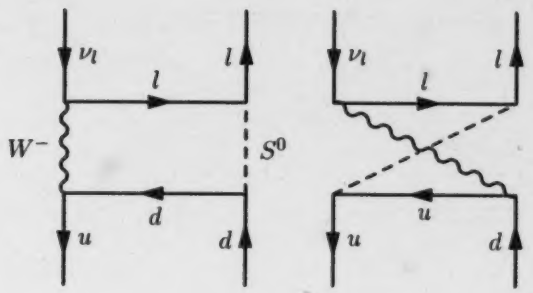

Figure 4.8: Dressed W exchange diagrams.

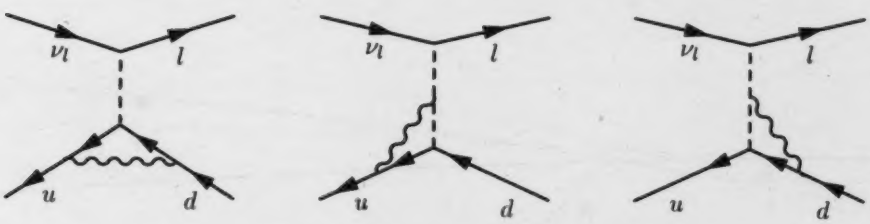

Figure 4.9: Radiative corrections to the quark-scalar vertex.

momentum at M_Z represents a conservative estimate, in that the scale of new physics is at the weak scale and therefore there is no scale separation for renormalization group running proper. In this case we find a non-vanishing contribution. The three graphs in figure 4.9 give the following result for the pion decay matrix element,

$$\begin{aligned}\mathcal{M}_{\text{Vertex}} &= -\frac{\sqrt{2}g^2\tilde{f}_\pi\lambda\lambda'}{64\pi^2\cos^2\theta_w M_Z^2}\left[\left(-\frac{4}{3}\sin^2\theta_w\right)\ln(2)+\cos(2\theta_w)\left(\ln(2)-\frac{1}{2}\right)\right][\bar{l}(1-\gamma_5)\nu_l] \\ &\approx 0.13\frac{\sqrt{2}g^2\tilde{f}_\pi\lambda\lambda'}{64\pi^2\cos^2\theta_w M_Z^2}[\bar{l}(1-\gamma_5)\nu_l]. \qquad (4.34)\end{aligned}$$

To get a second, independent, estimate of the threshold corrections, in a different renormalization prescription, we will imagine integrating out the weak scale degrees of freedom (W, Z and scalars) to get an effective low-energy theory. The resulting theory will have only dimension six four-fermion operators; to simplify our calculation let us imagine setting the scalar masses just below the mass of the W and Z and integrating out the W and Z first and then immediately integrating out the scalars, thus inducing the four-fermion operators. If we use a dimensionless regulator, the effective fermion-

scalar theory after integrating out the W and Z will have Yukawa couplings shifted by threshold effects neccessary to reproduce the residual effects of the W and Z in the resulting effective theory in which they are absent. These threshold corrections have been computed in [13, 14]. We then immediately integrate out the scalars, with their corrected Yukawa couplings, to get the final low-energy effective theory of fermions with four-fermion couplings. Using the results for the threshold corrections for Yukawa couplings from [13, 14], with the gauge charge representations of our particles, and then immediately integrating out the scalars at the weak scale (which we take to be M_Z) we get an effective induced interaction from the vertex corrections of:

$$\mathcal{M}_{\text{Vertex}} \approx 0.08 \frac{\sqrt{2} g^2 \tilde{f}_\pi \lambda \lambda'}{64\pi^2 \cos^2\theta_w M_Z^2} [\bar{l}(1-\gamma_5)\nu_l]. \tag{4.35}$$

That the estimates of eq.(4.34) and eq.(4.35), which use two entirely different regularization and renormalization prescriptions, agree to within a factor of two gives us confidence that estimates of the threshold corrections are of this order and are not artifacts of the regulator chosen. To be conservative, we will use the estimate of eq.(4.35) which in conjunction with eq.(4.15) and in the absence of right-handed neutrinos gives,

$$-3 \times 10^{-2} \leq \frac{K_s}{G_F} \leq 6 \times 10^{-3} \tag{4.36}$$

where,

$$|K_s| \equiv \frac{\lambda \lambda'}{M_Z^2}. \tag{4.37}$$

The above calculation gives a conservative estimate of the amplitude, including only contributions from threshold effects. We see in this toy example that even from threshold effects alone a pseudoscalar interaction will be radiatively induced.

4.5 Comparison with β-Decay Constraints

We can compare our bounds on scalar currents, with those arising in nuclear β-decay. The effective Hamiltonian for allowed β-decay has the general Lorentz form [15],

$$\begin{aligned} H = \frac{G_F}{\sqrt{2}} \{ & (\bar{\psi}_p \gamma_\mu \psi_n)(C_V \bar{\psi}_e \gamma_\mu \psi_\nu + C'_V \bar{\psi}_e \gamma_\mu \gamma_5 \psi_\nu) \\ & + (\bar{\psi}_p \gamma_\mu \gamma_5 \psi_n)(C_A \bar{\psi}_e \gamma_\mu \psi_\nu + C'_A \bar{\psi}_e \gamma_\mu \gamma_5 \psi_\nu) \\ & + (\psi_p \psi_n)(C_S \bar{\psi}_e \psi_\nu + C'_S \bar{\psi}_e \gamma_5 \psi_\nu) \\ & + \frac{1}{2}(\bar{\psi}_p \sigma_{\lambda\mu} \psi_n)(C_T \bar{\psi}_e \sigma_{\lambda\mu} \psi_\nu + C'_T \bar{\psi}_e \sigma_{\lambda\mu} \gamma_5 \psi_\nu) \}. \end{aligned} \tag{4.38}$$

A pseudoscalar term has not been included since it vanishes to leading order in nuclear β decay. In the absence of right-handed currents, $C_i = C_i'$ and as we have mentioned before, we consider purely scalar interactions. (Note that in the above, $\frac{1+\gamma_5}{2}$ is taken to be the left projector. This is opposite to our convention in the preceding sections. However by using this convention in this section, it will be easier to compare with the β-decay literature.) The transition probability per unit time is given by [15],

$$w_{if} = \frac{\xi}{4\pi^3} p_e E_e (E_{max} - E_e) \left(1 + a v_e \cos\theta + b \frac{2m_e}{E_e}\right) \sin\theta \, d\theta \tag{4.39}$$

where E_{max} is the maximum energy of the electron in beta decay, $v_e = p_e/E_e$ and,

$$\begin{aligned}
\xi &= \frac{1}{2}|M_F|^2 \left(|C_V|^2 + |C_V'|^2 + |C_S|^2 + |C_S'|^2\right) + \frac{1}{2}|M_{GT}|^2 \left(|C_A|^2 + |C_A'|^2 + |C_T|^2 + |C_T'|^2\right) \\
a\xi &= \frac{1}{2}|M_F|^2 \left(|C_V|^2 + |C_V'|^2 - |C_S|^2 - |C_S'|^2\right) - \frac{1}{6}|M_{GT}|^2 \left(|C_A|^2 + |C_A'|^2 - |C_T|^2 - |C_T'|^2\right) \\
b\xi &= \frac{1}{2}\mathrm{Re}\left(C_S C_V^* + C_S' C_V'^*\right)|M_F|^2 + \frac{1}{2}\mathrm{Re}\left(C_T C_A^* + C_T' C_A'^*\right)|M_{GT}|^2.
\end{aligned} \tag{4.40}$$

The angle, θ, is the angle between the electron and neutrino momenta and b is the Fierz interference term. The direct searches [2, 3, 4] for scalar interactions in β-decay consider pure Fermi transitions $0^+ \to 0^+$ as the parameter a has a particulary simple form. In this case the Gamow-Teller matrix elements are absent and the Fermi matrix elements divide out,

$$a = \frac{|C_V|^2 + |C_V'|^2 - |C_S|^2 - |C_S'|^2}{|C_V|^2 + |C_V'|^2 + |C_S|^2 + |C_S'|^2}. \tag{4.41}$$

Since in the standard model $C_V = C_V' = 1$, $a \neq 1$ implies evidence for an effective scalar interaction.

We need to rewrite our expressions for scalar interactions in terms of $\tilde{C}_s$ and $\tilde{C}_s'$ where $\tilde{C}_i = C_i/C_V$. The scalar couplings can be re-expressed,

$$S_A = \frac{\Lambda^2 G_F \cos\theta_c}{\sqrt{2}} (\tilde{C}_s + \tilde{C}_s') \tag{4.42}$$

$$S_B = \frac{\Lambda^2 G_F \cos\theta_c}{\sqrt{2}} (\tilde{C}_s - \tilde{C}_s') \tag{4.43}$$

where the S_A, S_B denote scalar interactions at the nucleon level. The operator analysis of section 4.3 was completed with quarks, thus we need to include the scalar form factor $< p|\bar{u}d|n >$ which can be estimated from lattice calculations [16], $< p|\bar{u}d|n > \approx 0.65 \pm 0.09$. By saturating the error in this quantity, we can obtain a conservative 2 σ constraint

equation on the scalar couplings from pion decay (see eq.(4.15)),

$$-1.0\times10^{-2} \leq \frac{1}{0.74}\frac{\tilde{f}_\pi \Delta_A}{f_\pi m_e}\mathrm{Re}(\tilde{C}_s+\tilde{C}'_s)+\frac{1}{0.74^2}\frac{\Delta_A^2\tilde{f}_\pi^2}{f_\pi^2 m_e^2}|\tilde{C}_s+\tilde{C}'_s|^2+\frac{1}{0.74^2}\frac{\Delta_B^2\tilde{f}_\pi^2}{f_\pi^2 m_e^2}|\tilde{C}_s-\tilde{C}'_s|^2 \leq 2.2\times10^{-3} \tag{4.44}$$

If we include only left-handed neutrinos in the theory, we are constrained to lie along the line $\tilde{C}_s = \tilde{C}'_s$ whereas if we include only right-handed neutrinos we are forced to lie along $\tilde{C}_s = -\tilde{C}'_s$. We can now examine a few special cases.

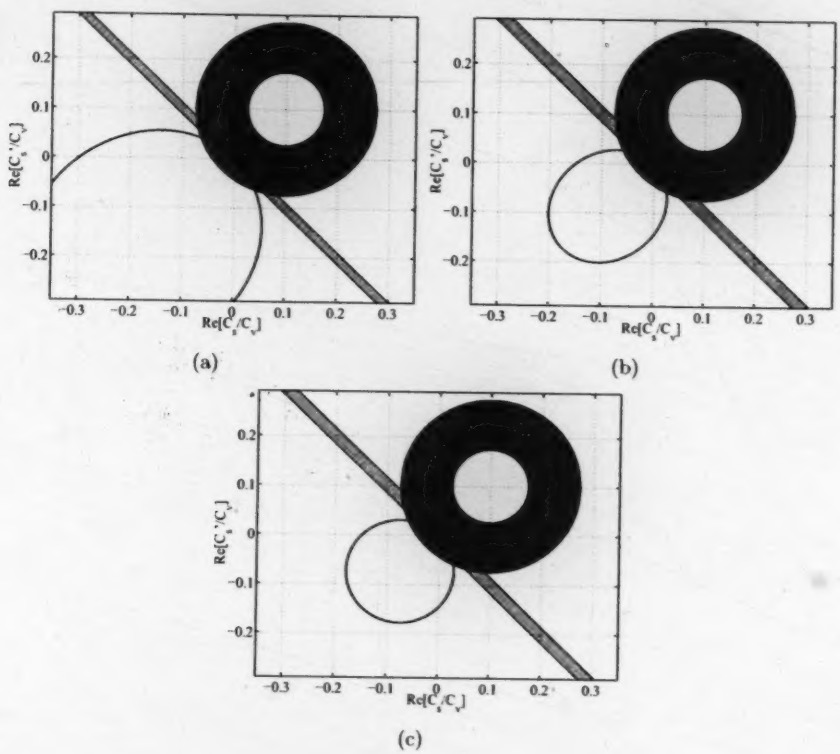

Figure 4.10: Constraint plots on the real parts of $\tilde{C}_s$ and $\tilde{C}'_s$ at Λ =200 GeV. Panel (a) corresponds to a phase of 0°; panel (b) to ±45°; and panel (c) to 45° and −45° for $\tilde{C}_s$ and $\tilde{C}'_s$ respectively. The diagonal band is the experimental limit set by the b-Fierz interference term from β-decay at the 90% confidence level and the solid annulus is the approximate experimental bound given in [3]. In all cases, the allowed region is the band between the two ellipses. An enlargement of the figures is displayed in figure 4.11.

In the absence of right-handed neutrinos, if we consider C_s and C'_s to be purely real and the scale Λ of the order of 200 GeV, the indirect limits from $\pi^{\pm} \to l^{\pm}\nu_l$ decay give

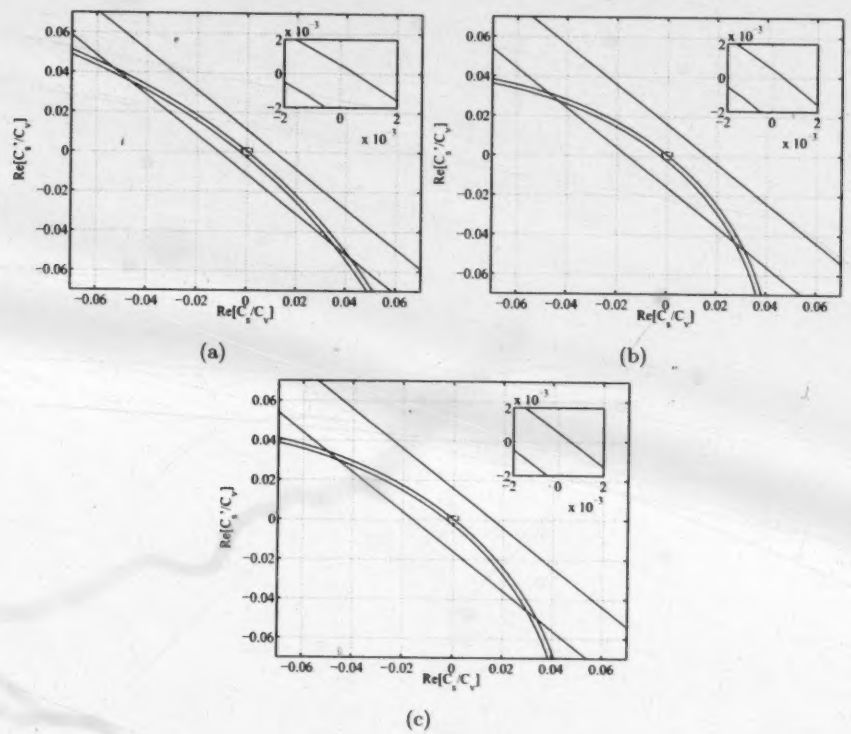

Figure 4.11: Constraint plots on the real parts of $\tilde{C}_s$ and $\tilde{C}'_s$ at Λ =200 GeV. Panel (a) corresponds to a phase of 0°; panel (b) to ±45°; and panel (c) to 45° and −45° for $\tilde{C}_s$ and $\tilde{C}'_s$ respectively. The diagonal band is the experimental limit set by the b-Fierz interference term from β-decay at the 90% confidence level. In all cases, the allowed region is the band between the two ellipses. The enlarged area more clearly shows the width of the region.

us the limit

$$-1.2 \times 10^{-3} \leq \tilde{C}_s \leq 2.7 \times 10^{-4}. \tag{4.45}$$

For comparison, the experimental 90% confidence limit determined from the b-Fierz interference term in β-decay (see eq.(4.40)) is $|\mathrm{Re}(\tilde{C}_s)| \leq 8 \times 10^{-3}$ [3, 5]. We see that the indirect limit from pion decay is stronger by over an order of magnitude. On the other hand, if we consider C_s and C'_s to be purely imaginary; again in the limit of left-handed couplings we obtain,

$$|\tilde{C}_s| \leq 1.2 \times 10^{-2} \tag{4.46}$$

where the scale Λ is of the order of 200 GeV. Again for comparison, the experimental limit on the size of the imaginary part at the 95% confidence level, with only left-handed

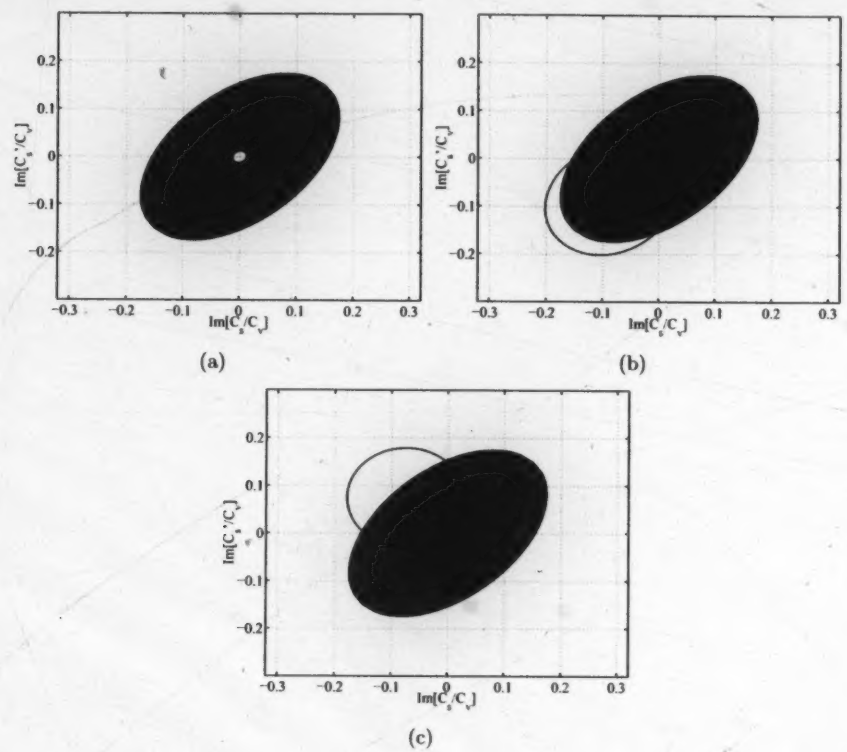

Figure 4.12: Constraint plots on the imaginary parts of $\tilde{C}_s$ and $\tilde{C}'_s$ at Λ =200 GeV. Panel (a) corresponds to a phase of $\pm 90°$; panel (b) to $\pm 45°$; and panel (c) to $45°$ and $-45°$ for $\tilde{C}_s$ and $\tilde{C}'_s$ respectively. The solid ellipse is the approximate experimental bound on the imaginary part of the couplings assuming nothing about the phase [3]. In panel (a), the unshaded interior ellipse is the constraint from pion decay. In the remaining plots, the allowed region is the band between the two ellipses. An enlargement of the figures is displayed in figure 4.13.

neutrinos, is approximately $|\mathrm{Im}(\tilde{C}_s)| \leq 1 \times 10^{-1}$ [3]. The indirect $\pi^{\pm} \to l^{\pm}\nu_l$ limit is stronger by approximately an order of magnitude. If we take $\tilde{C}_s = -\tilde{C}'_s$ so that we are in the limit of right-handed couplings and the b-Fierz interference term vanishes we find,

$$|\tilde{C}_s| \leq 1.0 \times 10^{-2}. \tag{4.47}$$

Again for comparison, at 1σ, the direct experimental constraint is $|\tilde{C}_s| \leq 6 \times 10^{-2}$[3]. In each case presented the scale of new physics was at $\Lambda = 200$ GeV corresponding to $\Delta_A(200\,\mathrm{GeV}) \approx 7.7 \times 10^{-4}$, $\Delta_B(200\,\mathrm{GeV}) \approx 8.9 \times 10^{-4}$. Because the pseudoscalar interactions are induced through renormalization group running from Λ down to the elec-

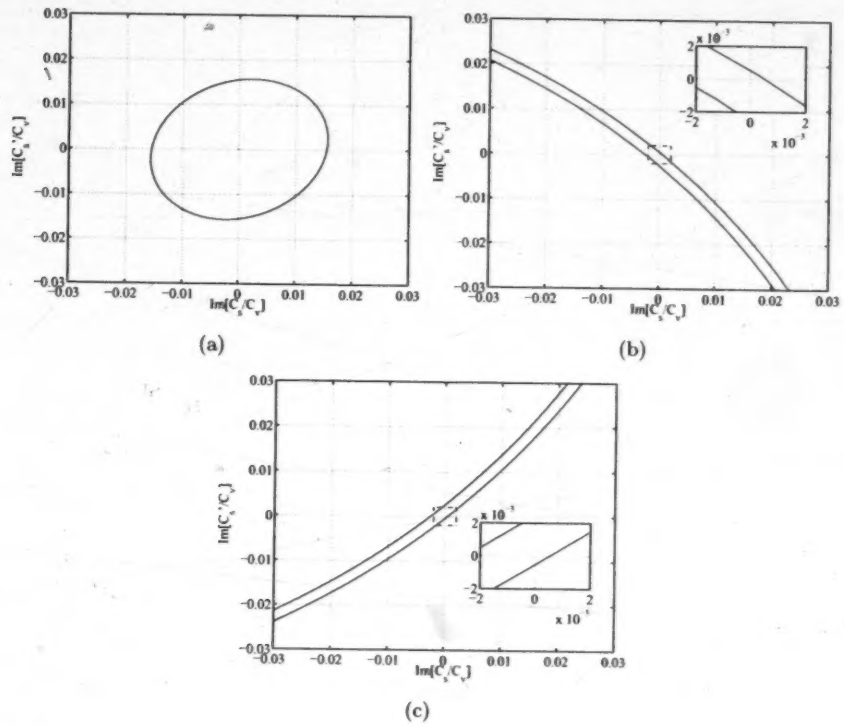

Figure 4.13: Constraint plots on the imaginary parts of $\tilde{C}_s$ and $\tilde{C}'_s$ at Λ =200 GeV. Panel (a) corresponds to a phase of $\pm 90°$; panel (b) to $\pm 45°$; and panel (c) to $45°$ and $-45°$ for $\tilde{C}_s$ and $\tilde{C}'_s$ respectively. In panel (a), the interior of the ellipse is the constraint. In the remaining plots, the allowed region is the band between the two ellipses. The enlarged area more clearly shows the width of the region.

troweak scale, the higher the scale of new physics is, the more competitive our results become relative to beta decay. As the scale of new physics is lowered, the constraints from $\pi^{\pm} \to l^{\pm}\nu_l$ become less stringent. However even in the worst case limit where the new scale is at the Z-mass and therefore we would no longer have an interval of renormalization group running, the renormalization threshold effects calculated in eq.(4.36) are still competitive. As an example, if we take C_s and C'_s to be real and ignore right-handed neutrinos we find that,

$$-2 \times 10^{-2} \leq \tilde{C}_s \leq 4 \times 10^{-3}. \tag{4.48}$$

Plots of the pion physics constraints for the more general situation (where the real and imaginary parts of C_s and C'_s vary independently) are given in figures 4.10, 4.11 4.12, and 4.13. We plot the constraints for the real and imaginary parts separately. Note from

eq.(4.44) that the phases of C_s and C_s' are important when constructing these separate plots. In order to convey the effects of the phases most clearly, we have chosen three interesting cases. In the real plots we consider: C_s and C_s' to each have a phase of $0°$; C_s and C_s' to each have a phase of $\pm 45°$; and the situation where C_s has as a phase of $45°$ and C_s' has a phase of $-45°$. In the imaginary plots we consider: C_s and C_s' to each have a phase of $\pm 90°$; C_s and C_s' each have a phase of $\pm 45°$; and the case where C_s has a phase of $45°$ and C_s' has a phase of $-45°$. All three plots in the imaginary case are well within the region allowed by the direct experimental bounds [3, 17].

There are two points of interest that warrant further discussion. First, note that in the limit of sufficiently large phases (i.e. $> 85°$) the ellipse bound in figure 4.11 moves entirely inside the b-Fierz interference limit allowed region. This is expected since phases approaching $90°$ imply that C_s and C_s' are almost completely imaginary. When this situation occurs and we are in the limit of left-handed couplings (i.e. along the line $C_s = C_s'$), there are two solutions consistent with the pion physics constraints and the b-Fierz interference bound. One solution is centered around 0 and the other is centered off 0 along the line $C_s = C_s'$ yet inside the b-Fierz interference limits. Even in these cases, the width of the ellipse bound is still of the order of 2×10^{-3}. Secondly, in order to move from the origin along the ellipse by more than the width of the allowed region requires a delicate cancellation between the terms in eq.(4.44). If we ignore the possibility of this cancellation, the region allowed by pion decay would collapse to a small region near the origin of length given by the width of the ellipse bounds.

4.6 Flavour Dependent Couplings

Thus far we have obtained limits on scalar interactions in the limit of universal flavour couplings. Let us now relax this assumption. One case that deserves attention is the limit of mass proportional couplings. This implies that $R_e/(m_e^2(m_\pi^2 - m_e^2)) = R_\mu/(m_\mu^2(m_\pi^2 - m_\mu^2))$ in eq.(4.10) and therefore there is no effect on the pion branching ratio,

$$\begin{aligned} \frac{\Gamma(\pi^- \to e\nu_e)}{\Gamma(\pi^- \to \mu\nu_\mu)} &= \frac{(m_\pi^2 - m_e^2)}{(m_\pi^2 - m_\mu^2)} \left[\frac{m_e^2(m_\pi^2 - m_e^2) + S_e}{m_\mu^2(m_\pi^2 - m_\mu^2) + S_\mu} \right] \\ &= T. \end{aligned} \tag{4.49}$$

This observation also holds in the presence of right-handed neutrinos. However, in this case, we still can bound the scalar couplings involved in β-decay by combining the $\pi^{\pm} \to l^{\pm}\nu_l$ limits with data from muon capture experiments. Recent experiments and analysis of muon capture on ^{3}He indicate that the muon-nucleon scalar coupling is

bounded by [18]

$$\frac{|S_\mu|}{\Lambda^2} \leq 4 \times 10^{-2} G_F \tag{4.50}$$

with a neutrino of left-handed chirality. Therefore, in the limit of mass proportional couplings, S_e/Λ^2 must be of the order of 200 times smaller due to the electron-muon mass ratio. This implies that $\tilde{C}_s$ is bounded,

$$|\tilde{C}_s| \leq 2 \times 10^{-4}. \tag{4.51}$$

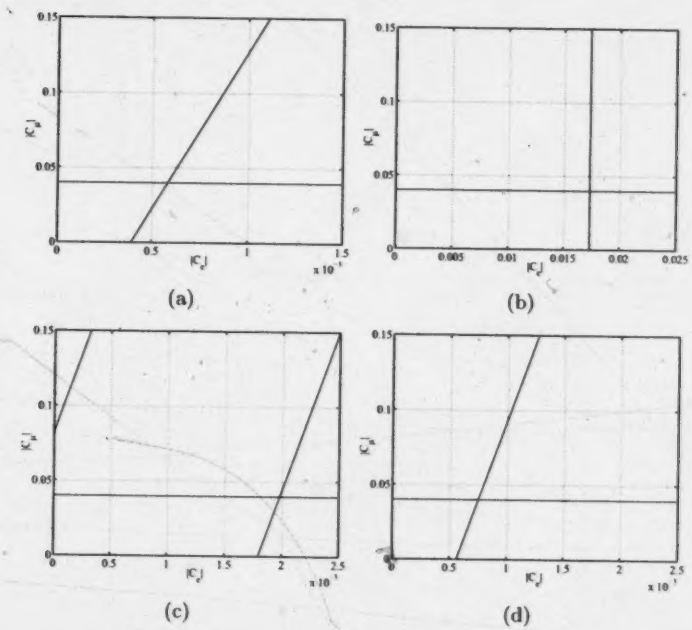

Figure 4.14: Constraint plots on the $|C_e|$ and $|C_\mu|$ couplings at $\Lambda = 200$ GeV. Panel (a) corresponds to phases for C_e and C_μ of 0°, 0°; panel (b) to 90°, 90°; panel (c) to 180°, 180°; panel (d) to ±45°, ±45° respectively. The allowed region is the bounded area in the lower left corner. The horizontal line is the muon capture bound [18].

In order to estimate the degree to which the presence of muon scalar interactions can weaken the limits that we infer from $\pi^{\pm} \to l^{\pm}\nu_l$, let us assume that the muon scalar coupling saturates the experimental bound eq.(4.50). Substituting this into the expression for the pion branching ratio eq.(4.13), ignoring right-handed neutrinos and

assuming a scale Λ of 200 Gev, eq.(4.15) is modified to the following form,

$$-3.3 \times 10^{-2} \leq \sqrt{2}\frac{\tilde{f}_\pi \mathrm{Re}(\rho)}{G_F \Lambda^2 f_\pi \cos\theta_c m_e} + \frac{|\rho|^2 \tilde{f}_\pi^2}{2G_F^2 \Lambda^4 f_\pi^2 \cos^2\theta_c m_e^2} \leq 7.3 \times 10^{-3}. \qquad (4.52)$$

We find this conservative approach has the effect of weakening our limits a factor of three at most compared to the analysis in section 4.5. The limits on scalar couplings with $\Lambda = 200\,\mathrm{GeV}$, from $\pi^{\pm} \to l^{\pm}\nu_l$ combined with muon capture scalar limits, are substantially stronger than limits on scalar couplings from direct β-decay searches.

Finally, we consider the allowed region for the electron-scalar and muon-scalar couplings in a model independent manner. Again the constraint equation derived from eq.(4.13) is,

$$-1.0 \times 10^{-2} \leq \left(\frac{1 + \sqrt{2}\frac{\tilde{f}_\pi \mathrm{Re}(C_e)\Delta_A}{f_\pi \cos\theta_c m_e} + \frac{|C_e|^2 \Delta_A^2 \tilde{f}_\pi^2}{2 f_\pi^2 \cos^2\theta_c m_e^2}}{1 + \sqrt{2}\frac{\tilde{f}_\pi \mathrm{Re}(C_\mu)\Delta_A}{f_\pi \cos\theta_c m_\mu} + \frac{|C_\mu|^2 \Delta_A^2 \tilde{f}_\pi^2}{2 f_\pi^2 \cos^2\theta_c m_\mu^2}} - 1 \right) \leq 2.2 \times 10^{-3}, \qquad (4.53)$$

where,

$$C_\mu = \frac{S_\mu}{G_F \Lambda^2} \quad C_e = \frac{S_e}{G_F \Lambda^2}. \qquad (4.54)$$

We display the results in figure 6.2 for a number of different phase conditions. We consider the cases where the complex phase of C_e and C_μ are 0°, 0°; 90°, 90°; 180°, 180°; ±45°, ±45°, respectively.

4.7 Discussion

By considering renormalization effects on universal (or alternatively first generation), and flavour diagonal scalar operators, we have derived limits on the size of the ratio between scalar and vector couplings from precision measurements of $\pi^{\pm} \to l^{\pm}\nu_l$ decay. As a typical constraint value, in the absence right-handed neutrinos, we find that $-1.2 \times 10^{-3} \leq \tilde{C}_s \leq 2.7 \times 10^{-4}$ for Λ of the order of 200 GeV. A more general comparison with the β-decay experiments (with the inclusion of right-handed neutrinos) is made in the plots in figure 4.11 and figure 4.13. We note that the most conservative estimate of the limits occurs when the new physics arises at the electroweak scale. In this case, the contribution to the induced pseudoscalar comes entirely from threshold corrections which we estimate from the calculations in section 4.4. The limit for real couplings in the absence of right-handed neutrinos from threshold contributions is $-3 \times 10^{-2} \leq \tilde{C}_s \leq 6 \times 10^{-3}$. In the scenario where we have arbitrary generation dependence of the scalar couplings, $\pi^{\pm} \to l^{\pm}\nu_l$ limits can be combined with limits on scalar interactions in muon capture to bound the first generation scalar couplings. These limits are illustrated in particular

cases in figure 6.2.

These observations have implications for current β-decay experiments. Direct searches for scalar interactions in β-decay will be most competitive if the new physics responsible for the effective scalar interactions arises at the electroweak scale in the explicit exchange of new scalar particles. In these circumstances, the indirect limits from threshold induced pseudoscalar interactions, eq.(4.48), are comparable to the direct β-decay scalar searches. Therefore, interest in searches for new scalar interactions with β-decay experiments remains undiminished.

On the other hand, for new effective scalar interactions arising as effective SU(2) $\times$ U(1) invariant operators at mass scales above 200 GeV (as expected in models with leptoquarks, composite quarks/leptons, or low scale quantum gravity) the constraints arising from the precision measurements of $\pi^{\pm} \to l^{\pm}\nu_l$ decay, combined with limits on scalar interactions in muon capture, can be stronger by an order of magnitude or more than the direct experimental searches. Furthermore, the relative strength of these searches becomes better, the higher the mass scale of the new physics compared to the electroweak scale. This argues strongly for improved experimental precision in measurements of muon capture, and $\pi^{\pm} \to l^{\pm}\nu_l$ decay. In particular we note that in the case of pion decay, the experimental error exceeds the uncertainty in the theoretical calculation by a factor of eight. A new measurement of $\pi^{\pm} \to l^{\pm}\nu_l$ decay with an order of magnitude greater precision would not only constrain physics beyond the standard model which could potentially contribute to tree level pion decay, but as we have argued above, will also indirectly provide tests of new scalar interactions of unparalleled precision.

Bibliography

[1] Particle Data Group, Phys. Rev. **D66**,(2002)

[2] A. Garcia *et al.*, nucl-ex/9904001.

[3] E. G. Adelberger *et al.* (ISOLDE), Phys. Rev. Lett. **83**, 1299 (1999), nucl-ex/9903002.

[4] E. G. Adelberger, Phys. Rev. Lett. **70**, 2856 (1993).

[5] For a review see: I. S. Towner and J. C. Hardy, nucl-th/9504015.

[6] For a review see: D. A. Bryman Comments Nucl. Part. Phys. **21** 101 (1993).

[7] W. J. Marciano and A. Sirlin, Phys. Rev. Lett. **71**, 3629 (1993).

[8] D. I. Britton *et al.*,Phys. Rev. Lett. **68**, 3000-3003 (1992).

[9] D. I. Britton *et al.*,Phys. Rev. D **49**, 17-20 (1993).

[10] D. I. Britton *et al.*,Phys. Rev. Lett. **70**, 3000-3003 (1992).

[11] For reviews see:
A. Manohar, hep-ph/9606222
D. Kaplan, nucl-th/9506035.

[12] S. Weinberg, Physica **96A**, 327-340 (1979).

[13] H. Arason, D. J. Castano, B. Keszthelyi, S. Mikaelian, E. J. Piard, P. Ramond, and B. D. Wright Phys.Rev. **D46**, 3945-3965 (1992).

[14] B. D. Wright hep-ph/9404217

[15] J. Jackson, S. Treiman, and H. Wyld Jr., Nucl. Phys. **4**, 206 (1957).

[16] S. J. Dong, J. F. Lagaë, and K. F. Liu, Phys. Rev. **D54**, 5496-5500 (1996), hep-ph/9602259.

[17] M. B. Schneider *et al.*, Phys. Rev. Lett. **51**, 1239 (1983).

[18] J. Govaerts and J.-L. Lucio-Martinez, Nucl. Phys. **A678**, 110 (2000), nucl-th/0004056.

Chapter 5

See-Saw Induced CMSSM Lepton Flavour Violation Post-WMAP

5.1 Introduction

The standard model contains three continuous global symmetries associated with lepton flavour. Neglecting non-perturbative effects arising from the weak SU(2) anomaly, the standard model conserves lepton flavour exactly, as the charged Yukawa matrix $\mathbf{Y_e}$ and the gauge interactions can simultaneously be made flavour diagonal. The solar [1]–[5], and atmospheric [6], neutrino deficit observations, which imply neutrino mass and mixing, (and their confirmation by reactor [7], and accelerator [8], experiments), presently provide the only direct observation of physics that cannot be accommodated within the standard model. The smallness of the inferred neutrino masses can be understood through the see-saw mechanism [9], which involves the introduction of a heavy Majorana fermion in a gauge singlet (right-handed neutrino) for each generation. The light neutrino masses are then induced through a Yukawa interaction of the form $N_i^c \mathbf{Y}_\nu^{ij} L_j H$, once the right-handed neutrinos are integrated out at the Majorana scale, M_R. The resulting induced neutrino mass operator arises at dimension 5 ($HHLL$) and, on dimensional grounds, would be expected to be the first observable extension beyond the renormalizable dimension 4 operators that compose the standard model interactions, given the standard model particle content at low energies.

Even without the addition of a see-saw sector generating neutrino masses, the standard model suffers from a gauge hierarchy problem, with quadratic divergences in radiative corrections to the Higgs mass parameter. These require unnatural fine-tuning of the input Higgs parameters, readjusted at each order in perturbation theory, in order to maintain the hierarchy of scales between the gravitational energy scale M_{Pl}, and the scale of electroweak breaking M_W. A natural solution to this problem is the supersymmetric

extension of the standard model, where the extra particles and interactions necessitated by supersymmetry contribute cancelling contributions to the destabilizing quadratic divergences in the Higgs potential, as required by the supersymmetry non-renormalization theorems. After soft supersymmetry breaking the cancellation of the quadratic divergences will still remain, though there will be finite shifts of the Higgs mass parameters by an amount proportional to the soft supersymmetry breaking. Model dependence enters in the choice of mechanism to impose the soft supersymmetry breaking. An especially attractive and well-motivated possibility is that the supersymmetry breaking is communicated (super-)gravitationally from a hidden sector in which supersymmetry is spontaneously broken, to the observable sector of the supersymmetric standard model (mSUGRA). Models with soft supersymmetry breaking masses of the form that this mechanism would impose, and where each of the soft supersymmetry breaking scalar masses, gaugino masses and trilinear couplings are universal and flavour diagonal at the Planck scale, comprise the constrained minimal supersymmetric standard model (CMSSM).

To incorporate see-saw neutrino masses in a supersymmetric extension of the standard model, we consider the minimal supersymmetric standard model with additional right-handed (singlet) neutrino supermultiplets and their superpotential interactions, where each of the soft supersymmetry breaking scalar masses, gaugino masses and trilinear couplings are universal and flavour diagonal at the Planck scale. New indirect sources of low-energy lepton-flavour violation (LFV) appear with the introduction of the singlet neutrino supermultiplets. Renormalization group running of the slepton mass matrices and trilinear couplings in the presence of right-handed neutrinos generates off diagonal elements that contribute to LFV processes [10],

$$(\Delta m_L^2)_{ij} \approx -\frac{1}{8\pi^2}(3+a^2)m_0^2(\mathbf{Y}_\nu{}^\dagger\mathbf{Y}_\nu)_{ij}\ln\left(\frac{M_{GUT}}{M_R}\right) \tag{5.1}$$

where M_R is the Majorana scale. As the see-saw mechanism violates lepton number by two units, the CMSSM with right-handed neutrino singlets continues to conserve R-parity; therefore the lightest supersymmetric particle (LSP) is stable. If it is assumed that the dark matter is composed of the LSP (which is expected to be the lightest neutralino), the CMSSM parameter space becomes tightly constrained by the WMAP satellite observations [11], as well as by laboratory searches. These constraints [12, 13, 14] have important implications for the rates of lepton-flavour violating processes.

In this study, we examine CMSSM lepton-flavour violation [15, 16, 17] in simple general classes [18] of see-saw models which are constructed to fit the low energy neutrino oscillation data. The parametrization of see-saw models is considered in Section 2. Two specific classes [18] of them (corresponding to hierarchical or degenerate Majorana masses

for the singlet right-handed neutrinos) form the model range of our calculations in Section 4. The models considered have their neutrino Yukawa couplings (and Majorana mass scale) chosen as large as reasonable, to maximize the rates for lepton-flavour violating decays; this is a conservative assumption, as we wish to consider how much of CMSSM parameter space (and see-saw model space) is still consistent with experimental limits on lepton-flavour violation, and this is conservatively determined under assumptions that maximize its calculated rate.

In Section 3 we discuss the range of parameter space of the CMSSM over which we perform our calculations. The CMSSM parameters are chosen such that their renormalization group running to low energies yields radiative electroweak symmetry breaking, and a resulting spectrum of particle masses that is consistent with experiment. In particular, we display our results over CMSSM parameter ranges determined by [12] and [13], which impose that the resulting models have LSP relic densities in the region determined by WMAP [11], and are consistent with the LEP direct search limits, and the rate for $b \to s\gamma$. See also [14] for other parameter determinations using WMAP and laboratory data.

In Section 4 we compute the branching ratio for the decay $\mu \to e\gamma$ [15, 16], in the classes of see-saw models considered, over the allowed range of CMSSM parameter space, and compare to present [19], and prospective [20], data for this process. We consider $\mu \to e\gamma$ because with the present level of experimental precision, lepton-flavour violation in the models and parameter ranges we consider would only be detectable in muon decays. Of the muon decays, since the rates for $\mu \to eee$, and $\mu N \to eN$, are largely dominated by electromagnetic penguin contributions (again, in the models and parameter ranges we consider), they are suppressed with respect to the rate for $\mu \to e\gamma$ by an extra factor of α. Since at the present time the experimental limit on $\mathrm{BR}(\mu \to e\gamma) \leq 1.2 \times 10^{-11}$ [19], is of comparable strength to the limits on $\mathrm{BR}(\mu \to eee) \leq 1.0 \times 10^{-12}$ [21], and $\mathrm{BR}(\mu N \to eN) \leq 6.1 \times 10^{-13}$ [22], the model class that we study will be consistent with all the present lepton-flavour violation data if it satisfies the present limit on $\mathrm{BR}(\mu \to e\gamma)$. We will find that even for a choice of neutrino Yukawa coupling (and Majorana scale) that maximizes the rates for lepton-flavour violation, that much of the model space and parameter range is consistent with present experimental limits, though future experiments should probe these ranges thoroughly, at least for the largest choices of Yukawa couplings.

In Section 5 we present our conclusions. For a thorough review of muon physics and muon flavour violation, see [25].

5.2 Supersymmetric See-Saw Parameterization

The leptonic part of the CMSSM see-saw superpotential is

$$\mathcal{L} = \mathbf{Y_e}^{ij}\epsilon_{\alpha\beta}H_d^\alpha e_i^c L_j^\beta + \mathbf{Y}_\nu{}^{ij}\epsilon_{\alpha\beta}H_u^\alpha N_i^c L_j^\beta + \frac{1}{2}\mathcal{M}^{ij}N_i^c N_j^c \tag{5.2}$$

above the Majorana scale. Here, L_i, $i = e, \mu, \tau$, is the left handed weak doublet, e_i^c is the charged lepton weak singlet, and H_u and H_d are the two Higgs doublets of opposite hypercharge. The anti-symmetric SU(2) tensor is defined by $\epsilon_{12} = +1$. N denotes the right-handed neutrino singlet. The Yukawa matrices $\mathbf{Y_e}$ and $\mathbf{Y}_\nu$ give masses to the charged leptons and Dirac masses to the neutrinos respectively. The Majorana matrix, $\mathcal{M}^{ij}$, gives the right-handed neutrinos their heavy Majorana mass. Below the Majorana scale the right-handed neutrinos are integrated out, and after renormalization down to the scale of electroweak symmetry breaking, induce a Majorana mass for the light left-handed neutrinos via the see-saw mechanism,

$$\mathbf{m}_\nu = \mathbf{Y}_\nu{}^T\mathcal{M}^{-1}\mathbf{Y}_\nu < H_u^0 >^2 \tag{5.3}$$

where $< H_u^0 >^2 = v_2^2 = v^2 \sin^2\beta$ and $v = (174\ \text{GeV})^2$ as set by the Fermi constant G_F. By transforming to a basis where $\mathbf{Y_e}$ and the gauge interactions are flavour diagonal, the left-handed neutrino mass matrix is diagonalized by the PMNS matrix $\mathbf{U}$,

$$\mathbf{U}^T\mathbf{m}_\nu\mathbf{U} = \text{diag}(m_1, m_2, m_3) \tag{5.4}$$

where $\mathbf{U}$ is a unitary matrix that connects flavour states to the mass eigenbasis. It is possible to parameterize the PMNS matrix as follows,

$$\mathbf{U} = \mathbf{U}'\text{diag}(e^{-i\phi/2}, e^{-i\phi'}, 1) \tag{5.5}$$

$$\mathbf{U}' = \begin{pmatrix} c_{13}c_{12} & c_{13}s_{12} & s_{13}e^{-i\delta} \\ -c_{23}s_{12} - s_{23}s_{13}c_{12}e^{i\delta} & c_{23}c_{12} - s_{23}s_{13}s_{12}e^{i\delta} & s_{23}c_{13} \\ s_{23}s_{12} - c_{23}s_{13}c_{12}e^{i\delta} & -s_{23}c_{12} - c_{23}s_{13}s_{12}e^{i\delta} & c_{23}c_{13} \end{pmatrix}. \tag{5.6}$$

where ϕ and ϕ' are additional CP violating phases and $\mathbf{U}'$ has the usual form of the CKM matrix. It was shown in [18] that the Yukawa matrix Y_ν can be re-expressed in a simple general form. By defining,

$$\kappa \equiv \frac{\mathbf{m}_\nu}{< H_u^0 >^2} = \mathbf{Y}_\nu{}^T\mathcal{M}^{-1}\mathbf{Y}_\nu \tag{5.7}$$

and using the PMNS matrix, it is possible to diagonalize κ,

$$\kappa_d = \mathbf{U}^T \mathbf{Y}_\nu{}^T \mathcal{M}^{-1} \mathbf{Y}_\nu \mathbf{U}. \tag{5.8}$$

where the d subscript denotes diagonalization. It is always possible to make an arbitrary field re-definition to rotate to a basis such that $\mathcal{M}$ is diagonal, hence $\mathcal{M}_d = \text{diag}(\mathcal{M}_1, \mathcal{M}_2, \mathcal{M}_3)$. In this case,

$$\mathbf{1} = \left(\sqrt{\mathcal{M}_d^{-1}} \mathbf{Y}_\nu \mathbf{U} \sqrt{\kappa_d^{-1}}\right)^T \left(\sqrt{\mathcal{M}_d^{-1}} \mathbf{Y}_\nu \mathbf{U} \sqrt{\kappa_d^{-1}}\right) \tag{5.9}$$

where a square root over a diagonal matrix denotes the positive square root of its entries. One then identifies

$$\mathbf{R} \equiv \sqrt{\mathcal{M}_d^{-1}} \mathbf{Y}_\nu \mathbf{U} \sqrt{\kappa_d^{-1}} \tag{5.10}$$

as an arbitrary orthogonal matrix. Then, the most general form of $\mathbf{Y}_\nu$ is [18]

$$\mathbf{Y}_\nu = \sqrt{\mathcal{M}_d} \mathbf{R} \sqrt{\kappa_d} \mathbf{U}^\dagger. \tag{5.11}$$

As pointed out by the authors of [18], the physical low-energy observables contained in $\mathbf{U}$ and κ_d are augmented by three positive mass eigenvalues associated with $\mathcal{M}$ and three (in general complex) parameters that define the orthogonal matrix $\mathbf{R}$. It should be stressed that the above equation is defined at the Majorana scale, M_R. It is useful to parameterize the neutrino Yukawa couplings with the use of an arbitrary orthogonal matrix, $\mathbf{R}$, as it allows a general examination of the origin of flavour violation in see-saw models.

Following [18] we will consider two classes of neutrino hierarchy models. In the first case we will examine a strong right-handed neutrino hierarchy and in the second, we will consider degenerate right-handed neutrinos. In both cases we will assume that the Yukawa couplings of the left-handed neutrinos are hierarchical. We will impose the condition that the largest eigenvalue of the $\mathbf{Y}_\nu{}^\dagger \mathbf{Y}_\nu$ matrix (denoted $|Y_0|^2$) coincide with the square of the top quark Yukawa coupling $|Y_t|^2$ at the unification scale M_{GUT}. This Yukawa unification condition is suggested in simple $SO(10)$ models, and has the effect of making the neutrino Yukawa couplings, and hence the rates for lepton-flavour violating processes, as large as reasonably possible. Since we are interested in the degree to which present experimental limits rule out regions of model and CMSSM parameter space, maximizing the expected rates gives us a conservative determination of the models and parameter ranges that are still viable. More specific details of the classes of models to be analyzed will be discussed in Section 4.

5.3 Supersymmetry Breaking and the CMSSM

Since supersymmetric particles have not yet been observed, the model Lagrangian must contain terms that break supersymmetry. If we assume that supersymmetry is broken softly, in that the supersymmetry violating terms are of mass dimension 2 and 3, then the Lagrangian has the following supersymmetry breaking terms,

$$\begin{aligned}
-\mathcal{L}_{soft} &= (\mathbf{m}^2_{\tilde{\mathbf{L}}})_{ij}\tilde{L}^\dagger_i\tilde{L}_j + (\mathbf{m}^2_{\tilde{\mathbf{e}}})_{ij}\tilde{e}^*_{Ri}\tilde{e}_{jR} + (\mathbf{m}^2_{\tilde{\nu}})_{ij}\tilde{\nu}^*_{Ri}\tilde{\nu}_{Rj} \\
&\quad +(\mathbf{m}^2_{\tilde{\mathbf{Q}}})_{ij}\tilde{Q}^\dagger_i\tilde{Q}_j + (\mathbf{m}^2_{\tilde{\mathbf{u}}})_{ij}\tilde{u}^*_{Ri}\tilde{u}_{jR} + (\mathbf{m}^2_{\tilde{\mathbf{d}}})_{ij}\tilde{d}^*_{Ri}\tilde{d}_{jR} \\
&\quad +\tilde{m}^2_{H_d}H^\dagger_d H_d + \tilde{m}^2_{H_u}H^\dagger_u H_u + (B\mu H_d H_u + \frac{1}{2}B_\nu \mathcal{M}_{ij}\tilde{\nu}^*_{Ri}\tilde{\nu}^*_{Rj} + \text{h.c.}) \\
&\quad [(\mathbf{A_d})_{ij}H_d\tilde{d}^*_{Ri}\tilde{Q}_j + (\mathbf{A_u})_{ij}H_u\tilde{u}^*_{Ri}\tilde{Q}_j + (\mathbf{A_l})_{ij}H_d\tilde{e}^*_{Ri}\tilde{L}_j + (\mathbf{A}_\nu)_{ij}H_u\tilde{\nu}^*_{Ri}L_j \\
&\quad +\frac{1}{2}M_1\tilde{B}^0_L\tilde{B}^0_L + \frac{1}{2}M_2\tilde{W}^a_L\tilde{W}^a_L + \frac{1}{2}M_3\tilde{G}^a\tilde{G}^a + \text{h.c.}]
\end{aligned} \tag{5.12}$$

Note the presence of terms containing $\mathbf{m}_{\tilde{\nu}}{}^2$ and $\mathbf{A}_\nu$ in eq.(5.12). These terms are only included above the Majorana scale. Below the Majorana scale, the soft part of the Lagrangian returns to that of the CMSSM. In the CMSSM scenario, supersymmetry is broken in a universal *i.e.*, flavour independent, manner giving the following relations

$$(\mathbf{m}^2_{\tilde{f}})_{ij} = m_0^2\mathbf{1} \quad \tilde{m}^2_{h_i} = m_0^2 \quad \mathbf{A_f}_{ij} = am_0\mathbf{Y_f}, \tag{5.13}$$

where m_0 is a universal scalar mass and a is a dimensionless constant. We restrict to the CMSSM in our studies and set the trilinear A-term soft parameter $a = 0$. The ranges for the other non-zero, Planck-scale, inputs to the CMSSM are chosen such that their renormalization group running to low energies yields radiative electroweak symmetry breaking, and a resulting spectrum of particle masses that is consistent with experiment. In particular, we display our results over CMSSM parameter ranges determined by [12] and [13], which not only impose that the resulting model have LSP relic densities in the range determined by WMAP [11], but that they have spectra consistent with the LEP direct search limits, as well as the rate for $b \to s\gamma$. Following these authors we ignore the focus point region in parameter space which occurs at very large m_0 and whose location depends on m_t and M_H in an extremely sensitive manner.

Note that the absence of off-diagonal terms leads to flavour conservation (up to effects of light neutrino mass splittings). However, these relations are imposed at the GUT scale and are therefore subject to renormalization group running. Above the Majorana scale, the neutrino sector modifies the CMSSM renormalization group equations (RGEs). In fact, the flavour violation is controlled by the off-diagonal terms in $\mathbf{Y}_\nu{}^\dagger\mathbf{Y}_\nu$ which contribute to the off-diagonal terms of $\mathbf{m}^2_{\tilde{\mathbf{L}}}$. In the leading log approximation to the

RGEs we have,

$$\begin{aligned}
(\mathbf{m}_{\tilde{\mathbf{L}}}{}^2)_{ij} &\approx -\frac{1}{8\pi^2}(3+a^2)m_0^2(\mathbf{Y}_\nu{}^\dagger\mathbf{Y}_\nu)_{ij}\ln\frac{M_{GUT}}{M_R} \\
(\mathbf{m}_{\tilde{\mathbf{e}}}{}^2)_{ij} &\approx 0 \\
(\mathbf{A_e})_{ij} &\approx -\frac{3}{8\pi^2}am_0Y_{l_i}(\mathbf{Y}_\nu{}^\dagger\mathbf{Y}_\nu)_{ij}\ln\frac{M_{GUT}}{M_R}
\end{aligned} \tag{5.14}$$

where Y_{l_i} denotes the Yukawa coupling of the charged lepton l_i. It is the presence of such terms that leads to significant flavour violation. We will see in the following sections how much flavour violation we should expect, and how the branching ratio for the process $\mu \to e\gamma$ is affected. The branching ratio for $\mu \to e\gamma$ can be estimated through mass insertion techniques [15, 16]:

$$\begin{aligned}
\mathrm{BR}(\mu \to e\gamma) &\sim \frac{\alpha^3}{G_F^2}\frac{(m_{\mathbf{L}})_{12}^2}{m_s^8}\tan^2\beta \\
&\sim \frac{\alpha^3}{G_F^2 m_s^8}\left|\frac{-1}{8\pi^2}(3+a^2)m_0^2\ln\frac{M_{GUT}}{M_R}\right|^2\left|\left(\mathbf{Y}_\nu{}^\dagger\mathbf{Y}_\nu\right)_{12}\right|^2\tan^2\beta
\end{aligned} \tag{5.15}$$

where m_s is a typical slepton mass. We note that the branching ratio is proportional to $\tan^2\beta$, which will give an increasing dependence on the ratio of Higgs vevs $\tan\beta$, and will be evident in our detailed results in the next section.

5.4 $\mu \to e\gamma$ In The CMSSM See-Saw

Following [18] we consider two classes of neutrino hierarchy models. In both cases the neutrino Yukawa couplings to the left-handed neutrinos are assumed to be hierarchical. In the first class of models the Majorana mass terms for the singlet right-handed see-saw neutrinos are assumed to be strongly hierarchical. In the second, we will assume that the right-handed singlet neutrinos have degenerate Majorana masses. We numerically integrate the one loop CMSSM RGEs with right-handed neutrino supermultiplets. In addition, we have re-derived the expressions [15] for the amplitude for $\mu \to e\gamma$, and we use the resulting full expressions (see Appendix) to calculate the branching ratios.

5.4.1 Hierarchical ν_Rs

As we saw in Section 2, $\mathbf{Y}_\nu$ can be expressed using an orthogonal matrix, $\mathbf{R}$. Following [18], and ignoring possible phases, it is useful to parameterize R as,

$$\mathbf{R} = \begin{pmatrix} c_2c_3 & -c_1s_3 - s_1s_2c_3 & s_1s_3 - c_1s_2c_3 \\ c_2s_3 & c_1c_3 - s_1s_2s_3 & -s_1c_3 - c_1s_2s_3 \\ s_2 & s_1c_2 & c_1c_2 \end{pmatrix}. \tag{5.16}$$

Since we are assuming that the left-handed neutrinos are hierarchical, we take

$$\kappa_2 = \sqrt{\frac{(\Delta m^2_\nu)_{\rm sol}}{v_2^4}} \quad \kappa_3 = \sqrt{\frac{(\Delta m^2_\nu)_{\rm atm}}{v_2^4}}, \tag{5.17}$$

and based on the bi-maximal LMA mixing solution we take the PMNS matrix to be,

$$\mathbf{U_{PMNS}} \approx \begin{pmatrix} .866 & .500 & 0 \\ -.354 & .612 & .707 \\ .354 & -.612 & .707 \end{pmatrix}. \tag{5.18}$$

If we assume a strong hierarchy in the right-handed sector, then

$$(\mathbf{Y}_\nu)_{ij} = \sqrt{\mathcal{M}_3}\delta_{i3}\mathbf{R}_{3l}(\sqrt{\kappa_d})_l\mathbf{U}^\dagger_{lj}. \tag{5.19}$$

The largest eigenvalue of eq.(5.19) is $Y_0 = \mathcal{M}_3(|\mathbf{R}_{32}|^2\kappa_2 + |\mathbf{R}_{33}|^2\kappa_3)$. We identify this with the top coupling at M_{GUT} as in the case of many $SO(10)$ models. By identifying the largest Yukawa in the neutrino sector with the top coupling LFV is maximized. We assume that $\mathbf{R}_{32} \neq 0$ or $\mathbf{R}_{33} \neq 0$. The pathology of the case where $\mathbf{R}_{32} = 0$ or $\mathbf{R}_{33} = 0$ is discussed in [18], which forms a small region of parameter space. With these assumptions, $M_R \sim 10^{15}$ GeV. This leaves us with one complex parameter. Following [18], we will assume that this parameter is real. Therefore, $\mathbf{Y}_\nu$ will depend on one angle, denoted by θ_1 in eq.(5.16).

First, consider figure 5.1. This plot shows BR($\mu \to e\gamma$) as a function of θ_1 and is made with parameters typical of the WMAP regions of [12], as indicated in the caption. The angle θ_1 varies over 0 to π and we only show the $\mu > 0$ case as the plots with $\mu < 0$ are very similar. Most of θ_1 is allowed for low to moderate $\tan\beta \lesssim 40$. Notice that there are two special places where the branching ratio becomes highly suppressed. These choices for θ_1 correspond to the vanishing of the off diagonal element $(\mathbf{Y}_\nu{}^\dagger\mathbf{Y}_\nu)_{12}$

which results in large flavour suppression. The special angles are,

$$\tan\theta_1 \approx -\sqrt{\frac{\kappa_3}{\kappa_2}}\frac{\mathbf{U}^*_{13}}{\mathbf{U}^*_{12}} \approx 0 \quad \tan\theta_1 \approx -\sqrt{\frac{\kappa_3}{\kappa_2}}\frac{\mathbf{U}^*_{23}}{\mathbf{U}^*_{22}}. \tag{5.20}$$

In order to quantify and further illustrate the regions that are both LFV and CMSSM compliant in this scenario, consider figures 5.2 and 5.3. The regions considered are a parameterization of the WMAP data from [12]. In figure 5.2, the bands correspond to $\tan\beta = 5, 10, 15, 20, 25, 30, 35, 40, 45, 50, 55$ for $\mu > 0$ and each colour represents the percentage of the θ_1 range that is allowed by the current bound on $\mu \to e\gamma$, $\mathrm{BR}(\mu \to e\gamma) < 1.2 \times 10^{-11}$. Grey indicates that less than 25% of θ_1 is allowed, while red, green and blue illustrate that between 25% and 50%, 50% and 75%, and between 75% and 100% is allowed respectively. Notice that there are two competing effects controlling the amount of LFV in these plots. As we move higher in $\tan\beta$, the branching ratio, $\mathrm{BR}(\mu \to e\gamma)$ increases as eq.(6.16). At the same time, the rate becomes suppressed at larger m_0 and $m_{1/2}$. As figure 5.2 illustrates, there are portions of the parameter space at high $\tan\beta$, (*i.e.* $\gtrsim 45$), that are consistent with the current LFV bound due to the high universal scalar and gaugino mass in those regions. Figure 5.3 shows the situation after a possible null result from MEG, ($\mathrm{BR}(\mu \to e\gamma) \lesssim 5 \times 10^{-14}$). We see that a large portion of the parameter space would be highly restricted, with most of the parameter space relegated to less than 25%. Therefore, the θ_1 range will be throughly probed by the up coming experiments, given this see-saw scenario. In the $\mu < 0$ case, the situation is slightly different. While the branching ratio of $\mu \to e\gamma$ is largely insensitive to the sign of μ, the WMAP compliant parameter space is not [13]. Figure 5.4 shows the constraints from lepton flavour violation with the current limit on $\mathrm{BR}(\mu \to e\gamma) < 1.2 \times 10^{-11}$ over the WMAP range for $\mu < 0$ and $a = 0$ with $\tan\beta = 10, 35$. Grey indicates that less than 25% of θ_1 is allowed, while red, green and blue illustrate that between 25% and 50%, 50% and 75%, and between 75% and 100% is allowed respectively. The funnel structure in figure 5.4 for $\mu < 0$ appears at lower $\tan\beta$ (*i.e.* ~ 35) compared to figure 5.2. This pushes the parameter space to larger values of m_0 and $m_{1/2}$ at lower $\tan\beta$ and therefore allows more room where the WMAP region is LFV compliant. Figure 5.5 shows how figure 5.4 changes after the expected results from MEG. If LFV is not observed in the near future, this scenario will only allow a small region of θ_1 corresponding to values near those given in eq.(5.20) with $\mu > 0$, or a relatively moderate region of θ_1 with $\mu < 0$.

5.4.2 Degenerate ν_Rs

Ignoring possible phases in $\mathbf{R}$, lepton-flavour violation becomes $\mathbf{R}$-independent, in the case of degenerate singlet right-handed neutrino Majorana masses. We see from eq.(5.11)

that, $\mathbf{Y}_\nu\mathbf{Y}_\nu{}^\dagger$, which controls the amount of lepton flavour violation becomes

$$\mathbf{Y}_\nu{}^\dagger\mathbf{Y}_\nu = \mathcal{M}\mathbf{U}\kappa_d\mathbf{U}^\dagger, \tag{5.21}$$

which is independent of $\mathbf{R}$. Again, we use the GUT relation $|Y_0| \sim \mathcal{M}\kappa_3 = |Y_t(M_{\rm GUT})|$ as in [18]. The situation here is quite different from the hierarchical case. Figure 5.6 shows the currently allowed region for $\mu \to e\gamma$ consistent with the CMSSM for $\mu > 0$ [12]. Notice that most of the parameter space is ruled out in this scenario; only $\tan\beta \lesssim 5$ and a small region at $\tan\beta \approx 50$ are consistent with the current LFV bounds. The upcoming limits will probe all of this currently allowed region. In the $\mu < 0$ [13] case more of the parameter space is allowed as the region is pushed to higher soft mass scales and therefore the LFV rates become suppressed as before. Figure 5.7 illustrates the allowed region consistent with the current LFV bounds for $\mu < 0$. Clearly the degenerate case, with maximized "unification" neutrino Yukawa couplings, is strongly constrained by the present data and will be be severely probed by the forth-coming generation of experiments.

5.5 Conclusion

In this chapter, we examined CMSSM lepton-flavour violation in simple general classes of see-saw models [18] which had been constructed to fit the data on low energy neutrino oscillations. The models considered have had their neutrino Yukawa couplings (and Majorana mass scale) chosen as large as reasonable, to maximize the rates for lepton-flavour violating decays. Nevertheless, when the CMSSM parameters for the models were restricted (following [12, 13]) to have LSP relic densities in the region determined by WMAP, and to be consistent with the LEP direct search limits, and the rate for $b \to s\gamma$, the resulting rate for lepton-flavour violation was such that over much of the allowed WMAP range, much of the model parameter space was consistent with the present experimental limit on BR($\mu \to e\gamma$) (and so, a fortiori, with present limits on the other (charged) lepton-flavour violating processes). We also noted that the next generation of $\mu \to e\gamma$ experiments should definitively probe the range of branching ratios suggested by these models at maximal Yukawa couplings, and also for ranges of smaller Yukawas depending on the CMSSM parameters and the exact see-saw model details.

A future detection of $\mu \to e\gamma$ would, however, represent not the end of lepton-flavour violation studies of these models, but rather just the beginning. To disentangle the details of CMSSM see-saw lepton flavour violation will require comparisons of rates for different LFV muon decays, including $\mu \to eee$, and $\mu N \to eN$. It will also require the observation of (charged) lepton-flavour violation in different generations, such as $\tau \to \mu\gamma$,

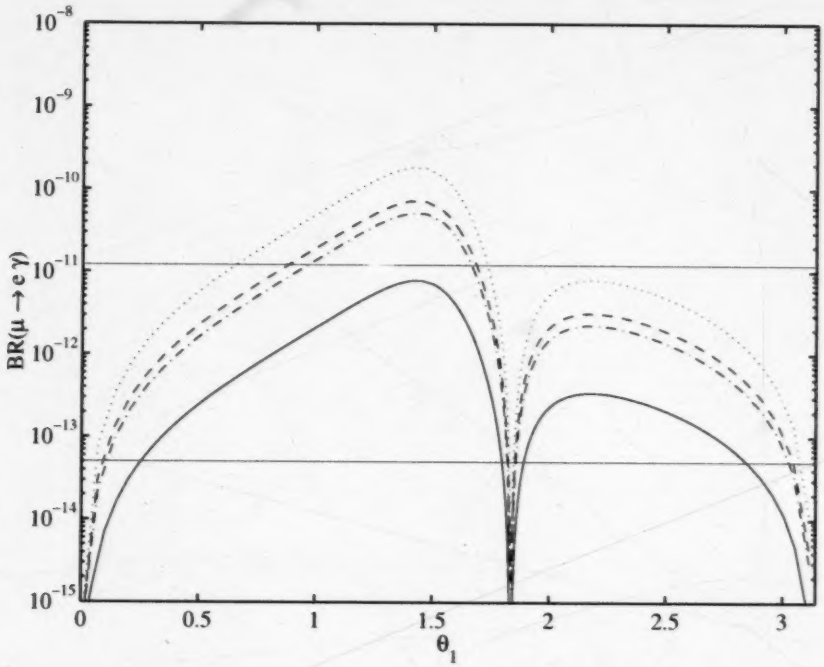

Figure 5.1: **Hierarchical ν_Rs**: BR($\mu \to e\gamma$) as a function of the seesaw parameter θ_1; $\mu > 0$ and $a = 0$. The solid curve corresponds to $\tan\beta = 5$, $m_0 = 140$ GeV, $m_{1/2} = 700$ GeV. The dash-dot curve corresponds to $\tan\beta = 10$, $m_0 = 125$ GeV, $m_{1/2} = 560$ GeV. The dashed curve corresponds to $\tan\beta = 20$, $m_0 = 200$ GeV, $m_{1/2} = 760$ GeV. The dotted curve corresponds to $\tan\beta = 40$, $m_0 = 390$ GeV, $m_{1/2} = 900$ GeV. Each parameter set is chosen to lie inside the CMSSM allowed region [12]. The upper horizontal line indicates the present experimental bound and the lower line indicates the expected upcoming experimental sensitivity from MEG.

$\tau \to e\gamma$, $\tau \to \mu ll$, and $\tau \to ell$, with l either e or μ. With a combination of observed rates for different LFV μ-decays, and the observation of LFV in τ decays, one can hope to begin to uncover both the precise nature of the low-energy soft supersymmetry breaking, as well as the origin of the lepton-flavour violating interactions responsible for inducing these decays. Fortunately, we can look forward to a new generation of dedicated $\mu \to e\gamma$ [20], and $\mu N \to eN$ [23],[24] experiments, as well as to τ sources of unprecedented flux, to help us find the experimental signatures of this new realm of physics.

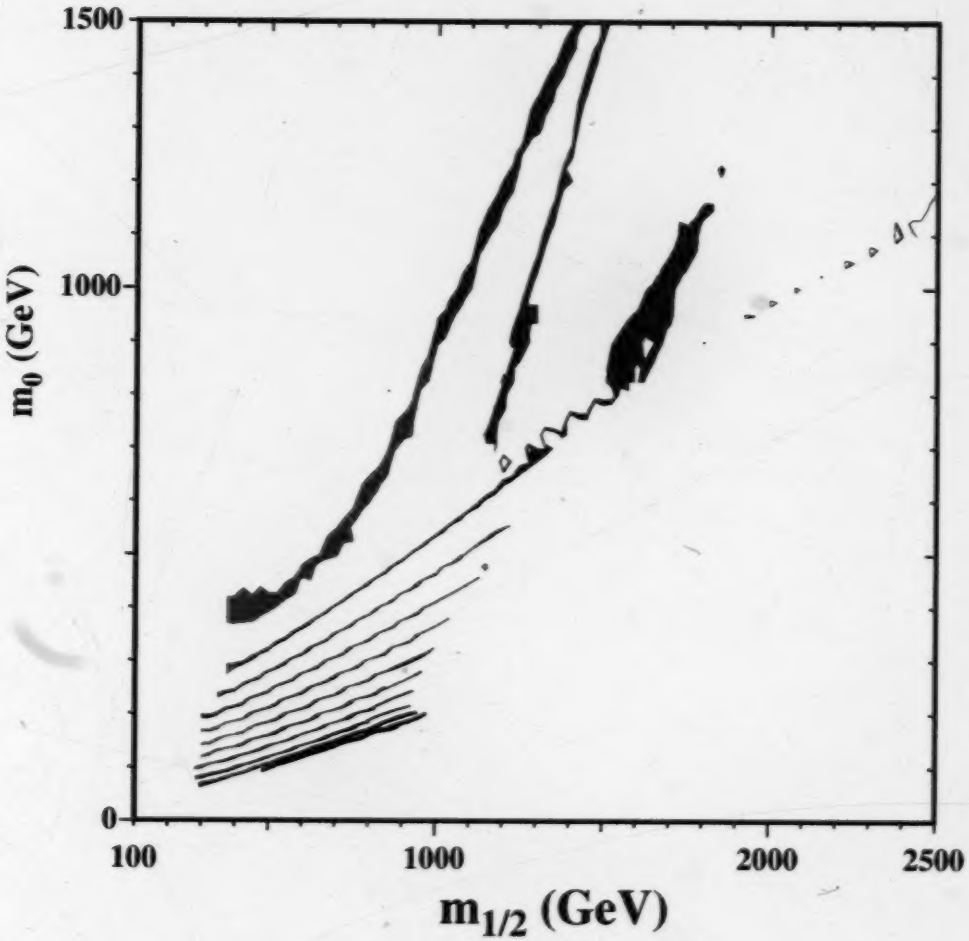

Figure 5.2: **Hierarchical ν_Rs**: WMAP and laboratory constraint parameterization of the CMSSM, and LFV compliance, based on the current LFV bound, $\mathrm{BR}(\mu \to e\gamma) < 1.2 \times 10^{-11}$ for $\tan\beta = 5$, 10, 15, 20, 25, 30, 35, 40, 45, 50, 55, $\mu > 0$ and $a = 0$. Grey indicates that less than 25% of the range of θ_1 is allowed. Red indicates that between 25% and 50% of θ_1 is allowed. Green and blue illustrate that 50% to 75%, and 75% to 100%, are allowed respectively. The constraint regions are reproduced from [12].

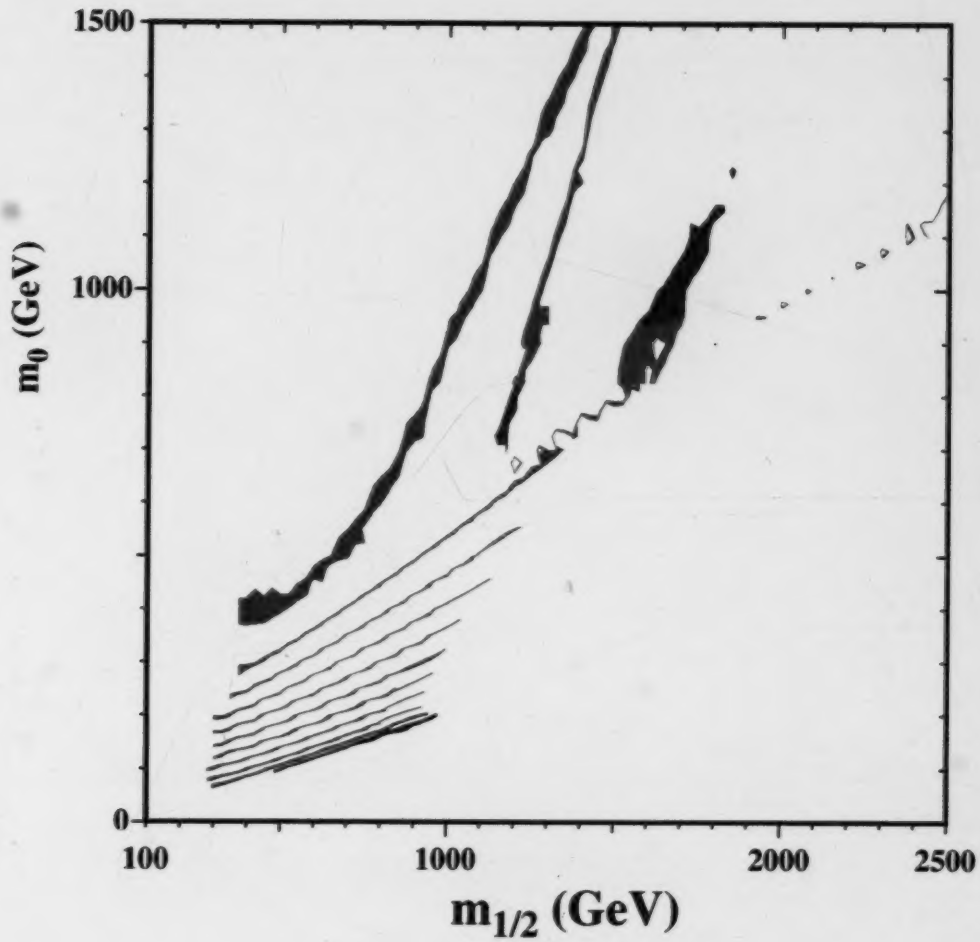

Figure 5.3: **Hierarchical ν_Rs**: WMAP and laboratory constraint parameterization of the CMSSM, and LFV compliance, based on the expected LFV bound from MEG, $\mathrm{BR}(\mu \to e\gamma) \lesssim 5 \times 10^{-14}$ for $\tan\beta = 5$, 10, 15, 20, 25, 30, 35, 40, 45, 50, 55, $\mu > 0$ and $a = 0$. Grey indicates that less than 25% of the range of θ_1 is allowed. Red indicates that between 25% and 50% of θ_1 is allowed. Green and blue illustrate that 50% to 75%, and 75% to 100%, are allowed respectively. The constraint regions are reproduced from [12].

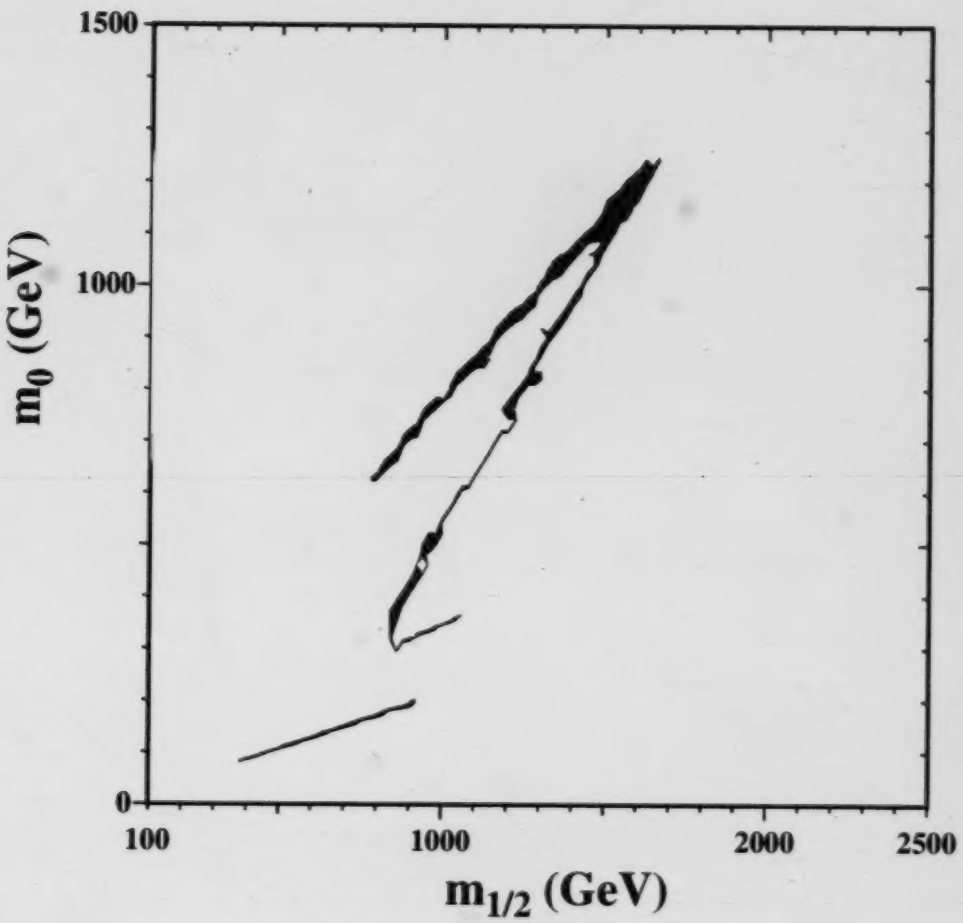

Figure 5.4: **Hierarchical ν_Rs**: WMAP and laboratory constraint parameterization of the CMSSM, and LFV compliance, based on the current LFV bound, $\mathrm{BR}(\mu \to e\gamma) < 1.2 \times 10^{-11}$ for $\tan\beta = 10, 35$, $\mu < 0$ and $a = 0$. Grey indicates that less than 25% of the range of θ_1 is allowed. Red indicates that between 25% and 50% of θ_1 is allowed. Green and blue illustrate that 50% to 75%, and 75% to 100%, are allowed respectively. The constraint regions are reproduced from [13].

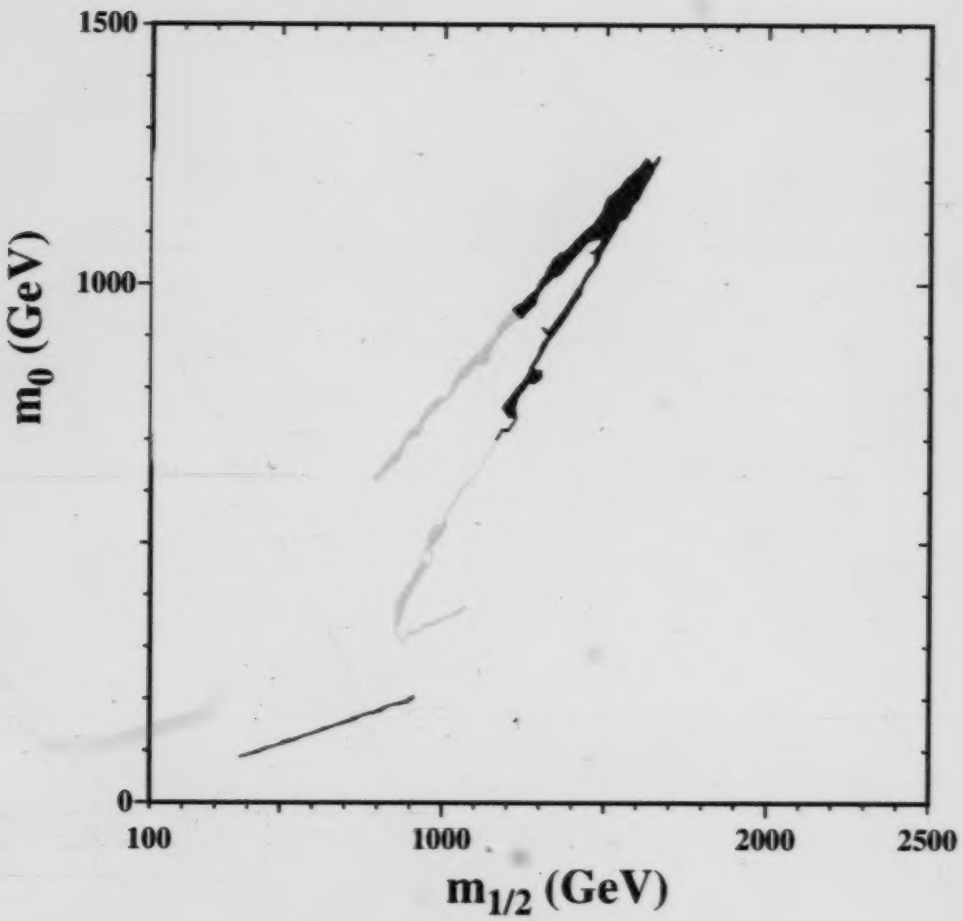

Figure 5.5: **Hierarchical ν_Rs**: WMAP and laboratory constraint parameterization of the CMSSM, and LFV compliance, based on the expected LFV bound from MEG, $\mathrm{BR}(\mu \to e\gamma) \lesssim 5 \times 10^{-14}$ for $\tan\beta = 10, 35$, $\mu < 0$ and $a = 0$. Grey indicates that less than 25% of the range of θ_1 is allowed. Red indicates that between 25% and 50% of θ_1 is allowed. Green and blue illustrate that 50% to 75% and 75% to 100% are allowed respectively. The constraint regions are reproduced from [13].

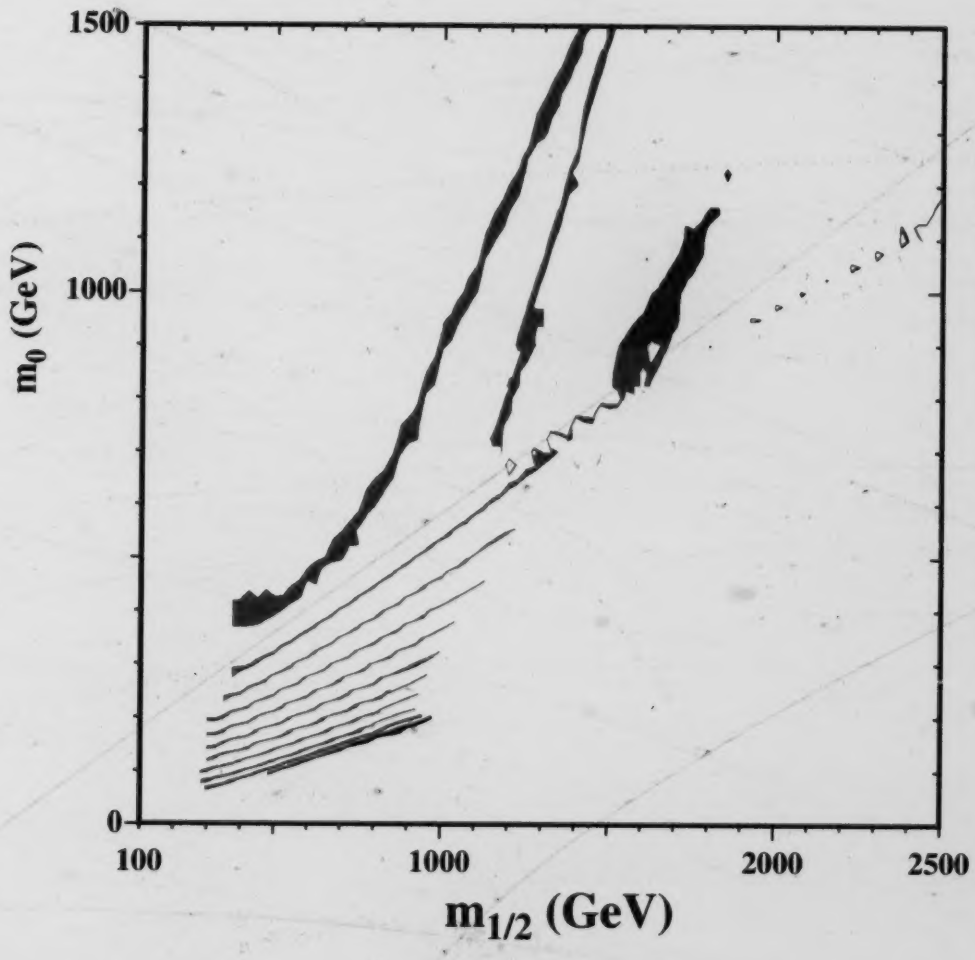

Figure 5.6: **Degenerate ν_Rs**: WMAP and laboratory constraint parameterization of the CMSSM, and LFV compliance, based on the current LFV bound, $\mathrm{BR}(\mu \to e\gamma) < 1.2 \times 10^{-11}$ for $\tan\beta = 5, 10, 15, 20, 25, 30, 35, 40, 45, 50, 55$, $\mu > 0$ and $a = 0$. Blue indicates the allowed region. The constraint regions are reproduced from [12].

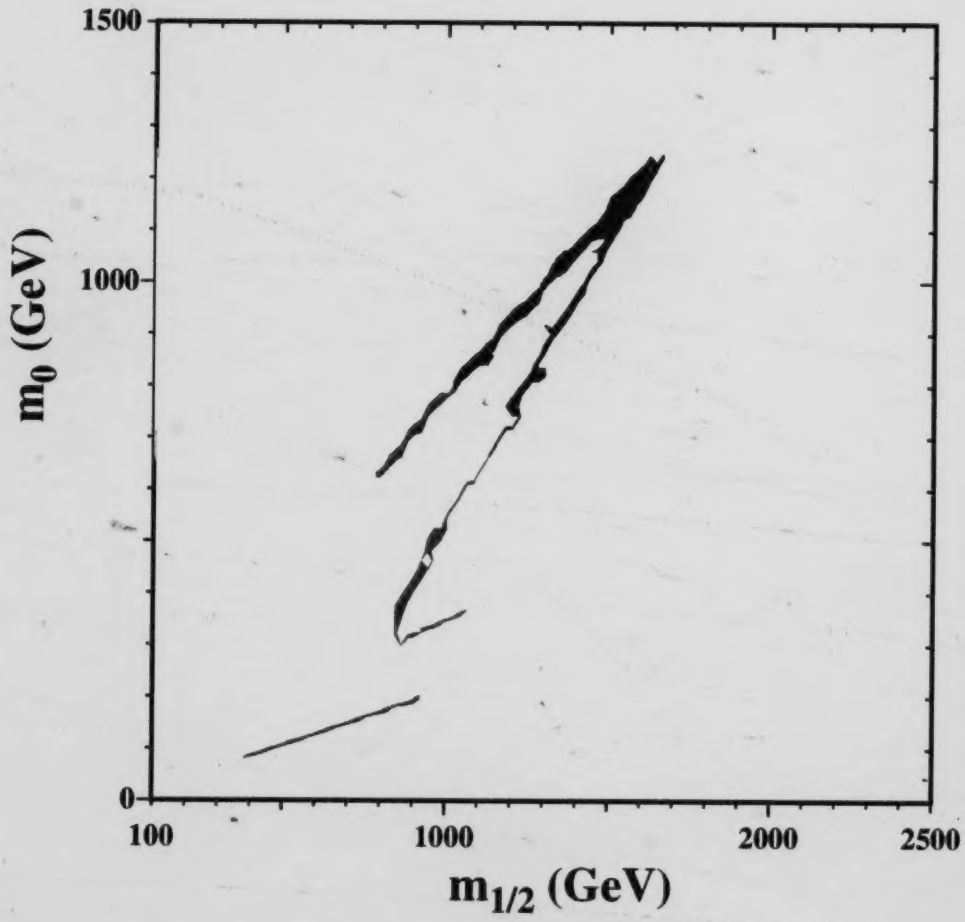

Figure 5.7: **Degenerate ν_Rs**: WMAP and laboratory constraint parameterization of the CMSSM, and LFV compliance, based on the current LFV bound, $\mathrm{BR}(\mu \to e\gamma) < 1.2 \times 10^{-11}$ for $\tan\beta = 10, 35$, $\mu < 0$ and $a = 0$. Blue indicates the allowed region. The constraint regions are reproduced from [13].

Bibliography

[1] R. Davis et al., Homestake Collaboration, Rev. Mod. Phys. **75** (2003), 985-994.

[2] J. N. Abdurashitov et al., SAGE Collaboration, Phys. Rev. Lett. B **328** (1994), 234-248;

Phys. Rev. Lett. **83** (1999), 4686-4689 [arXiv:hep-ex/9907131];

J. Exp. Theor. Phys. **95** (2002), 181-193 [arXiv:hep-ex/0204245].

[3] P. Anselmann et al., GALLEX Collaboration, Phys. Rev. Lett. **B285** (1992), 237-247;

Phys. Rev. Lett. **B357** (1995), 390-397; Erratum-ibid. B **361** (1996), 235-236;

Phys. Rev. Lett. **B477** (1999), 127-133;

Phys. Rev. Lett. **B490** (2000), 16-26 [arXiv:hep-ex/0006034].

[4] Y. Fukuda et al., Super-Kamiokande Collaboration, Phys. Rev. Lett. **86** (2001), 5651-5655 [arXiv:hep-ex/0103032];

Phys. Rev. Lett. **86** (2001), 5656-5660 [arXiv:hep-ex/0103033].

[5] Q. R. Ahmad et al., SNO Collaboration, Phys. Rev. Lett. **87** (2001), 071301 [arXiv:nucl-ex/0106015];

Phys. Rev. Lett. **89** (2002), 011301 [arXiv:nucl-ex/0204008];

Phys. Rev. Lett. **89** (2002), 011302 [arXiv:nucl-ex/0204009];

[arXiv:nucl-ex/0309004] submitted for publication.

[6] Y. Fukuda et al., Super-Kamiokande Collaboration, Phys. Rev. Lett. **81** (1998), 1562-1567 [arXiv:hep-ex/9807003];

Phys. Rev. Lett. **82** (1999), 2644-2648 [arXiv:hep-ex/9812014];

Phys. Rev. Lett. **85** (2000), 3999-4003 [arXiv:hep-ex/0009001].

[7] K. Eguchi et al., KAMLAND Collaboration, Phys. Rev. Lett. **90** (2003), 021802 [arXiv:hep-ex/0212021].

[8] M. H. Ahn et al., K2K Collaboration, Phys. Rev. Lett. **90** (2003), 041801 [arXiv:hep-ex/0212007].

[9] For reviews see: **Journeys Beyond The Standard Model**, P. Ramond, Perseus Books (1999); **Physics of Neutrinos**, M. Fukugita and T. Yanagida, Springer-Verlag (2003).

[10] F. Borzumati and A. Masiero, Phys. Rev. Lett. **57** (1986), 961.

[11] C. L. Bennett et al., WMAP Collaboration, Astrophys. J. Suppl. **148** (2003), 1 [arXiv:astro-ph/0302207];

D. N. Spergel et al., WMAP Collaboration, Astrophys. J. Suppl. **148** (2003), 175 [arXiv:astro-ph/0302209].

[12] J. R. Ellis, K. A. Olive, Y. Santoso and V. C. Spanos, Phys. Lett. **B565** (2003), 176-182 [arXiv:hep-ph/0303043].

[13] M. Battaglia, A. De Roeck, J. R. Ellis, F. Gianotti, K. A. Olive, and L. Pape [arXiv:hep-ph/0306219].

[14] J. R. Ellis, K. A. Olive, Y. Santoso, and V. C. Spanos [arXiv:hep-ph/0310356];

H. Baer and C. Balazs, JCAP **0305** (2003), 006 [arXiv:hep-ph/0303114];

H. Baer, C. Balazs, A. Belyaev, T. Krupovnickas and X. Tata, JHEP **0306** (2003), 054 [arXiv:hep-ph/0304303];

A. B. Lahanas and D. V. Nanopulos, Phys. Lett. **B568** (2003), 055 [arXiv:hep-ph/0303130];

U. Chattopadhyay, A. Corsetti, and P. Nath, Phys. Lett. **D68** (2003), 035005 [arXiv:hep-ph/0310103];

U. Arnowitt, B. Dutta, and B. Hu [arXiv:hep-ph/0310103].

[15] J. Hisano, T. Moroi, K. Tobe M. Yamaguchi, and T. Yanagida, Phys. Lett. **B357** (1995), 579 [arXiv:hep-ph/9501407].

[16] J. Hisano, T. Moroi, K. Tobe and M. Yamaguchi, Phys. Rev. **D53** (1996), 2442-2459 [arXiv:hep-ph/9510309].

[17] J. Hisano and D. Nomura, Phys. Rev.**D59** (1999), 116005 [arXiv:hep-ph/9810479];

W. Buchmuller,D. Delepine and F. Vissani, Phys. Lett. **B459** (1999), 171 [arXiv:hep-ph/9904219];

M. E. Gomez,G .K Leontaris, S. Lola and J. D. Vergados, Phys. Rev. **D59** (1999), 116009 [arXiv:hep-ph/9810251];

J. R. Ellis,M. E. Gomez, G. K. Leontaris and D. V. Nanopoulos, Eur. Phys. J. **C14** (2000), 319 [arXiv:hep-ph/9911459];

W. Buchmuller,D. Delepine, and L. T. Handoko, Nucl. Phys. **B576** (2000), 445 [arXiv:hep-ph/9912317];

J. L. Feng,Y. Nir, and Y. Shadmi, Phys. Rev. **D61** (2000), 113005 [arXiv:hep-ph/9911370];

T. Blazek and S.F. King, Phys. Lett. **B518** (2001), 109 [arXiv:hep-ph/0105005];

D. Carvalho, J. Ellis, M. Gomez and S. Lola, Phys. Lett. **B515** (2001), 323 [arXiv:hep-ph/0103256];

S. Lavignac, I. Masina and C.A. Savoy, Phys. Lett. **B520** (2001), 269 [arXiv:hep-ph/0106245];

S. Lavignac, I. Masina and C.A. Savoy, Nucl. Phys. **B633** (2002), 139 [arXiv:hep-ph/0202086];

J. R. Ellis, J. Hisano, S. Lola and M. Raidal, Nucl. Phys. **B621** (2002), 208 [arXiv:hep-ph/0109125];

J. R. Ellis and M. Raidal, Nucl. Phys. **B643** (2002), 229 [arXiv:hep-ph/0206174];

F. Deppisch, H. Pas, A. Redelbach, R. Ruckl and Y. Shimizu, Nucl.Phys.Proc.Suppl. **116** (2003), 316-320 [arXiv:hep-ph/0211138];

J. Ellis, J. Hisano and M. Raidal and Y. Shimizu, Phys. Rev. **D66** (2002), 115013 [arXiv:hep-ph/0206110];

J. R. Ellis, M. Raidal and T. Yanagida, [arXiv:hep-ph/0303242];

S. T. Petcov, S. Profumo and Y. Takanishi and C. E. Yaguna, Nucl. Phys. **B676** (2004), 453-480 [arXiv:hep-ph/0306195];

S. Pascoli, S. T. Petcov and C. E. Yaguna, Phys. Lett. **B564** (2003), 241-254 [arXiv:hep-ph/0301095];

S. Pascoli, S. T. Petcov and W. Rodejohann, Phys. Rev. **D68** (2003), 093007 [arXiv:hep-ph/0302054].

[18] J. A. Casas and A. Ibarra, Nucl.Phys. **B618** (2001), 171 [arXiv:hep-ph/0103065].

[19] M.L. Brooks et.al., [MEGA Collaboration]
Phys. Rev. Lett. **83** (1999), 1521 [arXiv:hep-ph/9905013].

[20] T. Mori, "Status and Future of $\mu \to e\gamma$: The PSI Experiment," Nucl. Phys. Proc. Suppl. 111, 194 (2002). Also, the MEG website `http://meg.web.psi.ch/`

[21] U. Bellgardt et. al., Nucl. Phys. **B229** (1988), 1.

[22] P. Wintz, "Results of the SINDRUM-II Experiment," *Prepared for 29th International Conference on High-Energy Physics (ICHEP 98), Vancouver, Canada, 23-29 Jul 1998*

[23] M. Hebert [MECO Collaboration], "Searching for Muon to Electron Conversion Below the 10^{-16} Level," Nucl. Phys. A 721, 461 (2003). Also, the MECO website `http://meco.ps.uci.edu/`

[24] A. Sato: presentation at NuFact03
http://www.cap.bnl.gov/nufact03/WG2/6june/sato.pdf

[25] Y. Kuno and Y. Okada, Rev. Mod. Phys. **73** (2001) 151 [arXiv:hep-ph/9909265].

Chapter 6

Lepton Flavour Violation in a Class of Lopsided SO(10) Models

6.1 Introduction

Neutrinos have been observed to oscillate between flavour states [1]–[8], which implies neutrino mass and mixing. In addition, the combined observations suggest that both the atmospheric and solar mixing angles are nearly maximal, known as the large angle mixing solution (LMA). Interestingly, the LMA solution implies that the lepton mixing scenario is radically different from the quark sector. Specifically, $|U_{\mu 3}|$ of the MNS matrix is much larger than $|V_{cb}|$ of the CKM matrix. Over the last few years a number of models that employ the see-saw mechanism [9] in conjunction with various flavour symmetries have been developed to address this difference [10]–[21]. Recently, a particularly interesting and highly successful class of supersymmetric SO(10) GUTs has emerged that makes use of asymmetric mass matrices known as lopsided textures [11, 12, 13]. In these models, the charged lepton sector is responsible for the large atmospheric mixing angle while the Majorana singlet neutrino matrix has a simple form that results in the large solar mixing angle. Throughout this chapter we will refer to these models as the AB model class [11].

After GUT breaking, these models can reduce to the R-parity conserving minimal supersymmetric standard model (MSSM) with specific model dependent relationships amongst the Yukawa couplings. In addition to the see-saw constraints already provided by the neutrino physics (and the demand that these models reproduce all the low energy physics of the standard model), the WMAP satellite observations [22] provide strong constraints on the available supersymmetric parameter space if the lightest supersymmetic particle (LSP) is assumed to compose the dark matter [23, 24, 25]. For a choice of CMSSM parameters, the definite flavour structure of the AB model class results in specific predictions of lepton flavour violation and in particular the rate for $\mu \to e\gamma$. We

determine how much of the presently viable CMSSM parameter space, as allowed by the WMAP observations, results in a $\mu \to e\gamma$ rate consistent with experimental limits for the AB model class.

We organize this chapter as follows. In section 6.2 we outline the essential details of the AB models, the supersymmetric parameter space, and the calculation for $\mu \to e\gamma$. We consider $\mu \to e\gamma$ since at the present time, with the current bound [26] of $\mathrm{BR}(\mu \to e\gamma) < 1.2 \times 10^{-11}$, this process gives the strongest constraints on lepton flavour violation in the class of models that we discuss. Furthermore, the MEG experiment at PSI [27] expects to improve on this bound with the expected sensitivity of $\mathrm{BR}(\mu \to e\gamma) \lesssim 5 \times 10^{-14}$. This experiment will provide stringent limits on models with charged lepton flavour violation. In section 6.3 we display our numerical results on $\mu \to e\gamma$ together with the combined constraints from the WMAP satellite observations and direct search limits, and in section 6.4 we present our conclusions. The appendix provides further calculational details.

6.2 The AB Model Definition

The AB model class is based on an SO(10) GUT with a $\mathrm{U}(1) \times \mathrm{Z}_2 \times \mathrm{Z}_2$ flavour symmetry and uses a minimum set of Higgs fields to solve the doublet-triplet splitting problem [11, 12, 13]. The interesting feature of these models is the use of a lopsided texture. The approximate form of the charged lepton and the down quark mass matrix in these models is given by

$$\mathbf{Y_E} \sim \begin{pmatrix} 0 & 0 & 0 \\ 0 & 0 & \epsilon \\ 0 & \sigma & 1 \end{pmatrix}, \quad \mathbf{Y_D} \sim \begin{pmatrix} 0 & 0 & 0 \\ 0 & 0 & \sigma \\ 0 & \epsilon & 1 \end{pmatrix}. \tag{6.1}$$

where $\sigma \sim 1$ and $\epsilon \ll 1$. As pointed out by the authors of [11], this asymmetric structure naturally occurs within a minimal SU(5) GUT where the Yukawa interaction for the down quarks and leptons is of the form $\lambda_{ij}\bar{\mathbf{5}}_i\mathbf{10}_j\mathbf{5_H}$ ($\mathbf{5_H}$ denotes the Higgs scalars). In an SU(5) GUT, the left-handed leptons and the charge conjugate right-handed down quarks belong to the $\bar{\mathbf{5}}$ while the $\mathbf{10}$ contains the charge conjugate right-handed leptons and the left-handed down quarks. Therefore the lepton and down quark mass matrices are related to each other by a left-right transpose. Since SU(5) is a subgroup of SO(10), this feature is retained in an SO(10) GUT. This lopsided texture has the ability to explain why $|U_{\mu 3}| >> |V_{cb}|$. Making use of this observation, the AB models contain the Dirac matrices $\mathbf{U}, \mathbf{N}, \mathbf{D}, \mathbf{L}$ for the up-like quarks, Dirac neutrino interaction, down-like quarks,

and the leptons respectively [13],

$$\mathbf{U} = \begin{pmatrix} \eta & 0 & 0 \\ 0 & 0 & \epsilon/3 \\ 0 & -\epsilon/3 & 1 \end{pmatrix} M_U, \quad \mathbf{N} = \begin{pmatrix} \eta & 0 & 0 \\ 0 & 0 & -\epsilon \\ 0 & \epsilon & 1 \end{pmatrix} M_U, \tag{6.2}$$

$$\mathbf{D} = \begin{pmatrix} 0 & \delta & \delta' e^{i\phi} \\ \delta & 0 & \sigma + \epsilon/3 \\ \delta' e^{i\phi} & -\epsilon/3 & 1 \end{pmatrix} M_D, \quad \mathbf{L} = \begin{pmatrix} 0 & \delta & \delta' e^{i\phi} \\ \delta & 0 & -\epsilon \\ \delta' e^{i\phi} & \sigma + \epsilon & 1 \end{pmatrix} M_D. \tag{6.3}$$

where

$$\begin{aligned} M_U &\approx 113\,\text{GeV}, & M_D &\approx 1\,\text{GeV}, \\ \sigma &= 1.78, & \epsilon &= 0.145, \\ \delta &= 8.6 \times 10^{-3}, & \delta' &= 7.9 \times 10^{-3}, \\ \phi &= 126^\circ, & \eta &= 8 \times 10^{-6}. \end{aligned} \tag{6.4}$$

The given values of M_D and M_U best fit the low energy data with $\tan\beta \approx 5$. However, the mass scale itself is set only after electroweak symmetry breaking and it is therefore possible, with the use of $\tan\beta$, to extract dimensionless Yukawa matrices $\mathbf{Y_U}, \mathbf{Y_N}, \mathbf{Y_D}$, and $\mathbf{Y_E}$. It is advantageous to use dimensionless couplings since the renormalization group equations are initialized above the electroweak symmetry breaking scale. The corresponding dimensionless up and down-like Yukawa matrices retain the form of equations (6.2, 6.3) but are scaled by overall dimensionless factors: M'_U and M'_D. By varying the overall dimensionless scale factors, other values of $\tan\beta$ can be accommodated while retaining accurate fits to the low energy data after renormalization group running. Our code implements the one-loop beta functions [28, 29, 30] for the CMSSM with neutrino singlets and reproduces the results of [11, 12, 13]. Futhermore, we obtain accurate (within the stated errors in [31]) fits to the low energy data for $\tan\beta = 5 - 50$ which corresponds to $M'_U = 0.82 - 0.85$ and $M'_D = 0.016 - 0.20$.

The lopsided texture of the AB model class nicely fits the large atmospheric mixing angle; however, in order to obtain the large solar mixing angle a specific hierarchical form of the heavy Majorana singlet neutrino matrix needs to be chosen [12, 13], namely,

$$\mathbf{M_N} = \begin{pmatrix} b^2\eta^2 & -b\epsilon\eta & a\eta \\ -b\epsilon\eta & \epsilon^2 & -\epsilon \\ a\eta & -\epsilon & 1 \end{pmatrix} \Lambda_N. \tag{6.5}$$

where the parameters ϵ and η are as defined in equation (6.4). The parameters a and b are of order 1 and $\Lambda_N \sim 2 \times 10^{14}$ GeV. Since the Majorana singlet neutrino matrix is not related to the Dirac Yukawa structure, it is not surprising that this matrix should take

on a form independent from the rest of the model. Once these choices have been made, the AB model class is highly predictive and accurately fits all the low energy standard model physics and the neutrino mixing observations.

It should be emphasized that all these relations are defined at the GUT scale and are therefore subject to renormalization group running. If we assume that the GUT symmetry breaks to the standard model gauge symmetries, SU(3)×SU(2)×U(1), and that supersymmetry is broken super-gravitionally through a hidden sector in a flavour independent manner, the AB model class will give well defined predictions for charged lepton flavour violation. There may also be contributions to the off-diagonal elements from renormalization group running between the GUT and gravity scales [32, 33]. Since the particulars of GUT and supersymmetry breaking – as well as the possibility of new physics above the GUT scale – can have model dependent effects on the branching ratio for $\mu \to e\gamma$, we do not consider an interval of running between the GUT and gravity scales.

The specific model predictions for the Dirac Yukawa couplings and the form of the Majorana singlet neutrino matrix will feed into the soft supersymmetry breaking slepton mass terms through renormalization group running, generating off diagonal elements that will contribute to flavour changing neutral currents [34]. The amount of flavour violation contained in the AB model class can be examined through the branching ratio of the process $\mu \to e\gamma$.

6.3 Numerical Results for $\mu \to e\gamma$

After GUT and supersymmetry breaking, the model class reduces to the constrained minimal supersymmetric standard model (CMSSM) with heavy gauge singlet neutrinos to make use of the see-saw mechanism. It should be noted that given our assumptions about how the GUT and supersymmetry breaks, the CMSSM studies of [23, 24, 25] directly impact this model class. As discussed in the previous section, the renormalization group running from the supersymmetry breaking scale to the weak scale alters the simple GUT relationship for the sfermion mass matrices. The diagonal part of the sfermion mass matrices is not strongly model dependent. The model dependence appears in the off-diagonal parts of the sfermion mass matrices which come from the particular textures of the model class - i.e. the mixings. Therefore, flavour changing neutral current processes are of primary interest, since they test the off-diagonal sfermion mass matrix structure. As discussed in the introduction, $\mu \to e\gamma$ is the best constraining process for this model class. We note that the prediction for the anomalous magnetic moment of the muon in this model class is consistent with the CMSSM analysis found in [23].

The leptonic part of the superpotential is

$$W = \epsilon_{\alpha\beta} H_{\rm d}^{\alpha} \mathbf{E} \mathbf{Y}_{\rm E} \mathbf{L}^{\beta} + \epsilon_{\alpha\beta} H_{\rm u}^{\alpha} \mathbf{N} \mathbf{Y}_{\rm N} \mathbf{L}^{\beta} + \frac{1}{2} \mathbf{N} \mathbf{M}_{\rm N} \mathbf{N} \tag{6.6}$$

where $\mathbf{Y}_{\rm E}$, $\mathbf{Y}_{\rm N}$ are Yukawa matrices, and $\mathbf{M}_{\rm N}$ is the singlet Majorana neutrino mass matrix. The totally antisymmetric symbol is defined $\epsilon_{12} = +1$. We explain our notation in detail in the appendix. On integrating out the heavy singlet neutrinos, equation (6.6) reduces to

$$W = \epsilon_{\alpha\beta} H_{\rm d}^{\alpha} \mathbf{E} \mathbf{Y}_{\rm E} \mathbf{L}^{\beta} - \frac{1}{2} \nu^{\rm T} \mathbf{m}_{\nu} \nu \tag{6.7}$$

where

$$\mathbf{m}_{\nu} = \frac{v^2}{2} \mathbf{Y}_{\rm N}^{\rm T} \mathbf{M}_{\rm N}^{-1} \mathbf{Y}_{\rm N} \sin^2 \beta \tag{6.8}$$

is the see-saw induced light neutrino mass matrix. The coefficients β and v are defined in terms of Higgs fields expectation values by

$$\frac{v^2}{2} = \langle H_{\rm d}^0 \rangle^2 + \langle H_{\rm u}^0 \rangle^2 = (174 \text{ GeV})^2, \qquad \tan\beta = \frac{\langle H_{\rm u}^0 \rangle}{\langle H_{\rm d}^0 \rangle}. \tag{6.9}$$

The neutrino mass matrix, equation (6.8), is in general not diagonal and this is the source of lepton flavour violating interactions.

We assume that supersymmetry is broken softly in that breaking occurs through operators of mass dimension 2 and 3. The soft supersymmetry breaking Lagrangian relevant to LFV studies is

$$\begin{aligned}
\mathcal{L}_{\text{breaking}} \;=\; & -\delta_{\alpha\beta} \tilde{\mathbf{L}}^{\alpha\dagger} \mathbf{m}_{\tilde{\rm L}}^2 \tilde{\mathbf{L}}^{\beta} - \tilde{\mathbf{E}} \mathbf{m}_{\tilde{\rm E}}^2 \tilde{\mathbf{E}}^{\dagger} - \tilde{\mathbf{N}} \mathbf{m}_{\tilde{\rm N}}^2 \tilde{\mathbf{N}}^{\dagger} \\
& - m_{\rm H_d}^2 \delta_{\alpha\beta} H_{\rm d}^{\alpha *} H_{\rm d}^{\beta} - m_{\rm H_u}^2 \delta_{\alpha\beta} H_{\rm u}^{\alpha *} H_{\rm u}^{\beta} \\
& + \left(-b \epsilon_{\alpha\beta} H_{\rm d}^{\alpha} H_{\rm u}^{\beta} - \frac{1}{2} \tilde{\mathbf{N}} \mathbf{B}_{\tilde{\rm N}} \tilde{\mathbf{N}} \;+\; \text{c. c.} \right) \\
& + \left(-\epsilon_{\alpha\beta} H_{\rm d}^{\alpha} \tilde{\mathbf{E}} \mathbf{A}_{\rm E} \tilde{\mathbf{L}}^{\beta} - \epsilon_{\alpha\beta} H_{\rm u}^{\alpha} \tilde{\mathbf{N}} \mathbf{A}_{\rm N} \tilde{\mathbf{L}}^{\beta} \;+\; \text{c. c.} \right) \\
& + \left(-\frac{1}{2} M_1 \tilde{B} \tilde{B} - \frac{1}{2} M_2 \tilde{W}^a \tilde{W}^a \;+\; \text{c. c.} \right)
\end{aligned} \tag{6.10}$$

(see the appendix for the notational details). The CMSSM assumes universal soft supersymmetry breaking parameters at the supersymmetry breaking scale, which we take to be of order the GUT scale, leading to the following GUT relations:

$$\mathbf{m}_{\tilde{\rm L}}^2 = \mathbf{m}_{\tilde{\rm E}}^2 = \mathbf{m}_{\tilde{\rm N}}^2 = m_0^2 \cdot \mathbf{I}, \tag{6.11}$$

$$m_{\rm H_d}^2 = m_{\rm H_u}^2 = m_0^2, \tag{6.12}$$

$$\mathbf{A}_{\rm E} = \mathbf{A}_{\rm N} = 0, \tag{6.13}$$

$$M_1 = M_2 = m_{1/2} \tag{6.14}$$

where m_0 and $m_{1/2}$ denote the universal scalar mass and the universal gaugino mass respectively ($\mathbf{I}$ is the 3×3 unit matrix). We conservatively assume that the trilinear terms $\mathbf{A_E}$ and $\mathbf{A_N}$ vanish at the supersymmetry breaking scale.

We run the parameters of the CMSSM using the renormalization group equations [28, 29, 30] working in a basis where the Majorana neutrino singlet matrix is diagonal, integrating out each heavy neutrino singlet at its associated scale. After integrating down to the electroweak scale, we rotate the Yukawa couplings to the mass eigenbasis. In order to understand the origin of flavour violation in this model class, we first give a qualitative estimate. The leading log approximation of the off-diagonal slepton mass term is given by

$$\left(\Delta \mathbf{m}_{\tilde{\mathrm{L}}}^2\right)_{ij} \approx -\frac{3}{8\pi^2} m_0^2 (\mathbf{Y_N}^\dagger \mathbf{Y_N})_{ij} \ln\left(\frac{M_{\mathrm{GUT}}}{\Lambda_{\mathrm{N}}}\right), \tag{6.15}$$

(assuming that the trilinears vanish at the GUT scale), and using this approximation together with mass insertion techniques [33, 28], the branching ratio for $\mu \to e\gamma$ is

$$\begin{aligned} \mathrm{BR}(\mu \to e\gamma) &\sim \frac{\alpha^3}{G_{\mathrm{F}}^2} \frac{\left(\left(\mathbf{m}_{\tilde{\mathrm{L}}}^2\right)_{12}\right)^2}{m_{\mathrm{s}}^8} \tan^2\beta \\ &\approx \frac{\alpha^3}{G_{\mathrm{F}}^2 m_{\mathrm{s}}^8} \left|\frac{3}{8\pi^2} m_0^2 \ln\frac{M_{\mathrm{GUT}}}{\Lambda_{\mathrm{N}}}\right|^2 \left|\left(\mathbf{Y_N}^\dagger \mathbf{Y_N}\right)_{12}\right|^2 \tan^2\beta \end{aligned} \tag{6.16}$$

where m_s is a typical sparticle mass. We see that since the flavour structure of the AB model class is specified so precisely, the branching ratio for $\mu \to e\gamma$ is well determined. In our calculation of the decay rate, we use the full one-loop expressions derived from the diagrams in figure 6.1 (see the appendix for more details).

The WMAP satellite observations [22] strongly limit the available CMSSM parameter space if the LSP composes the dark matter [23, 24, 25]. We display our results over CMSSM parameter ranges determined by [23] and [24], which not only impose that the resulting model have LSP relic densities in the range determined by WMAP [22], but that they have spectra consistent with the LEP direct search limits [31], as well as the rate for $b \to s\gamma$. Following these authors we ignore the focus point region in parameter space which occurs at very large m_0 and whose location depends on m_t and M_H in an extremely sensitive manner.

In figure 6.2, we show contours of the branching ratio $\mu \to e\gamma$ in the $m_{1/2}$-m_0 plane for a variety of $\tan\beta$ with the μ parameter both positive and negative. The parameters of the AB model class have been chosen such that all the low energy predictions fit the

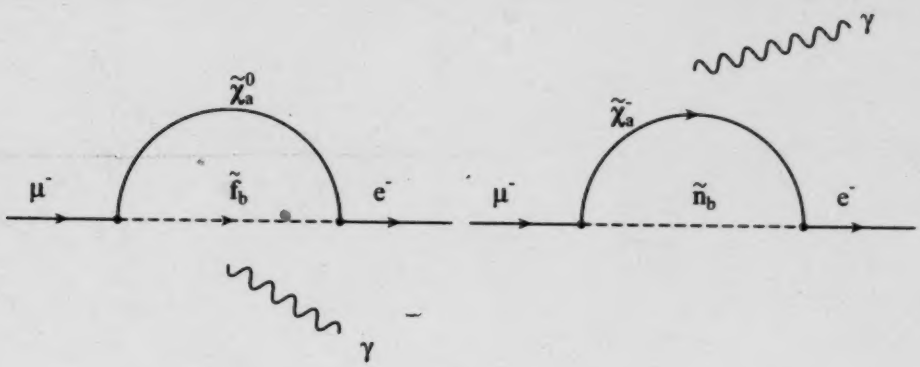

Figure 6.1: Feynman diagrams contributing to $\mu \to e\gamma$.

standard model data, and we have chosen $a = 1$ and $b = 2$ for the Majorana singlet neutrino mass matrix given in equation (6.5). As indicated in [13], there are a number of possible model choices for the Majorana singlet parameters a and b that are consistent with the LMA solution. However, we find that the rate for $\mu \to e\gamma$ is largely unaffected by the allowed range [13] for these parameters, $1.0 \lesssim a \lesssim 2.4$ and $1.8 \lesssim b \lesssim 5.2$. Panel (a) demonstrates the lepton flavour bounds for $\tan\beta = 5$ with $\mu > 0$. The small line-like shaded area in the lower part of the panel is the allowed region from the combined WMAP and laboratory limits. The remaining panels show that the contours of constant branching ratio migrate to the right of the plots (i.e. to high values of $m_{1/2}$ and m_0) as $\tan\beta$ is increased. In each case we overlay the approximate WMAP and laboratory constraint bounds represented by a shaded region [23]. The choice for the sign of μ is indicated in each panel. As $\tan\beta$ is pushed up, larger portions of the parameter space become excluded. This is an expected feature since the branching ratio is proportional to $\tan^2\beta$. Notice that by $\tan\beta \sim 25$, $\mu > 0$, the branching ratio allowed contours no longer have a significant overlap with the WMAP region. As a result, we find that the AB model class is consistent with the current experimental bound on $\mu \to e\gamma$ for low $\tan\beta$ (i.e. $\tan\beta \lesssim 20$) for $\mu > 0$. For completeness, in panels (b) and (e), we show two cases where $\mu < 0$. The branching ratio of $\mu \to e\gamma$ is largely insensitive to the sign of μ, however the WMAP region is moderately affected [24]. A small part of the allowed WMAP region is currently permitted for larger $\tan\beta$ (i.e. ~ 35) as indicated in panel (e). The upcoming limits [27] that MEG will establish, $\mathrm{BR}(\mu \to e\gamma) \lesssim 5 \times 10^{-14}$, will

effectively rule out this model class if LFV is not seen. Interestingly, if LFV is seen at MEG, this model will suggest that $\tan\beta$ is low based on flavour bounds alone.

6.4 Conclusions

The AB model class [11, 12, 13], based on a $U(1)\times Z_2 \times Z_2$ flavour symmetry, is a highly successful and predictive GUT scenario. This model class has the ability to accommodate all the observed neutrino phenomena and reproduce the low energy physics of the standard model. If it is assumed that supersymmetry is broken via mSUGRA and that the GUT breaks directly to the CMSSM, the AB model class is highly restrictive and hence allows for a precise determination for the rate of charged lepton flavour violation. In particular, we examined the process $\mu \to e\gamma$, since at the present time this flavour violating muon decay channel gives the strongest constraints on flavour changing neutral currents in the lepton sector.

As the WMAP satellite data [22] and laboratory direct searches [31] have already severely restricted the available CMSSM parameter space, the $\mu \to e\gamma$ flavour bounds allow a strong test of the AB model class. We find that given the current bounds [26] on $\mu \to e\gamma$, $\mathrm{BR}(\mu \to e\gamma) < 1.2 \times 10^{-11}$, the AB model class favours low to moderate $\tan\beta$ (i.e. $\lesssim 20$) with $\mu > 0$, however, there is a small region that is not excluded for $\tan\beta \lesssim 35$ with the sign of μ negative. If MEG at PSI [27] does not detect a positive LFV signal, $\mathrm{BR}(\mu \to e\gamma) \lesssim 5 \times 10^{-14}$, the AB model class will be effectively ruled out, given our conservative assumptions concerning GUT and supersymmetry breaking. It remains an open question as to whether or not other supersymmetry and/or GUT breaking schemes within the AB model class will be able to avoid these flavour violating bounds.

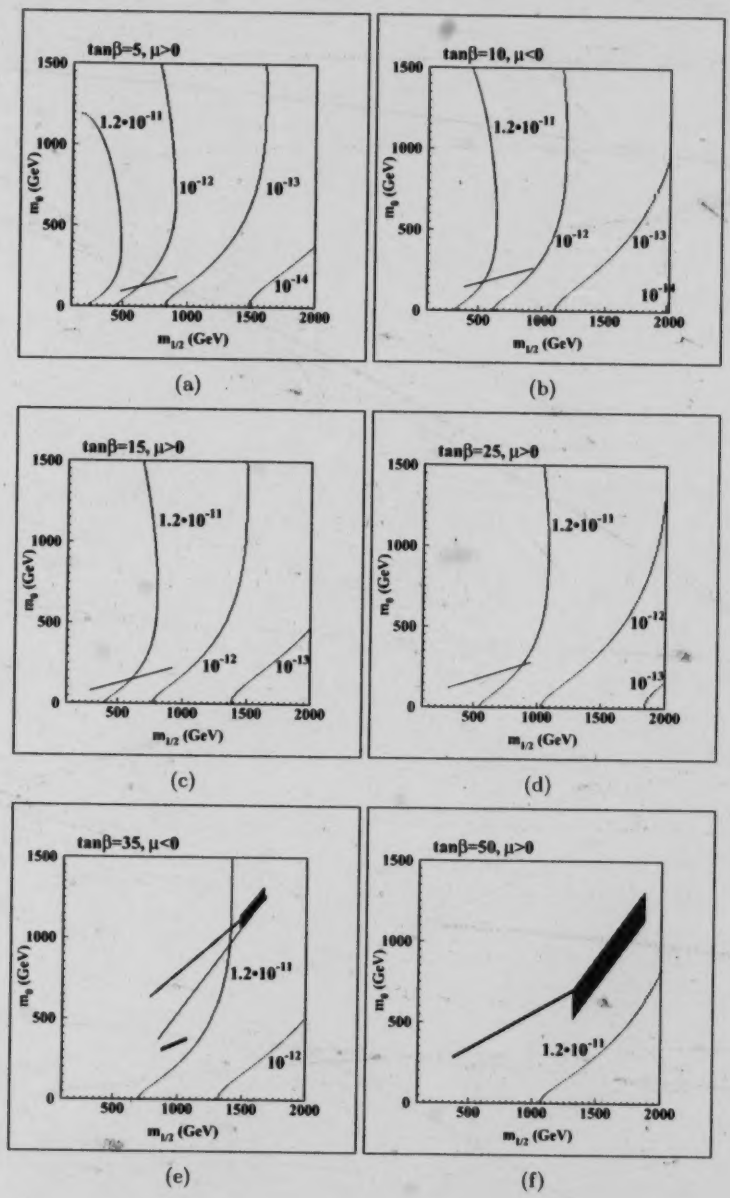

Figure 6.2: Contour Plots of BR($\mu \to e\gamma$) in the $m_0 - m_{1/2}$ plane: Panels (a),(c),(d), and (f) show the contours of the branching ratio for $\tan\beta = 5, 15, 25, 50$ respectively with $\mu > 0$. Panels (b) and (e) show the contours with $\tan\beta = 10, 35$ respectively with $\mu < 0$. In all cases the shaded region corresponds to the approximate combined WMAP and laboratory constraints.

Bibliography

[1] R. Davis et al., Homestake Collaboration, Rev. Mod. Phys. **75** (2003), 985-994.

[2] J. N. Abdurashitov et al., SAGE Collaboration, Phys. Rev. Lett. B **328** (1994), 234-248;

Phys. Rev. Lett. **83** (1999), 4686-4689 [arXiv:hep-ex/9907131];

J. Exp. Theor. Phys. **95** (2002), 181-193 [arXiv:hep-ex/0204245].

[3] P. Anselmann et al., GALLEX Collaboration, Phys. Rev. Lett. **B285** (1992), 237-247;

Phys. Rev. Lett. **B357** (1995), 390-397; Erratum-ibid. B **361** (1996), 235-236;

Phys. Rev. Lett. **B477** (1999), 127-133;

Phys. Rev. Lett. **B490** (2000), 16-26 [arXiv:hep-ex/0006034].

[4] Y. Fukuda et al., Super-Kamiokande Collaboration, Phys. Rev. Lett. **86** (2001), 5651-5655 [arXiv:hep-ex/0103032];

Phys. Rev. Lett. **86** (2001), 5656-5660 [arXiv:hep-ex/0103033].

[5] Q. R. Ahmad et al., SNO Collaboration, Phys. Rev. Lett. **87** (2001), 071301 [arXiv:nucl-ex/0106015];

Phys. Rev. Lett. **89** (2002), 011301 [arXiv:nucl-ex/0204008];

Phys. Rev. Lett. **89** (2002), 011302 [arXiv:nucl-ex/0204009];

[arXiv:nucl-ex/0309004] submitted for publication

[6] Y. Fukuda et al., Super-Kamiokande Collaboration, Phys. Rev. Lett. **81** (1998), 1562-1567 [arXiv:hep-ex/9807003];

Phys. Rev. Lett. **82** (1999), 2644-2648 [arXiv:hep-ex/9812014];

Phys. Rev. Lett. **85** (2000), 3999-4003 [arXiv:hep-ex/0009001].

[7] K. Eguchi et al., KAMLAND Collaboration, Phys. Rev. Lett. **90** (2003), 021802 [arXiv:hep-ex/0212021].

[8] M. H. Ahn et al., K2K Collaboration, Phys. Rev. Lett. **90** (2003), 041801 [arXiv:hep-ex/0212007].

[9] For reviews see: **Journeys Beyond The Standard Model**, P. Ramond, Perseus Books (1999); **Physics of Neutrinos**, M. Fukugita and T. Yanagida, Springer-Verlag (2003).

[10] K. S. Babu and S. M. Barr, Phys. Lett. **B381** (1996), 202-208 [arXiv: hep-ph/9511446].

[11] Carl H. Albright and S. M. Barr, Phys. Rev. **D62** (2000), 093008 [arXiv:hep-ph/0003251].

[12] C. H. Albright and S. M. Barr, Phys. Rev. **D64** (2001), 073010 [arXiv:hep-ph/0104294].

[13] C. H. Albright and S. Geer, Phys. Lett. **B532** (2002), 311-317 [arXiv:hep-ph/0112171].

[14] K. S. Babu, J. C. Pati and F. Wilczek, Nucl. Phys. **B566** (2000), 33-91 [arXiv:hep-ph/9812538].

[15] Z. Berezhiani and A. Rossi, Nucl. Phys. **B594** (2001), 113 [arXiv:hep-ph/0003084].

[16] T. Blazek, S. Raby and K. Tobe, Phys. Rev. **D62** (2000), 055001 [arXiv:hep-ph/9912482].

[17] W. Buchmuller and D. Wyler, Phys. Lett. **B521** (2001), 291 [arXiv:hep-ph/0108216].

[18] M.-C. Chen and K. T. Mahanthappa, Phys. Rev. **D65** (2002), 053010 [arXiv:hep-ph/0106093].

[19] R. Kitano and Y. Mimura, Phys. Rev. **D63** (2001), 016008 [arXiv:hep-ph/0008269].

[20] N. Maekawa, Prog. Theor. Phys. **106** (2001), 401 [arXiv:hep-ph/0104200].

[21] G. G. Ross and L. Velasco-Sevilla, Nucl. Phys. **B653** (2003), 3-26 [arXiv:hep-ph/0208218].

[22] C. L. Bennett et al., WMAP Collaboration, Astrophys. J. Suppl. **148** (2003), 1 [arXiv:astro-ph/0302207];

D. N. Spergel et al., WMAP Collaboration, Astrophys. J. Suppl. **148** (2003), 175 [arXiv:astro-ph/0302209].

[23] J. R. Ellis, K. A. Olive, Y. Santoso and V. C. Spanos, Phys. Lett. **B565** (2003), 176-182 [arXiv:hep-ph/0303043].

[24] M. Battaglia, A. De Roeck, J. R. Ellis, F. Gianotti, K. A. Olive, and L. Pape [arXiv:hep-ph/0306219].

[25] J. R. Ellis, K. A. Olive, Y. Santoso, and V. C. Spanos [arXiv:hep-ph/0310356];

H. Baer and C. Balazs, JCAP **0305** (2003), 006 [arXiv:hep-ph/0303114];

H. Baer, C. Balazs, A. Belyaev, T. Krupovnickas and X. Tata, JHEP **0306** (2003), 054 [arXiv:hep-ph/0304303];

A. B. Lahanas and D. V. Nanopoulos, Phys. Lett. **B568** (2003), 055 [arXiv:hep-ph/0303130];

U. Chattopadhyay, A. Corsetti, and P. Nath, Phys. Lett. **D68** (2003), 035005 [arXiv:hep-ph/0310103];

R. Arnowitt, B. Dutta, and B. Hu [arXiv:hep-ph/0310103].

[26] M. L. Brooks et. al, MEGA Collaboration Phys. Rev. Lett. **83** (1991), 1521 [arXiv:hep-ph/9905013].

[27] T. Mori, Nucl. Phys. Proc. Suppl. **111** (2002), 194; the MEG website: `http://meg.web.psi.ch/`

[28] J. Hisano, T. Moroi, K. Tobe and M. Yamaguchi, Phys. Rev. **D53** (1996), 2442-2459
[arXiv:hep-ph/9510309].

[29] S. P. Martin and M.T. Vaughn, Phys. Rev. **D50** (1994), 2282 [hep-ph/9311340].

[30] N. K. Falck, Z. Phys. **C30** (1986), 247.

[31] Particle Data Group, Phys. Rev. **D66** (2002).

[32] F. Barbieri, L. Hall, and A. Strumia, Nucl. Phys. **B445** (1995), 219-251 [arXiv:hep-ph/9501334].

[33] J. Hisano, and D.Nomura, Phys. Rev. **D59** (1999), 116005 [arXiv:hep-ph/9810479].

[34] F. Borzumati and A. Masiero, Phys. Rev. Lett. **57** (1986), 961,

Summary

In the last three chapters we have considered the effects of new scalar interactions on pion physics, the implications of the supersymmetric see-saw with MSSM LSP dark matter constraints for $\mu \to e\gamma$, and the predictions of lepton flavour violation from a class of lopsided $SO(10)$ grand unified models.

By considering renormalization effects on universal (or alternatively first generation), and flavour diagonal scalar operators, we have derived limits on the size of the ratio between scalar and vector couplings from precision measurements of $\pi^{\pm} \to l^{\pm}\nu_l$ decay. We note that the most conservative estimate of the limits occurs when the new physics arises at the electroweak scale. In this case, the contribution to the induced pseudoscalar comes entirely from threshold corrections. In the scenario where we have arbitrary generation dependence of the scalar couplings, $\pi^{\pm} \to l^{\pm}\nu_l$ limits can be combined with limits on scalar interactions in muon capture to bound the first generation scalar couplings. These observations have implications for current β-decay experiments. Direct searches for scalar interactions in β-decay will be most competitive if the new physics responsible for the effective scalar interactions arises at the electroweak scale in the explicit exchange of new scalar particles. In these circumstances, the indirect limits from threshold induced pseudoscalar interactions are comparable to the direct β-decay scalar searches [1, 2]. Therefore, interest in searches for new scalar interactions with β-decay experiments remains undiminished. On the other hand, for new effective scalar interactions arising as effective SU(2) $\times$ U(1) invariant operators at mass scales above 200 GeV (as expected in models with leptoquarks, composite quarks/leptons, or low scale quantum gravity) the constraints arising from the precision measurements of $\pi^{\pm} \to l^{\pm}\nu_l$ decay, combined with limits on scalar interactions in muon capture, can be stronger by an order of magnitude or more than the direct experimental searches. Furthermore, the relative strength of these searches becomes better, the higher the mass scale of the new physics compared to the electroweak scale. This argues strongly for improved experimental precision in measurements of muon capture, and $\pi^{\pm} \to l^{\pm}\nu_l$ decay. In particular we note that in the case of pion decay, the experimental error exceeds the uncertainty in the theoretical calculation by a factor of eight. A new measurement of $\pi^{\pm} \to l^{\pm}\nu_l$ decay with an order of magnitude greater precision would not only constrain physics beyond the standard model which could potentially contribute to tree level pion decay, but as we have argued above, will also indirectly provide tests of new scalar interactions of unparalleled precision.

We examined CMSSM lepton-flavour violation in simple general classes of see-saw models [3] which had been constructed to fit the data on low energy neutrino oscillations. The models considered have had their neutrino Yukawa couplings (and Majorana mass

scale) chosen as large as reasonable, to maximize the rates for lepton-flavour violating decays. Nevertheless, when the CMSSM parameters for the models were restricted to have LSP relic densities in the region determined by WMAP, and to be consistent with the LEP direct search limits, and the rate for $b \to s\gamma$, the resulting rate for lepton-flavour violation was such that over much of the allowed WMAP range, much of the model parameter space was consistent with the present experimental limit on BR($\mu \to e\gamma$) (and so, a fortiori, with present limits on the other (charged) lepton-flavour violating processes). We also noted that the next generation of $\mu \to e\gamma$ experiments should definitively probe the range of branching ratios suggested by these models at maximal Yukawa couplings, and also for ranges of smaller Yukawas depending on the CMSSM parameters and the exact see-saw model details.

The AB model class [4, 5, 6], based on a $U(1)\times Z_2 \times Z_2$ flavour symmetry, is a highly successful and predictive GUT scenario. This model class has the ability to accommodate all the observed neutrino phenomena and reproduce the low energy physics of the standard model. If it is assumed that supersymmetry is broken via mSUGRA and that the GUT breaks directly to the CMSSM, the AB model class is highly restrictive and hence allows for a precise determination of the rate of charged lepton flavour violation. In particular, we examined the process $\mu \to e\gamma$, since at the present time this flavour violating muon decay channel gives the strongest constraints on flavour changing neutral currents in the lepton sector. As the WMAP satellite data and laboratory direct searches have already severely restricted the available CMSSM parameter space, the $\mu \to e\gamma$ flavour bounds allow a strong test of the AB model class. We find that given the current bounds [8] on $\mu \to e\gamma$, BR($\mu \to e\gamma$) $< 1.2 \times 10^{-11}$, the AB model class favours low to moderate $\tan\beta$ (i.e. $\lesssim 20$) with $\mu > 0$, however, there is a small region that is not excluded for $\tan\beta \lesssim 35$ with the sign of μ negative. If MEG at PSI [9] does not detect a positive LFV signal, BR($\mu \to e\gamma$) $\lesssim 5 \times 10^{-14}$, the AB model class will be effectively ruled out, given our conservative assumptions concerning GUT and supersymmetry breaking. It remains an open question as to whether or not other supersymmetry and/or GUT breaking schemes within the AB model class will be able to avoid these flavour violating bounds.

Appendix A

Spinors

The Lorentz group satisfies the Lie algebra

$$[M^{\mu\nu}, M^{\rho\sigma}] = i\,(\eta^{\nu\rho}M^{\mu\sigma} + \eta^{\mu\sigma}M^{\nu\rho} - \eta^{\mu\rho}M^{\nu\sigma} - \eta^{\nu\sigma}M^{\mu\rho}) \tag{A.1}$$

and can be identified with the Lie algebra $SO(3,1)$. Therefore, writing the Hermitian generators M^{ij}, $i,j = 1,2,3$ as

$$J_i = \frac{1}{2}\epsilon_{ijk}M^{jk}, \tag{A.2}$$

the Lorentz algebra of eq.(A.1) guarantees that the operators J_i obey the usual $SU(2)$ commutation relations,

$$[J_i, J_j] = i\epsilon_{ijk}J_k. \tag{A.3}$$

Defining the non-compact boost generators as,

$$K_i = M_{0i} \tag{A.4}$$

we find that,

$$[K_i, K_j] = -i\epsilon_{ijk}J_k \tag{A.5}$$

$$[J_i, K_j] = i\epsilon_{ijk}K_k. \tag{A.6}$$

We may separate the these algebras by constructing the linear combination,

$$N_i = \frac{1}{2}(J_i + iK_i) \tag{A.7}$$

leading to the commutation relations

$$[N_i, N_j^\dagger] = 0 \tag{A.8}$$

$$[N_i, N_j] = i\epsilon_{ijk}N^k \tag{A.9}$$

$$[N_i^\dagger, N_j^\dagger] = i\epsilon_{ijk}N^{k\dagger}. \tag{A.10}$$

We see that the Lorentz group can be decomposed into two $SU(2)$ algebras and thus we may label states according to Casimir invariant of these two algebras. In particular we have the two basic irreducible representations $\left(\frac{1}{2}, \mathbf{0}\right)$, and $\left(\mathbf{0}, \frac{1}{2}\right)$. Let us consider these representations more closely.

The Lorentz algebra is satisfied by the operator,

$$\frac{1}{2}\Sigma^{\mu\nu} = \frac{i}{4}(\gamma^\mu\gamma^\nu - \gamma^\nu\gamma^\nu) \tag{A.11}$$

where the γ^μ matrices obey the Clifford algebra,

$$\{\gamma^\mu, \gamma^\nu\} = 2\eta^{\mu\nu} \tag{A.12}$$

with

$$\gamma = \begin{pmatrix} 0 & \sigma^\mu \\ \bar{\sigma}^\mu & 0 \end{pmatrix} \tag{A.13}$$

where,

$$\sigma^\mu = (\mathbf{I}_2, \sigma) \tag{A.14}$$

$$\sigma^\mu = (\mathbf{I}_2, -\sigma) = \sigma_\mu. \tag{A.15}$$

The matrices σ are the usual Pauli spin matrices. States that belong to this representation are formed by $\left(\frac{1}{2}, \mathbf{0}\right) + \left(\mathbf{0}, \frac{1}{2}\right) = \Psi_D = \Psi_L + \Psi_R$ and are called Dirac spinors. The Dirac spinor may be separated into its individual components Ψ_L and Ψ_R by applying the projection operators,

$$\Psi_L = \frac{1}{2}(1 - \gamma_5)\Psi_D \tag{A.16}$$

$$\Psi_R = \frac{1}{2}(1 + \gamma_5)\Psi_D \tag{A.17}$$

where $\gamma_5 = i\gamma_0\gamma_1\gamma_2\gamma_3$.

Since

$$\frac{1}{2}\Sigma^{ij} = \frac{1}{2}\begin{pmatrix} \sigma^k & 0 \\ 0 & \sigma^k \end{pmatrix} \tag{A.18}$$

$$\frac{1}{2}\Sigma^{0j} = \frac{1}{2}\begin{pmatrix} -i\sigma^j & 0 \\ 0 & i\sigma^j \end{pmatrix} \tag{A.19}$$

both spinors Ψ_L and Ψ_R transform in the same way under rotations but differently under boosts. Thus, we may write each state as

$$\left(\frac{\mathbf{1}}{\mathbf{2}},\mathbf{0}\right) = \Psi_L = \begin{pmatrix} \psi_\alpha \\ 0 \end{pmatrix} \tag{A.20}$$

$$\left(\mathbf{0},\frac{\mathbf{1}}{\mathbf{2}}\right) = \Psi_R = \begin{pmatrix} 0 \\ \bar{\chi}^{\dot{\alpha}} \end{pmatrix} \tag{A.21}$$

where $\alpha = 1,2$. The two component spinors ψ and $\bar{\chi}$ are referred to a Weyl spinors and thus we my write the Dirac spinor as

$$\Psi_D = \begin{pmatrix} \psi \\ \bar{\chi} \end{pmatrix}. \tag{A.22}$$

Introducing the charge conjugation operator $C = -i\gamma^0\gamma^2$ such that,

$$C^{-1}\gamma^\mu C = -\gamma^{T\mu} \tag{A.23}$$

$$\Psi_D^c = C\bar{\Psi}_D^T \tag{A.24}$$

leads to,

$$\Psi_D^c = -i\begin{pmatrix} -\sigma^2\bar{\chi}^* \\ \sigma^2\psi^* \end{pmatrix} \tag{A.25}$$

It is easy to see that $\sigma^2\psi^* \sim \left(\mathbf{0},\frac{\mathbf{1}}{\mathbf{2}}\right)$ and $\sigma^2\bar{\chi}^* \sim \left(\frac{\mathbf{1}}{\mathbf{2}},\mathbf{0}\right)$ i.e. $\sigma^2\psi^*$ transforms right-handed and $\sigma^2\bar{\chi}^*$ transforms left-handed. We may separately track the left and right-handed Weyl spinors by introducing the Van der Warden notation,

$$\bar{\psi}_{\dot{\alpha}} = (\psi_\alpha)^* \quad \chi^\alpha = (\bar{\chi}^{\dot{\alpha}})^* \tag{A.26}$$

such that,

$$(i\sigma^2)_{\alpha\beta} = \epsilon_{\alpha\beta} = \begin{pmatrix} 0 & 1 \\ -1 & 0 \end{pmatrix} \tag{A.27}$$

and

$$(-i\sigma^2)^{\dot{\alpha}\dot{\beta}} = \epsilon^{\dot{\alpha}\dot{\beta}} = \begin{pmatrix} 0 & -1 \\ 1 & 0 \end{pmatrix}. \tag{A.28}$$

We may raise an lower the spinor indices using $\epsilon_{\alpha\beta}$ and $\epsilon^{\dot{\alpha}\dot{\beta}}$,

$$\chi_\alpha = \epsilon_{\alpha\beta}\chi^\beta \tag{A.29}$$

$$\bar{\psi}^{\dot{\alpha}} = \epsilon^{\dot{\alpha}\dot{\beta}}\bar{\psi}_{\dot{\beta}}. \tag{A.30}$$

Using the Weyl spinors, the Dirac spinor may be written as,

$$\Psi_D = \begin{pmatrix} \psi_\alpha \\ \bar{\chi}^{\dot{\alpha}} \end{pmatrix} \quad \Psi_D^c = \begin{pmatrix} \chi_\alpha \\ \bar{\psi}^{\dot{\alpha}} \end{pmatrix} \tag{A.31}$$

Evidently, using the Van der Warden notation, the self conjugate Majorana spinor can be written as

$$\Psi_M = \Psi_M^c = \begin{pmatrix} \psi_\alpha \\ \bar{\psi}^{\dot{\alpha}} \end{pmatrix}. \tag{A.32}$$

We may always trade spinor indices for vector indices as we shall now see. The Lorentz transformation acting on the Dirac equation yields,

$$S(\Lambda)^{-1}\gamma^\mu S(\Lambda) = \Lambda^\mu_\nu \gamma^\nu \tag{A.33}$$

where,

$$S(\Lambda) = \exp\left\{-\frac{i}{4}\omega_{\mu\nu}\Sigma^{\mu\nu}\right\} \tag{A.34}$$

with $\omega_{\mu\nu} = -\omega_{\nu\mu}$. In the Weyl representation, we may re-express $\Sigma^{\mu\nu}$ as,

$$\frac{1}{2}\Sigma^{\mu\nu} = \begin{pmatrix} i\sigma^{\mu\nu} & 0 \\ 0 & i\bar{\sigma}^{\mu\nu} \end{pmatrix} \tag{A.35}$$

where

$$\sigma^{\mu\nu} = \frac{1}{4}(\sigma^\mu\bar{\sigma}^\nu - \sigma^\nu\bar{\sigma}^\mu) \tag{A.36}$$

$$\bar{\sigma}^{\mu\nu} = \frac{1}{4}(\bar{\sigma}^\mu\sigma^\nu - \bar{\sigma}^\nu\sigma^\mu). \tag{A.37}$$

By examining the action of the Lorentz group on the Weyl spinors, namely,

$$\psi'_\alpha = S_1(\Lambda)_\alpha^{\ \beta}\psi_\beta \tag{A.38}$$

$$\bar{\chi}^{\dot{\alpha}} = S_2(\Lambda)^{\dot{\alpha}}_{\ \dot{\beta}}\bar{\chi}^{\dot{\beta}} \tag{A.39}$$

with

$$S_1(\Lambda) = \exp\left\{\frac{1}{2}\omega_{\mu\nu}\sigma^{\mu\nu}\right\} \tag{A.40}$$

$$S_2(\Lambda) = \exp\left\{\frac{1}{2}\omega_{\mu\nu}\bar{\sigma}^{\mu\nu}\right\} \tag{A.41}$$

we see that $\sigma^{\mu\nu}$ and $\bar{\sigma}^{\mu\nu}$ control the spinor transformation properties and therefore they

carry the spinor indices,

$$(\sigma^{\mu\nu})_\alpha^{\ \beta} \quad (\bar{\sigma}^{\mu\nu})^{\dot{\alpha}}_{\ \dot{\beta}}. \tag{A.42}$$

As a result, we also have

$$\sigma^\mu_{\alpha\dot{\alpha}} \quad (\bar{\sigma}^\mu)^{\alpha\dot{\alpha}} \tag{A.43}$$

and it is not hard to show that,

$$S_1(\Lambda) = S_2(\Lambda)^\dagger. \tag{A.44}$$

We may now construct Lorentz invariant quantities by contracting the spinor indices using $\epsilon_{\alpha\beta}$ and $\epsilon^{\dot{\alpha}\dot{\beta}}$, and using the Grassmann algebra of the spinors themselves,

$$\chi^\alpha\psi_\alpha = \psi^\alpha\chi_\alpha = \chi\psi \tag{A.45}$$

$$\bar{\chi}_{\dot{\alpha}}\bar{\psi}^{\dot{\alpha}} = \bar{\psi}_{\dot{\alpha}}\bar{\chi}^{\dot{\alpha}} = \bar{\chi}\bar{\psi} \tag{A.46}$$

$$\bar{\chi}_{\dot{\alpha}}(\bar{\sigma}^\mu)^{\alpha\dot{\alpha}}\psi_\alpha = -\psi^\alpha(\sigma^\mu)_{\alpha\dot{\alpha}}\bar{\chi}^{\dot{\alpha}} = \bar{\chi}\bar{\sigma}^\mu\psi \tag{A.47}$$

$$\chi^\alpha(\sigma^{\mu\nu})_\alpha^{\ \beta}\psi_\beta = -\psi^\alpha(\sigma^{\mu\nu})_\alpha^{\ \beta}\chi_\beta = \chi\sigma^{\mu\nu}\psi \tag{A.48}$$

$$\bar{\chi}_{\dot{\alpha}}(\bar{\sigma}^{\mu\nu})^{\dot{\alpha}}_{\ \dot{\beta}}\bar{\psi}^{\dot{\beta}} = -\bar{\psi}_{\dot{\alpha}}(\bar{\sigma}^{\mu\nu})^{\dot{\alpha}}_{\ \dot{\beta}}\bar{\psi}^{\dot{\beta}} = \bar{\chi}\bar{\sigma}^{\mu\nu}\bar{\psi} \tag{A.49}$$

with

$$(\chi\psi)^\dagger = \psi^\dagger\chi^\dagger = \bar{\psi}\bar{\chi} = \bar{\chi}\bar{\psi} \tag{A.50}$$

and

$$(\chi\sigma^\mu\bar{\psi})^\dagger = \psi\sigma^\mu\bar{\chi} = -(\bar{\psi}\bar{\sigma}^\mu\chi)^\dagger \tag{A.51}$$

$$(\chi\sigma^{\mu\nu}\psi)^\dagger = \bar{\chi}\bar{\sigma}^{\mu\nu}\bar{\psi} = -(\psi\sigma^{\mu\nu}\chi)^\dagger. \tag{A.52}$$

From the completeness relations,

$$\delta_{\alpha\beta}\delta_{\gamma\delta} = \frac{1}{2}\left(\delta_{\alpha\delta}\delta_{\gamma\beta} + \sigma^i_{\alpha\delta}\sigma^i_{\gamma\beta}\right) \tag{A.53}$$

$$\delta_\alpha^{\ \beta}\delta^{\dot{\gamma}}_{\ \dot{\delta}} = \frac{1}{2}(\sigma^\mu)_{\alpha\dot{\delta}}(\bar{\sigma}_\mu)^{\dot{\gamma}\beta} \tag{A.54}$$

we may construct the complete set of Fierz identities.

Appendix B

$l_j \rightarrow l_i + \gamma$

The interactions leading to the lepton flavour violating process $l_j \rightarrow l_i + \gamma$ involve two effective Lagrangians: neutralino-lepton-slepton and chargino-lepton-sneutrino. Written in the mass eigenbasis they are

$$\mathcal{L} = \sum_{i=1}^{3}\sum_{a=1}^{4}\sum_{b=1}^{6} N^{\mathrm{L}}_{iab}\tilde{f}_b E_i \tilde{\chi}^0_a + N^{\mathrm{R}*}_{iab}\tilde{f}^*_b e_i \tilde{\chi}^0_a + \text{ c. c.} \tag{B.1}$$

and

$$\mathcal{L} = \sum_{i=1}^{3}\sum_{a=1}^{2}\sum_{b=1}^{3} C^{\mathrm{L}}_{iab}\tilde{\nu}_b E_i \tilde{\chi}^-_a + C^{\mathrm{R}*}_{iab}\tilde{\nu}^*_b e_i \tilde{\chi}^+_a + \text{ c. c.} \tag{B.2}$$

where

$$N^{\mathrm{L}}_{iab} = -\frac{g_2}{\sqrt{2}}\left(2\tan\theta_{\mathrm{W}}\left(\mathbf{U}_{\tilde{\mathrm{f}}}\right)^*_{b(i+3)}\left(\mathbf{O}_{\mathrm{ne}}\right)_{a1} + \frac{m_{\mathrm{l}_i}}{m_{\mathrm{W}}\cos\beta}\left(\mathbf{U}_{\tilde{\mathrm{f}}}\right)^*_{bi}\left(\mathbf{O}_{\mathrm{ne}}\right)_{a3}\right), \tag{B.3}$$

$$N^{\mathrm{R}}_{iab} = \frac{g_2}{\sqrt{2}}\left(\tan\theta_{\mathrm{W}}\left(\mathbf{U}_{\tilde{\mathrm{f}}}\right)^*_{bi}\left(\mathbf{O}_{\mathrm{ne}}\right)_{a1} + \left(\mathbf{U}_{\tilde{\mathrm{f}}}\right)^*_{bi}\left(\mathbf{O}_{\mathrm{ne}}\right)_{a2} - \frac{m_{\mathrm{l}_i}}{m_{\mathrm{W}}\cos\beta}\left(\mathbf{U}_{\tilde{\mathrm{f}}}\right)^*_{b(i+3)}\left(\mathbf{O}_{\mathrm{ne}}\right)_{a3}\right) \tag{B.4}$$

and

$$C^{\mathrm{L}}_{iab} = \frac{g_2 m_{\mathrm{l}_i}}{\sqrt{2}m_{\mathrm{W}}\cos\beta}\left(\mathbf{O}_{\mathrm{L}}\right)_{a2}\left(\mathbf{U}_{\tilde{\mathrm{n}}}\right)^*_{bi}, \tag{B.5}$$

$$C^{\mathrm{R}}_{iab} = -g_2\left(\mathbf{O}_{\mathrm{R}}\right)_{a1}\left(\mathbf{U}_{\tilde{\mathrm{n}}}\right)^*_{bi}. \tag{B.6}$$

The on-shell amplitude for $l_j \rightarrow l_i + \gamma$ can be written in the general form

$$\mathcal{M} = e\epsilon^*_\mu \bar{l}_i\left(p-q\right)\left(im_{\mathrm{l}_j}\sigma^{\mu\nu}q_\nu\left(A_{\mathrm{L}}\mathrm{L} + A_{\mathrm{R}}\mathrm{R}\right)\right)l_j\left(p\right); \tag{B.7}$$

here we have used Dirac spinors $l_i\left(p-q\right)$ and $l_j\left(p\right)$ for the charged leptons i and j with momenta $p-q$ and p, respectively; $\mathrm{L} = \left(1-\gamma^5\right)/2$ and $\mathrm{R} = \left(1+\gamma^5\right)/2$. Each of the

dipole coefficients $A_{\rm L}$ and $A_{\rm R}$ have contributions from the neutralino-lepton-slepton and the chargino-lepton-sneutrino interaction, namely,

$$A_{\rm L} = A_{\rm L}^{(\rm n)} + A_{\rm L}^{(\rm c)}, \tag{B.8}$$

$$A_{\rm R} = A_{\rm R}^{(\rm n)} + A_{\rm R}^{(\rm c)} \tag{B.9}$$

where $A_{\rm L}^{(\rm n)}$, $A_{\rm R}^{(\rm n)}$, $A_{\rm L}^{(\rm c)}$, $A_{\rm R}^{(\rm c)}$ can be evaluated from the Feynman diagrams in figure 6.1;

$$\begin{aligned} A_{\rm L}^{(\rm n)} &= \frac{1}{32\pi^2}\sum_{a=1}^{4}\sum_{b=1}^{6}\frac{1}{m_{\tilde{l}_b}^2}\left(N_{iab}^{\rm L}N_{jab}^{\rm L*}J_1\left(\frac{M_{\tilde{\chi}_a^0}^2}{m_{\tilde{l}_b}^2}\right)\right. \\ &\quad \left. + N_{iab}^{\rm L}N_{jab}^{\rm R*}\frac{|M_{\tilde{\chi}_a^0}|}{m_{l_j}}J_2\left(\frac{M_{\tilde{\chi}_a^0}^2}{m_{\tilde{l}_b}^2}\right)\right), \end{aligned} \tag{B.10}$$

$$\begin{aligned} A_{\rm L}^{(\rm c)} &= -\frac{1}{32\pi^2}\sum_{a=1}^{2}\sum_{b=1}^{3}\frac{1}{m_{\tilde{\nu}_b}^2}\left(C_{iab}^{\rm L}C_{jab}^{\rm L*}J_3\left(\frac{M_{\tilde{\chi}_a^-}^2}{m_{\tilde{\nu}_b}^2}\right)\right. \\ &\quad \left. + C_{iab}^{\rm L}C_{jab}^{\rm R*}\frac{M_{\tilde{\chi}_a^-}}{m_{l_j}}J_4\left(\frac{M_{\tilde{\chi}_a^-}^2}{m_{\tilde{\nu}_b}^2}\right)\right), \end{aligned} \tag{B.11}$$

$$A_{\rm R}^{(\rm n)} = A_{\rm L}^{(\rm n)}\Big|_{L\leftrightarrow R}, \tag{B.12}$$

$$A_{\rm R}^{(\rm c)} = A_{\rm L}^{(\rm c)}\Big|_{L\leftrightarrow R}. \tag{B.13}$$

The functions $J_1(x)$, $J_2(x)$, $J_3(x)$, $J_4(x)$ are defined as

$$J_1(x) = \frac{1-6x+3x^2+2x^3-6x^2\ln x}{6(1-x)^4}, \tag{B.14}$$

$$J_2(x) = \frac{1-x^2+2x\ln x}{(1-x)^3}, \tag{B.15}$$

$$J_3(x) = \frac{2+3x-6x^2+x^3+6x\ln x}{6(1-x)^4}, \tag{B.16}$$

$$J_4(x) = \frac{-3+4x-x^2+2\ln x}{(1-x)^3}. \tag{B.17}$$

Finally, the decay rate for $l_j^- \to l_i^- + \gamma$ is given by

$$\Gamma\left(l_j^- \to l_i^- + \gamma\right) = \frac{e^2}{16\pi}m_{l_j}^5\left(|A_{\rm L}|^2 + |A_{\rm R}|^2\right), \tag{B.18}$$

and $i = 1$, $j = 2$ for $\mu \to e + \gamma$.

Appendix C

The One-Loop RGEs for the MSSM-RN

The general form of the supersymmetric renormalization group equations [12, 11, 10] are

$$\frac{dX}{dt} = \frac{1}{16\pi^2}\dot{X} \tag{C.1}$$

where X is any of g_1, g_2, g_3, $\mathbf{Y_N}$, $\mathbf{Y_E}$, $\mathbf{Y_U}$, $\mathbf{Y_D}$, M_1, M_2, M_3, $m^2_{H_u}$, $m^2_{H_d}$, $\mathbf{m}^2_{\tilde{L}}$, $\mathbf{m}^2_{\tilde{N}}$, $\mathbf{m}^2_{\tilde{E}}$, $\mathbf{m}^2_{\tilde{Q}}$, $\mathbf{m}^2_{\tilde{U}}$, $\mathbf{m}^2_{\tilde{D}}$, $\mathbf{A_N}$, $\mathbf{A_E}$, $\mathbf{A_U}$, $\mathbf{A_D}$, and the dotted quantities are listed below:

$$\dot{g}_1 = 11g_1^3, \tag{C.2}$$

$$\dot{g}_2 = g_2^3, \tag{C.3}$$

$$\dot{g}_3 = -3g_3^3, \tag{C.4}$$

(C.5)

$$\dot{\mathbf{Y}}_\mathbf{N} = \mathbf{Y_N}\left(-g_1^2\mathbf{I} - 3g_2^2\mathbf{I} + 3\mathrm{Tr}\left(\mathbf{Y_U^\dagger Y_U}\right)\mathbf{I} + \mathrm{Tr}\left(\mathbf{Y_N^\dagger Y_N}\right)\mathbf{I} + 3\mathbf{Y_N^\dagger Y_N} + \mathbf{Y_E^\dagger Y_E}\right), \tag{C.6}$$

$$\dot{\mathbf{Y}}_\mathbf{E} = \mathbf{Y_E}\left(-3g_1^2\mathbf{I} - 3g_2^2\mathbf{I} + 3\mathrm{Tr}\left(\mathbf{Y_D^\dagger Y_D}\right)\mathbf{I} + \mathrm{Tr}\left(\mathbf{Y_E^\dagger Y_E}\right)\mathbf{I} + 3\mathbf{Y_E^\dagger Y_E} + \mathbf{Y_N^\dagger Y_N}\right), \tag{C.7}$$

$$\begin{aligned}\dot{\mathbf{Y}}_\mathbf{U} = \mathbf{Y_U}\Big(&-\frac{13}{9}g_1^2\mathbf{I} - 3g_2^2\mathbf{I} - \frac{16}{3}g_3^2\mathbf{I} + 3\mathrm{Tr}\left(\mathbf{Y_U^\dagger Y_U}\right)\mathbf{I} + \mathrm{Tr}\left(\mathbf{Y_N^\dagger Y_N}\right)\mathbf{I} \\ &+ 3\mathbf{Y_U^\dagger Y_U} + \mathbf{Y_D^\dagger Y_D}\Big),\end{aligned} \tag{C.8}$$

$$\dot{\mathbf{Y}}_\mathbf{D} = \mathbf{Y_D}\left(-\frac{7}{9}g_1^2\mathbf{I} - 3g_2^2\mathbf{I} - \frac{16}{3}g_3^2\mathbf{I} + 3\mathrm{Tr}\left(\mathbf{Y_D^\dagger Y_D}\right)\mathbf{I} + \mathrm{Tr}\left(\mathbf{Y_E^\dagger Y_E}\right)\mathbf{I}\right.$$

$$+3\mathbf{Y}_{\mathrm{D}}^{\dagger}\mathbf{Y}_{\mathrm{D}}+\mathbf{Y}_{\mathrm{U}}^{\dagger}\mathbf{Y}_{\mathrm{U}}\Big), \tag{C.9}$$

$$\dot{M}_1 = 22g_1^2M_1, \tag{C.10}$$

$$\dot{M}_2 = 2g_2^2M_2, \tag{C.11}$$

$$\dot{M}_3 = -6g_3^2M_3, \tag{C.12}$$

$$S = m_{\mathrm{H_u}}^2 - m_{\mathrm{H_d}}^2 + \mathrm{Tr}\left(\mathbf{m}_{\tilde{\mathrm{Q}}}^2 - 2\mathbf{m}_{\tilde{\mathrm{U}}}^2 + \mathbf{m}_{\tilde{\mathrm{D}}}^2 - \mathbf{m}_{\tilde{\mathrm{L}}}^2 + \mathbf{m}_{\tilde{\mathrm{E}}}^2\right), \tag{C.13}$$

$$\begin{aligned}\dot{m}_{\mathrm{H_u}}^2 = {} & 6\mathrm{Tr}\left(\mathbf{m}_{\tilde{\mathrm{Q}}}^2\mathbf{Y}_{\mathrm{U}}^{\dagger}\mathbf{Y}_{\mathrm{U}}+\mathbf{Y}_{\mathrm{U}}^{\dagger}\mathbf{m}_{\tilde{\mathrm{U}}}^2\mathbf{Y}_{\mathrm{U}}+m_{\mathrm{H_u}}^2\mathbf{Y}_{\mathrm{U}}^{\dagger}\mathbf{Y}_{\mathrm{U}}+\mathbf{A}_{\mathrm{U}}^{\dagger}\mathbf{A}_{\mathrm{U}}\right)\\ & +2\mathrm{Tr}\left(\mathbf{m}_{\tilde{\mathrm{L}}}^2\mathbf{Y}_{\mathrm{N}}^{\dagger}\mathbf{Y}_{\mathrm{N}}+\mathbf{Y}_{\mathrm{N}}^{\dagger}\mathbf{m}_{\tilde{\mathrm{N}}}^2\mathbf{Y}_{\mathrm{N}}+m_{\mathrm{H_u}}^2\mathbf{Y}_{\mathrm{N}}^{\dagger}\mathbf{Y}_{\mathrm{N}}+\mathbf{A}_{\mathrm{N}}^{\dagger}\mathbf{A}_{\mathrm{N}}\right)\\ & -2g_1^2M_1^2-6g_2^2M_2^2+g_1^2S,\end{aligned} \tag{C.14}$$

$$\begin{aligned}\dot{m}_{\mathrm{H_d}}^2 = {} & 2\mathrm{Tr}\left(\mathbf{m}_{\tilde{\mathrm{L}}}^2\mathbf{Y}_{\mathrm{E}}^{\dagger}\mathbf{Y}_{\mathrm{E}}+\mathbf{Y}_{\mathrm{E}}^{\dagger}\mathbf{m}_{\tilde{\mathrm{E}}}^2\mathbf{Y}_{\mathrm{E}}+m_{\mathrm{H_d}}^2\mathbf{Y}_{\mathrm{E}}^{\dagger}\mathbf{Y}_{\mathrm{E}}+\mathbf{A}_{\mathrm{E}}^{\dagger}\mathbf{A}_{\mathrm{E}}\right)\\ & +6\mathrm{Tr}\left(\mathbf{m}_{\tilde{\mathrm{Q}}}^2\mathbf{Y}_{\mathrm{D}}^{\dagger}\mathbf{Y}_{\mathrm{D}}+\mathbf{Y}_{\mathrm{D}}^{\dagger}\mathbf{m}_{\tilde{\mathrm{D}}}^2\mathbf{Y}_{\mathrm{D}}+m_{\mathrm{H_d}}^2\mathbf{Y}_{\mathrm{D}}^{\dagger}\mathbf{Y}_{\mathrm{D}}+\mathbf{A}_{\mathrm{D}}^{\dagger}\mathbf{A}_{\mathrm{D}}\right)\\ & -2g_1^2M_1^2-6g_2^2M_2^2-g_1^2S,\end{aligned} \tag{C.15}$$

$$\begin{aligned}\dot{\mathbf{m}}_{\tilde{\mathrm{L}}}^2 = {} & \mathbf{m}_{\tilde{\mathrm{L}}}^2\mathbf{Y}_{\mathrm{E}}^{\dagger}\mathbf{Y}_{\mathrm{E}}+\mathbf{Y}_{\mathrm{E}}^{\dagger}\mathbf{Y}_{\mathrm{E}}\mathbf{m}_{\tilde{\mathrm{L}}}^2+\mathbf{m}_{\tilde{\mathrm{L}}}^2\mathbf{Y}_{\mathrm{N}}^{\dagger}\mathbf{Y}_{\mathrm{N}}+\mathbf{Y}_{\mathrm{N}}^{\dagger}\mathbf{Y}_{\mathrm{N}}\mathbf{m}_{\tilde{\mathrm{L}}}^2\\ & +2\mathbf{Y}_{\mathrm{E}}^{\dagger}\mathbf{m}_{\tilde{\mathrm{E}}}^2\mathbf{Y}_{\mathrm{E}}+2m_{\mathrm{H_d}}^2\mathbf{Y}_{\mathrm{E}}^{\dagger}\mathbf{Y}_{\mathrm{E}}+2\mathbf{A}_{\mathrm{E}}^{\dagger}\mathbf{A}_{\mathrm{E}}\\ & +2\mathbf{Y}_{\mathrm{N}}^{\dagger}\mathbf{m}_{\tilde{\mathrm{N}}}^2\mathbf{Y}_{\mathrm{N}}+2m_{\mathrm{H_u}}^2\mathbf{Y}_{\mathrm{N}}^{\dagger}\mathbf{Y}_{\mathrm{N}}+2\mathbf{A}_{\mathrm{N}}^{\dagger}\mathbf{A}_{\mathrm{N}}\\ & -2g_1^2M_1^2\mathbf{I}-6g_2^2M_2^2\mathbf{I}-g_1^2S\mathbf{I},\end{aligned} \tag{C.16}$$

$$\dot{\mathbf{m}}_{\tilde{\mathrm{N}}}^2 = 2\mathbf{m}_{\tilde{\mathrm{N}}}^2\mathbf{Y}_{\mathrm{N}}\mathbf{Y}_{\mathrm{N}}^{\dagger}+2\mathbf{Y}_{\mathrm{N}}\mathbf{Y}_{\mathrm{N}}^{\dagger}\mathbf{m}_{\tilde{\mathrm{N}}}^2+4\mathbf{Y}_{\mathrm{N}}\mathbf{m}_{\tilde{\mathrm{L}}}^2\mathbf{Y}_{\mathrm{N}}^{\dagger}+4m_{\mathrm{H_u}}^2\mathbf{Y}_{\mathrm{N}}\mathbf{Y}_{\mathrm{N}}^{\dagger}+4\mathbf{A}_{\mathrm{N}}\mathbf{A}_{\mathrm{N}}^{\dagger}, \tag{C.17}$$

$$\begin{aligned}\dot{\mathbf{m}}_{\tilde{\mathrm{E}}}^2 = {} & 2\mathbf{m}_{\tilde{\mathrm{E}}}^2\mathbf{Y}_{\mathrm{E}}\mathbf{Y}_{\mathrm{E}}^{\dagger}+2\mathbf{Y}_{\mathrm{E}}\mathbf{Y}_{\mathrm{E}}^{\dagger}\mathbf{m}_{\tilde{\mathrm{E}}}^2+4\mathbf{Y}_{\mathrm{E}}\mathbf{m}_{\tilde{\mathrm{L}}}^2\mathbf{Y}_{\mathrm{E}}^{\dagger}+4m_{\mathrm{H_d}}^2\mathbf{Y}_{\mathrm{E}}\mathbf{Y}_{\mathrm{E}}^{\dagger}+4\mathbf{A}_{\mathrm{E}}\mathbf{A}_{\mathrm{E}}^{\dagger}\\ & -8g_1^2M_1^2\mathbf{I}+2g_1^2S\mathbf{I},\end{aligned} \tag{C.18}$$

$$\begin{aligned}\dot{\mathbf{m}}_{\tilde{\mathrm{Q}}}^2 = {} & \mathbf{m}_{\tilde{\mathrm{Q}}}^2\mathbf{Y}_{\mathrm{U}}^{\dagger}\mathbf{Y}_{\mathrm{U}}+\mathbf{Y}_{\mathrm{U}}^{\dagger}\mathbf{Y}_{\mathrm{U}}\mathbf{m}_{\tilde{\mathrm{Q}}}^2+2\mathbf{Y}_{\mathrm{U}}^{\dagger}\mathbf{m}_{\tilde{\mathrm{U}}}^2\mathbf{Y}_{\mathrm{U}}+2m_{\mathrm{H_u}}^2\mathbf{Y}_{\mathrm{U}}^{\dagger}\mathbf{Y}_{\mathrm{U}}+2\mathbf{A}_{\mathrm{U}}^{\dagger}\mathbf{A}_{\mathrm{U}}\\ & +\mathbf{m}_{\tilde{\mathrm{Q}}}^2\mathbf{Y}_{\mathrm{D}}^{\dagger}\mathbf{Y}_{\mathrm{D}}+\mathbf{Y}_{\mathrm{D}}^{\dagger}\mathbf{Y}_{\mathrm{D}}\mathbf{m}_{\tilde{\mathrm{Q}}}^2+2\mathbf{Y}_{\mathrm{D}}^{\dagger}\mathbf{m}_{\tilde{\mathrm{D}}}^2\mathbf{Y}_{\mathrm{D}}+2m_{\mathrm{H_d}}^2\mathbf{Y}_{\mathrm{D}}^{\dagger}\mathbf{Y}_{\mathrm{D}}+2\mathbf{A}_{\mathrm{D}}^{\dagger}\mathbf{A}_{\mathrm{D}}\\ & -\frac{2}{9}g_1^2M_1^2\mathbf{I}-6g_2^2M_2^2\mathbf{I}-\frac{32}{3}g_3^2M_3^2\mathbf{I}+\frac{1}{3}g_1^2S\mathbf{I},\end{aligned} \tag{C.19}$$

$$\begin{aligned}\dot{\mathbf{m}}^2_{\tilde{\mathrm{U}}} &= 2\mathbf{m}^2_{\tilde{\mathrm{U}}}\mathbf{Y}_\mathrm{U}\mathbf{Y}^\dagger_\mathrm{U} + 2\mathbf{Y}_\mathrm{U}\mathbf{Y}^\dagger_\mathrm{U}\mathbf{m}^2_{\tilde{\mathrm{U}}} + 4\mathbf{Y}_\mathrm{U}\mathbf{m}^2_{\tilde{\mathrm{Q}}}\mathbf{Y}^\dagger_\mathrm{U} + 4m^2_{\mathrm{H_u}}\mathbf{Y}_\mathrm{U}\mathbf{Y}^\dagger_\mathrm{U} + 4\mathbf{A}_\mathrm{U}\mathbf{A}^\dagger_\mathrm{U} \\ &\quad -\frac{32}{9}g_1^2M_1^2\mathbf{I} - \frac{32}{3}g_3^2M_3^2\mathbf{I} - \frac{4}{3}g_1^2S\mathbf{I}, \end{aligned} \tag{C.20}$$

$$\begin{aligned}\dot{\mathbf{m}}^2_{\tilde{\mathrm{D}}} &= 2\mathbf{m}^2_{\tilde{\mathrm{D}}}\mathbf{Y}_\mathrm{D}\mathbf{Y}^\dagger_\mathrm{D} + 2\mathbf{Y}_\mathrm{D}\mathbf{Y}^\dagger_\mathrm{D}\mathbf{m}^2_{\tilde{\mathrm{D}}} + 4\mathbf{Y}_\mathrm{D}\mathbf{m}^2_{\tilde{\mathrm{Q}}}\mathbf{Y}^\dagger_\mathrm{D} + 4m^2_{\mathrm{H_d}}\mathbf{Y}_\mathrm{D}\mathbf{Y}^\dagger_\mathrm{D} + 4\mathbf{A}_\mathrm{D}\mathbf{A}^\dagger_\mathrm{D} \\ &\quad -\frac{8}{9}g_1^2M_1^2\mathbf{I} - \frac{32}{3}g_3^2M_3^2\mathbf{I} + \frac{2}{3}g_1^2S\mathbf{I}, \end{aligned} \tag{C.21}$$

$$\begin{aligned}\dot{\mathbf{A}}_\mathrm{N} &= -g_1^2\mathbf{A}_\mathrm{N} - 3g_2^2\mathbf{A}_\mathrm{N} + 3\mathrm{Tr}\left(\mathbf{Y}^\dagger_\mathrm{U}\mathbf{Y}_\mathrm{U}\right)\mathbf{A}_\mathrm{N} + \mathrm{Tr}\left(\mathbf{Y}^\dagger_\mathrm{N}\mathbf{Y}_\mathrm{N}\right)\mathbf{A}_\mathrm{N} \\ &\quad -2g_1^2M_1\mathbf{Y}_\mathrm{N} - 6g_2^2M_2\mathbf{Y}_\mathrm{N} + 6\mathrm{Tr}\left(\mathbf{Y}^\dagger_\mathrm{U}\mathbf{A}_\mathrm{U}\right)\mathbf{Y}_\mathrm{N} + 2\mathrm{Tr}\left(\mathbf{Y}^\dagger_\mathrm{N}\mathbf{A}_\mathrm{N}\right)\mathbf{Y}_\mathrm{N} \\ &\quad +4\mathbf{Y}_\mathrm{N}\mathbf{Y}^\dagger_\mathrm{N}\mathbf{A}_\mathrm{N} + 5\mathbf{A}_\mathrm{N}\mathbf{Y}^\dagger_\mathrm{N}\mathbf{Y}_\mathrm{N} + 2\mathbf{Y}_\mathrm{N}\mathbf{Y}^\dagger_\mathrm{E}\mathbf{A}_\mathrm{E} + \mathbf{A}_\mathrm{N}\mathbf{Y}^\dagger_\mathrm{E}\mathbf{Y}_\mathrm{E}, \end{aligned} \tag{C.22}$$

$$\begin{aligned}\dot{\mathbf{A}}_\mathrm{E} &= -3g_1^2\mathbf{A}_\mathrm{E} - 3g_2^2\mathbf{A}_\mathrm{E} + 3\mathrm{Tr}\left(\mathbf{Y}^\dagger_\mathrm{D}\mathbf{Y}_\mathrm{D}\right)\mathbf{A}_\mathrm{E} + \mathrm{Tr}\left(\mathbf{Y}^\dagger_\mathrm{E}\mathbf{Y}_\mathrm{E}\right)\mathbf{A}_\mathrm{E} \\ &\quad -6g_1^2M_1\mathbf{Y}_\mathrm{E} - 6g_2^2M_2\mathbf{Y}_\mathrm{E} + 6\mathrm{Tr}\left(\mathbf{Y}^\dagger_\mathrm{D}\mathbf{A}_\mathrm{D}\right)\mathbf{Y}_\mathrm{E} + 2\mathrm{Tr}\left(\mathbf{Y}^\dagger_\mathrm{E}\mathbf{A}_\mathrm{E}\right)\mathbf{Y}_\mathrm{E} \\ &\quad +4\mathbf{Y}_\mathrm{E}\mathbf{Y}^\dagger_\mathrm{E}\mathbf{A}_\mathrm{E} + 5\mathbf{A}_\mathrm{E}\mathbf{Y}^\dagger_\mathrm{E}\mathbf{Y}_\mathrm{E} + 2\mathbf{Y}_\mathrm{E}\mathbf{Y}^\dagger_\mathrm{N}\mathbf{A}_\mathrm{N} + \mathbf{A}_\mathrm{E}\mathbf{Y}^\dagger_\mathrm{N}\mathbf{Y}_\mathrm{N}, \end{aligned} \tag{C.23}$$

$$\begin{aligned}\dot{\mathbf{A}}_\mathrm{U} &= -\frac{13}{9}g_1^2\mathbf{A}_\mathrm{U} - 3g_2^2\mathbf{A}_\mathrm{U} - \frac{16}{3}g_3^2\mathbf{A}_\mathrm{U} + 3\mathrm{Tr}\left(\mathbf{Y}^\dagger_\mathrm{U}\mathbf{Y}_\mathrm{U}\right)\mathbf{A}_\mathrm{U} + \mathrm{Tr}\left(\mathbf{Y}^\dagger_\mathrm{N}\mathbf{Y}_\mathrm{N}\right)\mathbf{A}_\mathrm{U} \\ &\quad -\frac{26}{9}g_1^2M_1\mathbf{Y}_\mathrm{U} - 6g_2^2M_2\mathbf{Y}_\mathrm{U} - \frac{32}{3}g_3^2M_3\mathbf{Y}_\mathrm{U} + 6\mathrm{Tr}\left(\mathbf{Y}^\dagger_\mathrm{U}\mathbf{A}_\mathrm{U}\right)\mathbf{Y}_\mathrm{U} + 2\mathrm{Tr}\left(\mathbf{Y}^\dagger_\mathrm{N}\mathbf{A}_\mathrm{N}\right)\mathbf{Y}_\mathrm{U} \\ &\quad +4\mathbf{Y}_\mathrm{U}\mathbf{Y}^\dagger_\mathrm{U}\mathbf{A}_\mathrm{U} + 5\mathbf{A}_\mathrm{U}\mathbf{Y}^\dagger_\mathrm{U}\mathbf{Y}_\mathrm{U} + 2\mathbf{Y}_\mathrm{U}\mathbf{Y}^\dagger_\mathrm{D}\mathbf{A}_\mathrm{D} + \mathbf{A}_\mathrm{U}\mathbf{Y}^\dagger_\mathrm{D}\mathbf{Y}_\mathrm{D}, \end{aligned} \tag{C.24}$$

$$\begin{aligned}\dot{\mathbf{A}}_\mathrm{D} &= -\frac{7}{9}g_1^2\mathbf{A}_\mathrm{D} - 3g_2^2\mathbf{A}_\mathrm{D} - \frac{16}{3}g_3^2\mathbf{A}_\mathrm{D} + 3\mathrm{Tr}\left(\mathbf{Y}^\dagger_\mathrm{D}\mathbf{Y}_\mathrm{D}\right)\mathbf{A}_\mathrm{D} + \mathrm{Tr}\left(\mathbf{Y}^\dagger_\mathrm{E}\mathbf{Y}_\mathrm{E}\right)\mathbf{A}_\mathrm{D} \\ &\quad -\frac{14}{9}g_1^2M_1\mathbf{Y}_\mathrm{D} - 6g_2^2M_2\mathbf{Y}_\mathrm{D} - \frac{32}{3}g_3^2M_3\mathbf{Y}_\mathrm{D} + 6\mathrm{Tr}\left(\mathbf{Y}^\dagger_\mathrm{D}\mathbf{A}_\mathrm{D}\right)\mathbf{Y}_\mathrm{D} + 2\mathrm{Tr}\left(\mathbf{Y}^\dagger_\mathrm{E}\mathbf{A}_\mathrm{E}\right)\mathbf{Y}_\mathrm{D} \\ &\quad +4\mathbf{Y}_\mathrm{D}\mathbf{Y}^\dagger_\mathrm{D}\mathbf{A}_\mathrm{D} + 5\mathbf{A}_\mathrm{D}\mathbf{Y}^\dagger_\mathrm{D}\mathbf{Y}_\mathrm{D} + 2\mathbf{Y}_\mathrm{D}\mathbf{Y}^\dagger_\mathrm{U}\mathbf{A}_\mathrm{U} + \mathbf{A}_\mathrm{D}\mathbf{Y}^\dagger_\mathrm{U}\mathbf{Y}_\mathrm{U}. \end{aligned} \tag{C.25}$$

Bibliography

[1] A. Garcia *et al.*, nucl-ex/9904001.

[2] E. G. Adelberger *et al.* (ISOLDE), Phys. Rev. Lett. **83**, 1299 (1999), nucl-ex/9903002.

[3] J. A. Casas and A. Ibarra, Nucl.Phys. **B618** (2001), 171 [arXiv:hep-ph/0103065].

[4] Carl H. Albright and S. M. Barr, Phys. Rev. **D62** (2000), 093008 [arXiv:hep-ph/0003251].

[5] C. H. Albright and S. M. Barr, Phys. Rev. **D64** (2001), 073010 [arXiv:hep-ph/0104294].

[6] C. H. Albright and S. Geer, Phys. Lett. **B532** (2002), 311-317 [arXiv:hep-ph/0112171].

[7] C. L. Bennett et al., WMAP Collaboration, Astrophys. J. Suppl. **148** (2003), 1 [arXiv:astro-ph/0302207];

D. N. Spergel et al., WMAP Collaboration, Astrophys. J. Suppl. **148** (2003), 175 [arXiv:astro-ph/0302209].

[8] M. L. Brooks et. al, MEGA Collaboration Phys. Rev. Lett. **83** (1991), 1521 [arXiv:hep-ph/9905013].

[9] T. Mori, Nucl. Phys. Proc. Suppl. **111** (2002), 194; the MEG website: `http://meg.web.psi.ch/`

[10] J. Hisano, T. Moroi, K. Tobe and M. Yamaguchi, Phys. Rev. **D53** (1996), 2442-2459 [arXiv:hep-ph/9510309].

[11] S. P. Martin and M.T. Vaughn, Phys. Rev. **D50** (1994), 2282 [hep-ph/9311340].

[12] N. K. Falck, Z. Phys. **C30** (1986), 247.